Maternal Adaptation to Pregnancy:

Altered Circadian Rhythms of Clock Genes in the Hypothalamus and Metabolic Tissues

by

Michaela Debra Wharfe, BSc (Hons)

This thesis is presented for the degree of

DOCTOR OF PHILOSOPHY

of The University of Western Australia

School of Anatomy, Physiology and Human Biology

Submitted: February, 2016

Preface

The experimental work presented in this thesis was undertaken in the School of Anatomy, Physiology and Human Biology, The University of Western Australia, under the supervision of Prof. Brendan J. Waddell, Dr. Peter J. Mark and Dr. Caitlin S. Wyrwoll, with the financial assistance of an Australian Postgraduate Award and an Ernst & Evelyn Havill Shacklock Top Up scholarship.

The work described is original and was carried out by myself except where specific contributions of other persons are acknowledged. All experimental chapters have been published. All co-authors have given formal permission for the published manuscripts to be printed in this thesis.

Michaela Debra Wharfe
February 2016

Abstract

Maternal physiological adaptations are crucial for pregnancy success by ensuring that fetal and placental demands are met whilst maintaining maternal homeostasis. There is growing recognition that whole body homeostasis is intimately linked to circadian variation. Accordingly, major physiological adaptations in pregnancy likely involve marked shifts in maternal circadian function. Circadian variation of physiological processes are driven by a network of clock genes that form transcriptional-translational feedback loops in both central (i.e. the suprachiasmatic nucleus; SCN) and peripheral tissues including the liver and adipose tissue. Therefore, the aims of this thesis were to characterise the impact of pregnancy on clock gene expression in key maternal tissues involved in HPA axis regulation and glucose and lipid metabolism as well as to determine subsequent downstream effects on the expression of tissue-specific genes that are known to be regulated in a circadian manner.

The initial study in this thesis tested the hypothesis that hypothalamic expression of clock genes change across mouse pregnancy and that this is linked to altered HPA axis activity. The anterior hypothalamus and plasma were collected from C57Bl/6J mice prior to and on days 6, 10, 14 and 18 of pregnancy (term=day 19) at 4-h intervals across a 24-h period. Hypothalamic expression of all clock genes changed markedly across gestation, particularly at mid-gestation when levels of each gene were elevated. The pregnancy-induced increase in maternal corticosterone (up to 14-fold higher by day 14) was not accompanied by a parallel shift in plasma adrenocorticotropic hormone (ACTH; 28% lower on day 14 compared with non-pregnant). Moreover, while circadian rhythmicity in corticosterone was maintained up to day 14, this was effectively lost by day 18. Thus, the central circadian clock undergoes marked adaptations throughout pregnancy, changes that likely contribute to maternal physiological adaptations. Importantly, however, neither hypothalamic clock genes nor plasma ACTH appear to drive the late-gestational increase in maternal corticosterone.

The second study tested the hypothesis that maternal adaptation to pregnancy involves changes in the hepatic expression of clock genes, which drive downstream shifts in the circadian expression of glucoregulatory genes. Maternal liver was collected at the same time-points as described for the initial study. Hepatic clock gene expression was substantially altered across pregnancy, most notably in late gestation when the circadian

rhythmicity of several clock genes was attenuated (e.g. 64% reduced amplitude for *Bmal1* on day 18). Similar reductions were observed in rhythmicity of the key glucoregulatory genes phosphoenolpyruvate carboxykinase 1 (*Pck1*), glucose-6-phophatase and glucokinase, and by day 18 *Pck1* was no longer rhythmic. Thus, marked adaptations in the liver clock occur during mouse pregnancy and may contribute to the altered circadian variation in glucoregulatory genes near term. We propose that the reduction of daily oscillations in glucose metabolism ensure a sustained supply of glucose to meet high fetal demands.

The third study hypothesised that pregnancy alters clock gene and downstream metabolic gene expression in white adipose tissue. Gonadal adipose tissue was collected from pregnant mice at the time-points described above. Adipose clock gene expression varied substantially across gestation, although the robust rhythmicity of expression was maintained throughout. In contrast, the circadian expression of the metabolic genes hormone sensitive lipase, adipocyte triglyceride lipase and lipoprotein lipase were lost with pregnancy onset. These findings demonstrate significant gestational adaptations in the adipose clock and a pregnancy-induced dissociation of adipose lipolytic and lipogenic genes from the circadian regulation of adipose clock genes during normal pregnancy.

Changes in the rhythmicity of maternal core body temperature (T_c) across pregnancy were also investigated as a possible mechanism driving pregnancy-induced changes in adipose clock gene expression. T_c was measured throughout gestation by intraperitoneal temperature loggers. T_c rhythm showed a 0.61°C decrease in mesor between days 6 and 18 and a 65% decrease in amplitude by term. These changes, however, were not linked to adipose clock gene expression during pregnancy.

Overall, these studies demonstrate for the first time that clock gene expression is markedly altered in key maternal tissues throughout normal mouse pregnancy. Furthermore, the effect of pregnancy on clock gene and downstream gene expression is highly tissue-dependent. In conclusion, pregnancy-induced changes in the circadian oscillations of both clock genes and metabolic genes are substantial and thus should be considered part of the normal maternal physiological adaptation to pregnancy.

Acknowledgements

I would firstly like to thank my supervisors, Brendan Waddell, Peter Mark and Caitlin Wyrwoll, for their invaluable guidance, constant enthusiasm, and mostly for the generous contribution of their time and knowledge.

I would also like to thank Michael Clarke for providing his time and facilities for LC-MS/MS analysis, as well as Hugh Barrett for his advice on cosinor analysis. Thanks also to Shane Maloney, Rachael Crew and Megan Ellyard for their help with optimising iButton surgeries. I would also like to acknowledge Cassandra Yap for the dissection and RNA extraction of the anterior hypothalamus samples.

My sincere thanks goes to several research and laboratory staff, including Jeremy Smith, Jessica Lewis, Dijana Tesic, Greg Cozens, Celeste Wale and Leah Attwood, who have helped me in many ways over the years and have been a pleasure to work with.

Thanks also to several teaching staff, including Kathy Sanders, Julie Hill, Caitlin Wyrwoll and Peter Mark, who provided me with the opportunity to teach undergraduate students, which has been a thoroughly rewarding experience.

I am grateful for the financial support of the Australian Postgraduate Award and the Ernst & Evelyn Havill Shacklock Top Up scholarship for the duration of my candidacy.

I am very thankful for the many friendships I have made during my PhD candidacy and for the wonderful working environment in Room 236. Special thanks to Rebekah Dawson, Rachael Crew, Cassandra Yap and Megan Ellyard, you have made this journey all the more worthwhile.

Thanks also to my proof readers Marcelle Williamson, Carole Williamson, and Rebekah Dawson.

Special thanks to my family, and particularly my parents and sister Marcelle, for their unconditional support and constant encouragement over the years. Your love and support over the last few months have been invaluable.

Lastly, I would like to thank my husband Luke, for his patience, endless support and constant encouragement. Your unwavering belief in me and ability to put things into perspective has helped me get where I am today.

Table of Contents

List of Figures

List of Tables

Thesis Format

General

This thesis is presented as nine chapters, the first four of which are the Introduction, Literature Review, Experimental Objectives and Materials and Methods. The results are presented as three experimental chapters of which all three have been published as original research papers. The final two chapters provide a general discussion of the overall findings and list all References cited in this thesis.

Language

The majority of this thesis is written according to Australian English. For chapters which are published however, language is kept according to specific Journal guidelines.

Presentation of data

The majority of data are presented in both graphical and tabular format. Figures are presented on individual pages, and where possible are placed directly after the text in which they are cited.

References

Published work referred to in the text is cited according to Harvard (UWA Science) format, with the author and year of publication included. Where the number of authors exceeds three, only the first three are mentioned, followed by et al. and the year of publication.

Abbreviations

°C	Degrees Celsius
11β-HSD	11-beta hydroxysteroid dehydrogenase enzyme
11-DHC	11-dehydrocorticosterone
ACTH	Adrenocorticotropic hormone
Actβ[1]	Beta actin
ANOVA	Analysis of variance
ANS	Autonomic nervous system
BLAST	Basic Local Alignment Search Tool
Bmal1	Brain and muscle *Arnt* like protein 1
CBG	Corticosterone binding globulin
cDNA	complementary DNA
CKIε	Casein kinase I epsilon
CLC	Cardiotrophin-like cytokine
Clock	Circadian locomotor output cycles kaput
Crh	Corticotropin releasing hormone
Cry	Cryptochrome
D	Day of pregnancy
Dbp	Albumin-D-site binding protein
dd H_2O	Double deionised water
DEPC	Diethylpyrocarbonate
DNA	Deoxyribonucleic acid
dNTPs	dinucleotide triphosphate

[1] This and all other gene abbreviations follow the convention of being italicised and having the only the first letter capitalised. The corresponding proteins are capitalised and are not italicised. These protein abbreviations are not included in this abbreviation list.

EDTA	Ethylenediamine tetra-acetic acid
g	Relative centrifugal force
G6Pase	Glucose-6-phosphatase
Gk	Glucokinase
Glut2	Glucose transporter 2
GR	Glucocorticoid receptor
GRE	Glucocorticoid response element
Gys2	Glycogen synthase 2
h	hour(s)
H_2O	Water
HPA	Hypothalamic-pituitary-adrenal
Hprt	Hypoxanthine-guanine phosphoribosyltransferase
IS	Internal standard
LC	Liquid chromatography
LC-MS/MS	Liquid chromatography tandem mass spectrometry
Lipe	Hormone sensitive lipase
Lpl	Lipoprotein lipase
LSD	Least significant difference
M	Molar = moles/litre
M-MLV	Moloney Murine leukemia virus
$MgCl_2$	Magnesium chloride
min	minute(s)
mRNA	messenger ribonucleic acid
n	Number of samples
ng	Nanograms
nm	Nanometres
NSB	Non-specific binding
P	Probability

Pck1	Phosphoenolpyruvate carboxykinase 1
PCR	Polymerase chain reaction
Per	Period
Pgc1α	Peroxisome proliferator-activated receptor gamma coactivator 1 alpha
Pk	Pyruvate kinase
PL	Placental lactogen
Pnpla2	Adipocyte triglyceride lipase
Ppar	Peroxisome proliferator activated receptors
Ppia	Peptidylprolyl isomerase A
PR	Progesterone receptor
PVN	Paraventricular nucleus
Pygl	Glycogen phosphorylase
r	Correlation coefficient
r^2	Coefficient of determination
Rev-erbα	Transcription factor reverse erythroblastosis virus α
RNA	Ribonucleic acid
RNase	Ribonuclease
Rorα	Retinoic acid receptor-related orphan receptor α
RT-qPCR	Quantitative reverse transcription polymerase chain reaction
SCN	Suprachiasmatic nuclei
Sdha	Succinate dehydrogenase complex, subunit A
sec	second(s)
SEM	Standard error of the mean
T_c	Core body temperature
Tbp	TATA box binding protein
UPLC	Ultra high performance liquid chromatography
W	Watts
ZT	Zeitgeber Time

Publications arising from this work

Wharfe, MD, Mark, PJ, Wyrwoll, CS, Smith, JT, Yap, C, Clarke, MW & Waddell, BJ 2016, 'Pregnancy-induced adaptations of the central circadian clock and maternal glucocorticoids', *Journal of Endocrinology*, vol. 228, no. 3, pp. 135-147 (Chapter 5)

Wharfe, MD, Wyrwoll CS, Waddell, BJ & Mark, PJ, 'Pregnancy-induced changes in the circadian expression of hepatic clock genes: implications for maternal glucose homeostasis', *American Journal of Physiology – Endocrinology and Metabolism*, vol. 311, no.3, pp. E575-E586 (Chapter 6)

Wharfe, MD, Wyrwoll CS, Mark, PJ & Waddell, BJ 'Pregnancy suppresses the daily rhythmicity of core body temperature and adipose metabolic gene expression in the mouse', *Endocrinology*, vol.157, no.3, pp. 3320-3331 (Chapter 7)

Chapter 1 Introduction

Maternal physiology is substantially adapted during pregnancy to enable the mother to provide sufficient nutrition to her developing fetus whilst concurrently maintaining her own wellbeing. These reversible modifications are widespread; cardiovascular, respiratory and renal systems are altered as well as the hypothalamic-pituitary-adrenal (HPA) axis, which regulates glucocorticoid release. During pregnancy, the metabolic requirements of the developing fetus change, and as such maternal metabolism is adapted early in pregnancy in anticipation of the high demand for nutrients during the period of rapid fetal growth in late gestation. Modifications to food intake and to the metabolism of glucose and lipids ensure there are sufficient energy stores available for use by the fetal-placental unit when needed.

Under normal conditions, circadian rhythms are integral for physiology to ensure that cellular processes occur at the optimal time of day and are coordinated to the 24-h light-dark cycle. In mammals, circadian rhythms are driven by a hierarchy of molecular clocks located throughout the body. Time-of-day information is transmitted via the retina to the central clock located in the suprachiasmatic nucleus (SCN) of the anterior hypothalamus. The SCN acts to coordinate peripheral clocks located in a range of tissues, such as the liver and adipose tissue, via neuro-humoral systemic cues that include glucocorticoids.

Circadian rhythms are driven at the molecular level by clock genes, which are rhythmically expressed within nearly every cell of the body over a period of 24-h, via a series of transcriptional-translational feedback loops. Clock genes are transcription factors for clock-controlled genes directly involved in processes such as metabolism, and thereby drive the rhythmic expression of metabolic genes. Consequently, up to 20% of transcripts expressed in any tissue are rhythmic. The importance of clock genes in metabolic function is apparent from the widespread metabolic aberrations of clock gene knock-out rodent models.

Despite the crucial role for clock genes in metabolic homeostasis, it is currently unclear how clock gene expression in central and peripheral tissue clocks is altered across pregnancy. Although recent studies show that pregnancy significantly impacts maternal clock gene expression, this previous work does not explore the changes across

pregnancy or the impact of altered clock gene expression on downstream metabolic pathways. Accordingly, the studies in this thesis are the first to determine whether the major metabolic adaptations during pregnancy involve marked shifts in maternal clock gene expression. Thus, the overall objectives of this thesis were to investigate changes in clock gene expression in the SCN, liver and adipose tissue during normal mouse pregnancy and to determine associated downstream effects on the circadian expression of tissue-specific genes important for maternal metabolism.

Pregnancy-induced changes in clock gene expression were first investigated in the SCN (Chapter 5), since the central clock is critical for whole body homeostasis. This was considered an important starting point as changes to the central clock may impact peripheral tissue clock function during pregnancy. This study also addressed the hypothesis that adapted clock gene expression in the SCN drives altered HPA axis activity during gestation.

The focus for the second study (Chapter 6) shifted to the liver peripheral clock since adaptations to liver function during pregnancy are critical for the supply of glucose, as the principal energy substrate, to the fetus. Thus the aim of this experiment was to assess whether changes in hepatic clock gene expression accompany maternal metabolic adaptations during pregnancy. Moreover, changes in the circadian variation of important hepatic glucoregulatory genes across pregnancy were also measured to determine whether alterations in clock gene expression drive maternal adaptations in glucose metabolism.

Adipose tissue plays an important role in metabolic adaptations to pregnancy due to its function as an energy store and the dynamic nature of energy needs across gestation. As such, the final study presented in this thesis (Chapter 7) investigated whether clock gene expression in white adipose tissue was altered across gestation and if such changes were associated with altered circadian rhythmicity of genes involved in lipid metabolism across pregnancy. Furthermore, altered rhythms in maternal core body temperature across pregnancy were explored as a potential mechanism driving changes in adipose tissue clock gene expression.

Collectively, the studies in this thesis comprehensively characterised the pregnancy-induced adaptations of maternal tissue clocks in mice for the first time. These data

highlight the central role of clock genes in maternal adaptations to pregnancy and provide a strong basis for future studies on pregnancy complications.

Chapter 2 Literature Review

2.1 C57Bl/6J mouse model

The common laboratory mouse (species *Mus musculus*) has been bred specifically for scientific research, with the C57Bl/6J strain being the most commonly used. The mouse is nocturnal, with most activity and feeding occurring during the dark period. Its short gestational length (~ 19-20 days), early onset of puberty, which occurs between five and eight weeks of age, and large litter size (~ 6-10 pups) makes it an ideal animal model for pregnancy studies (Rugh 1968).

2.1.1 Estrous cycle

The female mouse exhibits a 4-5 day estrous cycle which consists of four phases: pro-estrus, estrus, diestrus I and II. Proestrus equates to the pre-ovulatory day during which estradiol levels increase (Walmer et al. 1992). On the night of proestrus, the luteinizing hormone (LH) surge results in ovulation (Parkening, Collins & Smith 1982). Estradiol levels remain elevated throughout the morning of estrus before returning to basal levels by the afternoon and remaining low throughout diestrus I. In contrast, progesterone levels begin to rise on the morning of diestrus I and continue to do so until the morning of diestrus II. Progesterone levels decline thereafter and remain low for remainder of the cycle (Walmer et al. 1992). The female is only receptive to mating on the night of proestrus when ovulation occurs.

2.1.2 Pregnancy

2.1.2.1 Luteotrophins and progesterone

If mating occurs, cervical stimulation results in the production of twice-daily surges of prolactin from the anterior pituitary, which provides the initial trophic support, in combination with FSH, for the corpus luteum (CL) to prevent its regression (Choudary & Greenwald 1969). In mice, the CL is required to produce progesterone throughout the entire pregnancy. Prolactin is released in a semi-circadian manner with peaks in the early morning (0100-0900 h) and in the late afternoon (1500-2100 h), both of which are measurable throughout the first 9 to 10 days of gestation (Barkley, Bradford & Geschwind 1978; Soares et al. 1991).

By mid-pregnancy the major trophic support for the CL comes from the placenta, and from this stage ablation of the pituitary does not result in pregnancy loss (Strauss, Martinez & Kiriakidou 1996). The luteotrophic support includes mouse placental lactogen (mPL) 1 and 2, which are produced by trophoblastic giant cells. The concentration of mPL1 peaks on day 10, begins to decline on day 11 and remains low for the remainder of gestation, whilst that of mPL2 increases rapidly until day 14 and remains high until the end of pregnancy (Soares, Colosi & Talamantes 1982; Ogren et al. 1989). The placental lactogens exert their physiological effects by binding to the same CL membrane receptor (Galosy & Talamantes 1995). This luteotrophic support promotes growth of CL which reaches its maximum size on days 15 to 16. Accordingly, progesterone levels continue to rise throughout pregnancy with a transient increase around the time of implantation (day 5) before reaching a maximum on days 15 to 16 of gestation. From approximately day 17, there is a prepartum decline in progesterone (Barkley, Geschwind & Bradford 1979; Holinka, Tseng & Finch 1979), which coupled with increasing circulating estradiol, is believed to drive the reappearance of pituitary prolactin secretion prior to parturition (Grattan & Averill 1990).

2.1.2.2 Estrogens

The CL is the major source of estrogens (estradiol and estrone) during mouse gestation, and production is regulated by the availability of its androgen precursor which is converted first to estrone by P450 aromatase and then from estrone to estradiol by 17β-hydroxysteroid dehydrogenase-7 (Bowen-Shauver & Gibori 2003). Estradiol levels remain low for the first half of gestation, with exception of a brief surge in secretion on day 4 to 5 of pregnancy which is essential for implantation (Rugh 1968; McCormack & Greenwald 1974). Levels continue to increase after mid-gestation, until they reach a plateau from about day 17 (Barkley, Geschwind & Bradford 1979). During the first half of gestation the androgen precursors are produced by the ovarian follicles, and estrogen synthesis is under the regulation of LH and FSH. At mid-pregnancy, the source of androgens changes to the placenta due to the rapid decline in LH levels. Placental androgens are secreted into maternal circulation and converted to estrogens in the CL. The rising estradiol levels from mid-gestation are driven by increased androgen supply from the placenta (Barkley et al. 1977; Barkley, Geschwind & Bradford 1979).

2.1.2.3 Implantation and placentation

Implantation of the blastocyst into the progesterone-primed endometrium takes place on the night of day 5 and is dependent upon the estradiol surge. The transformation of fibroblastic stromal cells in preparation for pregnancy is known as decidualisation and is initiated by implantation of the blastocyst (Abrahamsohn & Zorn 1993). Initially, the mouse embryo develops a choriovitelline (or yolk sac) placenta, but by approximately day 10.5 of gestation, the definitive chorioallantoic placenta becomes functional (Georgiades, Ferguson-Smith & Burton 2002; Malassine, Frendo & Evain-Brion 2003).

2.1.3 Parturition

Parturition in our cohort of C57Bl/6J mice takes place on day 19-20 and like other nocturnal species, occurs predominantly during the light phase (Lincoln & Porter 1976). This circadian timing of birth requires an intact maternal SCN (Reppert et al. 1987) and may be 'gated' by circadian signals such as oxytocin (Olcese 2012).

2.1.4 Lack of melatonin in C57Bl/6J mice

In most mammalian species, melatonin is a rhythmically secreted hormone involved in the daily sleep/wake cycle and is synthesised from serotonin in the pineal gland. Serotonin is first converted to N-acetylserotonin by arylalkylamine N-acetyltransferase (AA-NAT) and then to melatonin by hydroxyindole-O-methyltransferase (HIOMT) (Kennaway & Wright 2002). AA-NAT activity is robustly rhythmic resulting in rhythmic melatonin synthesis (Klein et al. 1997). Surprisingly, all common laboratory mice, with the exception of the CBA and C3H strains, are melatonin deficient (Ebihara et al. 1986; Goto et al. 1989) due to mutations in AA-NAT (Roseboom et al. 1998) and HIOMT (Kennaway & Wright 2002). Importantly, the absence of melatonin appears to have no impact on behavioural or physiological rhythm generation in C57Bl/6J mice (Stehle, von Gall & Korf 2003).

2.2 Maternal adaptations to pregnancy

Pregnancy is arguably the most physiologically challenging state that an organism encounters across the life cycle. During pregnancy the mother undergoes a vast array of physiological changes to enable her to meet the requirements of her developing fetus, whilst also preparing for lactation and maintaining her own tissue function. The changes that take place are widespread, with the majority of maternal tissues being significantly modified. These adaptations extend from marked central modifications in brain function to fundamental changes in peripheral tissues including the liver and adipose tissue. Insufficient or dysregulated adaptations of maternal physiology can lead to serious pregnancy complications, as well as adverse developmental programming outcomes in adult offspring.

2.2.1 General adaptations

Coordinated physiological adaptations occur in the majority of maternal organ systems during pregnancy including: increased blood volume and cardiac output to ensure sufficient maternal-fetal exchange of nutrients and metabolic waste (Scott 1972; Robson et al. 1989); hyperplasia of pancreatic β-cells to increase production of maternal insulin (Nielsen et al. 1999); increased alveolar ventilation to meet the augmented respiratory requirements of the growing maternal and fetal tissue mass (Bonica 1973); and adjustments to the immune system to prevent immunological rejection of the developing fetus (Luppi 2003). Many of these changes are driven, at least in part, by placental production of gestational hormones including estrogen and progesterone (Weissgerber & Wolfe 2006).

2.2.2 Metabolic adaptations

Pregnancy imposes considerable metabolic challenges for the mother and as such is characterised by major metabolic adaptations. These modifications to maternal metabolism are designed to support the initial demands of embryonic/fetal development and then, later in pregnancy, rapid fetal growth. As a consequence, pregnancy may be considered to have two distinct metabolic phases (Hamosh et al. 1970; Knopp et al. 1973). The first of these phases spans the initial two thirds of gestation, trimesters one and two in humans and up to days 10 to 12 in rodents (Knopp et al. 1973; Metcalfe, Stock & Barron 1988). During this period the mother is hyperphagic (Weizenbaum,

Kenney & Adler 1979), yet fetal nutrient demand remains low, resulting in a positive energy balance. This enables enhanced fat storage in maternal adipose tissue in anticipation of the subsequent high fetal demand in late gestation (Herrera et al. 1988; Palacin et al. 1991) (refer to section 2.3.5.2 for details of the lipogenic pathway). The resultant net anabolism is primarily mediated by an increase in insulin sensitivity of peripheral tissues in early gestation (Munoz, Lopez-Luna & Herrera 1995; Gonzalez et al. 2002; Ramos et al. 2003) and is further enhanced by pregnancy-induced leptin resistance. The latter ensures that maternal appetite is not supressed despite the increase in leptin levels in parallel with growing fat stores (Henson & Castracane 2000; Herrera et al. 2000; Grattan, Ladyman & Augustine 2007). This period of 'facilitated anabolism' is primarily driven by estradiol and progesterone (Costrini & Kalhkhoff 1971).

The rapid fetal growth during the final third of pregnancy requires that the mother switch to a catabolic condition to meet high fetal demand. Requirements are greatest for glucose and amino acids, resulting in the concurrent development of maternal hypoglycaemia and hypoaminoacidemia (Herrera, Knopp & Freinkel 1969; Herrera et al. 1985). Enhanced breakdown of maternal fat stores (refer to Section 2.3.5.2 for details of the lipolytic pathway) (Knopp, Herrera & Freinkel 1970; Martin-Hidalgo et al. 1994) and the subsequent mobilisation of fatty acids, results in a state of hypertriglyceridemia (Montes et al. 1978). This is beneficial, since fatty acids and glycerol become a source of energy for the mother, which can be rapidly used under fasting conditions for gluconeogenesis (refer to Section 2.3.5.1) and ketone body synthesis, to minimise glucose utilisation (Herrera 2000). Additionally, the development of insulin resistance during this catabolic phase ensures most of the available glucose is free for use by the fetal-placental unit (Leturque et al. 1980; Knopp et al. 1970). Placental lactogen, progesterone, prolactin and glucocorticoids are the primary mediators of this period of catabolism (Kalkhoff, Richardson & Beck 1969; Landgraf et al. 1977; Kalkhoff, Kissebah & Kim 1978; Sutter-Dub et al. 1981).

2.2.3 Adaptations of the hypothalamic-pituitary-adrenal (HPA) axis

2.2.3.1 The HPA axis

The HPA axis regulates circulating levels of glucocorticoids, a group of steroid hormones crucial for not only the stress response but also metabolism (Munck & Koritz 1962; Vegiopoulos & Herzig 2007; Jitrapakdee 2012). Various stimuli, including stress

and circadian inputs, induce the secretion of corticotropin releasing hormone (CRH) from the hypothalamic paraventricular nucleus (PVN) into the portal blood vessels (Figure 2.1). Via this circulation, CRH reaches the anterior pituitary where it stimulates the secretion of adrenocorticotropic hormone (ACTH) from corticotroph cells. In turn, ACTH stimulates adrenocortical secretion of glucocorticoids (principally cortisol in humans and corticosterone in rodents) from the adrenal zona fasiculata. Once released into the circulation glucocorticoids can exert their effects via glucocorticoid receptors within target tissues (Baxter & Rousseau 1979; Jacobson 2005). Glucocorticoids are also capable of regulating their own release via negative feedback effects at the level of the PVN where they inhibit CRH, and at the level of the pituitary, where they inhibit ACTH (Jones, Hillhouse & Burden 1977; Dallman et al. 1987). Glucocorticoid secretion also exhibits a circadian rhythm (refer to Section 2.3), whereby levels are highest just before the onset of the active phase (morning in humans and evening in rodents) and then decrease to reach minimum levels during the inactive phase (Moore & Eichler 1972).

2.2.3.2 The effect of pregnancy on the HPA axis

Under basal (i.e. unstressed) conditions, pregnancy in both humans and rodents (rats and mice) is characterised by enhanced activity of the HPA axis after mid-gestation (Patrick et al. 1980; Atkinson & Waddell 1995; Douglas et al. 2003). Late in gestation the resultant increase in glucocorticoid levels may be important for mobilisation of maternal energy stores to meet the high fetal demand (Knopp et al. 1973; Metcalfe, Stock & Barron 1988). Late pregnancy is also characterised by suppression in HPA axis responses to stressors (Barlow, Morrison & Sullivan 1975; Brunton 2010). This is understood to be a protective adaptation to reduce exposure of the fetus to elevated levels of maternal glucocorticoids, which can have both immediate and long-term (i.e. programming) detrimental effects (Harris & Seckl 2011). This decreased responsiveness of the HPA axis may be explained by several mechanisms, the most likely being increased endogenous inhibitory opioid tone induced by actions of allopregnanolone, a progesterone metabolite (Brunton et al. 2009; Brunton 2010).

Pregnancy can also influence the metabolism of corticosterone. For example, in late gestation in the mouse there is an increase in plasma levels of corticosterone binding globulin (CBG) (Gala & Westphal 1967; Douglas et al. 2003) probably driven by

increasing estradiol concentrations (Uesa, Seal & Doe 1965). This increase in CBG is likely to reduce the metabolic clearance rate (MCR) of corticosterone by limiting its access to metabolizing tissues. Indeed, Waddell and Atkinson (1994) showed that the MCR of corticosterone relative to body weight falls during late gestation in the rat. Placental transport of corticosterone also changes across pregnancy. Glucocorticoid action is regulated by the 11β-hydroxysteroid dehydrogenase enzymes (11β-HSD1 and 2), which catalyse the interconversion of active corticosterone to inert 11-dehydrocorticosterone (11-DHC) (Waddell et al. 1998). For the majority of pregnancy, high placental expression of 11β-HSD2 prevents placental transport of corticosterone. Late gestation, however, is characterised by a fall in the synthesis and activity of 11β-HSD2 and a concurrent increase in 11β-HSD1 such that transplacental passage of corticosterone is increased (Brown et al. 1996; Mark et al. 2009). These changes in enzyme expression may influence maternal plasma 11-DHC concentration, however, this has not been measured in late gestation.

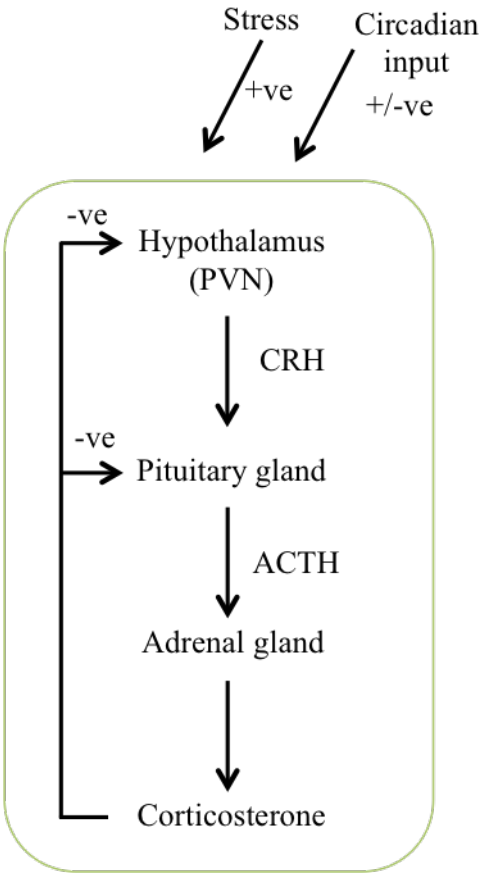

Figure 2.1 Schematic representation of the hypothalamic-pituitary-adrenal axis in rodents. Stress and circadian signals induce the secretion of CRH from the hypothalamic PVN, which stimulates the release of ACTH from the anterior pituitary gland. ACTH, in turn, stimulates the secretion of corticosterone from the adrenal gland, which has negative feedback effects at both the PVN and pituitary gland.

2.3 Circadian rhythms

The timing of physiological processes in mammals is regulated by an internal timing system, which results in nearly all aspects of physiology and behaviour displaying circadian [circa (about) diem (a day)] rhythms. These daily oscillations are seen in a multitude of processes at the molecular, cellular, organ, and whole organism levels. For example, glucocorticoid secretion, the sleep/wake cycle, body temperature, and metabolism all exhibit strong circadian rhythms (Mohawk, Green & Takahashi 2012).

Circadian rhythms are thought to have evolved to coordinate physiological processes with the 24-h light-dark cycle. This photoentrainment enables animals to predict and adapt their physiology and behaviour in order to optimise the timing of various processes. In the absence of all external environmental cues true circadian rhythms free run, with their phase lengthening to ~ 26.1 hours (Aschoff 1984). Accordingly, zeitgebers, or environmental cues such as light and temperature, play a vital role in keeping circadian phases regular and, in turn, ensuring an appropriate temporal relationship with the outside world (24-h).

Disruption of circadian coordination demonstrates the importance of circadian rhythms for maintenance of 'normal' physiology. Numerous studies have linked circadian irregularities, such as rotating shift work, to a wide range of pathological conditions including sleep, endocrine and metabolic disorders (including obesity), and cancer (Gery & Koeffler 2010; Delezie & Challet 2011; Eckel-Mahan et al. 2012; Landgraf, Shochtak & Oster 2012). Furthermore, there is emerging interest in the effects of circadian disruption during pregnancy on the long-term health outcomes of offspring (refer to Section 2.4).

In mammals, there is a hierarchy of circadian clocks located throughout the body (peripheral clocks), which is coordinated by the central clock in the suprachiasmatic nucleus (SCN) of the anterior hypothalamus (Rusak & Zucker 1979; Ralph et al. 1990) (Figure 2.2). Initially it was believed that the SCN was one of few tissues capable of generating circadian rhythms, but it is now well established that autonomous clocks are located in almost every cell of the body (Balsalobre, Damiola & Schibler 1998; Yoo et al. 2004).

2.3.1 The central clock

The central clock, located within the SCN of the anterior hypothalamus, is composed of approximately 20,000 neurons which exhibit autonomous circadian oscillations and together form a synchronised network of rhythmicity (Lowrey & Takahashi 2000). The robust circadian rhythm of the central clock acts to coordinate the body's multiple peripheral clocks; keeping them in an appropriate temporal relationship with one another, and ensuring synchrony of various metabolic processes (Yoo et al. 2004).

The central clock is entrained to the natural light-dark cycle via the retina, as light is the sole zeitgeber for the SCN. Electrical input signals pass from melanopsin-containing retinal ganglion cells through the retinohypothalamic tract where they terminate in the anterior hypothalamus (Gooley et al. 2001; Lucas et al. 2001; Do & Yau 2010). As a result, intrinsic SCN factors, vasoactive intestinal polypeptide and gastrin-releasing peptide, activate and synchronise SCN neurons to coordinate central rhythmicity (Maywood et al. 2006). Shifts in light-dark cycles can directly alter gene expression within the SCN and this subsequently results in rapid adaptation (via neural, behavioural and hormonal pathways) of whole body rhythms to the altered schedule (Kalsbeek et al. 2006) (refer to Section 2.3.4.2).

2.3.2 Peripheral clocks

Peripheral, non-neuronal tissues contain the molecular machinery necessary for circadian oscillation (refer to Section 2.3.3) (King et al. 1997; Tei et al. 1997), although the timing of rhythms may be up to 4 hours later than that of the SCN (Yamazaki et al. 2000). These peripheral clocks have been well characterised in the liver (Yamamoto et al. 2004), adipose tissue (Ando et al. 2005; Zvonic et al. 2006), kidney (Zuber et al. 2010), heart (Young, Razeghi & Taegtmeyer 2001), and adrenal gland (Bittman et al. 2003; Torres-Farfan et al. 2006). *In vitro*, peripheral cells are capable of circadian gene expression despite the absence of any SCN influence, consistent with the presence of endogenous peripheral clocks (Balsalobre, Damiola & Schibler 1998; Yamazaki et al. 2000; Yoo et al. 2004). Indeed, *in vivo* peripheral clocks can be entrained by alternative non-photic zeitgebers such as restricted feeding, which uncouples them from the SCN (Damiola et al. 2000; Stokkan et al. 2001; Hara et al. 2001). The physiological importance of peripheral clocks is illustrated by the high number of rhythmically

expressed genes that are responsible for vital tissue-specific functions, including most aspects of metabolism.

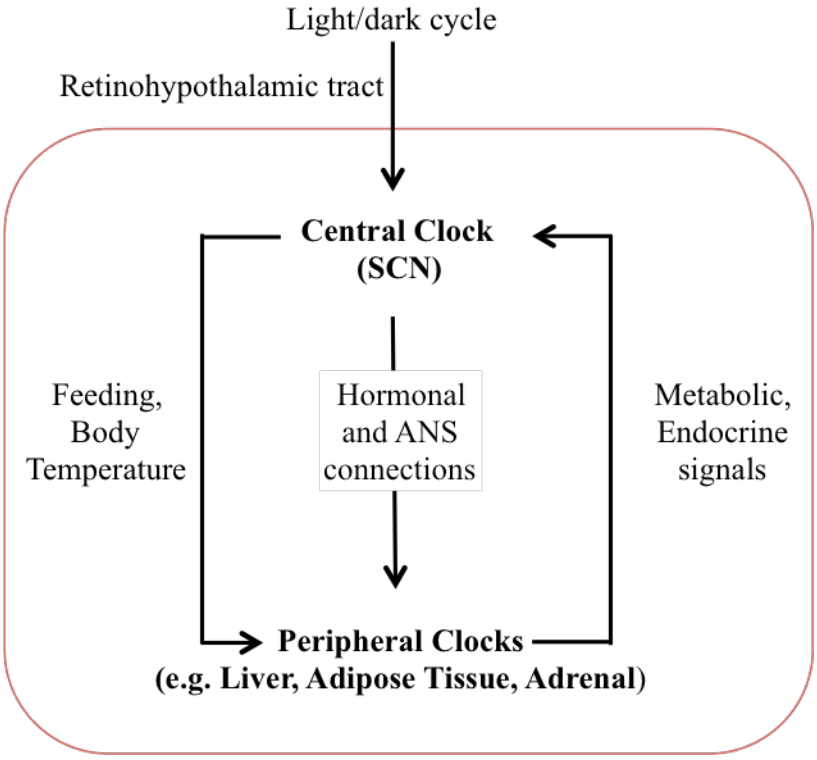

Figure 2.2 Schematic representation of the hierarchy of circadian clocks in mammals. The central clock receives time-of-day information and acts to coordinate circadian rhythms in peripheral clocks via hormonal, neural and behavioural pathways. Afferent projections to the central clock provide metabolic and endocrine information from peripheral clocks.

2.3.3 Molecular machinery of circadian clocks

Circadian rhythms are generated by a number of interacting positive and negative feedback loops of gene and protein expression (Figure 2.3). In the core circadian oscillatory loop, basic-helix-loop-helix (bHLH) PER-ARNT-SIM (PAS) family members, brain and muscle ARNTL-like protein 1 (BMAL1) and circadian locomotor output cycle kaput (CLOCK) form a protein heterodimer (BMAL1:CLOCK). This heterodimer translocates into the nucleus and activates transcription of the *Period* (*Per*) *1*, *Per 2*, *Cryptochrome* (*Cry*) *1* and *Cry 2* genes by binding to E box (5'–CACGTG–3') and E-box-like promoter sequences in their promoter regions (Reppert & Weaver 2002). The resultant increase in levels of *Per* and *Cry* mRNA is followed several hours later by an accumulation of PER and CRY proteins which form complexes in the cytoplasm, peaking at the end of the light phase. These protein complexes translocate into the nucleus where they associate with the CLOCK:BMAL1 heterodimer to inhibit its activity and thereby decrease transcription of *Per* and *Cry* genes (Figure 2.3).

In addition to CRY proteins forming a complex with PER proteins to repress the transcription of BMAL1:CLOCK, they also appear to regulate the activity of the heterodimer directly. The CRY proteins prevent phosphorylation of BMAL1 and CLOCK and inhibit the subsequent translocation of the heterodimer into the nucleus to drive transcription of *Per* and *Cry* genes (Dardente et al. 2007). The resultant fall in PER and CRY levels removes their negative feedback effects and the cycle is reinitiated (Reppert & Weaver 2002). The turnover of PER and CRY proteins is regulated by post-translational modifications, including the phosphorylation of the PER proteins by casein kinase I epsilon and delta and regulation of CRY protein by E3 ubiquitin ligase complexes (Akashi et al. 2002; Eide et al. 2005; Yoo et al. 2013). In this manner, the timing of the feedback cycle is regulated to approximately 24 hours.

Although functional, the core circadian oscillatory loop is unstable unless influenced by accessory loops. One of these accessory feedback loops drives rhythmic expression of *Bmal1* via two transcription factors. Thus, reverse erythroblastosis virus α (*Rev-erbα*) negatively regulates *Bmal1* transcription (Preitner et al. 2002), whereas retinoic acid receptor-related orphan receptor α (*Rorα*) stimulates it (Sato et al. 2004) (Figure 2.3). Both transcription factors act by binding to the retinoic-acid-receptor-related orphan receptor response element (RORE) proximal to the *Bmal1* promoter region (Ueda et al.

2005), therefore creating an alternating occupancy of the promoter to drive its rhythmic expression. In a similar manner, *Rev-erbα* also regulates the rhythmic expression of *Clock*, but this occurs to a lesser extent than for *Bmal1* (Preitner et al. 2002).

The core oscillators also confer rhythmicity on sets of downstream clock-controlled genes such as nuclear receptors, which are directly involved in the regulation of downstream metabolic pathways (Yang et al. 2006; Grimaldi et al. 2010; Lamia et al. 2011). Importantly, nuclear receptors such as the peroxisome proliferator-activated receptors (PPARs), the glucocorticoid receptor (GR), and PPARγ coactivator-1α (PGC1α) are themselves able to regulate clock function (Canaple et al. 2006; Liu et al. 2007; So et al. 2009). In this manner, signals of metabolic status conveyed by these nuclear receptors influence rhythmicity to ensure physiological functions occur at very specific and appropriate times of day.

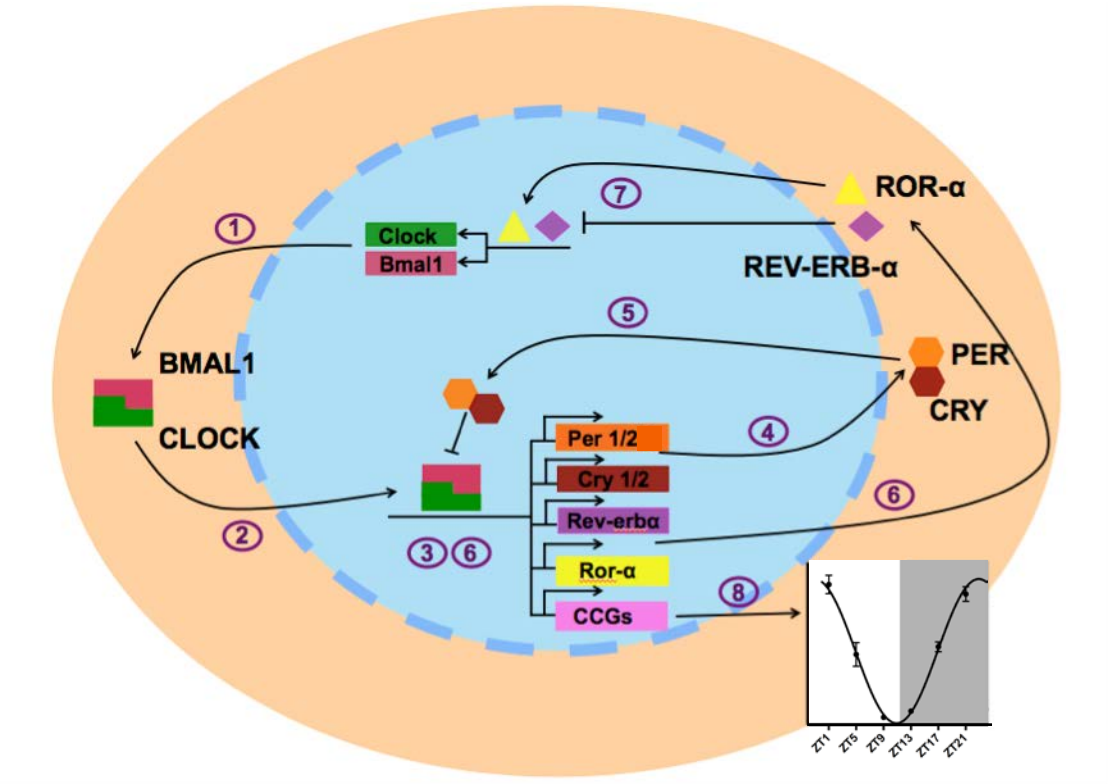

Figure 2.3 Schematic representation of the molecular clock machinery that drives circadian rhythms in central and peripheral clocks. The molecular mechanism involves several interacting positive and negative transcriptional and translational feedback loops. For detailed description see Section 2.3.3. CCGs: clock-controlled genes. ⟶ Activation ⊣ Inhibition

2.3.4 Regulation of central and peripheral clocks

2.3.4.1 Afferent signals to the SCN

Although light is the only zeitgeber for the central clock, the SCN receives metabolic and endocrine information from the periphery via numerous routes. Firstly, visceral information from peripheral tissues is transmitted to the SCN by the autonomic nervous system (ANS) via the nucleus tractus solitarius (Buijs et al. 2014). Secondly, while some hormones can cross the blood brain barrier and influence the SCN directly, information about those that cannot are relayed to the central clock from the ventromedial arcuate nucleus, and the intergeniculate leaflet via reciprocal connections between brain regions (Yi et al. 2006; Saderi et al. 2013). Finally, due to an absence of glucocorticoid and mineralocorticoid receptors in the SCN (Rosenfeld et al. 1988; Balsalobre et al. 2000), information about glucocorticoid levels is transmitted to the central clock via neural connections from other brain regions including the raphe nucleus (Amir et al. 2004; Lamont et al. 2005; Malek et al. 2007).

2.3.4.2 Efferent signals from the SCN

The phase of peripheral timekeepers *in vivo* is predominantly synchronised by both direct and indirect signals from the SCN. Although the genetic and biochemical mechanisms of synchronisation are complex and have not yet been fully elucidated, each peripheral oscillator is entrained to a specific adaptive relationship with the SCN that is determined by physiological requirements (Yamazaki et al. 2000). There are three pathways by which the SCN synchronises peripheral tissues and therefore physiological processes; these are neural, hormonal and behavioural.

The central clock coordinates peripheral oscillators such as the liver, adipose tissue and adrenal gland through both the parasympathetic and sympathetic pathways of the ANS (Bamshad et al. 1998; La Fleur et al. 2000; Ishida et al. 2005). In this way, light and circadian signals from the SCN can directly drive glucocorticoid synthesis from the adrenal gland without activation of the classic HPA axis (Ishida et al. 2005) (Figure 2.4). Simultaneously, the SCN is able to control the sensitivity of the adrenal gland to ACTH via sympathetic innervation and in this manner directly influences glucocorticoid secretion (Buijs et al. 1999; Oster et al. 2006; Ulrich-Lai, Arnhold & Engeland 2006).

Glucocorticoids themselves play an important role in the complex mechanism of communication with peripheral pacemakers (Le Minh et al. 2001; Pezuk et al. 2012). Dexamethasone, a synthetic glucocorticoid hormone analog, has been found to phase shift gene clock expression within the liver without having an effect on gene expression in the neurons of the SCN (Balsalobre et al. 2000). This glucocorticoid effect is most likely mediated via glucocorticoid response elements within promoter regions of clock genes such as *Per1* and *Per2* (Yamamoto et al. 2005; Reddy et al. 2007; So et al. 2009). That said, glucocorticoid hormones are unlikely to be the sole zeitgeber for peripheral tissues because mRNA cycles of clock genes in the liver show the same phase of accumulation in wild-type and mutant (GRAlfpCre) mice which contain a hepatocyte-specific inactivation of the glucocorticoid receptor gene (Balsalobre et al. 2000).

Furthermore, local hypothalamic secretion of humoral factors, such as transforming growth factor-α, cardiotrophin-like cytokine and prokineticin 2, driven by the SCN, is thought to contribute to the transmission of behavioural circadian rhythms such as locomotor activity by binding to receptors expressed in SCN output target cells around the third ventricle (Kramer et al. 2001; Cheng et al. 2002; Kraves & Weitz 2006).

Finally, the SCN regulates behavioural cycles of rest and activity in mammals via direct neural connections to other centres in the brain and via release of melatonin, and therefore indirectly controls peripheral oscillators through feeding behaviour. As feeding is the most potent zeitgeber for peripheral tissues, the SCN has control over these endogenous clocks by controlling overall feeding rhythms and behaviour (Damiola et al. 2000; Stokkan et al. 2001; Salgado-Delgado et al. 2013). Moreover, the central clock is able to influence core body temperature by direct input into thermoregulatory brain regions and via regulation of the rest/activity cycle. Core body temperature exhibits circadian variation and contributes to the entrainment of clock gene expression in peripheral tissues likely through the transcription factor heat-shock factor 1 (Brown et al. 2002; Buhr, Yoo & Takahashi 2010; Saini et al. 2012; Oishi et al. 2013).

Ultimately, temporal communication between the SCN and peripheral clocks is a complex combination of the three pathways described above. Indeed, a recent study looking at the contribution of each of these SCN outputs on peripheral tissue

rhythmicity found that simultaneous disruption of glucocorticoid and feeding rhythms were required for loss of clock gene rhythmicity within the liver (Su et al. 2016).

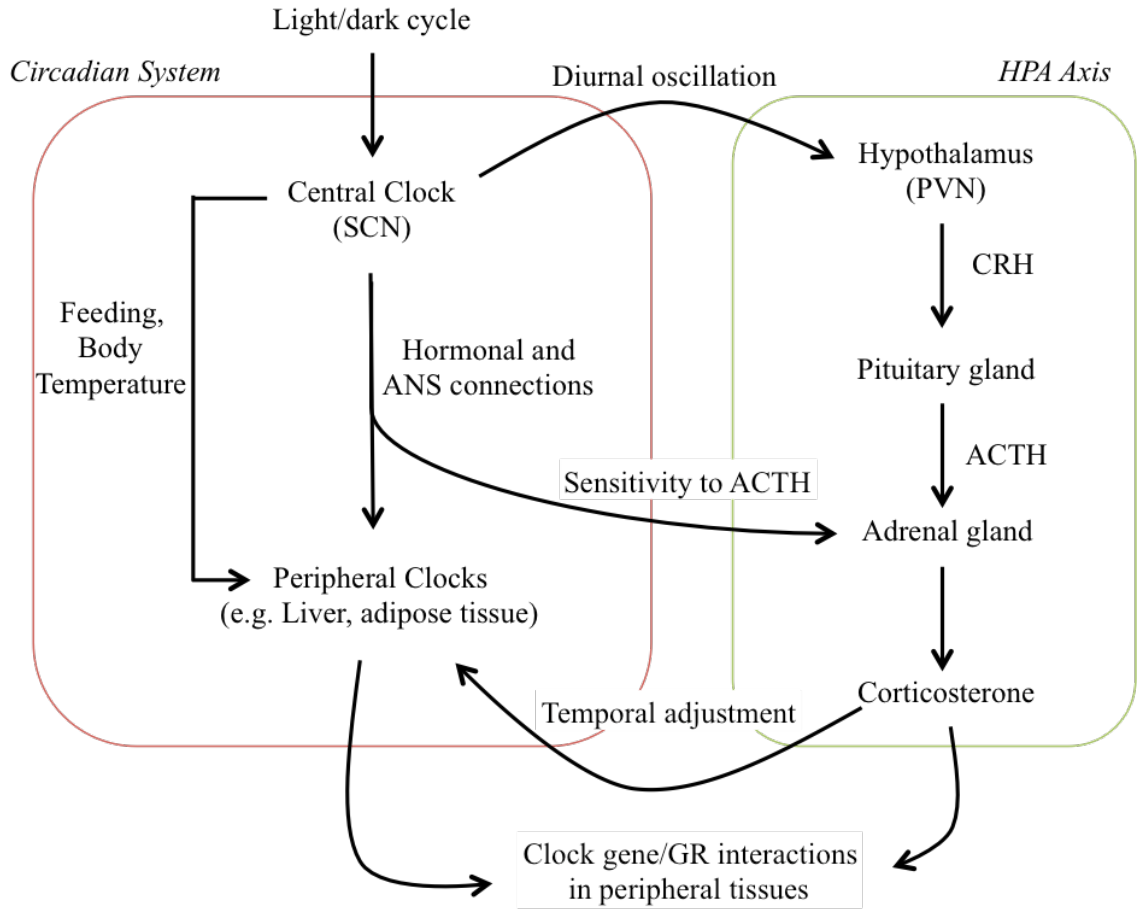

Figure 2.4 Overview of the links between the circadian system and the HPA axis. The SCN regulates adrenal corticosterone secretion at two levels: (i) the paraventricular nucleus via regulation of CRH; and (ii) the ANS via the effects on adrenocortical sensitivity to ACTH. Corticosterone can influence peripheral clocks through direct regulation of clock gene expression via glucocorticoid response elements located in the promoter regions of a number of clock genes. Adapted from Nader, Chrousos & Kino (2010).

2.3.5 Metabolic tissue clocks

An extensive number of fundamental metabolic pathways are regulated by the circadian system. Accordingly, metabolic tissue clocks are critical for overall body homeostasis. Liver and adipose tissue clocks are particularly important during pregnancy as metabolism of both glucose and lipids is substantially altered.

2.3.5.1 Liver

The liver plays a central role in energy homeostasis and metabolism and as such is important for the overall wellbeing of an organism (Klover & Mooney 2004). One of the most important biochemical pathways in the liver is glucose metabolism. Although food availability plays an important role in the daily changes in plasma glucose concentrations, rhythms persist in fasted rats because glucose metabolism is under circadian regulation (Escobar et al. 1998; La Fleur et al. 1999). Indeed, up to 15% of genes are rhythmically expressed in the rodent liver (Vollmers et al. 2012), the majority of which encode enzymes or regulatory proteins involved in metabolic pathways, most notably cholesterol homeostasis, fatty acid metabolism and glucose metabolism (Damiola et al. 2000; Akhtar et al. 2002; Panda et al. 2002). Prior to further discussion of the role of the liver clock in metabolism, the basic biological pathways of glucose metabolism are outlined. This description will focus primarily on the activity of the rate-limiting enzymes in glucose metabolism.

During fed conditions, plasma glucose levels increase and glucose is transported into the liver by the facilitative glucose transporter (GLUT) 2 (Figure 2.5). All imported glucose is phosphorylated to glucose-6-phosphate (G-6-P) by glucokinase (GK) to prevent diffusion out of the cell. High plasma insulin, as a result of feeding, activates glycogen synthase (GYS2) which catalyses the conversion of G-6-P to glycogen (glycogenesis) for storage (Bollen, Keppens & Stalmans 1998). Insulin limits glucose production by glycogen mobilisation (glycogenolysis), and from gluconeogenesis via transcriptional inhibition of the critical enzymes, glucose-6-phosphatase (*G6Pase*) and phosphoenolpyruvate carboxykinase 1 *(Pck1)* (see fasting description below) (Saltiel & Kahn 2001). Alternatively if carbohydrate intake is high enough, G-6-P can be converted to acetyl-CoA (AcCoA) by the glycolysis pathway, which is then available for fatty acid and triacylglycerol synthesis and ATP production (Figure 2.5) (Ferre & Foufelle 2007). The first step of this pathway involves the conversion of G-6-P to

fructose-6-phosphate (F-6-P) by phosphoglucose isomerase. Thereafter, F-6-P is converted to fructose-1,6-biphosphate (F-1,6-BP) by 6-phosphofructo-1-kinase (6PF-1K). The conversion of F-1,6-BP to phosphoenolpyruvate (PEP) occurs via series of complex enzymatic reactions, after which pyruvate kinase (PK) catalyses the conversion of PEP to pyruvate, which is decarboxylated to generate AcCoA (Figure 2.5).

During fasting, when glucose levels fall, secretion of glucagon from pancreatic α-cells and glucocorticoids from the adrenal gland stimulate glycogenolysis. This involves the conversion of glycogen to G-6-P by glycogen phosphorylase (PYGL) (Figure 2.5) (Bollen, Keppens & Stalmans 1998). If fasting conditions persist and glycogen stores are depleted, the synthesis of glucose from non-glucose precursors, including pyruvate and glycerol, occurs by gluconeogenesis (Jiang & Zhang 2003). The first step in the gluconeogenic pathway is the conversion of the non-glucose precursor (e.g. pyruvate) to oxaloacetate (OAA) by pyruvate carboxylase (PC) (Figure 2.5). OAA is then converted into PEP by PCK1, and then to F-1,6-BP. Thereafter, fructose-1,6-biphosphatase (FBPase) catalyses the hydrolysis of F-1,6-BP to F-6-P which is then converted to G-6-P. The synthesised G-6-P from both the glycogenolytic and gluconeogenic pathways is transported from the cytosol into the endoplasmic reticulum by the G-6-P transporter T_1 where it is converted by G6Pase into glucose (Jitrapakdee 2012). The resultant glucose is released into circulation via facilitative diffusion mediated by GLUT2 (Figure 2.5) (Thorens 1996). Consistent with a role for the circadian clock in glucose metabolism, many of these glucoregulatory genes are rhythmically expressed (Figure 2.5).

Hepatic clock genes play fundamental roles in these metabolic processes by controlling the expression of downstream genes and thereby imparting functional rhythmicity to the liver (Oishi et al. 2003). For instance, liver-specific *Bmal1*$^{-/-}$ mutant mice lose the robust circadian expression profile of most genes that are normally rhythmic, including those important in glucose metabolism such as *Glut2*, *Pk* and *Gk* (Kornmann et al. 2007; Lamia, Storch & Weitz 2008). Furthermore, *Pck1*, *Glut2*, *Gys2* and *G6Pase* have been identified as direct targets of BMAL1 in the liver using chromatin immunoprecipitation assays (Rey et al. 2011). Similarly, hepatic expression of *Clock* appears to be involved

in glucose homeostasis since *Clock*$^{\Delta 19}$ + MEL mice[2] display disrupted diurnal variation of plasma glucose, decreased glucose tolerance and altered expression of key glycolytic and gluconeogenic genes within the liver (Kennaway et al. 2007). Moreover, liver-specific *Cry* mutants do not exhibit glucagon-induced gluconeogenesis (Zhang et al. 2010). Furthermore, *Cry1* has been shown to repress transcription of *Pck1* after forming a complex with GR in hepatocytes (Lamia et al. 2011).

Glucose homeostasis is also substantially altered by the global loss of endogenous clock genes. For example, the *Clock*$^{\Delta 19}$ mutation results in damped oscillations of hepatic glycogen levels and expression of *Gys2* (Doi, Oishi & Ishida 2010) as do mice lacking a functional PER2 protein (Zani et al. 2013). Global *Bmal1*$^{-/-}$ mice exhibit increased insulin sensitivity along with a loss of rhythmicity in the hepatic expression of the key glucoregulatory genes, *Pck1*, *G6pase* and *Gk* (Rudic et al. 2004; Kennaway et al. 2013). Moreover, daily oscillations in *G6Pase* and *Pck1* are altered in cultured hepatocytes depleted of *Rev-erbα* (Yin et al. 2007).

[2] Modified *Clock*$^{\Delta 19}$ mice with retained central rhythmicity but a loss of peripheral rhythmicity.

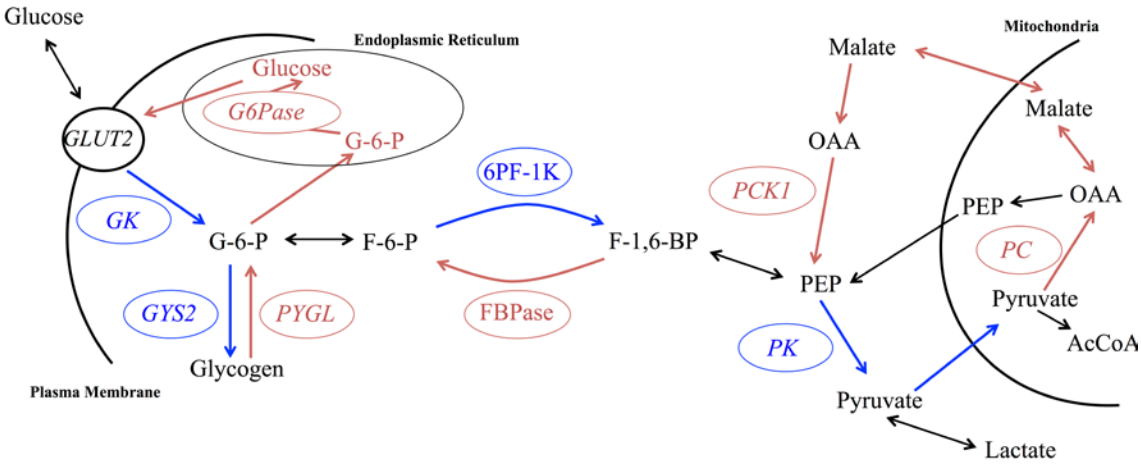

Figure 2.5 Schematic representation of glucose metabolism pathways in the liver. The blue arrows indicate pathways leading to glucose use or storage (i.e. glycolytic and glycogenic pathways), while those in red represent pathways of glucose production (i.e. gluconeogenic and glycogenolytic pathways). Genes that are rhythmically expressed are shown in italics. Adapted from Wallace & Barritt (2002).

2.3.5.2 White adipose tissue

White adipose tissue is a heterogeneous mixture of cell types that serves as the site of long-term energy storage and as an endocrine organ by its secretion of adipokines such as leptin (Rosen & Spiegelman 2006). Though food intake contributes to the daily rhythms in lipid metabolism, circadian rhythms of circulating plasma triacylglycerols persist in fasted rats (Escobar et al. 1998) since fat storage and release are regulated by the local adipose clock (Shostak, Meyer-Kovac & Oster 2013). In fact, approximately 13% of genes are rhythmically expressed in white adipose tissue, the majority of which encode for enzymes or regulatory proteins involved in lipid metabolism (Benavides, Siches & Llobera 1998; Zvonic et al. 2006; Sukumaran et al. 2010). Furthermore, strong circadian rhythms are present in both the expression of adipokine mRNAs and in their circulating plasma levels (Ahren 2000; Ando et al. 2005) .

Adipocytes store energy as triacylglycerols (formed via lipogenesis) in times of energy surplus and mobilise fatty acids and glycerol (lipolysis) when energy is in demand. In the fed state, increased levels of insulin upregulate the activity of lipoprotein lipase (LPL), the key enzyme involved in lipogenesis possibly via PPARγ (Figure 2.6) (Schoonjans et al. 1996; Vidal-Puig et al. 1997; Frayn, Arner & Yki-Jarvinen 2006). Consequently, circulating plasma triacylglycerols are hydrolysed into fatty acids and glycerol by LPL and taken up into adipocytes where triacylglycerols are resynthesised by esterification of these fatty acids (Frayn et al. 1995). Concurrently, insulin inhibits lipolysis via the inhibition of hormone sensitive lipase (LIPE) and adipocyte triglyceride lipase (PNPLA2), the key regulators of lipolysis (Figure 2.6) (Fruhbeck et al. 2014).

During fasting, decreased levels of insulin result in a reduction in lipogenesis and removal of the insulin-induced suppression of lipolysis. Consequently, adipose triacylglycerols are hydrolysed to glycerol and three fatty acids via the lipolytic pathway (Figure 2.6). The first step converts triacylglycerol to diacylglycerol (DG) catalysed by PNPLA2, DG is then hydrolysed to monoacylglycerol (MG) by LIPE which is then converted to glycerol by monoacylglycerol lipase (MGL) (Figure 2.6) (Fruhbeck et al. 2014). The resultant fatty acids and glycerol are then released into circulation and transported to tissues as required. In accordance with a role for the circadian clock in lipid metabolism, the majority of the above lipid-regulatory genes show circadian variation (Figure 2.6).

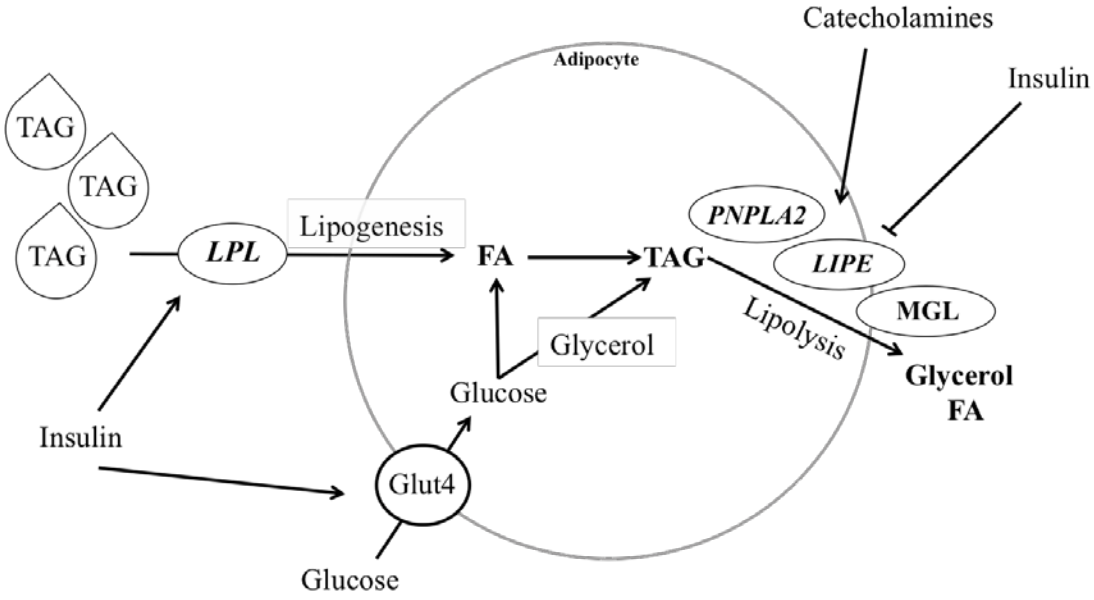

Figure 2.6 Schematic representation of lipid metabolism pathways in adipose tissue. Genes that are rhythmically expressed are shown in italics. Adapted from Henriksson & Lamia (2015).

Gene knock-out studies have highlighted the critical role for clock genes in the transcriptional regulation of many of the enzymatic pathways involved in lipid metabolism. Global loss of *Clock* in mice leads to the development of a metabolic syndrome-like condition consisting of hypertriglyceridemia, hyperleptinemia, and increased serum cholesterol (Turek et al. 2005). Furthermore, $Clock^{\Delta 19}$ mutants exhibit decreased rates of lipolysis, due to reduced adipose expression of both *Lipe* and *Pnpla2* (Shostak, Meyer-Kovac & Oster 2013). Moreover, specific loss of peripheral rhythmicity only ($Clock^{\Delta 19}$ + MEL mice) results in reduced plasma free fatty acids and a loss of rhythmicity of adipose *Pparγ* and *Pnpla2* expression (Kennaway et al. 2007; Kennaway et al. 2012). Global *Bmal1* deficiency results in elevated plasma triacylglycerol levels and circulating free fatty acids, as well as hyperleptinemia and decreased lipolysis (Rudic et al. 2004; Shimba et al. 2011; Shostak, Meyer-Kovac & Oster 2013; Kennaway et al. 2013). Additionally, chromatin immunoprecipitation assays have shown that the promoter regions of *Lipe* and *Pnpla2* are associated with *Bmal1* (Koike et al. 2012). *Per2* mutant mice display reduced plasma triacylglycerols and free fatty acids (Grimaldi et al. 2010). Loss of *Rev-erbα* leads to increased adiposity without increased hyperphagia and elevated expression of adipose *Lpl* (Delezie et al. 2012), whereas mice injected with *Rev-erbα* activating ligands display increased energy expenditure and suppressed adipose lipogenic gene expression (Solt et al. 2012).

2.4 Maternal circadian rhythms in pregnancy

Several epidemiological studies have observed associations between shift work and negative pregnancy outcomes such as low birth weight, premature birth and spontaneous abortion (Cone et al. 1998; Knutsson 2003; Zhu et al. 2004) suggestive of serious consequences of maternal circadian dysregulation during pregnancy. Moreover, studies in rodents exposed to environmental perturbations during pregnancy, such as repeated shifts of the light-dark cycle to mimic shift work, result in several negative pregnancy outcomes. For example, exposure of pregnant mice to either a 6-h phase delay or advance every 5-6 days substantially decreased pregnancy success rates with rates falling 50% in dams exposed to phase delays and by 78% in the phase advanced group (Summa, Vitaterna & Turek 2012). Furthermore, exposure of pregnant rats to a 12-h shift in the light cycle every 3-4 days resulted in the development of metabolic disorders in offspring including insulin resistance and altered glucose tolerance by 1 year of age, despite postnatal exposure to a normal 12-h light-dark cycle (Varcoe et al. 2011; Varcoe et al. 2013). Despite this clear evidence for adverse affects of circadian disruption, relatively little is known regarding circadian adaptation in normal pregnancy.

It has been established that circadian variation in hypothalamic-pituitary-adrenal axis activity is maintained in both humans (Patrick et al. 1980) and rats (Atkinson & Waddell 1995), with an overall elevation in absolute levels of glucocorticoids (cortisol and corticosterone, respectively) towards term. Although changes in absolute levels of corticosterone have been characterised at a single time point (0800 h) in mouse pregnancy (Douglas et al. 2003), the effect of pregnancy on the circadian profile of circulating corticosterone remains to be elucidated.

It is also well established that pregnancy substantially reduces activity levels in both humans and rodents (Richards 1966; Rousham, Clarke & Gross 2006; Gamo et al. 2013), but its effect on the circadian profile of activity is less well characterised. In the non-pregnant rodent the circadian profile is characterised by low levels of activity during the light phase, which increase substantially with the onset of darkness and progressively decline towards lights on (Kennaway et al. 2003; Gamo et al. 2013). Peak activity count (at 2000 h) is approximately 10 times greater than at the trough (1500 h) in mice (Gamo et al. 2013). Free-running circadian activity rhythms in late gestation

were found to be highly variable in rats with a circadian pattern difficult to detect (Rosenwasser, Hollander & Adler 1987), while the amplitude of the activity rhythm was found to be reduced in late gestation in hamsters (Scribner & Wynne-Edwards 1994). This late gestation decrease in activity likely conserves energy for use by the rapidly growing fetus, and as such, contributes to maternal metabolic adaptations. Although it remains to be confirmed, these changes may be driven by estradiol and progesterone across gestation, since these sex steroids are capable of modulating activity rhythms (Albers 1981).

Interestingly, despite maternal hyperphagia throughout gestation in rodents, the circadian rhythm of food intake does not change appreciably across pregnancy. Accordingly, the majority of food consumption during pregnancy still occurs exclusively in the dark phase, consistent with non-pregnant animals (Hitier et al. 1982; Varcoe et al. 2013).

In non-pregnant, nocturnal animals the circadian variation in core body temperature (T_c) is characterised by a trough during the light phase and a peak during the dark phase with an amplitude of approximately 0.75°C (Eliason & Fewell 1997). T_c rhythms are markedly altered during pregnancy in both rats and mice (Fewell 1995; Gamo et al. 2013). Indeed, in rats, circadian variation in T_c is lost from day 15 onwards, due to a loss of the normal dark phase increase (Fewell 1995). There is also a late pregnancy reduction in the mesor (circadian-rhythm adjusted mean) of T_c in both rats and mice (Fewell 1995; Gamo et al. 2013) that has been proposed to be an adaptive response to heat dissipation across the placenta. Accordingly, the increased heat gradient between fetus and mother likely enables the mother to act as a heat sink for the highly metabolically active fetus, to maintain optimal temperature *in utero*. The stimulus for altered circadian rhythmicity in body temperature remains unknown, however, a role for the placenta and/or fetus has been proposed due to the rapid restoration of normal body temperature rhythmicity immediately after birth (Fewell 1995). Also, because progesterone can exert thermogenic effects (Freeman et al. 1970), it has been suggested that its preterm decline may contribute to the late gestation temperature fall (Fewell 1995).

2.4.1 Clock gene expression during pregnancy

2.4.1.1 Maternal tissues

It is likely that clock gene expression is altered during pregnancy since several clock genes contain hormone response elements within their promoter regions including estrogen- and progesterone-response elements (Travnickova-Bendova et al. 2002; Nakamura et al. 2005). Furthermore, studies show that clock gene expression can be influenced by estradiol and progesterone in a range of tissues (Nakamura et al. 2005; He et al. 2007; Nakamura et al. 2010; Rubel et al. 2012). Indeed, several recent studies suggest that pregnancy significantly impacts clock gene expression in maternal tissues. For example, peak PER2 expression in the central clock has been shown to be phase advanced by 4-h on day 6 of rat pregnancy, while expression in non-SCN brain regions is characterised by phase shifts and a loss of rhythmicity (Schrader, Nunez & Smale 2010; Schrader, Nunez & Smale 2011). Late in gestation, marked changes in the circadian variation of several core clock genes occur in the maternal liver. Specifically, circadian oscillations of *Clock*, *Bmal1*, *Per1*, *Cry1* and *Cry2* were all dampened compared to non-pregnant rats (Figure 2.7). Moreover, hepatic *Clock* mRNA levels no longer displayed variation attributable to time-of-day (Wharfe, Mark & Waddell 2011), a surprising result given the central role for *Clock* in the core clock machinery. Further changes have been observed between late pregnancy and day one of lactation in the rat, where expression of *Clock* and *Bmal1* were found to be upregulated in the maternal liver, adipose tissue and mammary glands postpartum (Casey et al. 2009). Whether clock gene expression in metabolic tissues is altered across early to mid-pregnancy remains to be explored.

Clock genes are also rhythmically expressed in the uterus of non-pregnant rodents (Horard et al. 2004), and whilst the expression of most genes appears to be maintained across pregnancy (Akiyama et al. 2010; Ratajczak, Herzog & Muglia 2010), *Cry1* expression is upregulated on day 18 in the mouse uterus (Ratajczak, Herzog & Muglia 2010). Furthermore, *Per2* rhythmicity is lost in uterine stromal cells during decidualisation (Uchikawa et al. 2011). A role for clock genes in the timing of parturition, the onset of which shows clear circadian variation in mammals (Lincoln & Porter 1976), remains uncertain due to strain differences and ambiguity regarding patterns of expression in the different uterine cells (epithelial, stromal or myometrial) (Olcese 2012). Nevertheless, evidence suggests that timing of parturition is driven by

circadian signals from both the mother and fetus (Serón-Ferré, Ducsay & Valenzuela 1993; Olcese 2012). It is possible that clock genes may play a role in the transmission of these signals to the myometrium late in gestation.

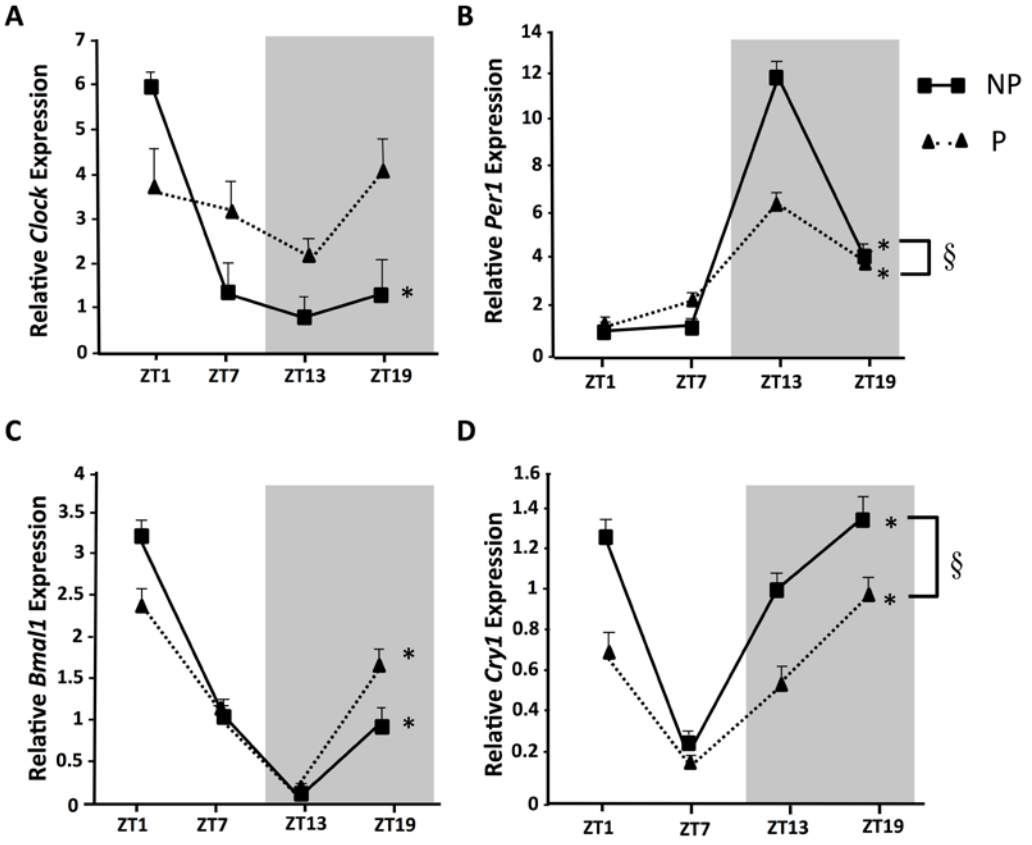

Figure 2.7 Hepatic expression of (A) *Clock*, (B) *Per1*, (C) *Bmal1* and (D) *Cry1* mRNAs in non-pregnant (NP) and pregnant (P) rats at zeitgeber times (ZT) 1, 7, 13 and 19 over days 21-22 of rat pregnancy. Values are the mean ± SEM. Grey shading represents the dark phase of the light cycle. *Significant time-of-day variation, $P < 0.05$; § overall difference between pregnant and non-pregnant profile ($P < 0.001$, two-way ANOVA). Modified from Wharfe et al. 2011.

2.4.1.2 The placenta

Clock genes have been identified in the whole mouse placenta (Ratajczak, Herzog & Muglia 2010), the two functionally distinct zones (labyrinth and junctional) of the rat placenta (Wharfe, Mark & Waddell 2011) and very recently in the human placenta at term (Perez et al. 2015). Although all clock genes are clearly expressed in the placenta, their rhythmicity appears to be relatively weak compared to that seen in adult tissues. Indeed, time-of-day variation was marginal and was limited to *Per1* and *Cry1* in the mouse placenta (Ratajczak, Herzog & Muglia 2010) and *Bmal1*, *Per1* and *Per2* in the rat placenta (Wharfe, Mark & Waddell 2011). Furthermore, the expected antiphase expression of *Bmal1* and *Per1/Per2* was absent (Wharfe, Mark & Waddell 2011), indicative of either an immature placental clock or transcriptional interactions between clock genes that differ between the placenta and adult tissues. While the physiological significance of the relatively stable placental clock remains to be explored, a preliminary report shows similarly weak time-of-day variation in the labyrinthine expression of the nutrient transporters *Glut1*, *Glut4*, Na+-coupled neutral amino acid transporter (*Snat*) 4 and fatty acid translocase (*CD36*) suggestive of a possible role for placental clock genes in the regulation of transplacental nutrient passage (Waddell et al. 2012).

2.4.1.3 The fetus

By late pregnancy in rodents all clock genes are expressed in the fetal SCN albeit at substantially lower levels than in adults and with no clear rhythmicity (Sladek et al. 2004; Shimomura et al. 2001; Ansari et al. 2009). Indeed, development of circadian oscillations of clock genes parallel the development of synapses within the fetal SCN which only reach completion on postnatal day 10 (Sumova et al. 2008). Despite the absence of clock gene rhythmicity, by day 19 the fetal rat SCN exhibits a 24-h rhythm in metabolic activity, as indicated by glucose utilization (Reppert & Schwartz 1984). It has been suggested that this rhythmicity may arise in response to cyclic maternal signals such as glucocorticoids or melatonin (Sumova et al. 2008; Serón-Ferré et al. 2012).

As observed in the fetal SCN, the fetal liver expresses all clock genes by embryonic day 20 in the rat but robust oscillations in expression are absent, with the exception of *Rev-erbα* (Sladek et al. 2007). By day 21, time-of-day variation is detectable for hepatic *Per2*, *Per3* and *Cry1* but as in the placenta, this variation does not follow the

conventional circadian pattern (Wharfe, Mark & Waddell 2011). It is possible that the relatively stable clock gene expression across a 24-h period is adaptive for continuous, rapid fetal growth. By postnatal day 30, rhythmic expression of all hepatic clock genes is in phase with adult rhythms (Sladek et al. 2007).

In contrast to the fetal SCN and liver, the fetal adrenal clock is functional by day 18 of rat pregnancy (Torres-Farfan et al. 2011). Indeed, at this stage the fetal adrenal gland displays a circadian rhythm in corticosterone content and expression of steroidogenic acute regulatory protein (StAR) opposite to that seen in the mother, as well as antiphase expression of *Bmal1* and *Per2* (Torres-Farfan et al. 2011). Despite the rhythmic expression of adrenal corticosterone content, plasma corticosterone levels in the rat fetus are not rhythmic (Wharfe, Mark & Waddell 2011). At this late stage of gestation the placental glucocorticoid barrier is almost entirely lost (Mark et al. 2009) and so the fetus is likely exposed to the maternal corticosterone rhythm. Accordingly, the out-of-phase fetal and maternal rhythms presumably account for the relatively constant fetal corticosterone levels at this time.

Chapter 3 Experimental Objectives

The overall aim of the experiments presented in this thesis was to characterise the impact of pregnancy on clock gene expression in key maternal tissues and to determine subsequent downstream effects on the circadian expression of tissue-specific genes. It is apparent from the review of literature that the circadian clock exerts temporal control over a wide range of physiological processes including glucocorticoid secretion and glucose and lipid metabolism, all of which are substantially altered during normal pregnancy. What is not known is whether circadian changes in clock gene expression accompany maternal adaptations throughout pregnancy or if such changes are linked to altered circadian variation in the expression of downstream genes directly involved in these adapted physiological processes. Therefore, the major hypotheses tested in this thesis were that normal pregnancy alters clock gene expression in maternal tissues, and this has downstream tissue-specific effects on a range of clock-controlled genes.

Study 1 (Chapter 5): Pregnancy-induced adaptations of the central circadian clock and maternal glucocorticoids

The objective of this study was to investigate the effect of pregnancy on clock gene expression within the anterior hypothalamus, the location of the central circadian clock. As circadian variation of the hypothalamic-pituitary-adrenal (HPA) axis is dependent upon the rhythmic expression of clock genes within this central clock, a key focus was to determine whether changes in hypothalamic clock gene expression are linked to altered HPA axis activity during pregnancy.

Measurements were made at 0800, 1200, 1600, 2000, 0000 and 0400 h prior to and on days 6, 10, 14 and 18 of mouse pregnancy (term = day 19). Levels of hypothalamic clock gene and *Crh* expression were measured, as well as plasma ACTH, corticosterone and 11-DHC.

Study 2 (Chapter 6): Pregnancy-induced changes in the circadian expression of maternal hepatic clock genes: implications for maternal glucose homeostasis

This study examined whether circadian changes in hepatic clock gene expression accompany maternal adaptations during pregnancy and also whether such changes influence the circadian expression of downstream glucoregulatory genes known to be rhythmic.

Levels of hepatic clock gene expression were determined at six time points as described for Study 1. In addition, expression of downstream genes directly involved in glucose metabolism, maternal plasma glucose, insulin and hepatic glycogen levels were also assessed.

Study 3 (Chapter 7): Pregnancy suppresses the daily rhythmicity of core body temperature and adipose metabolic gene expression in the mouse

The aims of this study were to investigate the effect of pregnancy on clock gene expression in white adipose tissue and to determine whether pregnancy alters the circadian variation of genes involved in lipid metabolism, which are known to be rhythmic. Furthermore, this study explored whether altered circadian variation in maternal T_c across pregnancy was linked to pregnancy-induced changes in adipose clock genes and whether these changes in T_c were associated with progesterone levels across mouse pregnancy.

Measurements were made at the same time points as described for Study 1. Adipose expression of clock genes and downstream genes directly involved in lipid metabolism were determined as well as maternal plasma progesterone. Maternal core body temperature was measured every 15 minutes throughout gestation, in a subset of animals, using surgically implanted temperature loggers.

Chapter 4 Materials and Methods

4.1 Animals

4.1.1 Mouse maintenance

All procedures involving the use of animals were conducted after approval by the Animal Ethics Committee of The University of Western Australia (AEC number RA/3/100/1070). Nulliparous C57Bl/6J mice, aged between 6 and 9 weeks old, were supplied by the Animal Resource Centre (Murdoch, WA, Australia) and housed in the Preclinical Facility at The University of Western Australia. Mice were maintained in two environmentally controlled rooms (average temperature 22°C, average humidity 55%), with food and water supplied *ad libitum*. In one room mice were exposed to a normal 12:12 light/dark cycle (lights on at 0700 h); in the other room the light cycle was reversed (lights on for 12h from 1900 h). Between 0700 and 1900 h mice in the reverse light cycle room were exposed to a constant red light (36 W, 620 nm) to allow normal animal care procedures to be carried out during work hours (refer to Section 4.1.2). Both groups of animals were allowed to acclimatise to their respective light cycles for two weeks before any experimental procedures were conducted. Lights on at 0700 h (or 1900 h in the reverse-light room) was classified as a new day and as zeitgeber time (ZT)-zero, and sampling times were defined relative to ZT-zero.

4.1.2 Pilot trial to determine the effect of red light exposure

Although 24-hour sampling of tissues is critical for circadian projects, around-the-clock collection of samples can be highly disruptive for researchers and animal-house staff. To overcome this problem, a reverse light cycle room was used, in which the normal lights were on from 1900 h to 0700 h. This enabled sampling of the dark phase time points (ZT13, 17 and 21) to be carried out during regular work hours. As animal monitoring and housekeeping also needed to be carried out during these hours, the reverse light cycle room was illuminated by a 36 W, 620 nm constant red light during the dark phase hours (0700 – 1900 h). This wavelength was chosen as it is above the spectral sensitivity of mouse vision (~ 360 – 590 nm), but remains within visible wavelengths for humans (~ 380 – 700 nm) (McLennan & Taylor-Jeffs 2004). Although a number of research groups use a combination of reverse light cycle and red light, it was of importance to investigate whether red light exposure altered the circadian

expression of clock genes in our cohort of animals prior to commencement of the main project.

Mice (n = 16 per room) were allowed to acclimatise to their respective light cycles (normal and reverse) for two weeks, after which they were monitored for estrous cycle stage (refer to Section 4.1.4). On diestrus I of the cycle, mice were anaesthetised and samples of liver were taken at 0800, 1200, 2000 or 0000 h (n = 4 per time point), thus simulating collection at ZT1, ZT5, ZT13, and ZT17 in each room (refer to Section 4.1.5). Total RNA was extracted from liver samples, reverse transcribed and quantitative polymerase chain reaction (refer to Section 4.2 for full protocols) was performed to determine the expression of *Bmal1* mRNA in the liver samples from these animals. Liver samples were standardised against reference genes *Ppia*, *Sdha* and *Tbp* using the GE Norm algorithm (Vandesompele et al. 2002). Time-of-day variation was detected in *Bmal1* expression ($P < 0.05$, two-way ANOVA), which peaked around ZT1 in both rooms, consistent with earlier profiles detected in rodent liver (Wharfe, Mark & Waddell 2011). Importantly, *Bmal1* expression was not different between the two rooms (Figure 4.1).

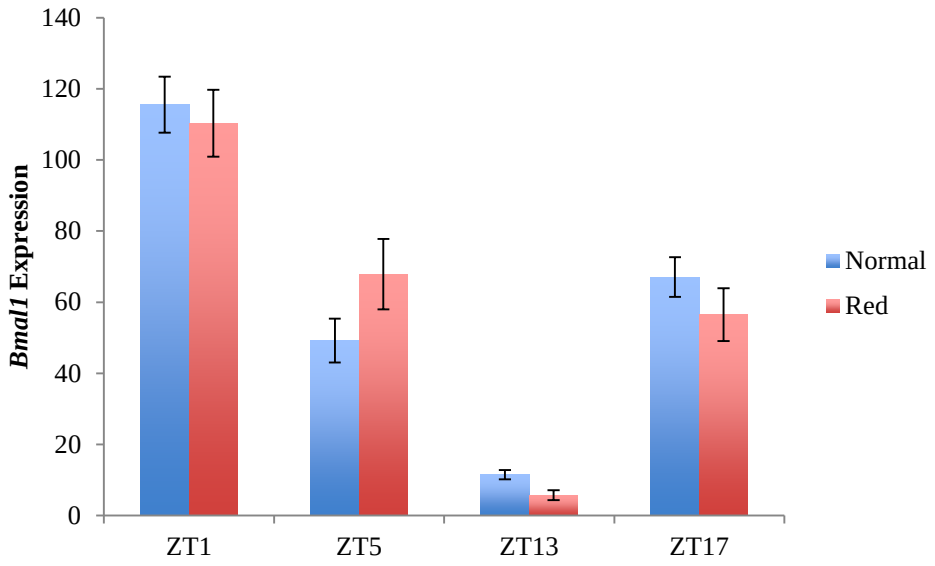

Figure 4.1 Hepatic *Bmal1* expression of mice exposed to either a normal light cycle with lights off during the dark phase or a reverse light cycle with exposure to constant red light during the dark phase. *Bmal1* expression profiles were comparable in both rooms (normal and reverse).

4.1.3 Measurement of maternal core body temperature

Maternal core body temperature was recorded every 15 min over a 23-day period, which spanned one estrous cycle and the length of gestation, using a Thermochron iButton temperature logger (DS1921G-F5; Embedded Data Systems, Kentucky, USA) implanted in the peritoneal cavity. Prior to implantation, the temperature loggers were partially dismantled according to the protocol outlined in Lovegrove (2009) with the kind assistance of Mr Greg Cozens. Removal of the stainless steel housing and circuit board resulted in a final weight of approximately 5% of the mouse's body weight. The validity and accuracy of dismantled temperature loggers has been previously verified (Lovegrove 2009). Prior to surgery temperature loggers were programmed and coated in two layers of inert paraffin wax (Sasol EXP986, Sasol Chemical Industries Ltd., Johannesburg, South Africa) to render them waterproof and immunologically inert. The final weight of implanted loggers was no more than 7.5% of the mouse's body weight. Loggers were sterilised for 24-h in 0.5% w/v chlorhexidine gluconate in 70% w/v ethanol solution.

A subset of animals (n = 3) were anaesthetised using isoflurane/nitrous oxide (0.2: 0.8) gas for the duration of the surgery. A portion of abdominal fur was shaved and the abdomen cleaned with 0.5% w/v chlorhexidine gluconate in 70% w/v ethanol solution. A small incision (approximately 1.5 cm) was made along the midline through the skin and the peritoneal wall. The temperature logger was then inserted into the peritoneal cavity, and the muscle and skin layers sutured individually using absorbable suture (Ethicon, New Jersey, USA) for both layers. Aseptic techniques were utilised throughout the surgical procedure. 0.05 mg/kg buprenorphine (Temgesic, Reckitt Benckiser, NSW, Australia) was injected subcutaneously to provide post-procedural analgesic relief. After one week post-surgery, animals were monitored for estrous cycle stage determination (refer to section 4.1.4).

Loggers were retrieved during tissue sampling on day 18 of gestation (refer to section 4.1.5). After recovery from the intraperitoneal cavity, temperature loggers were calibrated using a certified mercury-in-glass thermometer (National Association of Testing Authorities, Australia) in a water bath at 3°C increments from 33-41°C. Data were downloaded and read using eTemperature software (version 8.25, OnSolution Pty

Ltd, NSW, Australia). Data sets were corrected according to the calibration curve generated for each temperature logger.

4.1.4 Mating and pregnancy determination

Female mice were monitored for estrous cycle stage by vaginal lavage with saline and subsequent analysis of the cellular cytology according to the protocol outlined by Caligioni (2009); samples were taken between ZT6 and ZT13 each day. When pro-estrus was identified through the presence of abundant leukocytes, nucleated epithelial cells and cornified cells in the lavage, females were placed with males and left overnight to mate. Copulation was confirmed by visualization of a vaginal mucous plug the following morning and designated as day 1 of pregnancy.

In a separate group of non-pregnant mice, cycle stage was monitored for a minimum of three full estrous cycles using the protocol outlined above (Caligioni 2009). Mice with irregular cycles were excluded.

4.1.5 Collection and storage of blood and tissue

Tissues were collected from mice, in both normal and reverse cycle rooms, under isoflurane/nitrous oxide (0.2: 0.8) anaesthesia at 0800 (normal: ZT1/ reverse: ZT13), 1200 (ZT5/ ZT17) or 1600 h (ZT9/ ZT21) on either diestrus I of the cycle or day 6, 10, 14 or 18 of pregnancy (term = day 19). These days were selected to represent four important time points throughout pregnancy: post-implantation, mid-gestation, and the early and late fetal period. For collection of tissues in the dark phase, anaesthesia was carried out under red light before fitting the mouse with a light proof hood and collection of the tissues in white light. A blood sample was obtained by cardiac puncture and blood glucose measured immediately (Accu-Chek; Roche Diagnostics, Mannheim, Germany). The remainder of the blood was mixed with 10:1 (vol:vol) 0.6 M ethylenediamine tetra-acetic acid (EDTA) and centrifuged at 13,000 x *g* for 6 min to obtain plasma. The maternal brain was dissected out of the skull and frozen whole on crushed dry ice. A portion of the right side of the median lobe of the liver and a sample of gonadal adipose tissue were collected from each mother and immediately snap frozen in liquid nitrogen. All tissue and plasma samples were stored at -80°C until further analysis.

4.2 Quantitative reverse transcription polymerase chain reaction

4.2.1 Background

Quantitative reverse transcription polymerase chain reaction (RT-qPCR) is an accurate, reliable and quick technique that allows quantification of mRNA in tissue samples. Prior to PCR, RNA is extracted from tissue homogenate and then reverse transcribed into complementary DNA (cDNA) to act as a template for the PCR reaction. PCR consists of three phases: denaturation, annealing and extension. During the first phase, the DNA becomes single stranded, whilst in the second phase, primers hybridise to either end of a specific gene of interest to direct amplification of this region only. In the final phase, DNA polymerase binds to the primer-template hybrid and synthesizes a new strand of DNA complementary to the original template. Therefore, after multiple cycles, the specific PCR product is amplified many thousand fold. Quantitative PCR can be used to calculate the initial amount of template present in the sample via fluorescence. SYBR green, a fluorescent dye is included in the PCR reaction, and emits fluorescence by binding to the minor groove of the double stranded DNA. After each extension phase, fluorescence is recorded and the increasing amount of PCR product can be monitored. During the early phase of the qPCR reaction, product is amplified at a rate proportional to the initial starting amount of the target gene, thus providing opportunity for interpolation of concentration from a standard curve.

4.2.2 RNA sample preparation

4.2.2.1 Anterior Hypothalamus

The hypothalamus was dissected from the frozen brain on dry ice along the following boundaries stated in Quenell (2011): laterally 2 mm either side of the third ventricle from the optic chiasm to the posterior border of the mammillary bodies, and the thalamus dorsally. The hypothalamus was then bisected in the coronal plane immediately anterior to the pituitary stalk (Figure 4.2). Cassandra Yap, a fellow PhD candidate in the School of Anatomy, Physiology and Human Biology at UWA, carried out this dissection and the following RNA extraction as the brains from these animals were used for two separate projects.

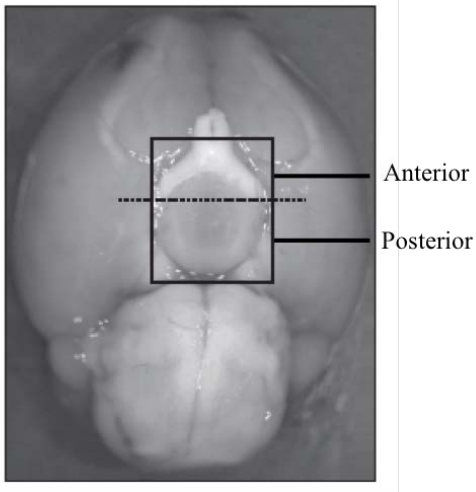

Figure 4.2 Anterior and posterior subdivisions of the mouse hypothalamus. The anterior hypothalamus was dissected from the frozen brain on dry ice. Adapted from Quennell (2011).

Total RNA from the whole anterior hypothalamus was extracted using QIAzol Lysis Reagent (Qiagen, Melbourne, VIC, Australia) according to the manufacturer's instructions. Ice-cold Qiazol (750 µl) was added to each sample in a 2 ml microfuge tube and homogenised using a hand-held homogeniser. Bromoanisole (37.5 µl) (Molecular Resources Center, Inc., Cincinnati, OH, USA) was added to the homogenate, thoroughly mixed and centrifuged at 12,000 x *g* for 15 min at 4°C (Eppendorf Centrifuge 5417R, Hamburg, Germany). Following centrifugation, the aqueous phase was transferred into a fresh tube and mixed with 375 µl of isopropanol to precipitate the RNA. Samples were stored at room temperature for 10 min and centrifuged at 12,000 x *g* for 5 min at 25°C. The supernatant was discarded and the RNA pellet was washed by adding 750 µl of 75% ethanol before centrifugation at 7,500 x *g* for 5 min at 25°C. The ethanol was discarded and the washing process repeated. After removal of the ethanol wash, the RNA pellet was air-dried for 5 min. The RNA was dissolved in 50 µl of RNase-free water, placed on ice for 5 min and thoroughly vortexed.

4.2.2.2 Liver

Samples (50 mg) of maternal liver were obtained by chipping the frozen tissue in a chilled porcelain mortar and pestle. Tissue samples were then transferred into chilled homogenising tubes and kept on dry ice to prevent RNA degradation. A POLYTRON-

Aggregate homogeniser (Kinematica Inc., Bohemia, NY, USA) was cleaned with RNaseZap (Ambion, Austin, TX, USA) to remove any potentially contaminating RNases. Samples were homogenised on ice in 1 ml of QIAzol Lysis reagent (Qiagen, Melbourne, VIC, Australia) using the homogeniser. The probe was rinsed with diethylpyrocarbonate (DEPC) water between samples to prevent cross-contamination. Bromoanisole (50 µl) (Molecular Resources Centre, Inc., Cincinnati, OH, USA) was added to each homogenised sample, which was vortexed prior to centrifugation at 12,000 x *g* for 15 min. All centrifugations were carried out at 4°C in a refrigerated centrifuge (Eppendorf Centrifuge 5417R, Hamburg, Germany). This resulted in the separation of the solution into three phases. An aliquot (400 µl) of the upper, aqueous phase was transferred into a new tube, to which 500 µl of cooled isopropanol was added. Samples were mixed and stored at room temperature for 10 min and then centrifuged at 12,000 x *g* for 5 min to pellet the precipitated RNA. The supernatant was decanted and the pellet washed with 1 ml of 75% ethanol followed by centrifugation at 12,000 x *g* for 5 min. This step was repeated, then the pellet air dried for approximately 8 min or until the pellet became semi-transparent. The RNA pellet was rehydrated in 50 µl of ultra pure water (Sigma-Aldrich, MO, USA) and stored at -80ºC until required.

4.2.2.3 Adipose tissue

Samples (100 mg) of gonadal fat were transferred into chilled homogenising tubes and kept on dry ice to prevent RNA degradation. Total RNA was extracted using a QIAGEN RNeasy Lipid Tissue Mini Kit (Melbourne, VIC, Australia) according to the manufacturer's instructions. Samples were homogenised on ice in 1 ml of QIAzol Lysis Reagent (Qiagen, Melbourne, VIC, Australia) using the POLYTRON-Aggregate homogeniser (Kinematica Inc., Bohemia, NY, USA). The probe was rinsed with diethylpyrocarbonate (DEPC) water between samples to prevent cross contamination. Samples were incubated at room temperature for 5 min, before 200 µl of choloroform was added and the mixture shaken vigorously. Following a 3 min incubation at room temperature, the samples were centrifuged at 12,000 x *g* for 15 min at 4°C (Eppendorf Centrifuge 5417R, Hamburg, Germany). An aliquot (~600 µl) of the upper, aqueous phase was transferred into a new tube to which 600 µl of 70% ethanol was added. Samples were then vortexed. An aliquot (700 µl) of each sample was transferred to an RNeasy Mini spin column in a 2 ml collection tube and centrifuged at 8,000 x *g* for 15 sec. The flow-through was discarded and the previous step repeated with the remainder

of the sample. The column was washed with 700 µl of Buffer RW1, centrifuged at 8,000 x *g* for 15 sec and the flow-through discarded. After this, 500 µl of buffer RPE was added to the RNeasy column and the sample centrifuged at 8,000 x *g* for 15 sec before the flow-through was discarded. This step was repeated with a 2 min centrifugation at 8,000 x *g*. The RNA was eluted by addition of 50 µl of RNase-free water to the RNeasy column and centrifugation at 8,000 x *g* for 1 min.

Purity and concentration of all RNA samples were quantified using the Nanodrop ND-1000 spectrophotometer at 260 nm and 280 nm (Thermo Scientific, Wilmington, DE, USA). All RNA samples were stored at -80°C until reverse transcription was carried out.

4.2.3 Reverse transcription

A portion of each RNA sample (1 µg for hypothalamic samples, 5 µg for liver and adipose samples) was combined with 0.5 µl of random hexamers (Promega, Sydney, NSW, Australia), 2.5 µl of 7.5 mg/ml Ficoll 70 and 2.5 µl of 2.5 mg/ml Ficoll 400 (Sigma-Aldrich, St Louis, MO, USA) and made up to 17.38 µl with double deionised water (ddH2O). Each sample was denatured in the thermocycler (MJ Research Inc. Watertown, MA, USA) at 70°C for 5 min before being immediately cooled on ice for 5 min to prevent secondary structure formation. Moloney Murine leukemia virus (M-MLV) reaction buffer (5 µl of 5 x buffer) was added to each sample followed by 1.35 µl of 10 mM dinucleotide triphosphates (dNTPs), 0.062 µl of RNAsin (40 U/µl); a recombinant ribonuclease inhibitor and 0.75 µl of M-MLV Reverse Transcriptase enzyme (200 U/µl); an RNA-dependent DNA polymerase (all reagents obtained from Promega Corp., Sydney, NSW, Australia). Reactions were then incubated in the thermocycler for 10 min at 25°C, 110 min at 42°C and 15 min at 70°C.

4.2.4 cDNA purification

The resultant cDNAs were purified using the UltraClean PCR Clean up spin kit (MoBio Laboratories Inc. Carlsbad, CA, USA) as per manufacturer's instructions. Spinbind buffer (125 µl) was mixed with the cDNA and the solution transferred to a spin column and centrifuged at 10,000 x *g* for 30 sec. The flow through solution was discarded and 300 µl of Spinclean added to the column before centrifugation at 10,000 x *g* for 30 sec.

The flow through was again discarded and the empty column was spun at 10,000 x *g* for 30 sec to remove any residual ethanol. The spin basket was then transferred to a new tube and the cDNA eluted by adding 100 µl of elution buffer directly onto the filter membrane before centrifuging at 10,000 x *g* for 60 sec. The column was then discarded and the resultant cDNA stored at -20°C.

4.2.5 Primer design

Primer BLAST (Basic Local Alignment Search Tool) (http://www.ncbi.nlm.nih.gov/tools/primer-blast/) was used to design specific primer sequences for each gene of interest in *Mus musculus* (taxid:10088) (Ye et al. 2012). PCR amplicon size was restricted to ~100-200 base pairs (with the exception of *Hprt*) and primers designed to span at least one intron on the corresponding genomic DNA. The generated primer sequences (synthesised by GeneWorks, Adelaide, SA, Australia) are listed in Table 4.1.

4.2.6 Optimisation of quantitative polymerase chain reaction (qPCR)

Preliminary qPCR runs were carried out to determine the specificity and efficiency of primers and to optimise PCR conditions. Magnesium chloride ($MgCl_2$) gradient tests were carried out at three different concentrations: 2 mM, 3 mM and 4 mM (Bioline, Alexandria, NSW, Australia). Following optimisation of each gene, a melt curve analysis from 70-99°C demonstrated a single PCR product (Figure 4.3A) which was confirmed to be the correct size by gel electrophoresis on a 1.5% agarose gel (Promega, Sydney, NSW, Australia) for 45 min at 110V (in 1x TAE buffer). Electrophoresed products were gel extracted using a QIAEX II gel extraction kit (Qiagen, Melbourne, VIC, Australia) and sequenced using Big Dye Terminator version 3.1 (Applied Biosystems, Mulgrave, VIC, Australia). Sequencing was carried out at the LotteryWest Biomedical Facility for Genomics, Perth, WA, Australia. This confirmed the identity of the PCR product in all amplicons. Final optimised PCR conditions are shown in Table 4.1.

4.2.7 qPCR

Quantitative PCR was performed in 10 µl reactions using the Rotorgene 6000 system (Corbett Research, Sydney, NSW, Australia). Each reaction contained 1 µl 10x Immolase buffer (Promega, Sydney, NSW, Australia), 0.2 µl 10 mM dNTPs (Promega, Sydney, NSW, Australia), 1/40,000 dilution of stock SYBR green (Molecular Probes, Eugene, OR, USA), 0.25 units of Immolase DNA polymerase (Promega, Sydney, NSW, Australia) and 0.2 µM of each forward and reverse primer (GeneWorks, Adelaide, SA, Australia). $MgCl_2$ concentrations for each reaction are detailed in Table 4.1. The PCR cycling conditions included an initial denaturation at 95°C for 10 min followed by amplification for 45 cycles at 95°C for 1 sec, an annealing temperature as specified in Table 4.1 for 15 sec; and 72°C extension for 5 sec.

4.2.8 Quantification of transcripts

External standards were generated from gel-extracted PCR products by 10-fold serial dilutions in elution buffer (1 - 10^{10}-fold dilutions; Figure 4.3B) and a standard curve for each gene constructed using Rotorgene software (Figure 4.3C). This standard curve was used to calculate the concentrations of the unknown samples.

Liver and adipose tissue samples were standardised against reference genes *Ppia*, *Sdha* and *Tbp* using the GE Norm algorithm (Vandesompele et al. 2002), whilst hypothalamic tissue samples were standardized against reference genes *Sdha*, *Hprt* and *Actβ*. All reference genes showed stable and constant expression across the 24-h period. Due to the large number of samples, common samples were included within all PCR runs from the same tissue to enable comparisons across multiple runs.

Table 4.1 PCR Conditions. Primer sequences, amplicon sizes, annealing temperatures (AT) and $MgCl_2$ concentrations used for RT-qPCR.

Gene	Forward/Reverse Primer sequence	Amplicon Size (bp)	AT (°C)	$MgCl_2$ (mM)
Clock	F, 5' - ACAACGCACACATAGGCCTTC– 3' R, 5' – TGGTGGTGCCCTGTGATCTA – 3'	175	60	3
Bmal1	F, 5' – CGTGCTAAGGATGGCTGTTC – 3' R, 5' – CTTCCCTCGGTCACATCCTA – 3'	166	60	3
Per1	F, 5' – TGCACTTCGGGAGCTCAAACTTC – 3' R, 5' – GTCCATGGCACAAGGCTCACC – 3'	169	59	2
Per2	F, 5' – AACAAATCCACCGGC – 3' R, 5' – CTCCGGTGAGACTCC – 3'	145	60	3
Cry1	F, 5' – AACGTCCCGAGCTGTAGCGGT – 3' R, 5' – GACGCTTCCCACTGCTGAGGC – 3'	139	60	2
Cry2	F, 5' – TGCCTCTCCTGCCGCCTCTT- 3' R, 5' – TGCGGTCCCAGGGGATCTGG – 3'	193	60	2
Rev-erbα	F, 5' – CGGGGCTCACTCGTCTCCCT – 3' R, 5' - GCTCGGGGAGGAGCCACTAGA – 3'	185	60	2
Rorα	F, 5' – CCCAACCGTGTCCATGGCAG – 3' R, 5' – TCCATCAATGCGTTTGGCAA – 3'	235	60	3

Gene	Forward/Reverse Primer sequence	Amplicon Size (bp)	AT (°C)	$MgCl_2$ (mM)
Crh	F, 5’ – AGGCATCCTGAGAGAAGTCC – 3’ R, 5’ – ACGACAGAGCCACCAGCAG – 3’	186	58	2
Pck1	F, 5’ – ATGAAGTTTGATGCCCAAGG – 3’ R, 5’ – ACCCCCATCGCTAGTCTCGG – 3’	100	60	2
G6Pase	F, 5’ – GGGCATCAATCTCCTCTGGG – 3’ R, 5’ – GTCCAGGACCCAATACG – 3’	100	60	2
Glut2	F, 5’ - TGGGCGGAATGGTCGCCTCAT – 3’ R, 5’ – GGGCTCCAGTCAATGAGAGGCT – 3’	102	60	2
Gk	F, 5’ – TTTGTGTCGCAGGTGGAGAG – 3’ R, 5’ – CACAATGTCGCAGTCGGC - 3’	102	60	2
Pk	F, 5’ – AGTCCCACACTTTGGAAGCA – 3’ R, 5’ – CTGGAGCCCCACTTAAAGCA – 3’	116	60	2
Pygl	F, 5’ – CCTATGGCTACGGCATTCGT – 3’ R, 5’ – TCTCCCAAGGGTTTCCATGC – 3’	111	60	2
Gys2	F, 5’ –CAGACACCTGACACTGAGCA – 3’ R, 5’ – CCTCCTCTTCATCATACCTC – 3’	200	60	2
Lpl	F, 5’ – CAGCAAGACCTTCGTGGTGA – 3’ R, 5’ – ATAATGTTGCTGGGCCCGAT – 3’	148	60	3

Gene	**Forward/Reverse Primer sequence**	**Amplicon Size (bp)**	**AT (°C)**	**$MgCl_2$ (mM)**
Lipe	F, 5’ – GGCTCACAGTTACCATCTCACC – 3’ R, 5’ – GAGTACCTTGCTGTCCTGTCC – 3’	107	60	3
Pnpla2	F, 5’ – CAACGCCACTCACATCTACGG – 3’ R, 5’ – TCACCAGGTTGAAGGAGGGAT – 3’	161	60	3
Pparγ	F, 5’ – AACTCTGGGAGATTCTCCTGTTGA – 3’ R, 5’ - CCTATGAGCACTTCACAAGAAGAAATT – 3’	131	58	4
Tbp	F, 5’ – GGGAGAATCATGGACCAGAA – 3’ R, 5’ – CCGTAAGGCATCATTGGACT – 3’	113	60	2
Ppia	F, 5’ – AGCATACAGGTCCTGGCATC – 3’ R, 5’ – TTCACCTTCCCAAAGACCAC – 3’	127	62	3
Sdha	F, 5’ – TGGGGAGTGCCGTGGTGTCA – 3’ R, 5’ – CTGTGCCGTCCCCTGTGCTG – 3’	149	60	2
Actβ	F, 5’ – TCCACACCCGCCACCAG – 3’ R, 5’ – GGCCTCGTCACCCACATAG – 3’	197	58	2
Hprt	F, 5’ – GCAGTACAGCCCCAAAATGG – 3’ R, 5’ – AGTCTGGCCTGTATCCAACAC – 3’	80	58	2

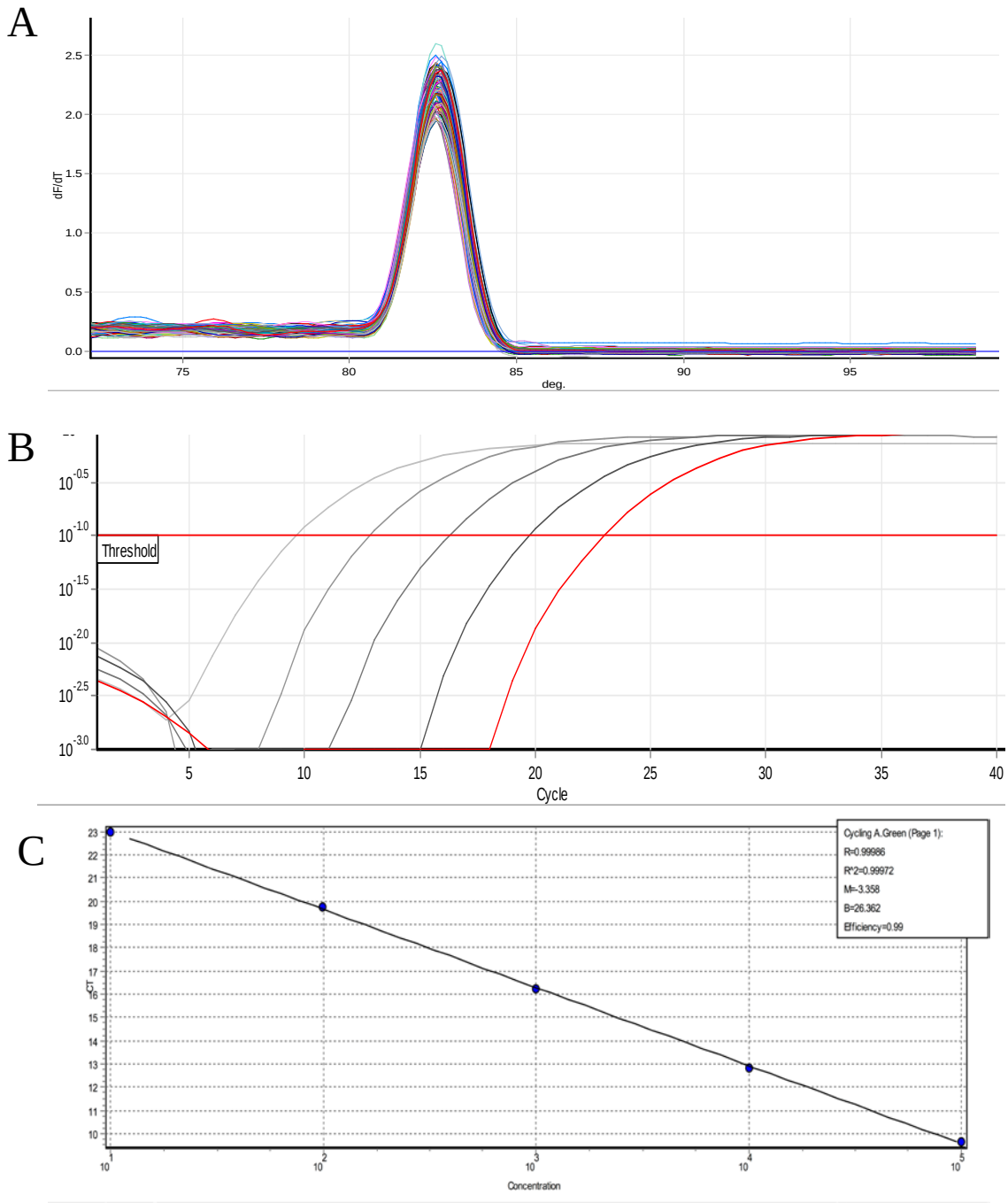

Figure 4.3 (A) Melt curve analysis, (B) standard amplification plot and (C) generated standard curve for *Bmal1* mRNA. For melt curve analysis, a single peak of amplified product was obtained for each sample. In the standard amplification plot, the threshold is indicated by the horizontal line and indicates the point at which all samples fall within the log-linear range of amplification. To generate a standard curve, the cycle number at which samples reach the log-linear phase of amplification is plotted against concentration, which enables concentration of unknown samples to be calculated.

4.3 Analysis of plasma adrenocorticotropic hormone (ACTH) and insulin

4.3.1 Background

Plasma ACTH and insulin concentrations were measured using Milliplex map assay kits produced by Millipore (Billerica, MA, USA; ACTH: CAT#MADKMAG-49K, Insulin: CAT#MADKMAG-71K). Multiplex assays consist of colour-coded beads, which are coated by a specific antibody that is able to bind and capture a specific analyte (i.e. ACTH or insulin). By including multiple beads, multiple assays can be conducted simultaneously on one sample. After binding of the analyte to the bead, a biotinylated detection antibody and reporter molecule (steptavidin-phycoerythrin) are added. The reporter molecule competes with the analyte to bind to the antibody. The resulting complex is passed through two lasers; the first excites the internal dyes, whilst the second excites the reporter molecule, which generates fluorescence. This allows the degree of analyte binding to be calculated and therefore, enables quantitation of the concentration of the analyte in the unknown samples.

4.3.2 Sample preparation

Plasma samples were thawed on ice and centrifuged at 13,000 x *g* for 5 min prior to assay. All reagents were allowed to reach room temperature as per manufacturer's instructions.

4.3.3 Assay protocol

Standards were generated by 4-fold serial dilutions of the reconstituted standard stock (ACTH: mouse pituitary; Insulin: mouse adipokine) in assay buffer. This generated concentrations ranging from 2.4 to 10,000 pg/ml (Insulin: 12.2 to 12,500 pg/ml). The plate was blocked with 200 µl/well of assay buffer, sealed and agitated on a plate shaker for 10 min at room temperature, after which the assay buffer was decanted and plate blotted to remove residual fluid. Each standard (ACTH: 25 µl; Insulin: 10 µl) was aliquoted in duplicate into the appropriate wells; 25 µl (Insulin: 10 µl) of assay buffer was used instead of standard, for the background wells. Reconstituted quality controls QC1 and QC2 (ACTH: 25 µl; Insulin: 10 µl) were also aliquoted in duplicate into the appropriate wells. Serum matrix (ACTH: 25 µl; Insulin: 10 µl; 0.08% Sodium Azide) was added to wells containing background, standards and quality controls. Prepared

plasma samples (10 µl) were aliquoted into the sample wells and in the ACTH assay made up to 50 µl with serum matrix. Antibody-immobilized beads (25 µl) were added to all wells, after which the plate was sealed, wrapped in foil and incubated with agitation on a plate shaker overnight (18-h) at 4°C. The following morning, the plate was washed by placing it on a hand-held magnet for 60 sec to allow for settling of the magnetic beads, after which the well contents were decanted and the plate gently tapped on absorbent paper towels. Wash buffer (200 µl of 10x; 0.05% Proclin) was added to all wells and agitated on a plate shaker for 30 sec. The plate was then reattached to the magnet and the wash procedure repeated once more (Insulin: twice more). Detection antibodies (50 µl) were aliquoted into each well and the plate was sealed, wrapped in foil and incubated with agitation on a plate shaker for 1-h at room temperature (Insulin: 30 min). The reporter molecule, streptavidin-phycoerythrin, was added to each well (50 µl) prior to a further 30 min incubation on a plate shaker at room temperature. Plate washing was repeated twice more (Insulin: three times) before 100 µl of drive fluid was added to all wells and beads were resuspended on a plate shaker for 5 min. The plates were read using a MAGPIX plate reader and analysed using xPONENT software (Merck Millipore, Billerica, MA, USA). This enabled the generation of a standard curve for each analyte (e.g. Figure 4.4), which was used to determine the concentration of ACTH and insulin in the unknown samples. Common samples were included in all plates to allow for comparison between runs. Quality controls fell within the expected ranges for all plates and the intra- and inter- assay coefficients for ACTH were 3.9% and 7.4%, respectively and for insulin were 7.1% and 16.9%.

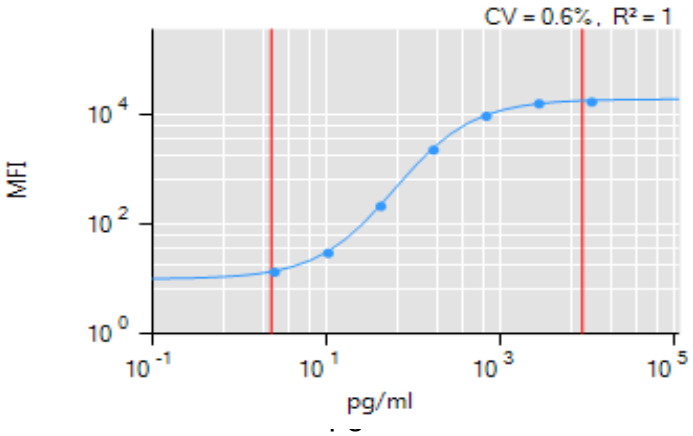

Figure 4.4 Standard curve for plasma ACTH quantitation. Values for 7 standards are shown with fluorescence (MFI) plotted against concentration (pg/ml).

4.4 Analysis of hepatic glycogen content

4.4.1 Background

Hepatic glycogen concentrations across pregnancy were assessed using a glycogen colorimetric assay produced by BioVision Inc. (Milpitas, CA, USA; CAT#K646-100). This assay relies on the ability of glucoamylase to hydrolyze glycogen to glucose, which is then specifically oxidized to produce a product that reacts with OxiRed probe. The colour produced can then be detected by spectrophotometry and is proportional to the amount of glycogen in the sample.

4.4.2 Sample preparation

Liver tissue (10 mg) was homogenized in 400 µl ddH_20 using the POLYTRON-Aggregate homogeniser (Kinematica Inc., Bohemia, NY, USA). Samples were heated to 95°C for 10 min, before centrifugation at 18,000 x *g* for 10 min.

4.4.3 Assay protocol

A stock standard solution was generated by an initial 10-fold dilution of the provided glycogen stock solution in MilliQ water (Merck Millipore, Billerica, MA, USA). Working standards were generated by adding 0, 1, 2, 3, 4 or 5 µl of diluted standard to a series of wells. Volumes within these wells were made up to 25 µl with hydrolysis buffer. The highest and lowest standards were aliquoted in duplicate. Prepared liver samples (1.5 µl) were aliquoted in duplicate and made up to 25 µl with hydrolysis buffer. Hydrolysis enzyme mix (1 µl) was added to standards and the first duplicate of each sample. No hydrolysis enzyme was added to the second duplicate to control for free glucose within the sample. The plate was mixed on a plate shaker and incubated for 30 min at room temperature. The reaction was initiated by adding 25 µl of reaction mix (23 µl development buffer, 1 µl development enzyme mix, 1 µl OxiRed Probe) to each well. The plate was mixed on a plate shaker and incubated for 30 min at room temperature, protected from light. The plates were then read at 570 nm on a BioTek ELx808 absorbance reader (BioTek Instruments Inc., Winooski, VT, USA).

The reading for the 0 standard was subtracted from each standard and sample reading. A standard curve was generated using Microsoft Excel software by plotting the adjusted standard readings against known concentrations (Figure 4.5). A line of best fit for the

standard curve was derived via the least squares method and used to calculate the concentrations of unknown samples (µg/well). The amount of glycogen (µg) in the homogenate was calculated from the known concentration (µg/well) by dividing by 1.5 (to get the µg of glycogen per µl of sample) and multiplying by 400 (to get the µg of glycogen in the whole homogenate). This concentration was then divided by the initial liver sample weight (g) and the free-glucose control was subtracted from the calculated concentration to obtain µg glycogen/g tissue.

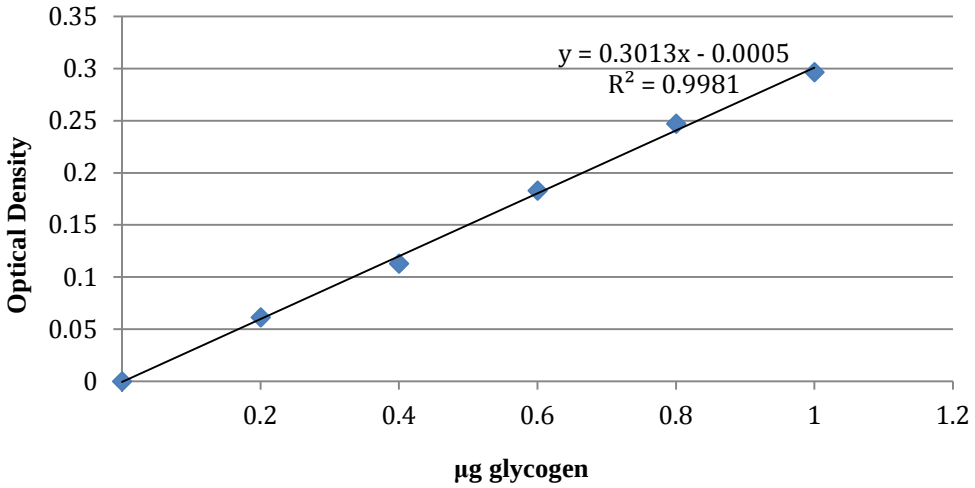

Figure 4.5 Standard curve for hepatic glycogen quantitation. Values for 6 standards with optical density plotted against concentration (µg glycogen).

4.5 Analysis of plasma corticosterone, 11-dehydrocorticosterone (11-DHC) and progesterone by LC-MS/MS

4.5.1 Background

Plasma corticosterone, 11-DHC and progesterone concentrations were analysed using liquid chromatography tandem mass spectrometry (LC-MS/MS) with the kind assistance of Assistant Professor Michael Clarke (Centre for Metabolomics, Perth, WA, Australia). The LC-MS/MS methodology is considered the 'gold standard' for measurement of plasma steroids, in part because it avoids the possibility for analyte cross-reaction that can occur in immunoassays. LC-MS/MS allows for the separation, identification and quantification of components of a complex mixture. The initial phase of LC-MS/MS is liquid chromatography, which allows for the separation of components within a mixture by introducing the sample into a mobile phase, which is then passed

through a column, known as the stationary phase. Components of the mixture move through the column at different velocities; the time at which the analyte elutes from the column is known as its retention time and is specific to each analyte. Mass spectrometry then allows for the identification of the resulting analyte by measuring its mass-to-charge ratio after ionization.

4.5.2 Sample preparation

Briefly, 50 µl of internal standard (Cortisol d4, 50 ng/ml; Progesterone d9, 5 ng/ml) was added to 50 µl of plasma or standard and subsequently vortexed in a glass tube. Steroids were extracted from plasma into methyl tertiary butyl ether (1 ml) by vigorous vortexing for 120 sec, before centrifugation for 5 min at 850 x *g*. Supernatant (900 µl) was transferred into an ultra high performance liquid chromatography (UPLC) injector vial, and then dried in a centrifugal vacuum evaporator for 30 min at 40°C. The analytes were resuspended in 70 µl of mobile phase (70% methanol, 0.1% formic acid, 29.9% water) before heating at 50°C for 10 min. During method development, recovery was assessed by spiking pure standards into test serum samples and measuring the response. The recovery, adjusted by the labelled internal standard, was between 98-103% of the predicted value for all analytes.

4.5.3 Protocol

Tandem MS was performed by injection of the sample (20 µl) onto an Agilent 6460 Triple Quadrupole mass spectrometer system coupled to 2 x 1290 UPLC series LC pumps. The LC system was run in two-dimensional mode, consisting of two columns; the first an Agilent Poroshell 120 EC-C18, 2.7 υm, 2.1 x 50 mm column (Agilent Technologies, Santa Clara, CA, USA). The second column was a Phenomenex Kinetex C18, 2.6 υm, 3.0 x 150 mm column (Phenomenex, Torrance, CA, USA). Mobile phase (A) comprised of Optima LCMS grade water (Thermo Fisher Scientific, Scoresby, VIC, Australia) + 0.1% formic acid and (B) Burdick and Jackson LCMS grade methanol (Chem-Supply, Gillman, SA, Australia) + 0.1% formic acid. The mobile phase flow rate was 0.2 ml/min through both columns and molecules were “heart cut” from column 1 to column 2 between a 1-2 min time window. A gradient was applied to both columns as follows; t = 0, 70% Burdick and Jackson LCMS grade methanol (B); t = 5, 80% B; t = 7, 98% B; t = 8, 98% B; t = 8.5, 60% B; t = 9, 70% B, t = 11, 70% B.

The MS system was operated in positive ionization mode and operating conditions were: gas temperature at 275°C, gas flow at 5 l/min, nebulizer pressure at 50 psi, sheath gas temperature at 325°C, sheath gas flow at 11 l/min, capillary voltage at 4000 V and charging voltage at 500 V. The following transitions were monitored during each data acquisition, Cortisol 363.2 → 121.0, Cortisol d4 367.2 → 121.0, 11- DHC 345.2 → 121.0, Corticosterone 347.3 → 329.1, Progesterone 315.3 → 109.2, Progesterone d9 324.3 → 100.2. Cortisol d4 was used as the internal standard for both 11-DHC and corticosterone and gave calibration curves with $r^2 > 0.999$ in both cases.

Assay precision was assessed during each batch by spiking EDTA plasma with compounds of interest, which were then used as quality controls. Intra- and inter-assay coefficients of variation for corticosterone were 1.4% and 9.7%, respectively, for 11-DHC were 3.2% and 17.5% and for progesterone were 0.3% and 7.7%.

Data were processed using Agilent MassHunter™ quantitative software.

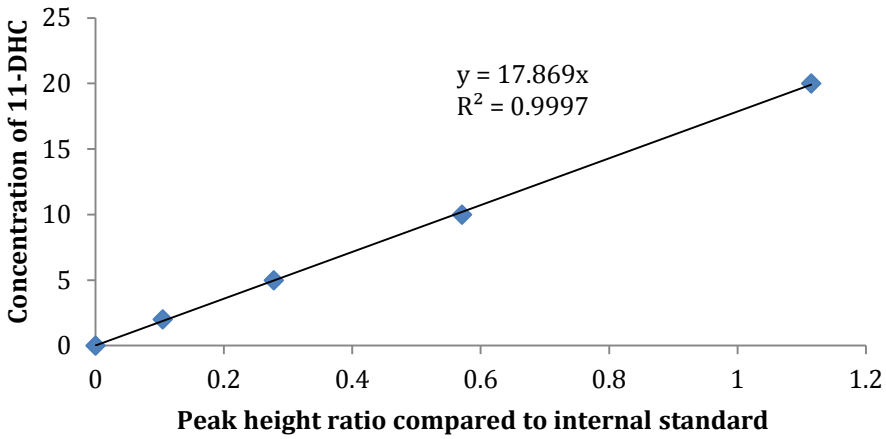

Figure 4.6 Standard curve for 11-DHC quantitation. Values for 5 standards are shown where concentration of 11-DHC is plotted against peak height ratio to internal standard.

4.6 Statistical analysis

All data are expressed as a mean ± SEM. Statistical analyses were conducted using GraphPad Prism 6.0 (GraphPad Software, La Jolla, CA, USA). When the data were not normally distributed (determined by D'Agostino and Pearson Omnibus normality test) values were log transformed before further analysis. For clarity of graphical presentation, all data are shown as untransformed values.

Two-way ANOVA was used to compare clock gene expression in non-pregnant mice and across pregnancy (with time-of-day and stage-of-pregnancy as factors). Similar analyses were carried out for downstream gene expression, hepatic glycogen and plasma concentrations of ACTH, corticosterone, 11-DHC, glucose, insulin and progesterone. When a significant interaction was observed between factors, time-of-day variation within each day was assessed by one-way ANOVA.

Assessment of circadian rhythmicity was made by cosinor analysis (Genstat Version 9, VSN International Ltd, Hemel Hempstead, UK), which is a sinusoidal approximation using a cosine function. Cosinor analysis approximates the following equation to experimental data using the least squares non-linear regression method:

$$y = M + A \times \cos((2\pi/TAU) \times (ZT - \Phi))$$

where y is the measured variable, M is the mesor (circadian rhythm adjusted mean),
A is the amplitude, ZT is the temporal fraction of the cycle, Φ is the acrophase (time of the peak of a rhythm) and TAU is the chosen period which in this case was 24 h (see Figure 4.7). A coefficient of determination (r^2) for non-linear functions was used as an index of cosinor rhythmicity. One-way ANOVA (GraphPad Prism 6.0, La Jolla, CA, USA) was used to determine whether each of the cosinor descriptors (mesor, amplitude and acrophase) varied with stage-of-pregnancy. For all ANOVAs, where the *F* test was significant ($P < 0.05$), *post hoc* LSD tests were used for pairwise comparisons. Gene expression is presented as relative to non-pregnant mesor levels, which were adjusted to 100.

Relationships between clock genes and downstream genes of interest in the liver and adipose tissue, as well as clock genes and corticosterone, were assessed by linear regression analysis (see Chapters 5-7 for specific applications).

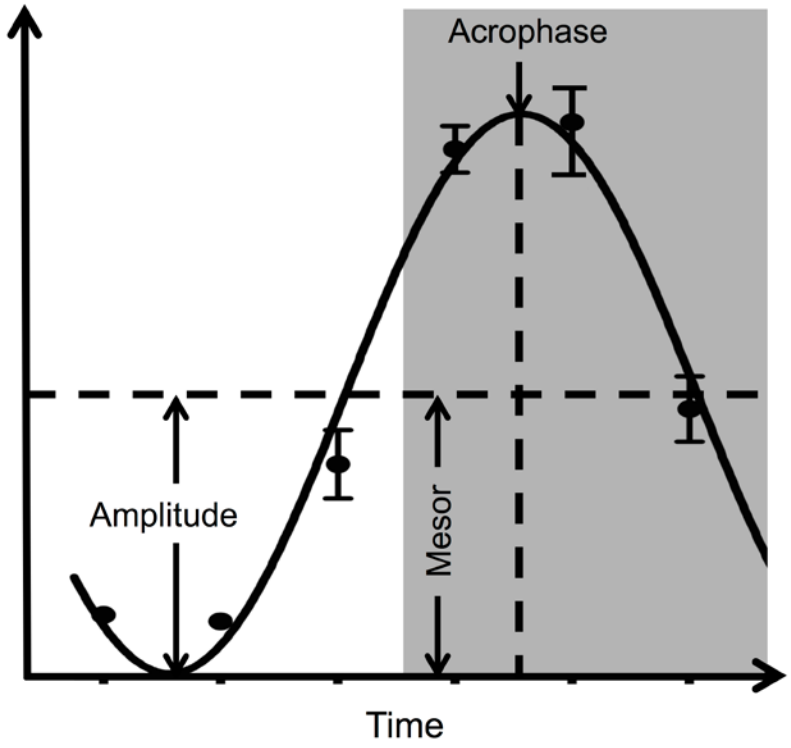

Figure 4.7 Schematic of a cosine curve with the circadian descriptors mesor, amplitude and acrophase. Adapted from Benavides (1998).

Chapter 5

Pregnancy-induced adaptations of the central circadian clock and maternal glucocorticoids

Preface

The major objective of this chapter was to investigate the effect of pregnancy on clock gene expression within the anterior hypothalamus, the location of the central circadian clock. Furthermore, as circadian variation of the hypothalamic-pituitary-adrenal (HPA) axis is dependent upon the rhythmic expression of clock genes within this central clock, a key focus was to determine whether changes in hypothalamic clock gene expression are linked to altered HPA axis activity during pregnancy.

This chapter was co-authored with Peter J. Mark, Caitlin S. Wyrwoll, Jeremy T. Smith, Cassandra Yap, Michael W. Clarke and Brendan J. Waddell and accepted for publication by the Journal of Endocrinology [vol. 228, no. 3, pp. 1-14] in December, 2015.

Michaela Wharfe performed all animal work and tissue sampling and was responsible for all of the analyses excluding the LC-MS/MS analysis and RNA extraction, representing about 75% of the laboratory work. Michaela Wharfe was also largely responsible (80%) for writing and submitting the manuscript.

5.1 Abstract

Maternal physiological adaptations, such as changes to the hypothalamic-pituitary-adrenal (HPA) axis, are central to pregnancy success. Circadian variation of the HPA axis is dependent upon clock gene rhythms in the hypothalamus, but it is not known if pregnancy-induced changes in maternal glucocorticoid levels are mediated via this central clock. We hypothesized that hypothalamic expression of clock genes changes across mouse pregnancy and this is linked to altered HPA activity. The anterior hypothalamus and maternal plasma were collected from C57Bl/6J mice prior to pregnancy and on days 6, 10, 14 and 18 of gestation (term = d19), across a 24-h period (0800, 1200, 1600, 2000, 0000, 0400 h). Hypothalamic expression of clock genes and *Crh* were determined by qPCR, plasma ACTH measured by Milliplex assay and plasma corticosterone by LC-MS/MS. Expression of all clock genes varied markedly across gestation, most notably at mid-gestation when levels of each gene were elevated. The pregnancy-induced increase in maternal corticosterone levels (by up to 14-fold on day 14) was not accompanied by a parallel shift in plasma ACTH (28% lower on day 14 compared with non-pregnant). Moreover, while circadian rhythmicity in corticosterone was maintained up to day 14 of gestation, this was effectively lost by day 18. Overall, our data show that the central circadian clock undergoes marked adaptations throughout mouse pregnancy, changes that are likely to contribute to maternal physiological adaptations. Importantly, however, neither hypothalamic clock genes nor plasma ACTH appear to drive the marked increase in maternal corticosterone after mid-gestation.

5.2 Introduction

Maternal physiological adaptations are central to pregnancy success, balancing fetal and placental demands with the maintenance of maternal homeostasis. Among these maternal adaptations, enhanced activity of the hypothalamic-pituitary-adrenal (HPA) axis after mid-gestation leads to increased glucocorticoid levels (Patrick et al. 1980; Atkinson & Waddell 1995). This HPA axis adaptation is crucial because it promotes the release of energy stores to meet high fetal demand (Atkinson & Waddell 1995), yet the regulation of HPA axis function in pregnancy remains poorly understood. The HPA axis is driven principally by corticotropin releasing hormone (CRH) released from the paraventricular nucleus (PVN), which stimulates pituitary secretion of adrenocorticotropic hormone (ACTH). In turn, ACTH stimulates adrenocortical secretion of glucocorticoids (cortisol in humans and corticosterone in rodents), which exert negative feedback effects at the hypothalamus and pituitary (Spiga et al. 2014). In pregnancy, the placenta may also provide direct trophic support to stimulate adrenal glucocorticoid secretion (Waddell 1993; Waddell & Burton 1993).

An additional feature of HPA axis function is its robust circadian variation, driven in part by the rhythmic expression of clock genes in the suprachiasmatic nucleus (SCN) (Nader, Chrousos & Kino 2010). These clock genes (*Bmal1*, *Clock*, *Per1*, *Per2*, *Cry1* and *Cry2*) form a molecular network of transcriptional-translational loops to drive their own rhythmic expression and that of downstream targets including CRH (via efferent projections from the SCN to the PVN) (Nader, Chrousos & Kino 2010). In the core oscillatory loop, a CLOCK-BMAL1 protein heterodimer activates the transcription of *Per* and *Cry* genes. This is followed several hours later by an accumulation of PER and CRY proteins, which form complexes in the cytoplasm. These complexes translocate to the nucleus where they associate with the CLOCK-BMAL1 heterodimer and thereby inhibit transcription of *Per* and *Cry* genes. The resultant fall in PER and CRY removes their negative feedback and the cycle is reinitiated. An accessory loop involves two transcription factors, *Rev-erbα* and *Rorα*, which have opposite effects on *Bmal1* transcription (inhibitory and stimulatory respectively) (Hastings, O'Neill & Maywood 2007).

In addition to this central clock, circadian variation in physiology is mediated via similar clock gene networks in key metabolic tissues, referred to as ‘peripheral clocks’.

The circadian rhythm of circulating glucocorticoids (generated via the HPA axis) provides a key coordination link between the central SCN clock and these peripheral clocks (Hastings, O'Neill & Maywood 2007), and as such plays a crucial role in overall metabolic homeostasis. Accordingly, changes in clock gene networks likely mediate maternal physiological adaptations to pregnancy. One previous report showed that peak PER2 expression in the SCN was phase advanced by 4-h at day 6 of gestation in the rat (Schrader, Nunez & Smale 2010). Whether pregnancy also alters expression of other clock genes, or if such changes influence downstream physiology including the HPA axis is unknown. Such changes may have important implications for pregnancy success, since circadian disruption is known to adversely affect fetal growth and developmental programming outcomes (Varcoe et al. 2011). In this study, therefore, we tested the hypothesis that hypothalamic expression of clock genes changes with the onset and progression of pregnancy, and that these changes are linked to altered HPA activity. Hypothalamic expression of clock genes and *Crh* and plasma ACTH and corticosterone levels were measured at six time points across the circadian day in the non-pregnant female mouse and at days 6, 10, 14 and 18 of mouse pregnancy.

5.3 Materials and Methods

5.3.1 Animals

Nulliparous C57Bl/6J mice (6-9 weeks old) were supplied by the Animal Resources Centre (Murdoch, Australia). All procedures involving the use of animals were conducted after approval by the Animal Ethics Committee of The University of Western Australia (AEC number RA/3/100/1070). Mice were maintained in two environmentally controlled rooms, with food and water supplied *ad libitum.* In one room mice were exposed to a normal 12:12 light/dark cycle (lights on at 0700 h); in the other room the light cycle was reversed (lights on for 12h from 1900 h). Between 0700 and 1900 h these mice were exposed to a constant red light (36 W, 620 nm). Preliminary studies showed no effect of exposure to red light on clock gene expression (unpublished observations). Both groups of animals were allowed to acclimatise to their respective light cycle for two weeks before any experimental procedures were conducted. Lights on at 0700 h (or 1900 h in the reverse-light room) was classified as a new day and as zeitgeber time (ZT)-zero, and sampling times were defined relative to ZT-zero. Female mice were mated overnight, and pregnancy was confirmed by visualization of a mucous plug the following morning (designated day 1 of pregnancy). In a separate group of non-pregnant mice, cycle stage was monitored for a minimum of three full estrous cycles by vaginal lavage (between ZT6 and 13) by the protocol of Caligioni (2009). Animals with irregular cycles were excluded.

5.3.2 Tissue collection

Tissues and plasma were collected from mice under isoflurane/nitrous oxide anaesthesia (0.2:0.8) at 4-h intervals commencing at ZT1 on either diestrus I of the cycle or day 6, 10, 14 or 18 of pregnancy (term = day 19). For collection of tissues in the dark phase, mice were anesthetized under red light then covered with a light-proof hood before collection of tissues under white light. In all mice a blood sample was obtained under anaesthesia by cardiac puncture (into an EDTA tube), and the whole brain was collected and frozen on crushed dry ice. Maternal blood was centrifuged and plasma and brains stored at -80 °C.

5.3.3 RNA sample preparation

Dissection of the anterior hypothalamus was carried out on dry ice, according to the protocol of Quennell (2011). Total RNA was extracted from the anterior hypothalamus using QIAzol (Qiagen, Doncaster, Australia) according to the manufacturer's instructions. RNA was quantitated using the Nanodrop ND-1000 spectrophotometer (Thermo Scientific, Wilmington, DE) at 260 nm, before 1 μg of total RNA was reverse transcribed at 42°C for 110 min by Mouse Moloney leukemia virus reverse transcriptase with random hexamers (Promega, Sydney, Australia). The resultant cDNAs were purified using an ultra-clean PCR spin kit (MoBio Laboratories, Inc., Carlsbad, CA) as per manufacturer's instructions.

5.3.4 Real time PCR

Analyses of mRNA expression levels for *Clock, Arntl* which encodes for *Bmal1*, *Per1*, *Per2*, *Cry1*, *Cry2, Nr1d1* which encodes for *Rev-erbα*, *Rorα, Crh* and the reference genes succinate dehydrogenase subunit A (*Sdha),* hypoxanthine-guanine phosphoribosyltransferase *(Hprt)* and beta actin (*Actβ*) were performed by real-time PCR on the Rotorgene 6000 system (Corbett Research, Sydney, Australia). Primer pairs for all these genes (see Table 5.1) were designed using Primer-BLAST (http://www.ncbi.nlm.nih.gov). All primer pairs were designed to span introns to prevent amplification of product from genomic DNA. The resulting amplicons were separated on 1.5% agarose gel containing ethidium bromide and sequenced to confirm specificity. Standard curves were created with 10-fold serial dilutions of gel-extracted (QIAEX II:Qiagen, Doncaster, Australia) PCR products and using the Rotorgene 6000 software. All samples were normalized against *Sdha, Hprt* and *Actβ* using the GeNorm algorithm (Vandesompele et al. 2002).

5.3.5 Measurement of plasma corticosterone and 11-dehydrocorticosterone (11-DHC)

Plasma corticosterone and 11-DHC concentrations were analysed using liquid chromatography tandem mass spectrometry (LC-MS/MS). The internal standard (IS) for both metabolites was cortisol d4. Briefly, 50 μl of IS (50 ng/mL) was added to 50 μl of plasma or standard and subsequently vortexed in a glass tube. Steroids were extracted into methyl tertiary butyl ether (1 ml) by vigorous vortexing. The supernatant was transferred into an ultra high performance liquid chromatography (UPLC) injector vial,

and then dried in a centrifugal vacuum evaporator. The analytes were resuspended in 70 µl of mobile phase (70% methanol, 0.1% formic acid, 29.9% water) before heating at 50°C for 10 min. Sample (20 µl) was injected onto an Agilent 6460 Triple Quadrupole mass spectrometer system coupled to 2 x 1290 UPLC series LC pumps. The LC system was run in 2D mode, consisting of two columns; the first an Agilent Poroshell 120 EC-C18, 2.7υm, 2.1 x 50 mm column (Agilent Technologies, Santa Clara, CA); the second was a Phenomenex Kinetex C18, 2.6 υm, 3.0 x 150 mm column (Torrance, CA). The mobile phase flow rate was 0.2 mL/min through both columns and molecules were "heart cut" from column 1 to column 2 between a 1-2 min time window. The instrument was operated in positive ionization mode. Assay precision was assessed during each batch by spiking EDTA plasma with compounds of interest, which were then used as quality controls. Intra- and inter-assay coefficients of variation for corticosterone were 1.4% and 3.2%, respectively, and for 11-DHC were 9.7% and 17.5%.

5.3.6 Measurement of plasma ACTH

Plasma ACTH concentrations were measured using a Milliplex Map assay kit (Cat#MADKMAG-49K; Merck Millipore, MA, USA). Samples were centrifuged at 13,000 x *g* for 5 min prior to analysis. The assay was performed as per manufacturer's instructions. Plates were read using a MAGPIX plate reader and analysed using xPONENT software (Merck Millipore, MA, USA). Intra- and inter-assay coefficients of variation for ACTH were 3.9% and 7.4% respectively. Values are expressed as pg/ml.

5.3.7 Statistical analysis

All data are expressed as a mean ± SEM, with an *n* of 6-8 per ZT on each day of pregnancy. Where data was not normally distributed (based on D'Agostino & Pearson omnibus normality test), values were log transformed prior to statistical analysis. Two-way ANOVA was used to compare hypothalamic clock gene expression in non-pregnant and pregnant mice (with time-of-day and pregnancy stage as factors). When a significant interaction was observed, time-of-day variation within each day was assessed by one-way ANOVA.

Circadian rhythms were assessed by cosinor analysis using a nonlinear regression model (Genstat Version 9, VSN International Ltd, Hemel Hempstead, UK). This analysis

generated the following rhythm descriptors: mesor (circadian rhythm adjusted mean), amplitude, acrophase (time of the peak of a rhythm) and cosinor r^2. One-way ANOVA (GraphPad Prism 6.0, GraphPad Software, San Diego, CA) was used to determine whether each of these cosinor descriptors varied with stage of pregnancy. For all ANOVAs, where the *F* test was significant ($P < 0.05$), *post hoc* LSD tests were used for pairwise comparisons. Relationships among corticosterone, clock genes and ACTH were assessed by linear regression analysis (GraphPad Prism 6.0, GraphPad Software, San Diego, CA).

For all results, differences attributable to time-of-day and day of pregnancy assessed by ANOVA are presented first. Where there is a significant effect of time, subsequent cosinor analyses are presented to determine the impact of day of pregnancy on circadian characteristics.

Table 5.1 Primers and PCR conditions used to measure hypothalamic clock genes *Crh*, and reference genes by RTq-PCR.

Gene	Forward/Reverse Primer sequence	Amplicon Size (bp)	Annealing Temp (°C)	$MgCl_2$ (mM)
Clock	F, 5' - ACAACGCACACATAGGCCTTC– 3' R, 5' – TGGTGGTGCCCTGTGATCTA – 3'	175	60	3
Bmal1	F, 5' – CGTGCTAAGGATGGCTGTTC – 3' R, 5' – CTTCCCTCGGTCACATCCTA – 3'	166	60	3
Per1	F, 5' – TGCACTTCGGGAGCTCAAACTTC – 3' R, 5' – GTCCATGGCACAAGGCTCACC – 3'	169	59	2
Per2	F, 5' – AACAAATCCACCGGC – 3' R, 5' – CTCCGGTGAGACTCC – 3'	145	60	3
Cry1	F, 5' – AACGTCCCGAGCTGTAGCGGT – 3' R, 5' – GACGCTTCCCACTGCTGAGGC – 3'	139	60	2
Cry2	F, 5' – TGCCTCTCCTGCCGCCTCTT- 3' R, 5' – TGCGGTCCCAGGGGATCTGG – 3'	193	60	2
Rev-erbα	F, 5' – CGGGGCTCACTCGTCTCCCT – 3' R, 5' - GCTCGGGGAGGAGCCACTAGA – 3'	185	60	2
Rorα	F, 5' – CCCAACCGTGTCCATGGCAG – 3' R, 5' – TCCATCAATGCGTTTGGCAA – 3'	235	60	3
Crh	F, 5' – AGGCATCCTGAGAGAAGTCC – 3' R, 5' – ACGACAGAGCCACCAGCAG – 3'	186	58	2
Actβ	F, 5' – TCCACACCCGCCACCAG – 3' R, 5' – GGCCTCGTCACCCACATAG – 3'	197	58	2
Hprt	F, 5' – GCAGTACAGCCCCAAAATGG – 3' R, 5' – AGTCTGGCCTGTATCCAACAC – 3'	80	58	2
Sdha	F, 5' – TGGGGAGTGCCGTGGTGTCA – 3' R, 5' – CTGTGCCGTCCCCTGTGCTG – 3'	149	60	2

5.4 Results

5.4.1 Hypothalamic clock gene expression

Hypothalamic expression of all clock genes, with the exception of *Rorα*, varied with time-of-day ($P < 0.001$, ANOVA) and with stage of pregnancy ($P < 0.001$; Figure 5.1 and 5.2). Significant *time-of-day* x *stage of pregnancy* interactions were evident for *Bmal1* ($P < 0.001$), *Cry1* ($P < 0.001$) and *Rev-erbα* ($P < 0.05$), indicating that pregnancy influenced the circadian expression of these clock genes.

Cosinor analysis revealed highly significant circadian variation for hypothalamic expression of all clock genes, again with the exception of *Rorα* (see Table 5.2 for r^2 and *P* values). The resultant circadian characteristics (mesor, amplitude and acrophase) for clock gene expression across pregnancy are shown in Table 5.3. A common feature among all clock genes was elevated overall expression (i.e. mesor increased by up to 1.5-fold) by day 10 of pregnancy (Figure 5.1 and 5.2), consistent with the ANOVA data. Overall expression of *Bmal1*, *Per2* and *Rev-erbα* remained elevated beyond mid-pregnancy, whereas mesor levels for *Clock*, *Cry1* and *Cry2* fell by day 14 before increasing again near term (day 18). Interestingly, the amplitude of the *Rev-erbα* profile had increased by day 10 but then returned to pre-pregnancy levels by day 18, whereas amplitudes remained unchanged across pregnancy for all other clock genes (Figure 5.2). Finally, hypothalamic expression of *Per1* fell slightly with the onset and progression of pregnancy apart from a transient rise at day 10.

For the majority of clock genes the time of peak expression (acrophase) showed little change across pregnancy (Figure 5.1 and 5.2). The key exceptions were a 3-h phase advance for *Bmal1* between days 14 and 18 ($P < 0.05$) and a delay in the acrophase of *Rev-erbα* which occurred later in the day with the progression of pregnancy, shifting from approximately ZT8 in non-pregnant mice to ZT11 by day 18 of pregnancy ($P < 0.05$).

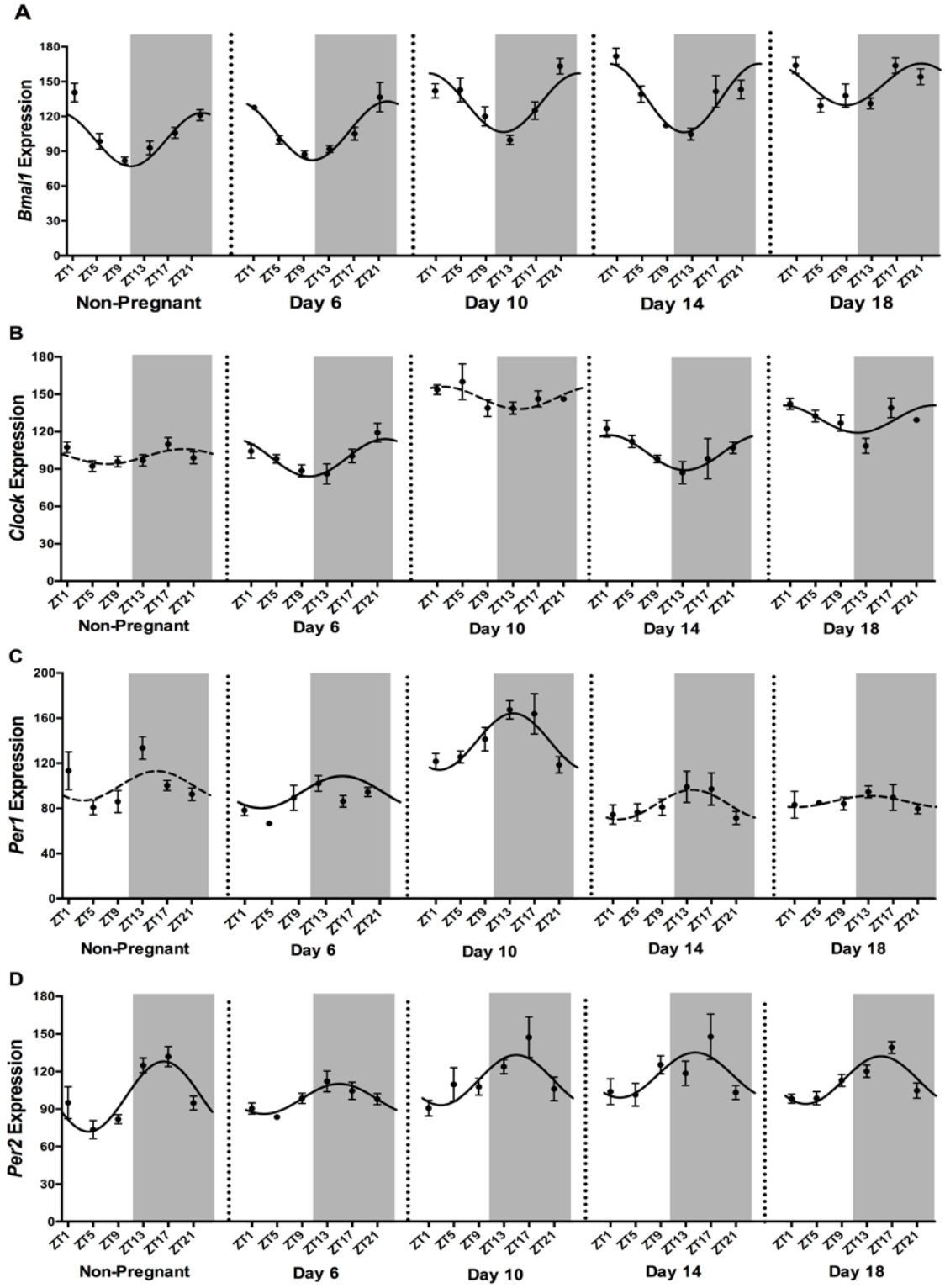

Figure 5.1 Hypothalamic expression of (A) *Bmal1*, (B) *Clock*, (C) *Per1* and (D) *Per2* at ZT1, 5, 9, 13, 17 and 21 in non-pregnant mice and in pregnant mice at days 6, 10, 14 and 18. Values are the mean ± SEM (n = 6-8/group). Grey shading represents the dark phase of the light cycle. The best-fit curve derived by cosinor analysis is shown as a solid line when significant ($P < 0.05$) and as a dashed line when non-significant.

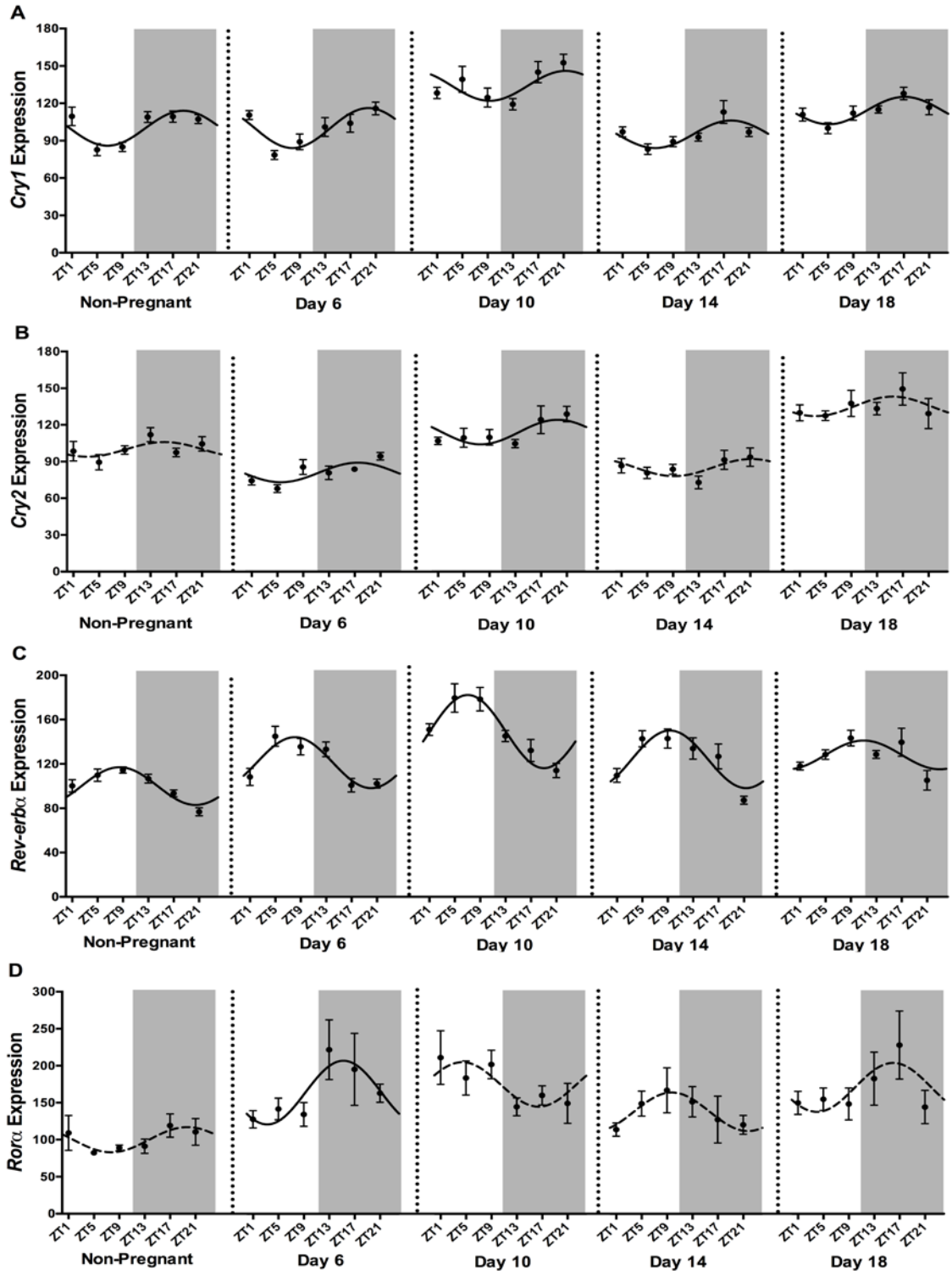

Figure 5.2 Hypothalamic expression of (A) *Cry1*, (B) *Cry2*, (C) *Rev-erbα* and (D) *Rorα* at ZT1, 5, 9, 13, 17 and 21 in non-pregnant mice and in pregnant mice at days 6, 10, 14 and 18. Values are the mean ± SEM (n = 6-8/group). Grey shading represents the dark phase of the light cycle. The best-fit curve derived by cosinor analysis is shown as a solid line when significant ($P < 0.05$) and as a dashed line when non-significant.

Table 5.2 Values for r^2 derived from cosinor analyses of anterior hypothalamic clock gene expression.

	Non-Pregnant	Day 6	Day 10	Day 14	Day 18
Bmal1	0.556	0.529	0.445	0.474	0.267
	($P < 0.0001$)	($P < 0.0001$)	($P < 0.0001$)	($P < 0.0001$)	($P = 0.0011$)
Clock	0.071	0.304	0.069	0.166	0.162
	(NS)	($P < 0.001$)	(NS)	($P < 0.05$)	($P < 0.05$)
Per1	0.066	0.190	0.342	0.092	0
	(NS)	($P < 0.05$)	($P < 0.0001$)	($P = 0.068$)	(NS)
Per2	0.496	0.278	0.196	0.146	0.497
	($P < 0.0001$)	($P < 0.001$)	($P < 0.05$)	($P < 0.05$)	($P < 0.0001$)
Cry1	0.364	0.333	0.127	0.243	0.267
	($P < 0.0001$)	($P < 0.0001$)	($P < 0.05$)	($P < 0.05$)	($P < 0.05$)
Cry2	0.044	0.159	0.107	0.055	0.004
	(NS)	($P < 0.05$)	($P < 0.05$)	(NS)	(NS)
Rev-erbα	0.546	0.461	0.525	0.414	0.143
	($P < 0.0001$)	($P < 0.0001$)	($P < 0.0001$)	($P < 0.0001$)	($P < 0.05$)
Rorα	0.083	0.127	0.061	0.073	0.051
	(NS)	($P < 0.05$)	(NS)	(NS)	(NS)

Relevant *P* values are shown in parentheses unless non-significant (NS).

Table 5.3 Mesor, amplitude and acrophase derived from cosinor analyses of anterior hypothalamic clock gene expression.

		Non-Pregnant	Day 6	Day 10	Day 14	Day 18	*P* value
Bmal1	Mesor	100 ± 2^{a}	102 ± 3^{a}	125 ± 3^{b}	129 ± 3^{b}	140 ± 3^{c}	<0.0001
	Amplitude	23 ± 3	24 ± 4	24 ± 4	28 ± 5	17 ± 4	NS
	Acrophase	22.8 ± 0.5^{ac}	22.4 ± 0.6^{ac}	23.8 ± 0.7^{bc}	23.7 ± 0.6^{bc}	20.4 ± 0.9^{a}	<0.05
Clock	Mesor	100 ± 2^{a}	99 ± 2^{a}	147 ± 3^{b}	103 ± 3^{a}	130 ± 3^{c}	<0.0001
	Amplitude	-	15 ± 3	-	14 ± 5	11 ± 4	NS
	Acrophase	-	22.2 ± 0.9	-	25.4 ± 1.3	23.8 ± 2.5	NS
Per1	Mesor	100 ± 4^{a}	86 ± 3^{b}	139 ± 4^{c}	83 ± 4^{b}	86 ± 3^{b}	<0.0001
	Amplitude	-	13 ± 4	25 ± 5	-	-	NS
	Acrophase	-	15.4 ± 1.2	13.6 ± 0.8	-	-	NS
Per2	Mesor	100 ± 3^{a}	98 ± 2^{a}	113 ± 4^{b}	117 ± 5^{b}	113 ± 2^{b}	<0.0001
	Amplitude	28 ± 5	12 ± 3	20 ± 6	18 ± 6	19 ± 3	NS
	Acrophase	16.3 ± 0.6	14.9 ± 0.9	14.9 ± 1.1	14.5 ± 1.3	15.2 ± 0.7	NS
Cry1	Mesor	100 ± 2^{a}	100 ± 2^{a}	134 ± 3^{b}	95 ± 2^{a}	114 ± 2^{c}	<0.0001
	Amplitude	14 ± 3	16 ± 3	12 ± 4	11 ± 3	11 ± 3	NS
	Acrophase	18.6 ± 0.8	19.8 ± 0.9	21.3 ± 1.5	18.2 ± 1.1	17.1 ± 1.1	NS
Cry2	Mesor	100 ± 2^{a}	81 ± 2^{b}	114 ± 3^{c}	85 ± 2^{b}	135 ± 4^{d}	<0.0001
	Amplitude	-	8 ± 3	10 ± 4	-	-	NS
	Acrophase	-	17.5 ± 1.3	19.6 ± 1.5	-	-	NS
Rev-erbα	Mesor	100 ± 2^{a}	121 ± 3^{b}	149 ± 3^{c}	124 ± 3^{b}	128 ± 3^{b}	<0.0001
	Amplitude	17 ± 2^{ac}	23 ± 4^{acd}	33 ± 5^{db}	26 ± 5^{cb}	13 ± 5^{a}	<0.05
	Acrophase	8.5 ± 0.6^{ac}	8.1 ± 0.7^{ac}	7.0 ± 0.6^{c}	9.3 ± 0.7^{ab}	11.0 ± 1.3^{b}	<0.05
Rorα	Mesor	100 ± 5^{a}	164 ± 11^{bc}	175 ± 10^{b}	138 ± 8^{c}	171 ± 13^{b}	<0.0001
	Amplitude	-	43 ± 16	-	-	-	-
	Acrophase	-	15.2 ± 1.4	-	-	-	-

Values are mean ± SEM and are expressed relative to the mesor value in the Non-Pregnant group (set at 100). Acrophase is expressed in clocktime. Within each group, values without common notation differ significantly ($P < 0.05$; one-way ANOVA and Fisher's LSD test).

5.4.2 Hypothalamic Crh expression

Surprisingly, *Crh* expression in the hypothalamus showed only a trend for variation with time-of-day ($P = 0.056$, ANOVA) but did vary markedly with stage of pregnancy ($P < 0.001$; Figure 5.3A). Post-hoc analysis demonstrated a clear peak in overall *Crh* expression at day 10 of pregnancy followed by a decline to non-pregnant levels at day 14 and 18. Consistent with the absence of significant time-of-day variation (by ANOVA), cosinor analysis of *Crh* expression showed no significant rhythmic variation at any stage (see Table 5.4 for r^2 and *P* values).

5.4.3 Plasma ACTH

Plasma ACTH varied significantly with time-of-day ($P < 0.05$, ANOVA) and stage of pregnancy ($P < 0.0001$), with a dramatic decline in levels observed by day 18 (83% lower than non-pregnant, Figure 5.3B).

Cosinor analysis showed highly significant circadian variation for plasma ACTH on days 6, 10 and 18 of pregnancy (see Table 5.4 for r^2 and *P* values). The mesor, amplitude and acrophase for these days of gestation are presented in Table 5.5. The mesor of plasma ACTH increased 1.3-fold between diestrus and early gestation (days 6 and 10), before decreasing by 43% on day 14 and a further 77% on day 18 ($P < 0.0001$, Figure 5.3B). While the amplitude did not change across pregnancy, the acrophase was delayed approximately 7-h by day 18 of pregnancy ($P < 0.001$, Table 5.5).

5.4.4 Plasma corticosterone

Plasma corticosterone varied with time-of-day ($P < 0.001$, ANOVA), with all profiles characterised by a daily peak soon after lights-off at ZT13 (Figure 5.3C). Pregnancy had a dramatic effect on absolute levels of plasma corticosterone ($P < 0.001$), with overall increases observed between non-pregnant and both day 14 (11-fold) and day 18 (14-fold). There was also a significant *time-of-day* x *stage of pregnancy* interaction ($P < 0.05$), indicating that the circadian variation in plasma corticosterone was influenced by the stage of pregnancy.

Cosinor analysis showed highly significant circadian variation for plasma corticosterone on days 6, 10 and 14 of pregnancy (see Table 5.4 for r^2 and *P* values). While there was

only a trend for cosinor rhythmicity prior to pregnancy, clear time-of-day variation existed within this group ($P < 0.05$, ANOVA) with a 2.3-fold increase in levels between ZT1 and ZT13 ($P < 0.01$, unpaired *t* test). Interestingly, rhythmic variation in corticosterone appeared to be lost by day 18, with high levels maintained across the full 24-h period. The derived mesor, amplitude and acrophase for plasma corticosterone at each stage of gestation are shown in Table 5.5. The mesor of plasma corticosterone was similar before and at days 6 and 10 of pregnancy, but had increased by approximately 10-fold 4 days later (at day 14; $P < 0.001$), and by another 1.2-fold by day 18 ($P < 0.001$; Figure 5.3C). The amplitude of the corticosterone rhythm displayed a similar pattern ($P < 0.001$), remaining unchanged up to day 10 but then increasing dramatically (almost 20-fold) by day 14 before falling by day 18 (but still 5.5-fold greater than before pregnancy) (Figure 5.3C). The acrophase of the corticosterone rhythm remained unchanged across pregnancy (Figure 5.3C).

5.4.5 Plasma 11-DHC

Plasma levels of the corticosterone metabolite 11-DHC generally paralleled the circadian pattern of corticosterone, varying with time-of-day ($P < 0.001$, ANOVA) and showing peak levels soon after lights-off. Plasma 11-DHC also varied with stage of pregnancy ($P < 0.001$; Figure 5.3D), and there was significant interaction between *time-of-day* x *stage of pregnancy* ($P < 0.05$).

As with plasma corticosterone, cosinor analysis showed highly significant circadian variation for plasma 11-DHC on days 6 and 14 of pregnancy (see Table 5.4 for r^2 and *P* values) with a trend for rhythmicity evident on day 10. The mesor remained relatively stable until day 10 but then increased more than 7-fold by days 14 and 18 ($P < 0.001$; Table 5.5, Figure 5.3D). The amplitude of the plasma 11-DHC rhythm increased 10-fold between days 6 and 14, but by day 18 rhythmic variation in 11-DHC was effectively absent (Figure 5.3D).

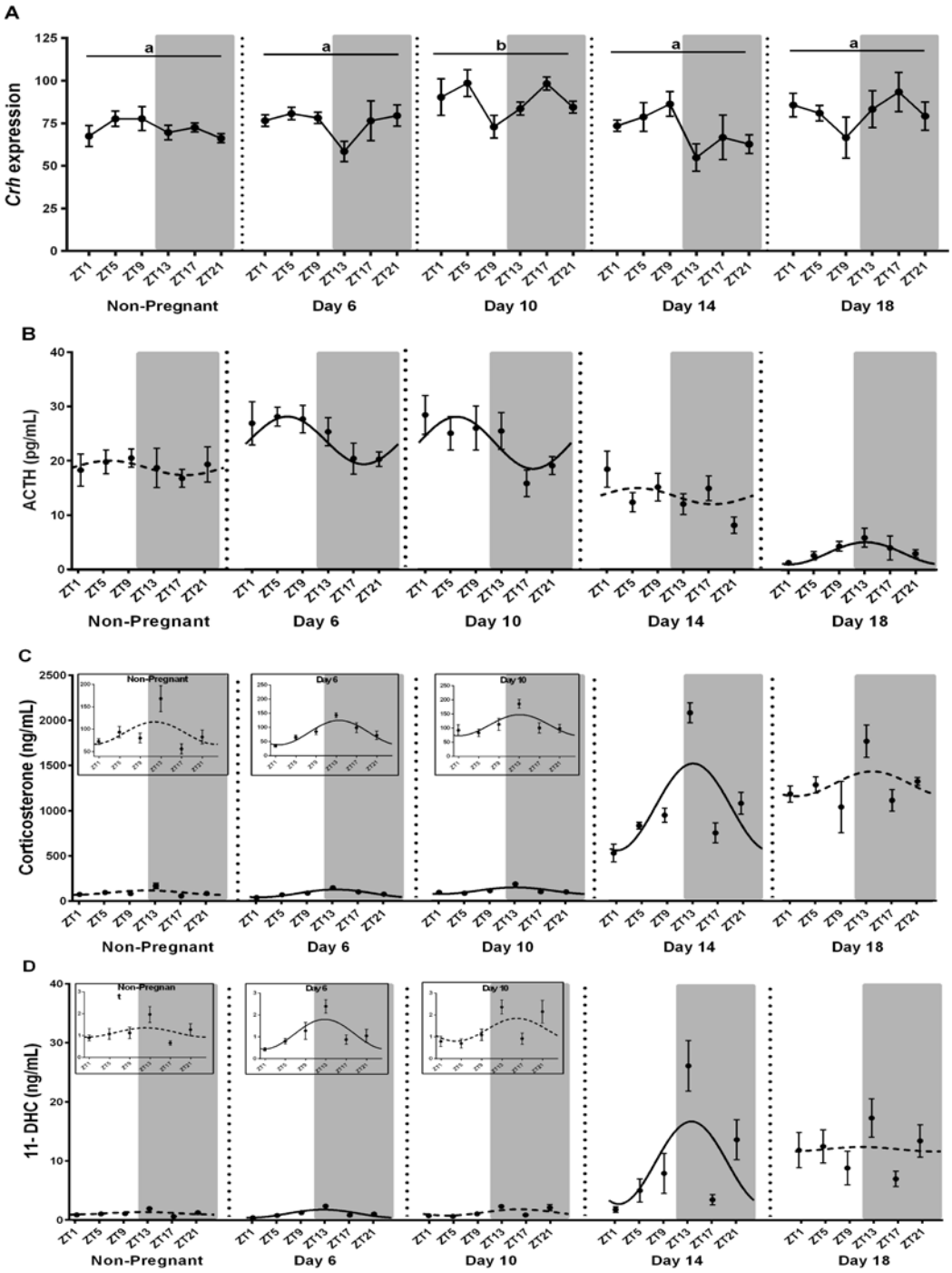

Figure 5.3 Hypothalamic expression of (A) *Crh* and plasma concentrations of (B) ACTH (pg/ml), (C) corticosterone (ng/ml) and (D) 11-DHC (ng/ml) at ZT1, 5, 9, 13, 17 and 21 in non-pregnant mice and pregnant mice at days 6, 10, 14 and 18. Values are the mean ± SEM (n = 6-8/group). Grey shading represents the dark phase of the light cycle. For *Crh* expression, cosinor curves are not shown since this analysis showed no statistical significance at any stage. For these profiles, values without common notation differ significantly ($P < 0.001$; two-way ANOVA and *post hoc* LSD test). For plasma corticosterone and 11-DHC, insets are included for non-pregnant and days 6 and 10 of pregnancy to show the same data on a reduced *y*-axis scale. The best-fit curve derived by cosinor analysis is shown as a solid line when significant ($P < 0.05$) and as a dashed line when non-significant.

Table 5.4 Values for r^2 derived from cosinor analyses of anterior hypothalamic expression of *Crh* mRNA, plasma ACTH, corticosterone and 11-DHC.

	Non-Pregnant	Day 6	Day 10	Day 14	Day 18
Crh	0.032 (NS)	0.037 (NS)	0 (NS)	0.089 (NS)	0.002 (NS)
ACTH	0 (NS)	0.160 ($P < 0.05$)	0.121 ($P < 0.05$)	0 (NS)	0.145 ($P < 0.05$)
Corticosterone	0.076 ($P = 0.089$)	0.435 ($P < 0.001$)	0.171 ($P = 0.004$)	0.344 ($P < 0.001$)	0 (NS)
11-DHC	0 (NS)	0.243 ($P < 0.001$)	0.081 (NS)	0.165 ($P < 0.05$)	0 (NS)

Relevant *P* values are shown in parentheses unless non-significant (NS).

Table 5.5 Mesor, amplitude and acrophase derived from cosinor analyses of plasma ACTH, corticosterone and 11-DHC and the calculated corticosterone to 11-DHC ratio across pregnancy.

		Non-Pregnant	Day 6	Day 10	Day 14	Day 18	*P* value
ACTH	Mesor (pg/ml)	18.7 ± 1.1[a]	23.8 ± 1.0[b]	23.3 ± 1.2[b]	13.5 ± 1.0[c]	3.1 ± 0.5[d]	<0.0001
	Amplitude (pg/ml)	-	4.4 ± 1.4	4.8 ± 1.7	-	2.0 ± 0.7	NS
	Acrophase	-	6.6 ± 1.3[a]	6.0 ± 1.4[a]	-	13.1 ± 1.5[b]	<0.001
Corticosterone	Mesor (ng/ml)	91.5 ± 7.8[a]	81.3 ± 5.0[a]	110.8 ± 7.7[a]	1038.2 ± 65.9[b]	1293.9 ± 69.5[c]	<0.0001
	Amplitude (ng/ml)	-	43.4 ± 7.2[a]	37.2 ± 11.0[a]	481.5 ± 93.3[b]	-	<0.0001
	Acrophase	-	13.5 ± 0.6	13.1 ± 1.1	13.1 ± 0.7	-	NS
11-DHC	Mesor (ng/ml)	1.14 ± 0.11[a]	1.13 ± 0.12[a]	1.33 ± 0.15[a]	9.73 ± 1.47[b]	12.02 ± 1.20[b]	<0.0001
	Amplitude (ng/ml)	-	0.68 ± 0.17[a]	-	6.98 ± 2.08[b]	-	<0.001
	Acrophase	-	12.8 ± 0.9	-	13.6 ± 1.1	-	NS
Ratio Corticosterone : 11-DHC		88 ± 14[a]	86 ± 11[a]	118 ± 19[a]	205 ± 36[b]	140 ± 26[a]	<0.05

Values are mean ± SEM. Within each group, values without common notation differ significantly ($P < 0.05$; one-way ANOVA and Fisher's LSD test).

5.4.6 Ratio of Corticosterone:11-DHC

The ratio of corticosterone to 11-DHC remained relatively stable until day 10 but then increased by day 14 (1.75-fold; $P = 0.002$), before returning to non-pregnant levels by day 18 (Table 5.5, Figure 5.4).

5.4.7 Correlations between plasma corticosterone and hypothalamic clock genes and plasma ACTH

We also explored possible relationships between clock gene expression and circulating corticosterone (Supplementary Table 5.1, see section on supplementary data given at the end of this article). Thus, plasma corticosterone was negatively correlated with hypothalamic *Bmal1* (at days 6 and 14 of pregnancy), *Clock* (days 6, 10, 14 and 18) and *Cry2* (day 14). In contrast, a positive association was observed between plasma corticosterone and *Rora* (at day 6). Finally, plasma ACTH was positively correlated with corticosterone only on day 10 of pregnancy.

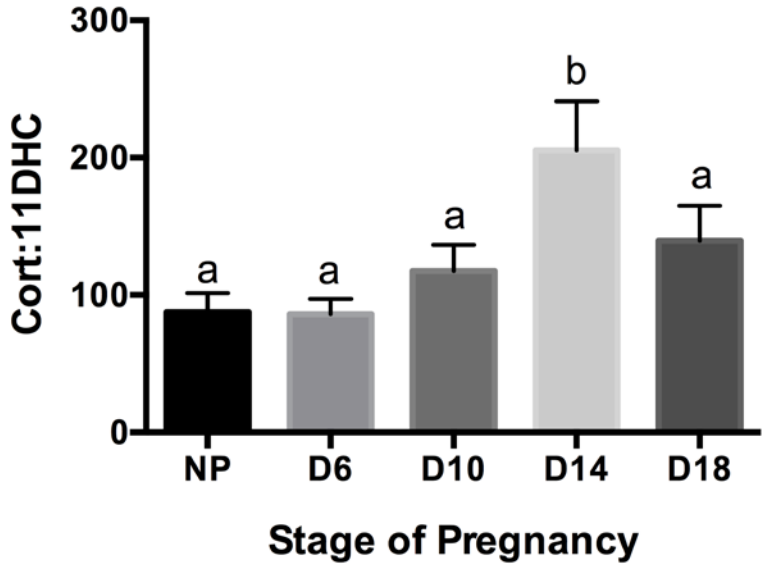

Figure 5.4 Ratio of corticosterone to 11-DHC in maternal plasma from non-pregnant and pregnant mice on days 6, 10, 14 and 18. Values are the mean ± SEM (n = 39-48/group). Values without common notation differ significantly (P = 0.002; one-way ANOVA and *post hoc* LSD test).

5.5 Discussion

This study demonstrates for the first time that the hypothalamic expression of the core (*Clock*, *Bmal1*, *Per1*, *Per2*, *Cry1* and *Cry2)* and accessory (*Rev-erbα* and *Rorα*) clock genes changes markedly during pregnancy in the mouse. Our data also characterise substantial shifts in absolute levels and circadian variation of plasma corticosterone and its key metabolite, 11-DHC, after mid-gestation. Importantly, the marked elevation in circulating glucocorticoids was not associated with comparable changes in either hypothalamic *Crh* mRNA expression or plasma ACTH, suggesting that higher corticosterone levels may be driven by factors beyond the conventional HPA axis (e.g. placental trophic support for the adrenal).

Clock genes are a set of rhythmically expressed transcription factors that drive rhythms in downstream genes directly involved in numerous physiological processes (Reppert & Weaver 2002; Hastings, O'Neill & Maywood 2007). Hypothalamic expression of all clock genes changed with the onset and progression of pregnancy, with clear effects on the mesor of each clock gene (an indicative measure of overall expression) evident by mid-gestation. Specifically, by day 10 of pregnancy each clock gene mesor was elevated above pre-pregnancy levels and, in the majority of cases, expression was highest at this stage (up to 1.5-fold). These increases in clock gene expression suggest a major shift in the function of the central clock in pregnancy, presumably to drive gestational adaptations in maternal behaviour and physiology. Together with our previous findings of pregnancy-induced changes to liver clock genes late in rat gestation (Wharfe, Mark & Waddell 2011), the present data suggest that widespread alterations to the circadian system are a feature of maternal physiological adaptations to pregnancy. Further studies are required to determine the mechanisms by which pregnancy-induced changes in central and peripheral clocks occur, but a role for the highly dynamic hormonal milieu of pregnancy seems likely. Indeed, a number of clock genes contain estrogen and progesterone response elements within their promoter regions (Nakamura et al. 2005; He et al. 2007; Nakamura et al. 2010), and ERα, ERβ and PR are expressed within the SCN (Blaustein & Wade 1978; Blaustein et al. 1988; Vida et al. 2008). Previous studies also show that clock gene expression is influenced by estradiol in the SCN (Nakamura et al. 2001; Nakamura et al. 2005), and by progesterone in the uterus (He et al. 2007; Nakamura et al. 2010; Rubel et al. 2012). Moreover, clock gene expression can be regulated by corticosterone, as glucocorticoid response elements are

present within the promoter regions of *Per1*, *Per2* and *Rev-erbα* (Balsalobre et al. 2000; Yamamoto et al. 2005; So et al. 2009). Corticosterone, however, is unlikely to drive pregnancy-induced changes in the central clock directly since glucocorticoid receptor expression is absent or minimal within the SCN (Rosenfeld et al. 1988; Balsalobre et al. 2000; Kalsbeek et al. 2012).

In contrast to the changes in hypothalamic expression of clock genes, that of *Crh* remained relatively stable across pregnancy. Similarly, while *Crh* expression showed a trend for overall time-of-day variation, this did not match the conventional cosinor pattern observed for the clock genes. These observations may appear surprising given that ablation studies (both anatomical and transgenic) have highlighted the importance of the SCN in the regulation of the diurnal secretion of corticosterone (Moore & Eichler 1972; Sellix et al. 2006). Interestingly, while a previous study also observed arrhythmic hypothalamic *Crh* mRNA expression in the mouse, rhythmic expression of *Crh* heteronuclear (hn) RNA was detected, indicative of circadian variation in *Crh* at this pre-processing stage (Watts, Tanimura & Sanchez-Watts 2004). This suggests that hypothalamic *Crh* expression at the heteronuclear RNA level may be influenced by the rhythmic expression of SCN clock genes, but this is obscured by other regulatory factors at the mRNA level. Moreover, the central clock also appears to influence the HPA axis independently of CRH, possibly via changes in adrenocortical sensitivity to ACTH across the circadian day (Kaneko et al. 1981). This effect is mediated centrally via the autonomic nervous system (ANS) (Buijs et al. 1999).

Our data also show for the first time that the full circadian profile of maternal corticosterone increases dramatically after mid-gestation in the mouse (i.e. at days 14 and 18). Elevation of the full circadian profile of glucocorticoids has previously been reported for human (Patrick et al. 1980) and rat pregnancy (Atkinson & Waddell 1995), but the magnitude of the increase observed here in the mouse is several-fold greater. Moreover, these higher levels of corticosterone occurred even though absolute levels of plasma ACTH fell markedly over the same period. This apparent decoupling of circulating ACTH and corticosterone suggests that factors outside the conventional HPA axis influence plasma corticosterone in pregnancy. For example, enhanced adrenal responsiveness appears to drive increased maternal corticosterone levels after mid-gestation in the rat (Atkinson & Waddell 1995), an effect likely mediated via rising estrogen levels (Atkinson & Waddell 1997; Figueiredo et al. 2007). Other ‘non-HPA

axis' factors that could enhance maternal levels of corticosterone include a fall in its metabolic clearance rate due to higher plasma corticosteroid binding globulin (CBG) levels (Gala & Westphal 1967; Douglas et al. 2003), or a contribution from the fetal adrenal. The latter is consistent with activation of the fetal HPA axis late in development (Cottrell et al. 2012) and the coincident loss of the placental glucocorticoid barrier (Brown et al. 1996) which may also explain the loss of maternal corticosterone rhythmicity by day 18 of gestation. Finally, a number of studies suggest that the placenta could provide direct trophic support to the adrenal, thereby stimulating adrenal corticosterone secretion independently of the HPA axis (Waddell 1993; Waddell & Burton 1993).

Given the established links between the central clock and adrenal sensitivity (via the ANS) (Buijs et al. 1999) and with the HPA axis (Nader, Chrousos & Kino 2010), one might expect a positive relationship between hypothalamic clock gene expression and corticosterone levels. On the contrary, our data show that there was no such association for the majority of clock genes, and where a relationship was observed (3 of 8 genes), it was predominantly negative. The single exception was for *Rorα*, which showed a positive association with corticosterone on day 6 of gestation. Further studies are required to determine whether the multiple regulatory pathways that link the central clock and the adrenal cortex (e.g. via adrenal sensitivity and regulation of clock gene expression indirectly by corticosterone) obscure such correlations.

The biologically-inert metabolite of corticosterone, 11-DHC, was detectable in plasma at all stages of pregnancy but at much lower concentrations than corticosterone. For the first time we have shown that throughout pregnancy the circadian profiles of 11-DHC generally paralleled the corresponding corticosterone profiles, including the apparent loss of rhythmicity at day 18. The ratio of corticosterone to 11-DHC increased substantially at day 14, possibly due to greater plasma CBG binding of corticosterone and an associated reduction in the proportion metabolised to 11-DHC (Barlow, Morrison & Sullivan 1974; Barlow, Morrison & Sullivan 1975). This conversion is catalysed by the 11β-hydroxysteroid dehydrogenase enzymes (11β-HSD1 and 11β-HSD2), and opposite changes in their expression occur in the two placental zones late in rodent pregnancy (Mark et al. 2009). These changes in enzyme expression are likely to influence total 11β-HSD enzymatic capacity and thereby impact on the plasma corticosterone:11-DHC ratio near term.

It is possible that alterations to the circadian system during pregnancy, such as those seen in the central clock and HPA axis, may contribute to gestational adaptations in maternal metabolism. Indeed, the central clock is known to influence peripheral tissue clocks via neural and humoral signals (Hastings, O'Neill & Maywood 2007). Furthermore, links between the clock gene network and metabolism (Froy 2010) indicate that changes to circadian rhythms of clock gene expression in peripheral tissues regulate expression of downstream genes governing physiological processes including glucose and lipid metabolism, both of which are adapted in pregnancy (Suman Rao, Shashidhar & Ashok 2013). For example, the steady increase in absolute levels of hypothalamic *Bmal1* across gestation may contribute to the sustained availability of nutrients from peripheral tissue stores by driving altered neural and/or humoral signals via the PVN (Kalsbeek et al. 2006). Previous studies show that hepatic *Bmal1* is particularly important in relation to regulation of hepatic glucose metabolism (Lamia, Storch & Weitz 2008), whilst *Rev-erbα* plays a key role in lipid metabolism within the liver and adipose tissue (Delezie et al. 2012). Accordingly, it will be of interest to explore how changes in the central and peripheral circadian clocks influence maternal metabolic adaptations in pregnancy.

In conclusion, this study shows that the central circadian clock undergoes marked adaptations with the onset and progression of mouse pregnancy. Importantly, neither clock genes nor plasma ACTH appear to drive the dramatic increase in the maternal glucocorticoid levels observed after mid-gestation. The pregnancy-induced changes in the central circadian clock and the HPA axis likely promote pregnancy success by driving maternal physiological adaptations to meet the metabolic demands of fetal growth.

Supplementary data

This is linked to the online version of the paper at http:dx.doi.org/10.1530/JOE-15-0405.

Declaration of interest

The authors declare that there is no conflict of interest that could be perceived as prejudicing the impartiality of the research reported.

Funding

This research did not receive any specific grant from any funding agency in the public, commercial or not-for-profit sector.

Acknowledgements

The authors are grateful to Professor Hugh Barrett (the University of Western Australia) for his advice on cosinor analysis.

5.6 Supplementary data

Supplementary Table 5.S1 Linear regression analysis of anterior hypothalamic clock genes and plasma ACTH with plasma corticosterone across pregnancy.

	Non-Pregnant	Day 6	Day 10	Day 14	Day 18
Cort : Bmal1	-0.30	-0.48	-0.27	-0.62	-0.01
	(NS)	($P = 0.004$)	(NS)	($P < 0.001$)	(NS)
Cort : Clock	-0.18	-0.36	-0.34	-0.43	-0.37
	(NS)	($P = 0.033$)	($P = 0.037$)	($P = 0.009$)	($P = 0.031$)
Cort : Per1	0.03	0.36	0.29	0.10	0.08
	(NS)	(NS)	(NS)	(NS)	(NS)
Cort : Per2	-0.03	0.22	0.02	-0.02	-0.03
	(NS)	(NS)	(NS)	(NS)	(NS)
Cort : Cry1	-0.09	-0.07	-0.07	-0.12	0.10
	(NS)	(NS)	(NS)	(NS)	(NS)
Cort : Cry2	0.07	0.30	-0.16	-0.36	0.29
	(NS)	(NS)	(NS)	($P = 0.031$)	(NS)
Cort : Rev-erbα	-0.05	0.19	0.01	-0.01	0.19
	(NS)	(NS)	(NS)	(NS)	(NS)
Cort : Rorα	-0.24	0.37	-0.01	0.10	0.02
	(NS)	($P = 0.029$)	(NS)	(NS)	(NS)
Cort : ACTH	0.27	0.12	0.65	-0.08	-0.25
	(NS)	(NS)	($P < 0.0001$)	(NS)	(NS)

Correlation coefficients (r) and significance levels are shown for each day of pregnancy.

Chapter 6

Pregnancy-induced changes in the circadian expression of hepatic clock genes: implications for maternal glucose homeostasis

Preface

The major objective of this chapter was to determine whether circadian changes in hepatic clock gene expression accompany maternal adaptations during pregnancy and also whether such changes influence the circadian expression of downstream glucoregulatory genes.

This chapter was co-authored with Caitlin S. Wyrwoll, Brendan J. Waddell and Peter J. Mark and accepted for publication by the American Journal of Physiology – Endocrinology and Metabolism [vol. 311, no. 3, pp. E575-E586] in July, 2016.

Michaela Wharfe performed all animal work and tissue sampling and was responsible for all analyses, representing 100% of the laboratory work. Michaela Wharfe was also largely responsible (80%) for writing and submitting the manuscript.

6.1 Abstract

Adaptations in maternal carbohydrate metabolism are particularly important in pregnancy because glucose is the principal energy substrate used by the fetus. As metabolic homeostasis is intricately linked to the circadian system via the rhythmic expression of clock genes, it is likely that metabolic adaptations during pregnancy also involve shifts in maternal circadian function. We hypothesized that maternal adaptation in pregnancy involves changes in the hepatic expression of clock genes, which drive downstream shifts in circadian expression of glucoregulatory genes. Maternal liver and plasma (n = 6-8/group) were collected across 24-h periods (0800, 1200, 1600, 2000, 0000, 0400 h) from C57Bl/6J mice under isoflurane/nitrous oxide anesthesia prior to and on days 6, 10, 14 and 18 of pregnancy (term = day 19). Hepatic expression of clock genes and glucoregulatory genes were determined by RT-qPCR. Hepatic clock gene expression was substantially altered across pregnancy, most notably in late gestation when the circadian rhythmicity of several clock genes was attenuated (up to 64% reduced amplitude on day 18). These changes were associated with a similar decline in rhythmicity of the key glucoregulatory genes *Pck1*, *G6Pase* and *Gk*, and by day 18 *Pck1* was no longer rhythmic. Overall, our data show marked adaptations in the liver clock during mouse pregnancy, changes that may contribute to the altered circadian variation in glucoregulatory genes near term. We propose that the observed reduction of daily oscillations in glucose metabolism ensure a sustained supply of glucose to meet the high demands of fetal growth.

6.2 Introduction

During pregnancy, maternal metabolic adaptations are crucial to meet the nutrient demands of the developing fetus. Two distinct maternal metabolic phases are evident across pregnancy (Knopp et al. 1973; Metcalfe, Stock & Barron 1988); the first, anabolic phase occurs up to approximately day 10 in the mouse when fetal demand is low, and the second, catabolic phase spans the latter half of pregnancy (days 11-19) when fetal nutrient demand is high. In essence, the anabolic phase ensures storage of energy in anticipation of subsequent high fetal demand, whereas the catabolic phase delivers these resources when needed for rapid fetal growth (Knopp et al. 1973; Constancia et al. 2002).

There is growing recognition that metabolic homeostasis is intimately linked to circadian variation (for review see Bailey, Udoh & Young 2014). The coupling of circadian and metabolic function is thought to maximize the efficiency of energy uptake, storage and utilization through coordinated alignment of biochemical processes with organism behaviour. Accordingly, the major metabolic adaptations of pregnancy are likely to involve marked shifts in maternal circadian function, but few studies have addressed this possibility. Circadian variation in cellular function is driven by a network of clock genes (*Clock*, *Bmal1*, *Period 1-2*, *Cryptochrome 1-2*, *Rev-erbα*, *Rorα*) that form transcriptional-translational feedback loops in both central (i.e. the suprachiasmatic nucleus; SCN) and peripheral tissues including the liver (for review see Partch, Green & Takahashi 2014). We previously observed that hepatic clock gene expression in the rat is lower near the end of pregnancy compared to non-pregnant animals (Wharfe, Mark & Waddell 2011), but it is not clear whether progressive adaptations occur earlier in pregnancy. It is also unknown if changes in hepatic clock genes influence the circadian expression of downstream metabolic genes to alter nutrient availability.

Adaptations in maternal carbohydrate metabolism are particularly important in pregnancy because glucose is the principal energy substrate used by the fetus (Jones & Rolph 1985; Kalhan & Parimi 2000). Glucose metabolism exhibits robust circadian variation, with a large number of genes encoding glucoregulatory enzymes displaying rhythmic expression (Ishikawa & Shimazu 1976; Akhtar et al. 2002; Panda et al. 2002; Storch et al. 2002; Reddy et al. 2006). In the liver for example, phosphoenolpyruvate

carboxykinase 1 (*Pck1*) displays clear circadian variation, with peak expression evident at 2000 h (Kennaway et al. 2013). Moreover, an important role for clock genes in the regulation of glucose metabolism is evidenced by numerous transgenic mouse models, such as $Clock^{mut}$, $Clock^{\Delta 19}$ and $Bmal1^{-/-}$, all of which show disrupted circadian profiles of either plasma glucose or glucoregulatory gene expression (Rudic et al. 2004; Kennaway et al. 2007; Lamia, Storch & Weitz 2008; Kennaway et al. 2013).

In this study, therefore, we hypothesized that maternal metabolic adaptation in pregnancy involves changes in the hepatic expression of clock genes. We further hypothesized that these clock gene changes drive downstream shifts in circadian expression of rhythmically expressed metabolic genes involved in glucose homeostasis. To test these hypotheses, hepatic expression of clock genes and key genes involved in glucose metabolism were measured, along with hepatic glycogen and plasma glucose and insulin at six time points across the circadian day in the non-pregnant mouse and at four stages of pregnancy (days 6, 10, 14 and 18).

6.3 Materials and Methods

6.3.1 Animals

Nulliparous C57Bl/6J mice (6-9 weeks old) were supplied by the Animal Resources Centre (Murdoch, Australia). All procedures involving the use of animals were conducted after approval by the Animal Ethics Committee of The University of Western Australia (AEC number RA/3/100/1070). Mice were housed 4-per-cage throughout the study and maintained in two environmentally controlled rooms, with food and water supplied *ad libitum.* In one room mice were exposed to a normal 12:12 light/dark cycle (lights on at 0700 h); in the other room the light cycle was reversed (lights on for 12h from 1900 h). In the latter, mice were exposed to a constant red light (36 W, 620 nm) between 0700 and 1900 h. Both groups of animals were allowed to acclimatise to their respective light cycle for two weeks before any experimental procedures were conducted. Preliminary studies showed no effect of light cycle reversal or exposure to red light on *Bmal1* and *Rorα* gene expression across a 24-h period, as measured by qPCR (unpublished data). Lights on at 0700 h (or 1900 h in the reverse-light room) was classified as a new day and as zeitgeber time (ZT)-zero, with sampling times defined relative to ZT-zero. Mice were mated overnight and pregnancy was confirmed by visualization of a mucous plug the following morning (designated day 1 of pregnancy). In a separate group of non-pregnant mice, estrous cycle stage was monitored for a minimum of three full cycles by vaginal lavage (between ZT6 and 13) by the protocol of Caligioni (2009).

6.3.2 Tissue Collection

Liver samples and plasma were collected from mice under isoflurane/nitrous oxide (0.2:0.8) anesthesia at 4-h intervals commencing at ZT1 on either diestrus I of the cycle or days 6, 10, 14 or 18 of pregnancy (term = day 19) with an *n* of 6-8 per ZT. For collections in the dark phase, anesthesia was carried out under red light before fitting the mouse with a lightproof hood and collecting the tissues in white light. In all mice, a blood sample was obtained under anesthesia by cardiac puncture (into an EDTA tube) and a portion of the maternal liver (right side of the median lobe) was collected. Tissue samples were snap frozen in liquid nitrogen. Maternal blood glucose was measured immediately (Accu-Chek; Roche Diagnostics, Mannheim, Germany), and the remainder

of each blood sample was centrifuged at 13,000 x *g* to obtain plasma. Plasma and liver samples were stored at -80 °C.

6.3.3 RNA sample preparation

Total RNA was extracted from liver samples using QIAzol (Qiagen, Doncaster, Australia) as per the manufacturer's instructions. After quantitation of RNA using the NanoDrop ND-1000 spectrophotometer (NanoDrop,Wilmington, DE, USA), total RNA (5 μg) was reverse transcribed at 42°C for 110 min by Mouse Moloney leukemia virus reverse transcriptase with random hexamers (Promega, Sydney, Australia). The resultant cDNAs were purified using an ultra-clean PCR spin kit (MoBio Laboratories, Inc., Carlsbad, CA, USA) as per manufacturer's instructions.

6.3.4 Real-time PCR

Analyses of mRNA expression levels of the following genes were performed by real-time PCR on the Rotorgene 6000 system (Corbett Research, Sydney, Australia): the clock genes *Clock, Arntl* which encodes *Bmal1*, *Per1*, *Per2*, *Cry1*, *Cry2* and *Nr1d1* which encodes *Rev-erbα*, the glucoregulatory genes *Slc2a2* which encodes glucose transporter 2 (*Glut2*), glucokinase (*Gk*), pyruvate kinase (*Pk*), phosphoenolpyruvate carboxykinase 1 (*Pck1*), glucose-6-phosphate (*G6Pase*), glycogen synthase 2 (*Gys2*) and glycogen phosphorylase (*Pygl*) and the reference genes TATA box binding protein (*Tbp*), peptidylprolyl isomerase A (*Ppia*) and succinate dehydrogenase subunit A (*Sdha*). Primer pairs for all genes (see Table 6.1) were designed using Primer-BLAST (http://www.ncbi.nlm.nih.gov) (Ye et al. 2012). All primer pairs were designed to span introns to prevent amplification of product from genomic DNA. The resulting amplicons were sequenced to confirm specificity. Standard curves were created with 10-fold serial dilutions of gel-extracted (QIAEX II; Qiagen, Doncaster, Australia) PCR products and using the Rotorgene 6000 software. All samples were normalized against *Sdha*, *Ppia* and *Tbp* using the GeNorm algorithm (Vandesompele et al. 2002). Common samples were included in all reverse transcription and qPCR reactions to validate comparisons between different runs.

6.3.5 Measurement of hepatic glycogen

Hepatic glycogen concentrations were assessed using a commercial colorimetric assay kit (BioVision Inc. Milpitas, CA, USA; Cat#K646-100). Liver tissue (10 mg) was homogenized in 400 µl ddH_20 using the POLYTRON-Aggregate homogenizer (Kinematica Inc., Bohemia, NY, USA). Samples were heated to 95°C for 10 min, before centrifugation at 18,000 x *g* for 10 min. Sample (1.5 µl) was aliquoted in duplicate and made up to 25 µl with hydrolysis buffer. A duplicate sample was used as a free-glucose control (no addition of hydrolysis enzyme) and was subtracted from the determined concentration to calculate the final glycogen concentration. The assay was performed as per manufacturer's instructions, with plates read at 570 nm on the Biotek ELx808 absorbance reader (BioTek Instruments Inc., Winooski, VT, USA).

6.3.6 Measurement of plasma insulin

Plasma insulin concentrations were measured using a commercially available Milliplex Map assay kit (Mouse Adipokine; Cat#MADKMAG-71K; Merck Millipore, MA, USA) as per manufacturer's instructions. Plates were read using a MAGPIX plate reader and analysed using xPONENT software (Merck Millipore, MA, USA). The intra- and inter-assay coefficients of variation for insulin were 7.1% and 16.9%, respectively.

6.3.7 Statistical Analysis

All data are expressed as the mean ± SEM, with an *n* of 6-8 per ZT on each day of pregnancy. Where data were not normally distributed (based on D'Agostino and Pearson omnibus test), values were log transformed. Variance in plasma glucose, insulin and glycogen was determined by two-way ANOVA (with time-of-day and pregnancy stage as factors). When a significant interaction was observed, time-of-day variation within each day was assessed by one-way ANOVA. Statistical analyses were conducted using GraphPad Prism 6.00 (GraphPad Software, La Jolla, CA, USA).

Circadian rhythms were assessed by cosinor analysis using a non-linear regression model (Genstat Version 9, VSN International Ltd, Hemel Hempstead, UK). This analysis generated the following rhythm descriptors: mesor (circadian rhythm adjusted mean), amplitude, acrophase (time of the peak of a rhythm) and cosinor r^2 as a measure of fit. One-way ANOVA was used to determine whether each of these cosinor

descriptors varied with stage of pregnancy. For all ANOVAs, where the *F* test was significant ($P < 0.05$), *post hoc* LSD tests were used for pairwise comparisons. Relationships between clock genes and downstream metabolic genes were assessed by linear regression analysis.

Table 6.1 Primers and PCR conditions used to measure hepatic clock genes, glucoregulatory genes and reference genes by RT-qPCR.

Gene	Forward/Reverse Primer sequence	Amplicon Size (bp)	Annealing Temp (°C)	$MgCl_2$ (mM)
Clock	F, 5' - ACAACGCACACATAGGCCTTC– 3' R, 5' – TGGTGGTGCCCTGTGATCTA – 3'	175	60	3
Bmal1	F, 5' – CGTGCTAAGGATGGCTGTTC – 3' R, 5' – CTTCCCTCGGTCACATCCTA – 3'	166	60	3
Per1	F, 5' – TGCACTTCGGGAGCTCAAACTTC – 3' R, 5' – GTCCATGGCACAAGGCTCACC – 3'	169	59	2
Per2	F, 5' – AACAAATCCACCGGC – 3' R, 5' – CTCCGGTGAGACTCC – 3'	145	60	3
Cry1	F, 5' – AACGTCCCGAGCTGTAGCGGT – 3' R, 5' – GACGCTTCCCACTGCTGAGGC – 3'	139	60	2
Cry2	F, 5' – TGCCTCTCCTGCCGCCTCTT- 3' R, 5' – TGCGGTCCCAGGGGATCTGG – 3'	193	60	2
Rev-erbα	F, 5' – CGGGGCTCACTCGTCTCCCT – 3' R, 5' - GCTCGGGGAGGAGCCACTAGA – 3'	185	60	2
Glut2	F, 5' - TGGGCGGAATGGTCGCCTCAT – 3' R, 5' – GGGCTCCAGTCAATGAGAGGCT – 3'	102	60	2

Gene	Forward/Reverse Primer sequence	Amplicon Size (bp)	Annealing Temp (°C)	$MgCl_2$ (mM)
Pk	F, 5' – AGTCCCACACTTTGGAAGCA – 3' R, 5' – CTGGAGCCCCACTTAAAGCA – 3'	116	60	2
Pck1	F, 5' – ATGAAGTTTGATGCCCAAGG – 3' R, 5' – ACCCCCATCGCTAGTCTCGG – 3'	159	59	3
G6Pase	F, 5' – GGGCATCAATCTCCTCTGGG – 3' R, 5' – GTCCAGGACCCAATACG – 3'	100	60	2
Gys2	F, 5' –CAGACACCTGACACTGAGCA – 3' R, 5' – CCTCCTCTTCATCATACCTC – 3'	200	60	2
Pygl	F, 5' – CCTATGGCTACGGCATTCGT – 3' R, 5' – TCTCCCAAGGGTTTCCATGC – 3'	111	60	2
Tbp	F, 5' – GGGAGAATCATGGACCAGAA – 3' R, 5' – CCGTAAGGCATCATTGGACT – 3'	113	60	2
Ppia	F, 5' – AGCATACAGGTCCTGGCATC – 3' R, 5' – TTCACCTTCCCAAAGACCAC – 3'	127	62	3
Sdha	F, 5' – TGGGGAGTGCCGTGGTGTCA – 3' R, 5' – CTGTGCCGTCCCCTGTGCTG – 3'	149	60	2

Glut2, glucose transporter 2 (official full name: solute carrier family 2, member 2 (Slc2a2)); *Gk*, glucokinase; *Pk*, pyruvate kinase; *Pck1*, phosphoenolpyruvate carboxykinase 1; *G6Pase*, glucose-6-phosphatase; *Gys2*, glycogen synthase 2; *Pygl*, glycogen phosphorylase; *Tbp*, TATA box binding protein; *Ppia*, peptidylprolyl isomerase A; *Sdha*, succinate dehydrogenase complex, subunit A

6.4 Results

6.4.1 Maternal characteristics

Maternal weight before pregnancy was similar in all groups (21.6 +/- 0.1 g overall), but successive increases ($P < 0.05$; ANOVA, LSD test) were observed thereafter (day 6: 23.6 +/- 0.2 g; day 10: 25.5 +/- 0.3 g; day 14: 30.3 +/- 0.3 g; day 18: 36.7 +/- 0.6 g). Fetal number was also consistent among groups (day 10: 8.7 +/- 0.2; day 14: 8.0 +/- 0.2; day 18: 7.8 +/- 1.2).

6.4.2 Plasma glucose and insulin, and hepatic glycogen levels across gestation

Overall, maternal plasma glucose varied with stage-of-pregnancy ($P < 0.0001$, two-way ANOVA) with levels declining with advancing gestation (Figure 6.1A). Although levels did not vary significantly with time-of-day, importantly, there was a significant *time-of-day* x *stage-of-pregnancy* interaction ($P < 0.05$, two-way ANOVA). Thus, circadian variation was present in plasma glucose before pregnancy and on day 6 ($P < 0.05$, one-way ANOVA) but no time-of-day effect was detected from day 10 onwards (Figure 6.1B).

Plasma insulin also varied significantly with stage-of-pregnancy ($P < 0.001$, two-way ANOVA) with absolute levels markedly higher after mid-gestation (Figure 6.1C). Plasma insulin also varied with time-of-day and there was a significant *time-of-day* x *stage-of-pregnancy* interaction ($P < 0.05$). Specifically, plasma insulin did not vary across a 24-h period on days 10, 14 and 18, despite the significant fit to a cosine curve on day 10 (one-way ANOVA; Figure 6.1D).

Absolute levels of hepatic glycogen remained unchanged up to mid-gestation but increased thereafter (up to 1.5-fold by day 18; $P < 0.0001$, two-way ANOVA; Figure 6.1E). Hepatic glycogen levels showed the expected robust circadian profile with stores accumulating during the dark phase and being depleted during the light phase ($P < 0.0001$, two-way ANOVA; Figure 6.1F).

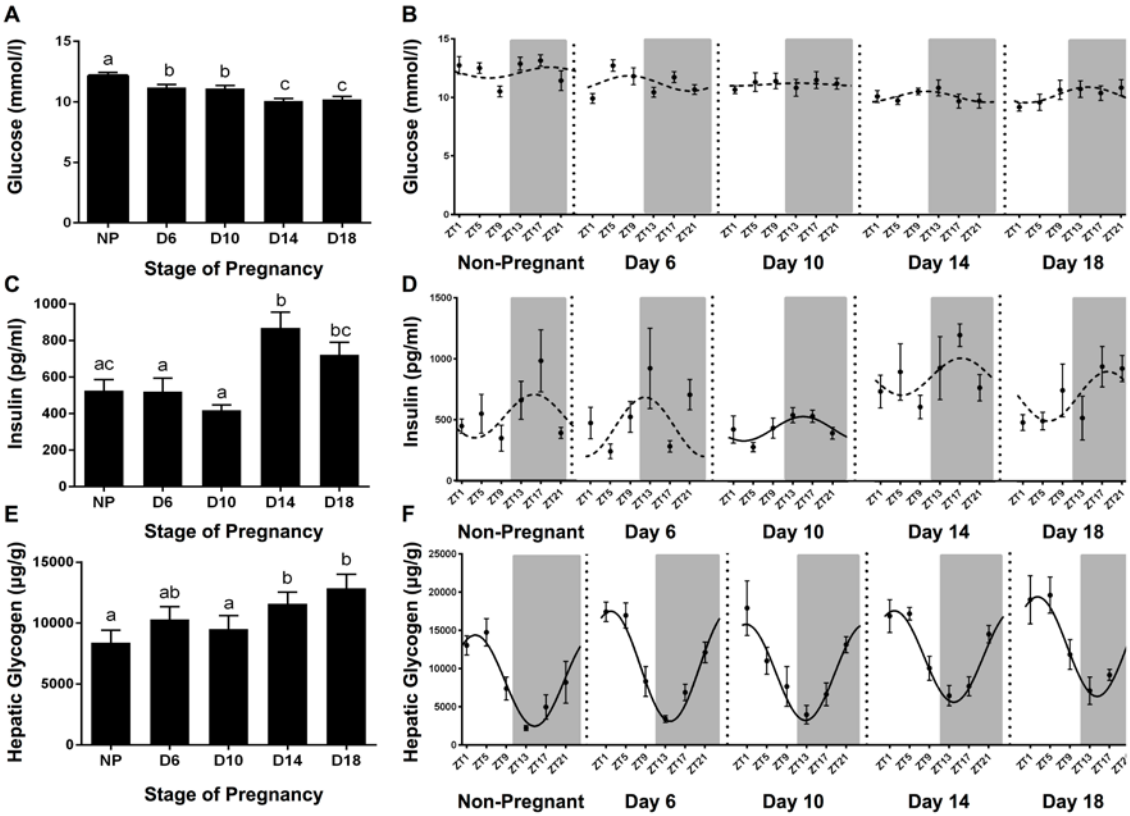

Figure 6.1 Mean plasma concentrations of (A) glucose (mmol/l) and (C) insulin (pg/ml) and (E) hepatic glycogen content (µg/g) in non-pregnant mice and pregnant mice on days 6, 10, 14 and 18. Values are ± SEM (n = 30-48/group). Values without common notation differ significantly ($P < 0.05$; two-way ANOVA and *post hoc* LSD test). Plasma concentrations of (B) glucose (mmol/l) and (D) insulin (pg/ml) and (F) hepatic glycogen content (µg/g) at ZT1, 5, 9, 13, 17 and 21 in non-pregnant mice and pregnant mice on days 6, 10, 14 and 18. Values are ± SEM (n = 6-8/group). Grey shading represents the dark phase of the light cycle. The best-fit curve derived by cosinor analysis is shown as a solid line when significant ($P < 0.05$) and as a dashed line when non-significant.

6.4.3 Changes in hepatic clock gene expression across gestation

In accordance with clock genes being rhythmically expressed, cosinor analysis revealed highly significant circadian variation in their hepatic expression (see Table 6.2 for r^2 and *P* values). The resultant circadian characteristics (mesor, amplitude and acrophase) across pregnancy are shown in Table 6.2.

For all genes except *Clock*, both absolute levels (mesor) and the amplitude of expression were greatest either before or early in pregnancy (day 6; Figures 6.2 and 6.3). From mid-pregnancy onwards both the mesor and amplitude of each gene decreased, reaching minimal levels on either day 14 or day 18; only mesors for *Cry1* and *Cry2* increased from day 14 to day 18 (Figure 6.3A and 6.3B). Interestingly, the mesor and amplitude of *Clock* expression were highest on day 10, after which absolute levels decreased below those seen before pregnancy (Figure 6.2B). The amplitude of *Clock* expression returned to non-pregnant levels on day 14.

For the majority of clock genes, the time of peak expression (acrophase) showed little change across pregnancy (Figures 6.2 and 6.3). The exceptions were *Bmal1* and *Per1*, the peaks of which were both delayed by approximately 1-h from day 6 onwards ($P < 0.05$; Table 6.2).

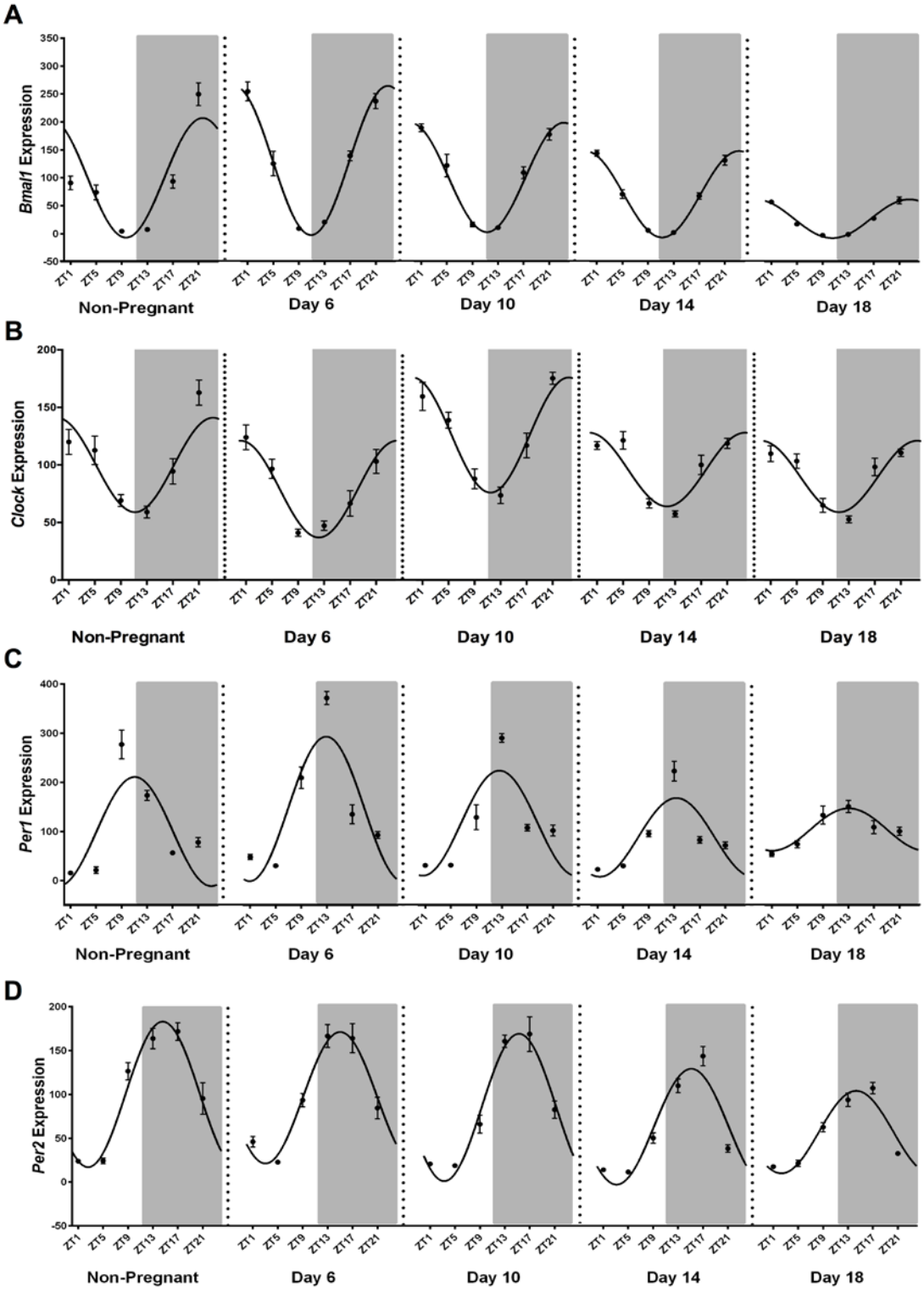

Figure 6.2 Hepatic expression of (A) *Bmal1*, (B) *Clock*, (C) *Per1* and (D) *Per2* at ZT1, 5, 9, 13, 17 and 21 in non-pregnant mice and pregnant mice at days 6, 10, 14 and 18. Values are ± SEM (n = 6-8/group) and are expressed relative to the non-pregnant mesor (adjusted to 100). Grey shading represents the dark phase of the light cycle. The best-fit curve derived by cosinor analysis is show as a solid line when significant ($P < 0.05$) and as a dashed line when non-significant.

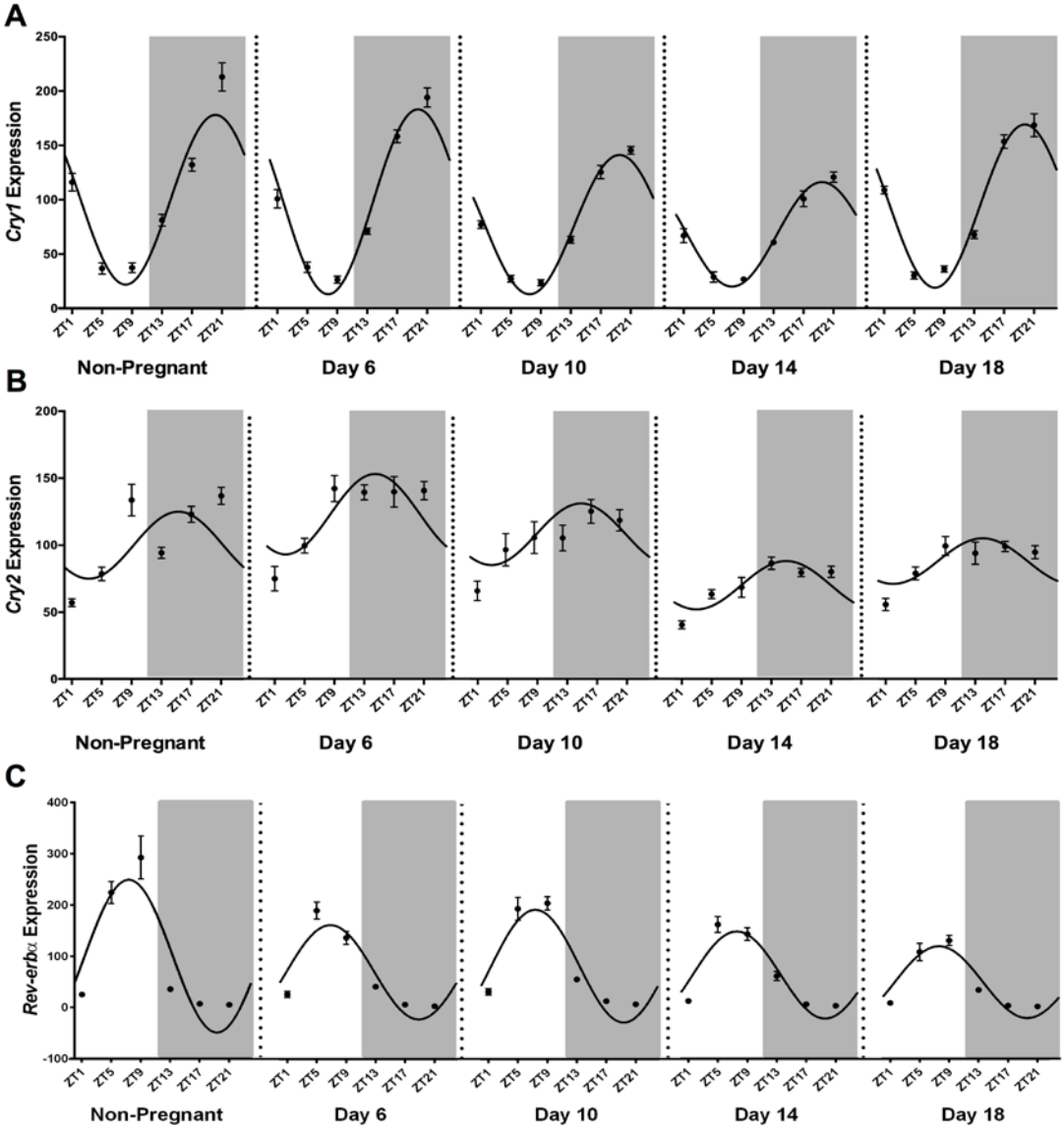

Figure 6.3 Hepatic expression of (A) *Cry1*, (B) *Cry2* and (C) *Rev-erbα* at ZT1, 5, 9, 13, 17 and 21 in non-pregnant mice and pregnant mice on days 6, 10, 14 and 18. Values are ± SEM (n = 6-8/group) and are expressed relative to the non-pregnant mesor (adjusted to 100). Grey shading represents the dark phase of the light cycle. The best-fit curve derived by cosinor analysis is shown as a solid line when significant ($P < 0.05$) and as a dashed line when non-significant.

Table 6.2 Mesor, amplitude, acrophase and r^2 derived from cosinor analyses of hepatic clock gene expression.

		Non-Pregnant	Day 6	Day 10	Day 14	Day 18	*P* value
Bmal1	Mesor	100 ± 9^{ac}	153 ± 6^{b}	119 ± 5^{a}	85 ± 3^{c}	36 ± 2^{d}	<0.0001
	Amplitude	107 ± 13^{ac}	150 ± 9^{b}	110 ± 6^{a}	87 ± 4^{c}	39 ± 2^{d}	<0.0001
	Acrophase	21.7 ± 0.4^{a}	22.9 ± 0.2^{b}	23.3 ± 0.2^{b}	23.2 ± 0.2^{b}	22.6 ± 0.2^{b}	<0.001
	Cosinor r^2	0.62 ($P < 0.0001$)	0.87 ($P < 0.0001$)	0.88 ($P < 0.0001$)	0.92 ($P < 0.0001$)	0.88 ($P < 0.0001$)	
Clock	Mesor	100 ± 4^{a}	79 ± 4^{b}	126 ± 4^{c}	96 ± 3^{ad}	90 ± 3^{d}	<0.0001
	Amplitude	41 ± 6^{ab}	42 ± 5^{ab}	50 ± 5^{b}	32 ± 4^{a}	31 ± 4^{a}	<0.05
	Acrophase	23.2 ± 0.6	24.2 ± 0.5	23.5 ± 0.4	23.8 ± 0.5	23.5 ± 0.5	NS
	Cosinor r^2	0.50 ($P < 0.0001$)	0.63 ($P < 0.0001$)	0.73 ($P < 0.0001$)	0.62 ($P < 0.0001$)	0.65 ($P < 0.0001$)	
Per1	Mesor	100 ± 11^{ac}	146 ± 10^{b}	117 ± 8^{a}	88 ± 7^{c}	104 ± 5^{ac}	<0.0001
	Amplitude	111 ± 15^{a}	147 ± 14^{b}	107 ± 12^{a}	80 ± 9^{a}	43 ± 7^{c}	<0.0001
	Acrophase	11.1 ± 0.5^{a}	12.9 ± 0.4^{b}	12.6 ± 0.4^{b}	13.3 ± 0.5^{b}	13.1 ± 0.6^{b}	<0.05
	Cosinor r^2	0.54 ($P < 0.0001$)	0.70 ($P < 0.0001$)	0.64 ($P < 0.0001$)	0.62 ($P < 0.0001$)	0.47 ($P < 0.0001$)	
Per2	Mesor	100 ± 4^{a}	96 ± 4^{a}	85 ± 4^{b}	63 ± 4^{c}	57 ± 2^{c}	<0.0001
	Amplitude	83 ± 6^{a}	75 ± 6^{ab}	84 ± 6^{a}	66 ± 5^{b}	47 ± 3^{c}	<0.0001
	Acrophase	14.6 ± 0.3	15.0 ± 0.3	15.3 ± 0.3	15.1 ± 0.3	14.3 ± 0.3	NS
	Cosinor r^2	0.81 ($P < 0.0001$)	0.77 ($P < 0.0001$)	0.81 ($P < 0.0001$)	0.79 ($P < 0.0001$)	0.82 ($P < 0.0001$)	
Cry1	Mesor	100 ± 4^{a}	98 ± 3^{a}	77 ± 2^{b}	68 ± 2^{c}	94 ± 3^{a}	<0.0001
	Amplitude	78 ± 6^{a}	85 ± 4^{a}	64 ± 3^{bd}	48 ± 3^{c}	75 ± 4^{ad}	<0.0001
	Acrophase	20.1 ± 0.3	19.8 ± 0.2	19.5 ± 0.1	19.5 ± 0.2	19.8 ± 0.2	NS
	Cosinor r^2	0.82 ($P < 0.0001$)	0.90 ($P < 0.0001$)	0.94 ($P < 0.0001$)	0.86 ($P < 0.0001$)	0.91 ($P < 0.0001$)	
Cry2	Mesor	100 ± 4^{a}	123 ± 4^{b}	108 ± 5^{a}	70 ± 2^{c}	88 ± 3^{d}	<0.0001
	Amplitude	25 ± 6	30 ± 6	23 ± 6	18 ± 3	17 ± 4	NS
	Acrophase	15.3 ± 1.0	14.5 ± 0.7	14.9 ± 0.1	15.0 ± 0.7	14.0 ± 0.8	NS
	Cosinor r^2	0.28 ($P < 0.001$)	0.36 ($P < 0.0001$)	0.21 ($P < 0.05$)	0.40 ($P < 0.0001$)	0.31 ($P < 0.001$)	
Rev-erbα	Mesor	100 ± 11^{a}	70 ± 6^{b}	82 ± 6^{ab}	63 ± 5^{bc}	49 ± 5^{c}	<0.0001
	Amplitude	149 ± 16^{a}	92 ± 8^{b}	110 ± 9^{c}	85 ± 7^{cd}	70 ± 7^{d}	<0.0001
	Acrophase	7.4 ± 0.4	6.9 ± 0.3	7.4 ± 0.3	7.6 ± 0.3	7.6 ± 0.4	NS
	Cosinor r^2	0.65 ($P < 0.0001$)	0.74 ($P < 0.0001$)	0.77 ($P < 0.0001$)	0.77 ($P < 0.0001$)	0.73 ($P < 0.0001$)	

Mesor, amplitude and acrophase values are mean ± SEM. Mesor and amplitude are expressed relative to the mesor value in the Non-Pregnant group (set at 100). Acrophase is expressed in clocktime. Within each group, values without common notation differ significantly ($P < 0.05$; one-way ANOVA and Fisher's LSD test). Values for r^2 are shown with relevant *P* values in parentheses unless non-significant (NS).

6.4.4 Expression of *Glut2*, *Gk* and *Pk* show transient increases in early pregnancy but are low thereafter

Expression of the glucose transporter *Glut2* (Figure 6.4A) was clearly rhythmic at all stages examined (see Table 6.3 for r^2 and *P* values), with the maximal mesor observed on day 6 (1.4-fold higher than before pregnancy). Thereafter, overall *Glut2* expression fell to a minimum by day 14 (mesor 46% lower than pre-pregnancy) before increasing slightly at day 18 (but still lower than pre-pregnancy).

Hepatic expression of *Gk* and *Pk* was rhythmic in the first half of pregnancy (Figures 6.4B and 6.4C), and while this was maintained for *Gk*, *Pk* rhythmicity was lost after mid-gestation (see Table 6.3). Overall expression of both genes increased early in gestation (mesor of each approximately 1.3-fold higher on day 6) before returning to non-pregnant levels on day 10. Expression of *Gk* decreased further by day 14 then increased slightly on day 18, whereas *Pk* expression returned to the high levels seen at day 6 and remained elevated to term ($P < 0.05$; Figure 6.4; Table 6.3). Interestingly, there was a large amount of variability in *Pk* expression on days 14 and 18 that was not seen earlier in gestation (Figure 6.4C).

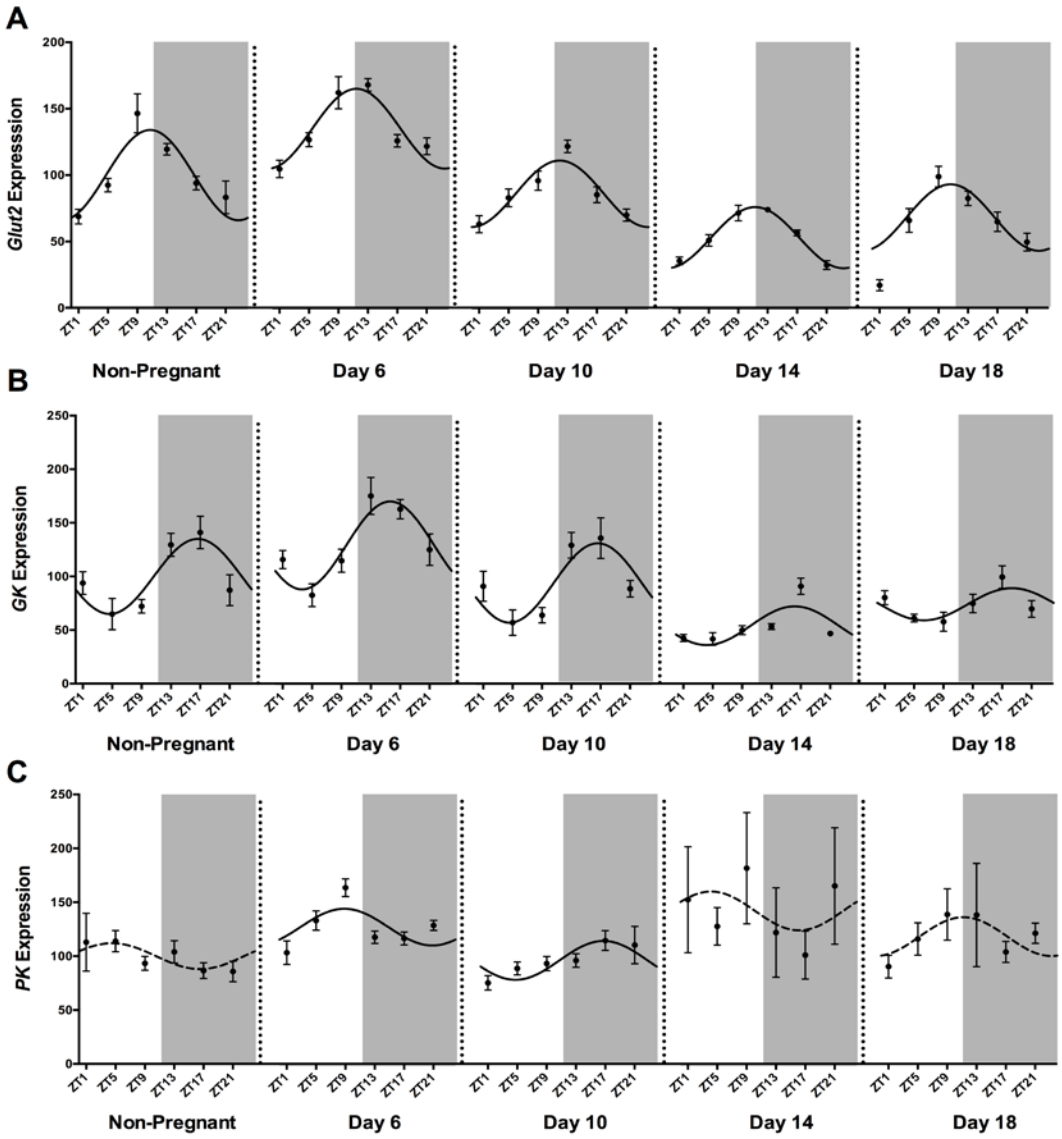

Figure 6.4 Hepatic expression of (A) *Glut2*, (B) *Gk* and (C) *Pk* at ZT1, 5, 9, 13, 17 and 21 in non-pregnant mice and pregnant mice on days 6, 10, 14 and 18. Values are ± SEM (n = 6-8/group) and are expressed relative to the non-pregnant mesor (adjusted to 100). Grey shading represents the dark phase of the light cycle. The best-fit curve derived by cosinor analysis is shown as a solid line when significant ($P < 0.05$) and as a dashed line when non-significant.

Table 6.3 Mesor, amplitude, acrophase and r^2 derived from cosinor analyses of hepatic downstream gene expression.

		Non-Pregnant	Day 6	Day 10	Day 14	Day 18	*P* value
Glut2	Mesor	100 ± 4^{a}	135 ± 3^{b}	86 ± 3^{c}	53 ± 1^{d}	68 ± 3^{e}	<0.0001
	Amplitude	34 ± 5	30 ± 4	25 ± 4	23 ± 2	25 ± 4	NS
	Acrophase	10.7 ± 0.6	11.5 ± 0.5	12.0 ± 0.6	11.3 ± 0.4	10.6 ± 0.6	NS
	Cosinor r^2	0.50 (*P* < 0.0001)	0.51 (*P* < 0.0001)	0.50 (*P* < 0.0001)	0.72 (*P* < 0.0001)	0.48 (*P* < 0.0001)	
GK	Mesor	100 ± 5^{a}	129 ± 5^{b}	94 ± 5^{a}	54 ± 2^{c}	74 ± 3^{d}	<0.0001
	Amplitude	35 ± 7^{ac}	41 ± 7^{a}	37 ± 8^{a}	18 ± 4^{c}	15 ± 5^{b}	<0.0001
	Acrophase	16.7 ± 0.8	15.7 ± 0.7	16.6 ± 0.8	16.2 ± 0.7	18.3 ± 1.3	NS
	Cosinor r^2	0.34 (*P* < 0.0001)	0.39 (*P* < 0.0001)	0.31 (*P* < 0.0001)	0.35 (*P* < 0.0001)	0.15 (*P* < 0.05)	
PK	Mesor	100 ± 6^{a}	127 ± 4^{b}	96 ± 4^{a}	142 ± 17^{b}	118 ± 9^{ab}	<0.05
	Amplitude	-	17 ± 5	18 ± 6	-	-	NS
	Acrophase	-	8.9 ± 1.2^{a}	16.8 ± 1.4^{b}	-	-	<0.0001
	Cosinor r^2	0.01 (NS)	0.15 (*P* < 0.05)	0.10 (*P* < 0.05)	0 (NS)	0.04 (NS)	
Pck1	Mesor	100 ± 7^{a}	88 ± 6^{ad}	61 ± 5^{bc}	51 ± 3^{c}	77 ± 4^{d}	<0.0001
	Amplitude	58 ± 10^{a}	61 ± 9^{a}	40 ± 7^{ac}	26 ± 4^{bc}	-	<0.01
	Acrophase	10.8 ± 0.6	11.7 ± 0.6	11.8 ± 0.7	10.2 ± 0.6	-	NS
	Cosinor r^2	0.44 (*P* < 0.0001)	0.49 (*P* < 0.0001)	0.40 (*P* < 0.0001)	0.47 (*P* < 0.0001)	0.05 (NS)	
G6Pase	Mesor	100 ± 6^{a}	88 ± 4^{a}	60 ± 4^{bc}	57 ± 3^{c}	75 ± 3^{d}	<0.0001
	Amplitude	-	32 ± 6	-	17 ± 5	17 ± 5	NS (0.06)
	Acrophase	-	21.1 ± 0.8^{a}	-	4.2 ± 1.0^{b}	22.6 ± 1.1^{a}	<0.0001
	Cosinor r^2	0.08 (NS)	0.35 (*P* < 0.0001)	0 (NS)	0.21 (*P* < 0.05)	0.21 (*P* < 0.05)	
Gys2	Mesor	100 ± 5^{a}	99 ± 3^{a}	75 ± 2^{b}	91 ± 2^{a}	117 ± 4^{c}	<0.0001
	Amplitude	60 ± 7^{a}	48 ± 5^{a}	28 ± 3^{b}	50 ± 3^{a}	49 ± 6^{a}	<0.001
	Acrophase	12.0 ± 0.4^{a}	12.9 ± 0.4^{ab}	13.6 ± 0.5^{b}	12.4 ± 0.3^{a}	12.3 ± 0.5^{a}	<0.05
	Cosinor r^2	0.64 (*P* < 0.0001)	0.67 (*P* < 0.0001)	0.62 (*P* < 0.0001)	0.84 (*P* < 0.0001)	0.59 (*P* < 0.0001)	
Pygl	Mesor	100 ± 3^{a}	126 ± 4^{b}	91 ± 3^{c}	51 ± 1^{d}	70 ± 3^{e}	<0.0001
	Amplitude	-	20 ± 6	-	8 ± 2	-	NS
	Acrophase	-	2.0 ± 1.1^{a}	-	5.6 ± 0.9^{b}	-	<0.05
	Cosinor r^2	0 (NS)	0.18 (*P* < 0.05)	0.07 (NS)	0.25 (*P* < 0.001)	0 (NS)	

Mesor, amplitude and acrophase values are mean ± SEM. Mesor and amplitude are expressed relative to the mesor value in the Non-Pregnant group (set at 100). Acrophase is expressed in clocktime. Within each group, values without common notation differ significantly ($P < 0.05$; one-way ANOVA and Fisher's LSD test). Values for r^2 are shown with relevant *P* values in parentheses unless non-significant (NS).

6.4.5 Gluconeogenic gene expression falls for most of pregnancy but increases slightly near term

Hepatic expression of the rate-limiting gluconeogenic gene, *Pck1*, showed robust circadian rhythmicity at diestrus I, but the amplitude of this variation declined progressively in pregnancy (55% decrease by day 14; $P < 0.01$; Figure 6.5A; Table 6.3). Indeed, rhythmicity in *Pck1* expression was effectively lost by day 18.

Expression of the second key gluconeogenic gene, *G6Pase*, was also rhythmic on days 6, 14 and 18 of pregnancy (Figure 6.5B and Table 6.3). Interestingly, like those of *Pck1*, *G6Pase* rhythms were somewhat attenuated from day 10 onwards (trend for reduced amplitude; $P = 0.059$; Figure 6.5B; Table 6.3).

Changes in *Pck1* and *G6Pase* expression followed remarkably similar patterns across gestation. Mesors of both genes were highest before pregnancy but then fell 40% by day 10 and remained lower at day 14 ($P < 0.0001$; Figure 6.5; Table 6.3), consistent with a reduced demand for gluconeogenesis in early to mid-pregnancy. On day 18, absolute levels increased (1.5-fold from day 14) but remained at levels lower than those seen before pregnancy ($P < 0.0001$; Figure 6.5; Table 6.3).

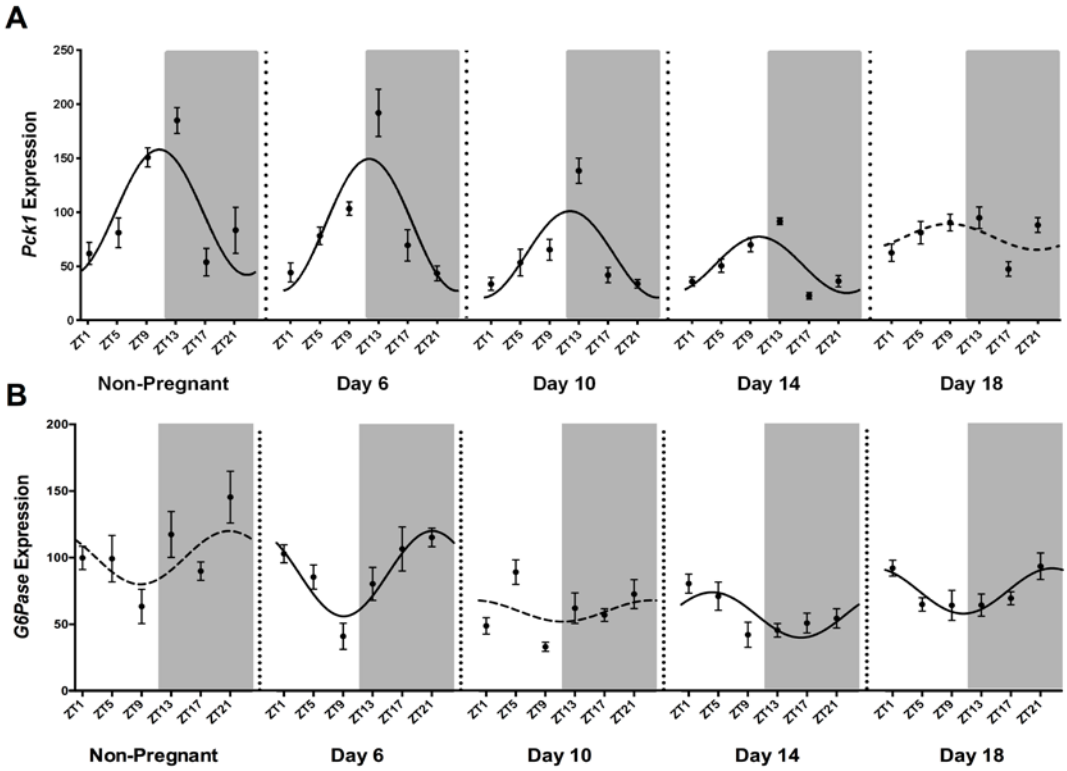

Figure 6.5 Hepatic expression of (A) *Pck1* and (B) *G6Pase* at ZT1, 5, 9, 13, 17 and 21 in non-pregnant mice and pregnant mice on days 6, 10, 14 and 18. Values are ± SEM (n = 6-8/group) and are expressed relative to the non-pregnant mesor (adjusted to 100). Grey shading represents the dark phase of the light cycle. The best-fit curve derived by cosinor analysis is shown as a solid line when significant ($P < 0.05$) and as a dashed line when non-significant.

6.4.6 Changes in glycogenic and glycogenolytic gene expression are consistent with increased glycogen storage in late gestation

Consistent with our findings of increased hepatic glycogen stores in late pregnancy, we observed higher hepatic expression of the glycogenic gene, *Gys2*, and decreased expression of the glycogenolytic gene, *Pygl*, from mid-gestation (Figures 6.6A and 6.6B). Cosinor analysis revealed that while *Gys2* expression was clearly rhythmic on all days of pregnancy, *Pygl* only showed significant circadian variation on days 6 and 14 (see Table 6.3 for r^2 and *P* values). Pregnancy affected all circadian characteristics of *Gys2* (Table 6.3), with the mesor and amplitude at day 10 both lower than in non-pregnant animals (by up to 46%; $P < 0.001$; Figure 6.6A). While the *Gys2* amplitude then returned to pre-pregnancy levels for the remainder of gestation, the mesor reached its highest level on day 18 ($P < 0.001$; Figure 6.6A).

The mesor of *Pygl* varied across gestation, being highest on day 6 before falling to a minimum on day 14. While expression then increased near term, it remained at a level lower than pre-pregnancy ($P < 0.0001$; Figure 6.6B; Table 6.3).

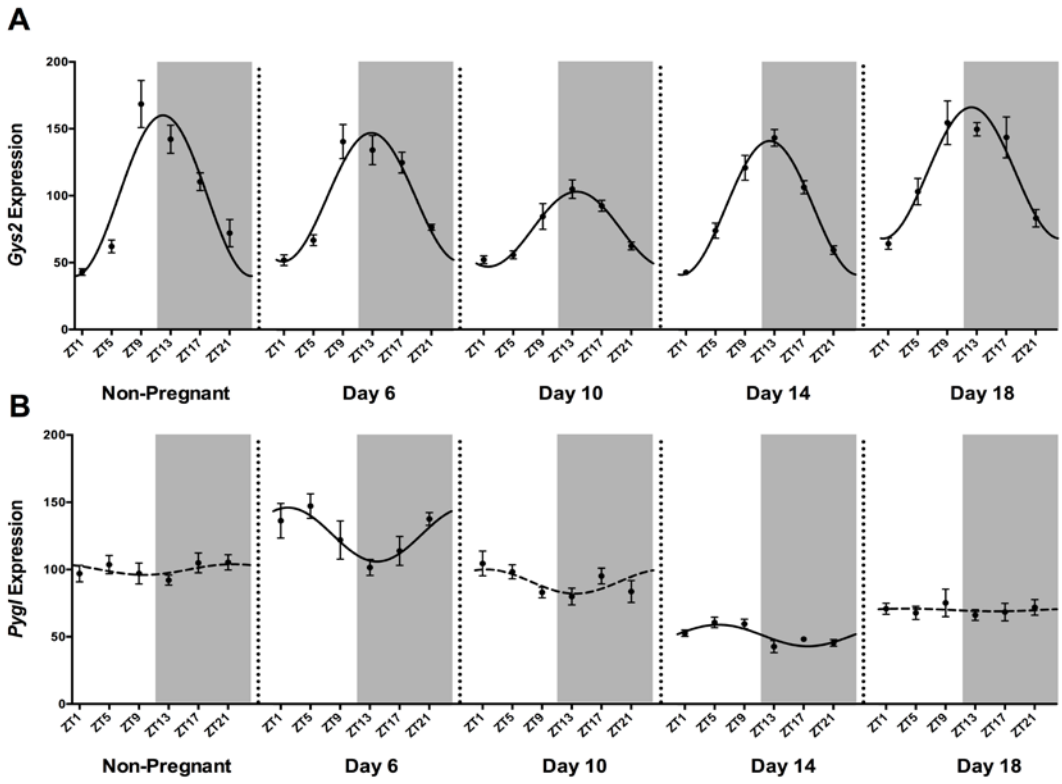

Figure 6.6 Hepatic expression of (A) *Gys2* and (B) *Pygl* at ZT1, 5, 9, 13, 17 and 21 in non-pregnant mice and pregnant mice on days 6, 10, 14 and 18. Values are ± SEM (n = 6-8/group) and are expressed relative to the non-pregnant mesor (adjusted to 100). Grey shading represents the dark phase of the light cycle. The best-fit curve derived by cosinor analysis is shown as a solid line when significant ($P < 0.05$) and as a dashed line when non-significant.

6.4.7 Correlations between hepatic clock genes and glucoregulatory genes

(i) *Glut2:* Negative correlations were observed between *Glut2* and each of *Bmal1*, *Clock* and *Cry1* on all days of pregnancy, with the exception of *Cry1* on day 10 ($P < 0.05$; Table 6.4). In contrast, *Glut2* was positively correlated with *Per1*, *Per2* and *Cry2* throughout pregnancy and *Rev-erbα* prior to pregnancy and on days 14 and 18 ($P < 0.05$; Table 6.4).

(ii) *Gk and Pk:* There was a positive association between *Gk* and *Per2* expression on all days of pregnancy, and between *Gk* and *Cry1* before pregnancy and on days 10 and day 18 ($P < 0.05$; Table 6.5). *Rev-erbα* was negatively correlated with *Gk* on all days examined except day 14 ($P < 0.05$; Table 6.5). No significant correlations were observed between hepatic *Pk* expression and any of the clock genes.

(iii) *Gluconeogenic genes: Pck1* was negatively correlated with *Bmal1*, *Clock* and *Cry1* on days 6 and 14 of pregnancy but not days 10 and 18 ($P < 0.05$; Table 6.6). In contrast, *Per1* was positively correlated with *Pck1* on all days except day 18 ($P < 0.05$; Table 6.6). *G6Pase* was positively correlated with *Bmal1*, *Clock* and *Cry1* for most of pregnancy with the exception of day 10 for each gene, day 14 for *Cry1* and pre-pregnancy for *Bmal1* and *Clock* ($P < 0.05$; Table 6.6).

(iv) *Glycogenic and glycogenolytic genes: Gys2* was negatively correlated with both *Bmal1* and *Clock* on all days of gestation ($P < 0.05$, Table 6.7). In contrast, there were positive associations between *Gys2* and *Per1*, *Per2* and *Cry2* throughout gestation ($P < 0.05$). *Rev-erbα* was positively correlated with *Gys2* only during late gestation (days 14 and 18; $P < 0.05$; Table 6.7). No significant correlations were observed between *Pygl* and any hepatic clock genes.

Table 6.4 Linear regression analysis of the hepatic clock genes with *Glut2* throughout pregnancy.

	Non-Pregnant	Day 6	Day 10	Day 14	Day 18
Bmal1 : Glut2	-0.48	-0.72	-0.68	-0.80	-0.70
	($P < 0.05$)	($P < 0.0001$)	($P < 0.0001$)	($P < 0.0001$)	($P < 0.0001$)
Clock : Glut2	-0.41	-0.62	-0.58	-0.68	-0.61
	($P < 0.05$)	($P < 0.0001$)	($P < 0.0001$)	($P < 0.0001$)	($P < 0.0001$)
Per1 : Glut2	0.64	0.68	0.66	0.57	0.39
	($P < 0.0001$)	($P < 0.0001$)	($P < 0.0001$)	($P < 0.0001$)	($P < 0.05$)
Per2 : Glut2	0.43	0.45	0.48	0.43	0.38
	($P < 0.05$)	($P < 0.001$)	($P < 0.001$)	($P < 0.05$)	($P < 0.05$)
Cry1 : Glut2	-0.40	-0.38	-0.25	-0.46	-0.41
	($P < 0.05$)	($P < 0.05$)	(NS)	($P < 0.01$)	($P < 0.05$)
Cry2 : Glut2	0.49	0.52	0.31	0.38	0.50
	($P < 0.01$)	($P < 0.01$)	($P < 0.05$)	($P < 0.05$)	($P < 0.01$)
Rev-erbα : Glut2	0.58	0.21	0.24	0.51	0.52
	($P < 0.0001$)	(NS)	(NS)	($P < 0.001$)	($P < 0.001$)

Only genes that showed significant correlations for the majority of pregnancy are shown. Correlation coefficients (r) and significance levels are shown for each day of pregnancy.

Table 6.5 Linear regression analysis of hepatic clock genes with *GK* throughout pregnancy.

	Non-Pregnant	**Day 6**	**Day 10**	**Day 14**	**Day 18**
Per2 : GK	0.53	0.68	0.63	0.67	0.40
	($P < 0.001$)	($P < 0.0001$)	($P < 0.0001$)	($P < 0.0001$)	($P < 0.05$)
Cry1 : GK	0.31	0.25	0.36	0.28	0.42
	($P < 0.05$)	(NS)	($P < 0.05$)	($P = 0.06$)	($P < 0.05$)
Rev-erbα : GK	-0.56	-0.49	-0.51	-0.25	-0.46
	($P < 0.001$)	($P < 0.001$)	($P < 0.001$)	(NS)	($P < 0.05$)

Only genes that showed significant correlations for the majority of pregnancy are shown. Correlation coefficients (r) and significance levels are shown for each day of pregnancy.

Table 6.6 Linear regression analysis of hepatic clock genes with *Pck1* and *G6Pase* throughout pregnancy.

	Non-Pregnant	Day 6	Day 10	Day 14	Day 18
Bmal1 : Pck1	-0.52	-0.64	-0.69	-0.69	-0.17
	($P < 0.05$)	($P < 0.0001$)	($P < 0.0001$)	($P < 0.0001$)	(NS)
Clock : Pck1	-0.49	-0.58	-0.55	-0.55	-0.14
	($P < 0.05$)	($P < 0.05$)	($P < 0.0001$)	($P < 0.0001$)	(NS)
Per1 : Pck1	0.65	0.80	0.77	0.68	0.25
	($P < 0.0001$)	($P < 0.0001$)	($P < 0.0001$)	($P < 0.0001$)	(NS)
Cry1 : Pck1	-0.34	-0.38	-0.28	-0.43	-0.12
	($P < 0.05$)	($P < 0.05$)	($P = 0.069$)	($P < 0.001$)	(NS)
Bmal1 : G6Pase	0.30	0.60	0.17	0.39	0.55
	(NS)	($P < 0.0001$)	(NS)	($P < 0.001$)	($P < 0.001$)
Clock : G6Pase	0.30	0.57	0.31	0.64	0.38
	(NS)	($P < 0.05$)	($P = 0.058$)	($P < 0.001$)	($P < 0.05$)
Cry1 : G6Pase	0.33	0.55	0.05	0.10	0.45
	($P < 0.05$)	($P < 0.0001$)	(NS)	(NS)	($P < 0.05$)

Only genes that showed significant correlations for the majority of pregnancy are shown. Correlation coefficients (r) and significance levels are shown for each day of pregnancy.

Table 6.7 Linear regression analysis of hepatic clock genes with *Gys2* throughout pregnancy.

	Non-Pregnant	Day 6	Day 10	Day 14	Day 18
Bmal1 : Gys2	-0.55	-0.63	-0.64	-0.85	-0.66
	($P < 0.001$)	($P < 0.0001$)	($P < 0.0001$)	($P < 0.0001$)	($P < 0.0001$)
Clock : Gys2	-0.66	-0.64	-0.65	-0.69	-0.44
	($P < 0.0001$)	($P < 0.0001$)	($P < 0.0001$)	($P < 0.0001$)	($P < 0.05$)
Per1 : Gys2	0.75	0.69	0.79	0.77	0.77
	($P < 0.0001$)	($P < 0.0001$)	($P < 0.0001$)	($P < 0.0001$)	($P < 0.0001$)
Per2 : Gys2	0.73	0.63	0.72	0.61	0.69
	($P < 0.0001$)	($P < 0.0001$)	($P < 0.0001$)	($P < 0.0001$)	($P < 0.0001$)
Cry2 : Gys2	0.53	0.58	0.42	0.59	0.58
	($P < 0.0001$)	($P < 0.0001$)	($P < 0.001$)	($P < 0.001$)	($P < 0.001$)
Rev-erbα : Gys2	0.29	-0.025	-0.048	0.35	0.42
	($P = 0.0695$)	(NS)	(NS)	($P < 0.05$)	($P < 0.05$)

Only genes that showed significant correlations for the majority of pregnancy are shown. Correlation coefficients (r) and significance levels are shown for each day of pregnancy.

6.5 Discussion

This study shows for the first time that maternal adaptation to pregnancy in the mouse includes marked shifts in the hepatic expression of the core clock genes, *Bmal1*, *Clock*, *Per1*, *Per2*, *Cry1*, *Cry2*, and the accessory clock gene *Rev-erbα*. While the rhythmicity of these genes was generally maintained across pregnancy, the amplitude of their circadian variation declined. These changes were associated with a similar reduction in the circadian variation of hepatic genes involved in glucose homeostasis. We suggest that this relative reduction in the circadian variation of hepatic glucose metabolism after mid-gestation ensures a sustained supply of glucose to meet the high demands of fetal growth.

We recently reported that pregnancy results in changes to the central circadian clock in the mouse, an effect likely to influence various aspects of maternal circadian biology (Wharfe et al. 2016a). The key change in the SCN (an increase in the mesor of the majority of clock genes on day 10) (Wharfe et al. 2016a) appears quite different to the changes reported here for the liver. We hypothesized that maternal metabolic adaptation in pregnancy involves changes in the hepatic expression of clock genes that drive downstream shifts in hepatic expression of genes involved in glucose homeostasis. Hepatic expression of all clock genes changed with the progression through pregnancy. Most notably, while the expression of each remained rhythmic throughout, the majority of genes (*Bmal1*, *Per1*, *Per2*, *Rev-erbα*) showed a greatly reduced amplitude in late pregnancy. Associated with these reductions were gene-specific shifts in the peaks and troughs of expression; for example, the peak (but not the trough) for *Bmal1* was markedly reduced at day 18. On the other hand, both the peak and trough of *Per1* expression were reduced at day 18. These fundamental changes in the profiles of the clock gene rhythms are likely to impact on a wide range of downstream hepatic genes, including those regulating glucose metabolism.

As observed for clock genes, the circadian rhythmicity of several genes involved in glucose homeostasis was also greatly attenuated in late pregnancy. Specifically, while *Pck1* and *Pk* lost their circadian rhythmicity entirely (as evidenced by a loss of significant cosinor fit), the amplitude of expression was progressively reduced throughout pregnancy for *Gk* and *Pck1*. Thus, the overall patterns of change in expression of hepatic clock genes and glucose-related genes appears similar across

gestation, but whether clock gene changes drive the glucose gene changes remains unclear. Certainly, previous studies with transgenic mice suggest that hepatic clock genes do indeed drive circadian variation in glucoregulatory genes, including *Glut2*, *Pck1* and *Gys2* (Kornmann et al. 2007; Lamia, Storch & Weitz 2008; Doi, Oishi & Ishida 2010; Rey et al. 2011), but, their relationships appear to vary depending on the gene and timeframe (circadian vs. stage of pregnancy). For example, the positive correlations observed between *Per1* and each of *Glut2*, *Pck1* and *Gys2* suggest that *Per1* may drive transcription of these genes across the circadian period (24-h). That said, the link between *Per1* and these glucoregulatory genes across pregnancy is less clear. For instance, while *Per1* is strongly positively correlated with both *Glut2* and *Gys2* at each stage of pregnancy, only *Per1* and *Glut2* show parallel overall changes across gestation. Indeed, *Per1* and *Gys2* display opposite changes throughout pregnancy, suggesting factors other than clock genes regulate *Gys2* expression across pregnancy.

An important caveat to interpretation of *Pck1* data in this study is that this enzyme is involved not just in glucose homeostasis, but also in glyceroneogenesis (Beale et al. 2004) and lactate metabolism (Adeva et al. 2013). Furthermore, insulin is a known negative regulator of hepatic *Pck1* expression (Zhang et al. 2011), and thus the late gestational rise in plasma insulin could account for the observed reduction in *Pck1* mesor and amplitude as gestation progressed. Consequently *Pck1* expression patterns may be the result of an integration of regulatory inputs from a variety of pathways.

While it is clear that deletion of clock genes has profound effects on both fertility and metabolism (e.g. *Bmal1*$^{-/-}$ mice are infertile (Boden et al. 2010) and exhibit a loss of rhythmicity in hepatic glucose metabolism (Lamia, Storch & Weitz 2008)), the overall significance of the observed clock gene adaptations in pregnancy remains to be fully elucidated. Thus, in those models where pregnancy can be established, there are somewhat surprisingly only subtle, or no, effects on fetal growth (Kennaway 2005; Turek et al. 2005), although many studies do not report birthweight. This apparent lack of effect may be due to a redundancy that exists within the circadian clock gene machinery. In this context it is also noteworthy that chronodisruption in rat pregnancy, which likely disturbs all clock gene profiles, reduces fetal growth in some (Gozeri et al. 2008) but not all models (Varcoe et al. 2011). Importantly, chronodisruption does result in adverse programming outcomes in offspring (Varcoe et al. 2011), which suggests that

maladaptations during pregnancy do impact offspring wellbeing. Consequently, a more complete understanding of pregnancy-induced adaptations in circadian machinery in metabolic pathways is critical.

Maternal physiological adaptations to pregnancy are driven, at least in part, by increased levels of estrogen and progesterone in the maternal circulation. Whether these sex steroids underpin the hepatic clock gene changes observed here is uncertain, but previous studies do show progesterone and/or estrogen response elements within the promoter regions of several clock genes (Nakamura et al. 2005; Gery et al. 2007; Nakamura et al. 2010). However, the effects of both estrogen (e.g. stimulation of hepatic *Per1* and *Per2* (Nakamura et al. 2005)) and progesterone (upregulation of *Clock*, *Cry1* and *Per1* in the uterus (He et al. 2007; Rubel et al. 2012)) on clock gene expression are the opposite to those observed across gestation in the present study. Accordingly, factors other than sex steroids likely account for the hepatic clock gene changes observed in pregnancy.

Maternal glucocorticoids may also influence pregnancy-induced changes in hepatic clock gene rhythms. Recently, we reported that plasma levels of corticosterone increase 14-fold from before pregnancy to day 18 (Wharfe et al. 2016a), and previous studies show that glucocorticoid response elements are present in the promoter regions of numerous clock genes (*Bmal1*, *Per1*, *Per2*, *Cry1*, *Rev-erbα*) (Balsalobre et al. 2000; Yamamoto et al. 2005; Reddy et al. 2007; So et al. 2009). But again, pregnancy-induced changes in hepatic clock genes do not parallel those induced by either restraint stress or dexamethasone treatment, both of which increase hepatic *Bmal1*, *Per1* and *Cry1* expression (Yamamoto et al. 2005; Reddy et al. 2007). Thus it appears that during pregnancy other factors override the usual glucocorticoid-driven regulation of clock gene expression. Furthermore, glucocorticoids also stimulate hepatic gluconeogenesis, and specifically the transcription of the *Pck1* and *G6Pase* genes, in non-pregnant animals (reviewed in (Jitrapakdee 2012)). The reason we did not see increased *Pck1* or *G6Pase* in association with the elevated corticosterone levels in late gestation is unclear.

The central circadian clock located in the SCN of the hypothalamus can also profoundly influence peripheral tissue clocks via the autonomic nervous system (Kalsbeek et al. 2004; Cailotto et al. 2005). Although the hepatic clock is not fully dependent on the SCN for continued rhythmicity, it is certainly influenced by it (Terazono et al. 2003; Su

et al. 2016). Moreover, we recently reported marked changes in hypothalamic clock gene expression in mouse pregnancy, characterised by elevated clock gene expression on day 10 of gestation for all genes, as well as additional gene-specific changes (Wharfe et al. 2016a). Further study is required to establish whether these central clock changes exert a downstream influence on the hepatic clock and associated changes in glucose metabolism.

In the present study, the circadian rhythms of glucose related genes in the non-pregnant animal are consistent with those observed by others (Cailotto et al. 2008; Lamia, Storch & Weitz 2008; Oishi, Uchida & Itoh 2012). Importantly, however, our data show for the first time a striking reduction in rhythmicity of these metabolic genes late in pregnancy has not previously been reported. It is possible that this reduction in rhythmicity of the glucoregulatory genes has the selective advantage of enabling continuous metabolic activity late in pregnancy to meet the high and unrelenting demands of the rapidly growing fetus. Importantly, recent studies show that changes in glucoregulatory gene expression correlate with enzyme activity e.g. *Pck1* (Cailotto et al. 2008) and with hepatic glucose output (Pocai et al. 2005a; Pocai et al. 2005b; Pocai et al. 2006). Therefore, the pregnancy-induced changes in the daily variation of these genes are likely reflected in altered circadian oscillations of metabolic activity in late gestation.

The timing and amount of food consumption was not measured in this cohort of animals, but previous studies have characterized the influence of pregnancy on these aspects in rodents. Whilst there is evidence that food intake increases during rat pregnancy (Weizenbaum, Kenney & Adler 1979), the majority of food consumption still occurs during the dark phase, consistent with patterns in non-pregnant animals. Furthermore, the acrophase of clock gene rhythms, which is the feature most responsive to altered timing of food intake, was largely unaffected across pregnancy.

Although plasma insulin levels were only rhythmic on day 10 of gestation, there was still considerable variability in plasma insulin levels, with levels typically rising over the transition from light to dark, coincident with likely increases in food intake (Varcoe et al. 2013). Importantly, plasma insulin was elevated after mid-gestation, consistent with previous findings in rodents (Knopp et al. 1973) likely due to the well-established maternal insulin resistance of peripheral tissues in late gestation.

In conclusion, this study shows that the peripheral liver clock undergoes substantial adaptations with the progression of mouse pregnancy. These pregnancy-induced changes may contribute to the altered circadian variation in glucoregulatory genes in late pregnancy in a gene-specific manner. Reductions in the oscillations of these metabolic genes may thus be considered part of the maternal physiological adaptations to pregnancy that are geared towards meeting the high metabolic demands of fetal growth.

Grants

This research did not receive any specific grant from any funding agency in the public, commercial or not-for-profit sector.

Disclosures

The authors have nothing to disclose.

Chapter 7

Pregnancy suppresses the daily rhythmicity of core body temperature and adipose metabolic gene expression in the mouse

Preface

The major objective of this study was to investigate the effect of pregnancy on clock gene expression in white adipose tissue and to determine whether pregnancy impacts the circadian variation of genes involved in lipid metabolism. Furthermore, changes in maternal core body temperature rhythms were explored as a potential driver of pregnancy-induced changes in clock gene expression.

This chapter was co-authored with Caitlin S. Wyrwoll, Peter J. Mark and Brendan J. Waddell and accepted for publication by Endocrinology [vol. 157, no. 9, pp. 3320-3331] in July, 2016.

Michaela Wharfe performed all animal work and tissue sampling and was responsible for all analyses, representing 100% of the laboratory work. Michaela Wharfe was also largely responsible (80%) for writing and submitting the manuscript.

7.1 Abstract

Maternal adaptations in lipid metabolism are crucial for pregnancy success due to the role of white adipose tissue as an energy store and the dynamic nature of energy needs across gestation. Because lipid metabolism is regulated by the rhythmic expression of clock genes, it was hypothesised that maternal metabolic adaptations involve changes in both adipose clock gene expression and the rhythmic expression of downstream metabolic genes. Maternal core body temperature (T_c) was investigated as a possible mechanism driving pregnancy-induced changes in clock gene expression. Gonadal adipose tissue and plasma were collected from C57Bl/6J mice before and on days 6, 10, 14 and 18 of pregnancy (term = d19) at 4 hourly intervals across a 24-h period. Adipose expression of clock genes and downstream metabolic genes were determined by RT-qPCR and T_c was measured by intraperitoneal temperature loggers. Adipose clock gene expression showed robust rhythmicity throughout pregnancy, but absolute levels varied substantially across gestation. Rhythmic expression of the metabolic genes *Lipe*, *Pnpla2* and *Lpl* was clearly evident before pregnancy; however, this rhythmicity was lost with the onset of pregnancy. T_c rhythm was significantly altered by pregnancy with a 65% decrease in amplitude by term and a 0.61°C decrease in mesor between days 6 and 18. These changes in T_c, however, did not appear to be linked to adipose clock gene expression across pregnancy. Overall, our data show marked adaptations in the adipose clock in pregnancy, with an apparent decoupling of adipose clock and lipolytic/lipogenic gene rhythms from early in gestation.

7.2 Introduction

Maternal metabolic adaptation is crucial for pregnancy success by ensuring that the demands of fetal growth are met whilst still maintaining maternal homeostasis. Two distinct maternal metabolic phases are apparent across pregnancy (Knopp et al. 1973; Metcalfe, Stock & Barron 1988); the first of these occurs over days 1-10 of gestation in the mouse and is principally anabolic. During this period, fetal demand is relatively low and so energy is stored in anticipation of increased fetal demand via rapid fetal growth during the second, catabolic phase of gestation (days 11-19) (Knopp et al. 1973). Central to these adaptations are modifications to adipose tissue lipid metabolism linked to its primary function as a long-term energy store. Thus, an increase in fat deposition in adipose tissue (lipogenesis) is a hallmark of early pregnancy, whereas this transitions to adipose tissue mobilisation (lipolysis) in later stages (Knopp et al. 1973; Ramos et al. 2003).

Lipid metabolism exhibits robust circadian rhythmicity (Suzuki, Shimomura & Satoh 1983; Refinetti 1996) driven, at least in part by the rhythmic expression of clock genes (*Clock*, *Bmal1*, *Period* (*Per*) *1*, *Per2* and *Cryptochrome* (*Cry*) *1*, *Cry2*) and accessory clock genes (*Rev-erbα* and *Rorα*) within white adipose tissue itself (Zvonic et al. 2006). Local clock genes drive the rhythmic expression of key enzymes and transporters involved in lipid pathways to enable anticipation of feeding times and thereby ensure appropriate temporal coordination of adipose tissue lipogenesis and lipolysis (Ptitsyn et al. 2006; Sukumaran et al. 2010; Shostak, Meyer-Kovac & Oster 2013). Indeed, studies have shown that BMAL1 binds to the promoter regions of the key lipolytic enzymes, hormone sensitive lipase (*Lipe*) and adipocyte triglyceride lipase (*Pnpla2*) (Koike et al. 2012; Shostak, Meyer-Kovac & Oster 2013) while *Per2* regulates the transcriptional activity of peroxisome proliferator-activated receptor gamma (PPARγ), a nuclear hormone receptor important for adipose tissue lipogenesis (Grimaldi et al. 2010). Moreover, rhythmicity of *Pparγ*, *Lipe* and *Pnpla2* expression are lost in clock gene knock-out models (Kennaway et al. 2012; Shostak, Meyer-Kovac & Oster 2013).

Given the integral role of clock genes in lipid homeostasis, metabolic adaptations of pregnancy are likely to involve changes in the circadian expression of clock genes in metabolic tissues. Indeed, we recently reported that maternal adaptation to pregnancy in the mouse involves major shifts in rhythmic function, including pregnancy-induced

changes in the expression of clock genes in the suprachiasmatic nucleus (SCN) (Wharfe et al. 2016a) and a suppression of rhythmicity towards term in both hepatic clock genes and genes involved in glucose homeostasis (Wharfe et al. 2016b). In the present study therefore, we tested the hypothesis that adipose expression of clock genes and downstream metabolic genes are also suppressed in late pregnancy. Because recent studies have shown that *Bmal1* and *Per2* rhythms can be entrained by 24-h temperature cycles (Brown et al. 2002; Saini et al. 2012; Oishi et al. 2013) and rhythmicity of core body temperature (T_c) is altered by pregnancy in rodents (Fewell 1995; Eliason & Fewell 1997; Gamo et al. 2013), we also tested the hypothesis that T_c rhythms are associated with suppressed adipose clock gene expression during pregnancy. Furthermore, we aimed to determine whether pregnancy-induced changes in T_c are linked to changes in progesterone levels across mouse pregnancy as has been reported previously for the rat (Fewell 1995; Eliason & Fewell 1997).

7.3 Materials and Methods

7.3.1 Animals

Nulliparous C57Bl/6J mice (6-9 weeks old) were supplied by the Animal Resources Centre (Murdoch, Australia). All procedures involving the use of animals were conducted after approval by the Animal Ethics Committee of The University of Western Australia (AEC number RA/3/100/1070). Mice were maintained in 12:12 light/dark cycle as described previously (Wharfe et al. 2016a). Lights on at 0700 h (or 1900 h in the reverse-light room) was classified as a new day and as zeitgeber time (ZT)-zero, and sampling times were defined relative to ZT-zero. Estrous cycle stage was monitored for a minimum of three full cycles by vaginal lavage (between ZT6 and 13) by the protocol of Caligioni (2009). Mice were mated overnight at proestrus, and pregnancy was confirmed by visualization of a mucous plug the following morning (designated day 1 of pregnancy).

7.3.2 Measurement of core body temperature

Prior to mating, a temperature logger (DS1921G-F5 Thermochron iButton, Embedded Data Systems, Kentucky, USA) was surgically implanted into the peritoneal cavity of a subset of animals (n = 3) under isoflurane/nitrous oxide (0.2: 0.8) anaesthesia. Prior to implantation, these temperature loggers were partially dismantled according to the protocol of Lovegrove (2009), to reduce their weight for use in the mouse. After coating the logger in wax (Sasol EXP986, Sasol Chemical Industries Ltd., Johannesburg, South Africa) the final weight was no more than 7.5% of the mouse's body weight.

Animals were allowed to recover for 1 week post-surgery before smearing for estrous cycle stage. Temperature loggers recorded body temperature every 15 minutes and were retrieved during tissue sampling on day 18 of gestation. After recovery, temperature loggers were calibrated using a certified mercury-in-glass thermometer (National Association of Testing Authorities, Australia) in a water bath at 3°C increments from 33-41°C. Data were downloaded and read using eTemperature software (version 8.25, OnSolution Pty Ltd, Baulkham Hills, Australia). Data sets were corrected according to the calibration curve generated for each temperature logger. Final data sets consisted of 23 days of measurements.

7.3.3 Tissue Collection

Gonadal adipose tissue samples and plasma (*n* = 6-8 per ZT) were collected from mice under isoflurane/nitrous oxide (0.2: 0.8) anaesthesia at 4-h intervals commencing at ZT1 on either diestrus I of the cycle or days 6, 10, 14 or 18 of pregnancy (term = day 19). For collection of tissues in the dark phase, anaesthesia was carried out under red light before fitting the mouse with a light proof hood and obtaining tissues in white light. A blood sample was obtained under anaesthesia by cardiac puncture (into an EDTA tube) and a portion of gonadal adipose tissue was collected. Tissue samples were snap frozen in liquid nitrogen, and the blood sample centrifuged at 13,000 x *g* to obtain plasma. Plasma and adipose tissue samples were stored at -80°C.

7.3.4 RNA sample preparation

Total RNA was extracted from adipose samples using an RNeasy lipid tissue mini kit (Qiagen, Doncaster, Australia) as per the manufacturer's instructions. After quantitation of RNA using the NanoDrop ND-1000 spectrophotometer (NanoDrop, Wilmington, DE, USA), total RNA (5 μg) was reverse transcribed at 42°C for 110 min by Mouse Moloney leukemia virus reverse transcriptase with random hexamers (Promega, Sydney, Australia). The resultant cDNAs were purified using an ultra-clean PCR spin kit (MoBio Laboratories, Inc., Carlsbad, CA) as per manufacturer's instructions.

7.3.5 Real-time PCR

Analyses of mRNA expression levels of the following genes were performed by real-time PCR on the Rotorgene 6000 system (Corbett Research, Sydney, Australia): the clock genes *Clock, Arntl* which encodes *Bmal1*, *Per1, Per2, Cry1, Cry2, Nr1d1* which encodes *Rev-erbα, Rorα*; the metabolic genes lipoprotein lipase (*Lpl*), *Lipe*, *Pnpla2* and *Pparγ*; and the reference genes succinate dehydrogenase complex, subunit A (*Sdha*), peptidylprolyl isomerase A (*Ppia*) and TATA box binding protein (*Tbp*). Primer pairs for all genes (see Table 1) were designed using Primer-BLAST (http://www.ncbi.nlm.nih.gov/tools/primer-blast/) (Ye et al. 2012). All primer pairs were designed to span introns to prevent amplification of product from genomic DNA. The resulting amplicons were sequenced to confirm specificity. Standard curves were created with 10-fold serial dilutions of gel-extracted (QIAEX II; Qiagen, Doncaster, Australia) PCR products using the Rotorgene 6000 software. All samples were

normalized against *Sdha*, *Ppia* and *Tbp* using the GeNorm algorithm (Vandesompele et al. 2002). None of the reference genes varied significantly with either time of day or stage of gestation.

7.3.6 Measurement of plasma progesterone

Plasma progesterone concentrations were analysed using liquid chromatography tandem mass spectrometry (LC-MS/MS) by the protocol described previously (Wharfe et al. 2016a). For this metabolite the internal standard used was progesterone d9 (5 ng/ml) and the intra- and inter-assay coefficients of variation (CV) were 0.3% and 7.7%, respectively.

7.3.7 Statistical Analysis

All data are expressed as the mean ± SEM. Where data were not normally distributed (based on D'Agostino and Pearson omnibus normality test), values were log transformed prior to statistical analysis. Variation in metabolic gene expression and plasma progesterone was assessed by two-way ANOVA, with time-of-day and pregnancy stage as factors. When a significant interaction was observed, time-of-day variation within each day was assessed by one-way ANOVA. Statistical analyses were conducted using GraphPad Prism 6.00 (GraphPad Software, La Jolla, CA, USA).

Rhythmic variation was assessed by cosinor analysis using a non-linear regression model (Genstat Version 9, VSN International Ltd, Hemel Hempstead, UK). This analysis generated the following rhythm descriptors: mesor (rhythm adjusted mean), amplitude, acrophase (time of the peak of a rhythm) and cosinor r^2 as a measure of fit. One-way ANOVA was used to determine whether each of these cosinor descriptors varied with stage-of-pregnancy. For all ANOVAs, where the *F* test was significant ($P < 0.05$), *post hoc* LSD tests were used for pairwise comparisons. Relationships between clock genes and downstream metabolic genes were assessed by linear regression analysis.

Table 7.1 Primers and PCR conditions used to measure adipose clock genes, metabolic genes and reference genes by RT-qPCR.

Gene	Forward/Reverse Primer sequence	Amplicon Size (bp)	Annealing Temp (°C)	$MgCl_2$ (mM)
Clock	F, 5' - ACAACGCACACATAGGCCTTC– 3'	175	60	3
	R, 5' – TGGTGGTGCCCTGTGATCTA – 3'			
Bmal1	F, 5' – CGTGCTAAGGATGGCTGTTC – 3'	166	60	3
	R, 5' – CTTCCCTCGGTCACATCCTA – 3'			
Per1	F, 5' – TGCACTTCGGGAGCTCAAACTTC – 3'	169	59	2
	R, 5' – GTCCATGGCACAAGGCTCACC – 3'			
Per2	F, 5' – AACAAATCCACCGGC – 3'	145	60	3
	R, 5' – CTCCGGTGAGACTCC – 3'			
Cry1	F, 5' – AACGTCCCGAGCTGTAGCGGT – 3'	139	60	2
	R, 5' – GACGCTTCCCACTGCTGAGGC – 3'			
Cry2	F, 5' – TGCCTCTCCTGCCGCCTCTT- 3'	193	60	2
	R, 5' – TGCGGTCCCAGGGGATCTGG – 3'			
Rev-erbα	F, 5' – CGGGGCTCACTCGTCTCCCT – 3'	185	60	2
	R, 5' - GCTCGGGGAGGAGCCACTAGA – 3'			
Rorα	F, 5' – CCCAACCGTGTCCATGGCAG – 3'	235	60	3
	R, 5' – TCCATCAATGCGTTTGGCAA – 3'			

Gene	Forward/Reverse Primer sequence	Amplicon Size (bp)	Annealing Temp (°C)	$MgCl_2$ (mM)
Lpl	F, 5' – CAGCAAGACCTTCGTGGTGA – 3' R, 5' – ATAATGTTGCTGGGCCCGAT – 3'	148	60	3
Lipe	F, 5' – GGCTCACAGTTACCATCTCACC – 3' R, 5' – GAGTACCTTGCTGTCCTGTCC – 3'	107	60	3
Pnpla2	F, 5' – CAACGCCACTCACATCTACGG – 3' R, 5' – TCACCAGGTTGAAGGAGGGAT – 3'	161	60	3
Pparγ	F, 5' – AACTCTGGGAGATTCTCCTGTTGA – 3' R, 5' - CCTATGAGCACTTCACAAGAAGAAATTACC – 3'	131	58	4
Tbp	F, 5' – GGGAGAATCATGGACCAGAA – 3' R, 5' – CCGTAAGGCATCATTGGACT – 3'	113	60	2
Ppia	F, 5' – AGCATACAGGTCCTGGCATC – 3' R, 5' – TTCACCTTCCCAAAGACCAC – 3'	127	62	3
Sdha	F, 5' – TGGGGAGTGCCGTGGTGTCA – 3' R, 5' – CTGTGCCGTCCCCTGTGCTG – 3'	149	60	2

Lpl, lipoprotein lipase; *Lipe*, hormone sensitive lipase; *Pnpla2*, adipocyte triglyceride lipase; *Pparγ*, peroxisome proliferator-activated receptor gamma; *Tbp*, TATA box binding protein; *Ppia*, peptidylprolyl isomerase A; *Sdha*, succinate dehydrogenase complex, subunit A

7.4 Results

7.4.1 Adipose tissue clock gene expression varies across gestation

Consistent with the role of clock genes as a set of rhythmically expressed transcription factors, cosinor analysis showed highly significant daily rhythmic variation for all adipose clock genes at each pregnancy stage, with the exception of *Rorα* on day 10 (see Table 7.2 for r^2 and *P* values).

A common feature among all clock genes, except *Clock*, was that absolute expression levels were lowest on day 6 (i.e. mesors decreased by up to 47% compared to non-pregnant; $P < 0.0001$; Figures 7.1 and 7.2, Table 7.2). Thereafter, the mesor reached maximal levels on either day 14 or 18 of gestation for all genes ($P < 0.0001$), with the exception of *Cry1* and *Rev-erbα*. Another notable feature was that the lowest amplitude of expression for several genes (*Bmal1*, *Clock*, *Cry1* and *Rev-erbα*) occurred in late gestation (Figures 7.1 and 7.2, Table 7.2).

Pregnancy also resulted in subtle gene-specific changes to the time of peak expression (acrophase) for *Bmal1*, *Cry2*, *Rev-erbα* and *Rorα* (Figures 7.1 and 7.2, Table 7.2). Thus, between days 14 and 18, peak expression of *Bmal1* was advanced by approximately 1-h, whilst the acrophase of *Cry2* was advanced approximately 4-h between days 10 and 18 ($P < 0.05$). In contrast, the acrophase of *Rev-erbα* was delayed by around 2-h from day 6 onwards ($P < 0.0001$), whereas peak *Rorα* expression was delayed 3-h on day 14 ($P < 0.05$; Table 7.2).

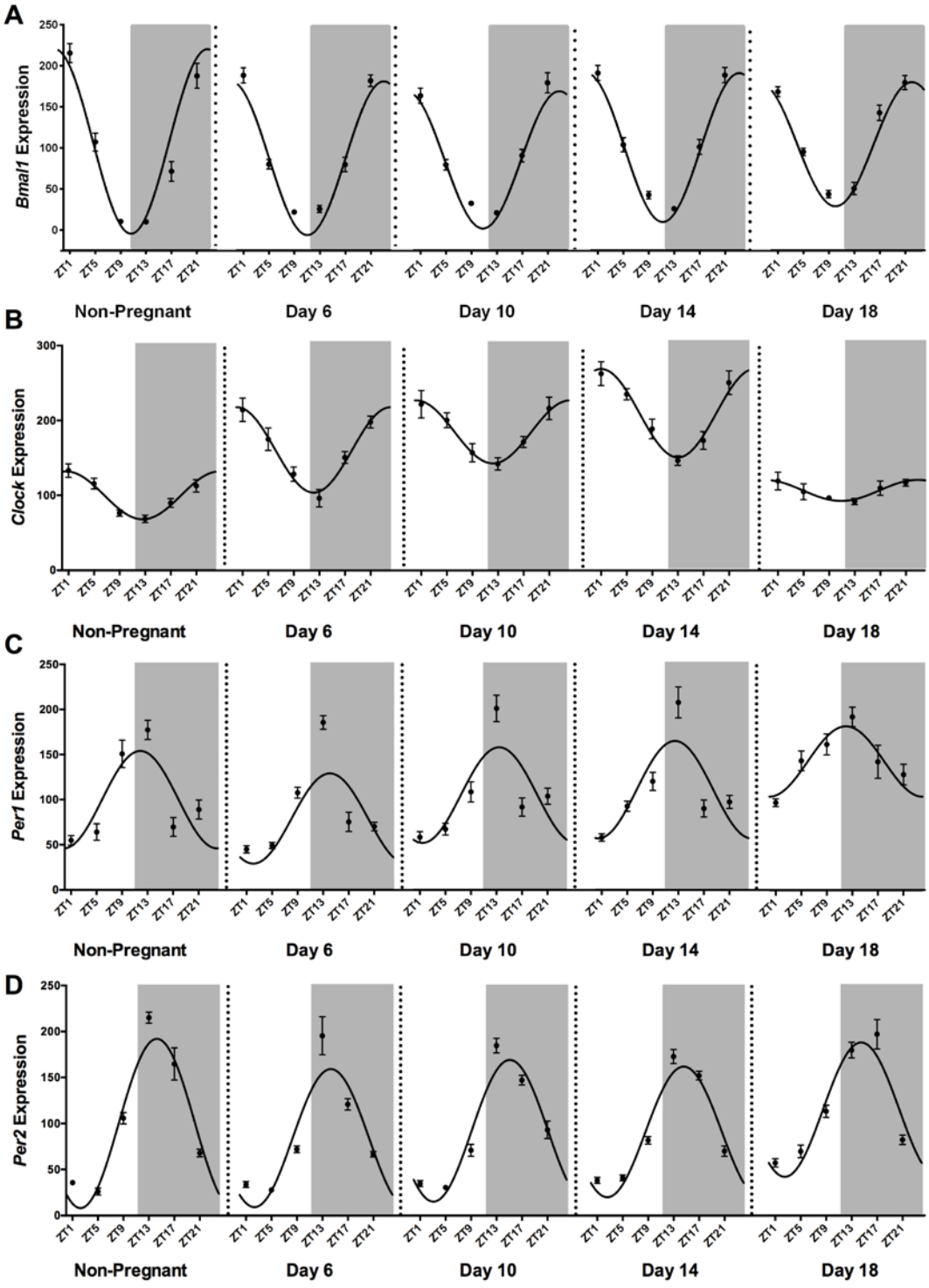

Figure 7.1 Adipose tissue expression of (A) *Bmal1*, (B) *Clock*, (C) *Per1* and (D) *Per2* at ZT1, 5, 9, 13, 17 and 21 in non-pregnant mice and in pregnant mice on days 6, 10, 14 and 18. Values are the mean ± SEM (n = 6-8/group) and are expressed relative to non-pregnant mesor levels (adjusted to 100). Grey shading represents the dark phase of the light cycle. The best-fit curve derived by cosinor analysis is shown as a solid line ($P < 0.05$).

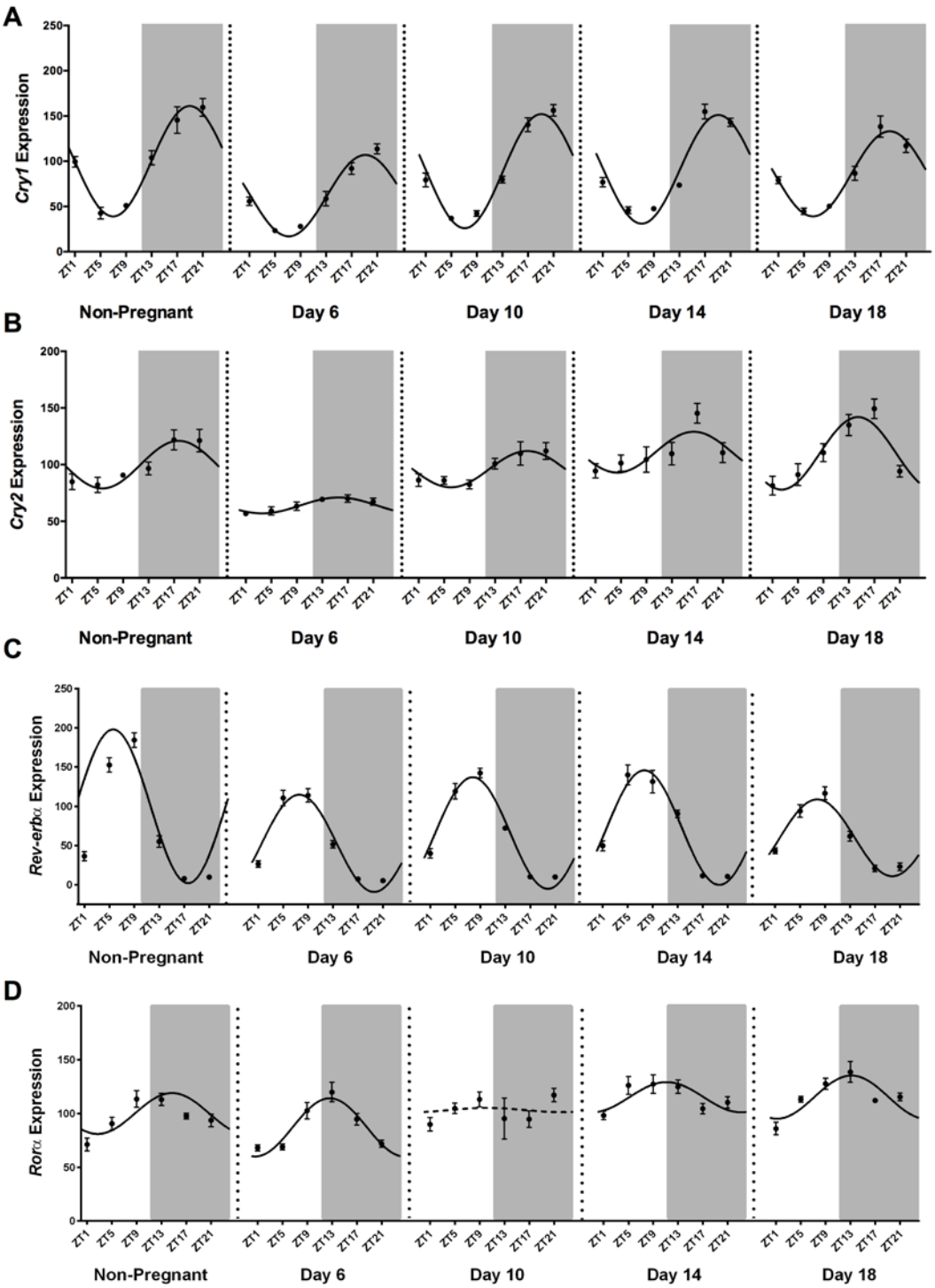

Figure 7.2 Adipose tissue expression of (A) *Cry1*, (B) *Cry2*, (C) *Rev-erbα* and (D) *Rorα* at ZT1, 5, 9, 13, 17 and 21 in non-pregnant mice and in pregnant mice on days 6, 10, 14 and 18. Values are the mean ± SEM (n = 6-8/group) and are expressed relative to non-pregnant mesor levels (adjusted to 100). Grey shading represents the dark phase of the light cycle. The best-fit curve derived by cosinor analysis is shown as a solid line when significant ($P < 0.05$) and as a dashed line when non-significant.

Table 7.2 Mesor, amplitude, acrophase and r^2 derived from cosinor analyses of adipose clock gene expression.

		Non-Pregnant	Day 6	Day 10	Day 14	Day 18	*P* value
Bmal1	Mesor	100 ± 4^{a}	88 ± 3^{b}	86 ± 3^{b}	101 ± 3^{a}	105 ± 3^{a}	<0.0001
	Amplitude	113 ± 6^{a}	94 ± 4^{b}	84 ± 5^{bc}	91 ± 5^{b}	76 ± 4^{c}	<0.0001
	Acrophase	23.6 ± 0.2^{a}	23 ± 0.2^{ad}	22.8 ± 0.2^{bd}	23.2 ± 0.2^{ad}	22 ± 0.2^{c}	<0.0001
	Cosinor r^2	0.89 ($P < 0.0001$)	0.90 ($P < 0.0001$)	0.87 ($P < 0.0001$)	0.89 ($P < 0.0001$)	0.88 ($P < 0.0001$)	
Clock	Mesor	100 ± 3^{a}	161 ± 5^{b}	185 ± 5^{c}	210 ± 5^{d}	107 ± 3^{a}	<0.0001
	Amplitude	32 ± 4^{a}	57 ± 7^{bd}	42 ± 7^{ad}	59 ± 7^{b}	14 ± 5^{c}	<0.0001
	Acrophase	0.6 ± 0.5	0.1 ± 0.5	0.2 ± 0.6	1.0 ± 0.5	22.9 ± 1.3	NS
	Cosinor r^2	0.59 ($P < 0.0001$)	0.60 ($P < 0.0001$)	0.42 ($P < 0.0001$)	0.60 ($P < 0.0001$)	0.13 ($P < 0.05$)	
Per1	Mesor	100 ± 6^{a}	79 ± 6^{b}	105 ± 6^{a}	111 ± 6^{a}	143 ± 5^{c}	<0.0001
	Amplitude	54 ± 8	50 ± 8	53 ± 8	54 ± 8	39 ± 7	NS
	Acrophase	11.9 ± 0.6	14.1 ± 0.6	13.4 ± 0.6	12.5 ± 0.6	12 ± 0.7	NS (0.053)
	Cosinor r^2	0.48 ($P < 0.0001$)	0.44 ($P < 0.0001$)	0.46 ($P < 0.0001$)	0.48 ($P < 0.0001$)	0.38 ($P < 0.0001$)	
Per2	Mesor	100 ± 4^{a}	84 ± 5^{b}	92 ± 3^{a}	91 ± 3^{a}	115 ± 4^{c}	<0.0001
	Amplitude	92 ± 6	75 ± 7	77 ± 5	71 ± 4	73 ± 6	NS
	Acrophase	14.3 ± 0.2	14.3 ± 0.4	15.1 ± 0.2	14.6 ± 0.2	14.5 ± 0.3	NS
	Cosinor r^2	0.84 ($P < 0.0001$)	0.70 ($P < 0.0001$)	0.85 ($P < 0.0001$)	0.88 ($P < 0.0001$)	0.76 ($P < 0.0001$)	
Cry1	Mesor	100 ± 4^{a}	62 ± 2^{b}	89 ± 3^{c}	91 ± 3^{c}	86 ± 3^{c}	<0.0001
	Amplitude	61 ± 5^{a}	45 ± 3^{b}	63 ± 4^{a}	60 ± 4^{a}	47 ± 4^{b}	<0.001
	Acrophase	19.0 ± 0.3	19.2 ± 0.3	19.1 ± 0.2	19.0 ± 0.2	18.4 ± 0.3	NS
	Cosinor r^2	0.77 ($P < 0.0001$)	0.79 ($P < 0.0001$)	0.87 ($P < 0.0001$)	0.85 ($P < 0.0001$)	0.74 ($P < 0.0001$)	
Cry2	Mesor	100 ± 3^{a}	64 ± 1^{b}	96 ± 3^{a}	111 ± 4^{c}	110 ± 3^{c}	<0.0001
	Amplitude	21 ± 4^{ad}	7 ± 2^{bc}	16 ± 4^{ac}	18 ± 5^{ac}	32 ± 5^{d}	<0.001
	Acrophase	17.7 ± 0.8^{ac}	15.6 ± 1.1^{ac}	18.1 ± 0.9^{a}	16.4 ± 1.2^{ac}	14.4 ± 0.6^{bc}	<0.05
	Cosinor r^2	0.36 ($P < 0.0001$)	0.19 ($P < 0.01$)	0.27 ($P < 0.001$)	0.40 ($P < 0.0001$)	0.48 ($P < 0.0001$)	
Rev-erbα	Mesor	100 ± 5^{a}	53 ± 3^{b}	66 ± 3^{cd}	73 ± 4^{d}	60 ± 3^{bc}	<0.0001
	Amplitude	98 ± 8^{a}	62 ± 4^{bc}	71 ± 4^{b}	73 ± 5^{b}	49 ± 4^{c}	<0.0001
	Acrophase	5.6 ± 0.3^{a}	7.6 ± 0.2^{b}	7.8 ± 0.2^{b}	7.7 ± 0.3^{b}	7.8 ± 0.3^{b}	<0.0001
	Cosinor r^2	0.79 ($P < 0.0001$)	0.84 ($P < 0.0001$)	0.90 ($P < 0.0001$)	0.82 ($P < 0.0001$)	0.78 ($P < 0.0001$)	
Rorα	Mesor	100 ± 2^{a}	87 ± 2^{b}	103 ± 3^{a}	115 ± 3^{c}	115 ± 3^{c}	<0.0001
	Amplitude	19 ± 4	27 ± 3	-	14 ± 4	20 ± 4	NS
	Acrophase	0.2 ± 0.7^{ab}	0.8 ± 0.5^{a}	-	21.4 ± 1.1^{b}	0.3 ± 0.7^{a}	<0.05
	Cosinor r^2	0.38 ($P < 0.05$)	0.57 ($P < 0.0001$)	0 (NS)	0.19 ($P < 0.05$)	0.35 ($P < 0.0001$)	

Mesor, amplitude and acrophase values are mean ± SEM. Mesor and amplitude are expressed relative to the mesor value in the Non-Pregnant group (set at 100). Acrophase is expressed in clocktime. Within each group, values without common notation differ significantly ($P < 0.05$; one-way ANOVA and Fisher's LSD test). Values for r^2 are shown with relevant *P* values in parentheses unless non-significant (NS).

7.4.2 Adipose lipoprotein lipase expression is elevated at mid-pregnancy

While adipose expression of the key lipogenic gene, *Lpl*, showed clear daily rhythmic variation prior to pregnancy, during pregnancy this rhythmicity was significant only on days 6 and 14 ($P < 0.05$; see Table 7.3 for r^2 and P values). Absolute levels of *Lpl* expression varied significantly with stage-of-pregnancy ($P < 0.0001$, two-way ANOVA). Although *Lpl* did not vary with time of day, there was a significant *time-of-day* x *stage-of-pregnancy* interaction ($P < 0.001$ two-way ANOVA) such that an effect of time-of-day was present only prior to pregnancy. Overall *Lpl* expression was highest on days 10 and 14 of pregnancy (Figure 7.3A), but then fell to levels 32% lower than pre-pregnancy on day 18, suggestive of decreased lipogenesis ($P < 0.0001$, one-way ANOVA; Figure 7.3A). A similar pattern of change was observed by comparison of *Lpl* mesors across pregnancy (one-way ANOVA; Table 7.3).

7.4.3 Daily rhythmic variation of lipolytic gene expression is lost with the onset of pregnancy

Adipose expression of both *Lipe* and *Pnpla2* showed highly significant daily rhythmic variation before pregnancy ($P < 0.0001$; Figure 7.3B) consistent with previous findings in the mouse (Shostak, Meyer-Kovac & Oster 2013). Strikingly, however, rhythmicity of both these lipolytic genes was lost for the entirety of pregnancy (see Figure 7.3B and Table 7.3 for r^2 and P values).

Overall, *Lipe* expression varied with stage-of-pregnancy, time-of-day and there was a significant *time-of-day* x *stage-of-pregnancy* interaction ($P < 0.01$, two-way ANOVA). Consistent with the cosinor analysis, *Lipe* varied with time-of-day prior to pregnancy, but expression did not vary across a 24-h period at any stage during gestation (one-way ANOVA). *Pnpla2* expression was not affected by time-of-day but did vary with stage-of-pregnancy ($P < 0.0001$, two-way ANOVA).

The pregnancy-induced changes in absolute levels of the lipolytic genes were consistent with a mid-gestation transition from an anabolic to a catabolic state; both *Lipe* and *Pnpla2* remained either unchanged or decreased on day 6 of pregnancy, before reaching peak levels on day 14. Despite the increased lipolysis observed in rats late in gestation (Knopp et al. 1973; McNamara & Bauman 1978), absolute levels of both lipolytic genes were substantially decreased on day 18 ($P < 0.0001$, *Lipe*: one-way ANOVA; *Pnpla2*:

two-way ANOVA; Figure 7.3). A similar pattern of change was observed by comparison of mesors across pregnancy (one-way ANOVA; Table 7.3).

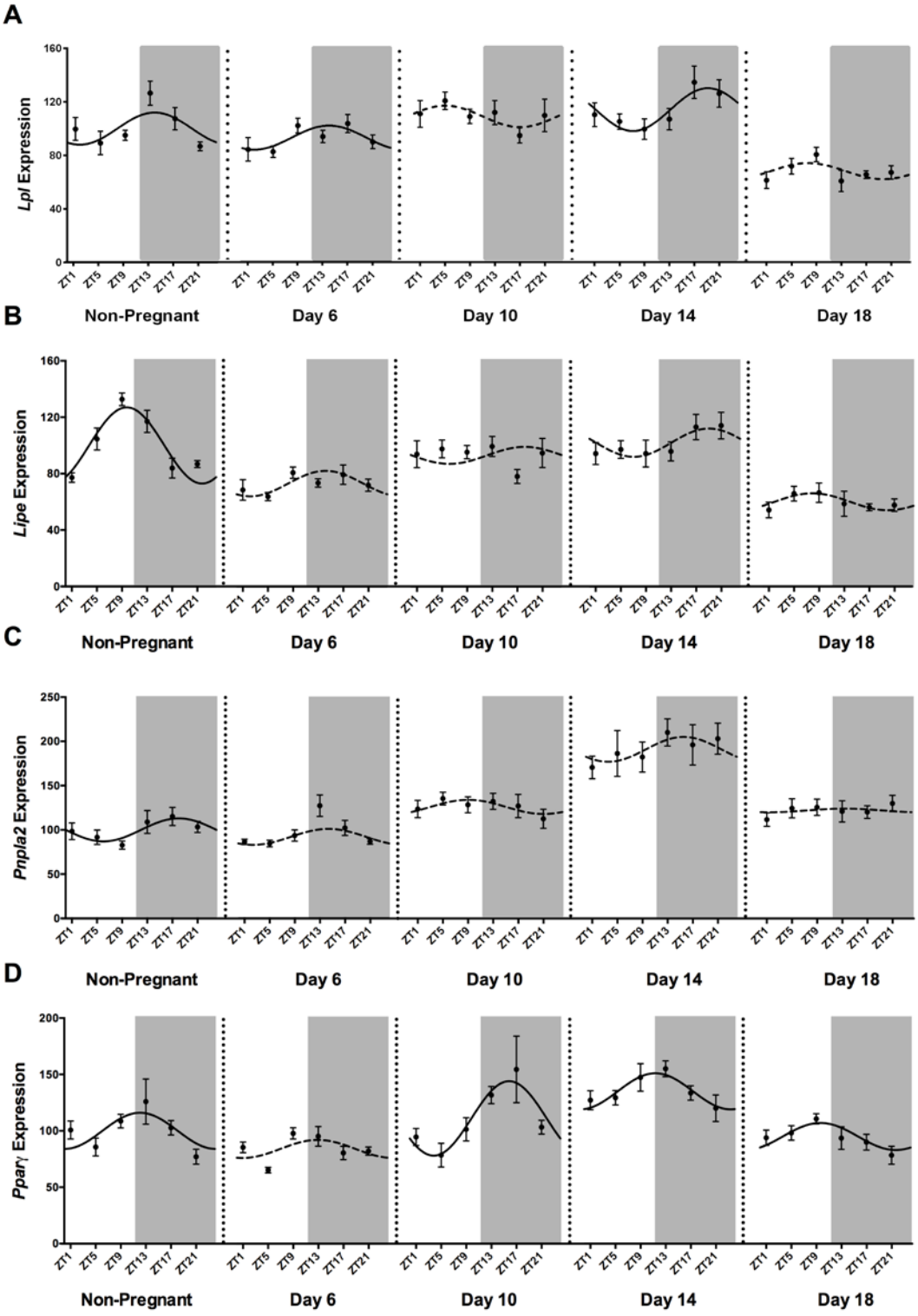

Figure 7.3 Adipose tissue expression of (A) *Lpl*, (B) *Lipe*, (C) *Pnpla2* and (D) *Pparγ* at ZT1, 5, 9, 13, 17 and 21 in non-pregnant mice and in pregnant mice on days 6, 10, 14 and 18. Values are the mean ± SEM (n = 6-8/group) and are expressed relative to non-pregnant mesor levels (adjusted to 100). Grey shading represents the dark phase of the light cycle. The best-fit curve derived by cosinor analysis is shown as a solid line when significant ($P < 0.05$) and as a dashed line when non-significant.

Table 7.3 Mesor, amplitude, acrophase and r^2 derived from cosinor analyses of adipose tissue downstream gene expression.

		Non-Pregnant	Day 6	Day 10	Day 14	Day 18	*P* value
Lpl	Mesor	100 ± 3^{a}	93 ± 3^{a}	109 ± 3^{b}	114 ± 4^{b}	68 ± 2^{c}	<0.0001
	Amplitude	12 ± 5	9 ± 4	-	16 ± 5	-	NS
	Acrophase	14.0 ± 1.4^{a}	14.1 ± 1.4^{a}	-	19.2 ± 1.2^{b}	-	<0.05
	Cosinor r^2	0.11 ($P < 0.05$)	0.10 ($P < 0.05$)	0.02 (NS)	0.14 ($P < 0.05$)	0.02 (NS)	
Lipe	Mesor	100 ± 3^{a}	73 ± 2^{b}	93 ± 0^{c}	102 ± 3^{a}	60 ± 2^{d}	< 0.0001
	Amplitude	27 ± 4	-	-	-	-	-
	Acrophase	9.8 ± 0.5	-	-	-	-	-
	Cosinor r^2	0.54 ($P < 0.0001$)	0.05 (NS)	0 (NS)	0.06 (NS)	0.02(NS)	
Pnpla2	Mesor	100 ± 4^{a}	92 ± 3^{a}	126 ± 4^{b}	191 ± 8^{c}	122 ± 4^{b}	<0.0001
	Amplitude	13 ± 5	-	-	-	-	-
	Acrophase	18 ± 1.5	-	-	-	-	-
	Cosinor r^2	0.11 ($P < 0.05$)	0.08 (NS)	0 (NS)	0 (NS)	0 (NS)	
Pparγ	Mesor	100 ± 4^{ad}	84 ± 2^{be}	111 ± 6^{ac}	135 ± 4^{c}	92 ± 3^{de}	<0.05
	Amplitude	16 ± 6	-	33 ± 8	16 ± 5	12 ± 5	NS (0.06)
	Acrophase	12.1 ± 1.3^{ab}	-	15.8 ± 0.9^{ac}	11.4 ± 1.2^{bc}	9.6 ± 1.5^{b}	<0.05
	Cosinor r^2	0.11 ($P < 0.05$)	0.07 ($P = 0.07$)	0.24 ($P < 0.001$)	0.14 ($P < 0.01$)	0.09 ($P < 0.05$)	

Mesor, amplitude and acrophase values are mean ± SEM. Mesor and amplitude are expressed relative to the mesor value in the Non-Pregnant group (set at 100). Acrophase is expressed in clocktime. Within each group, values without common notation differ significantly ($P < 0.05$; one-way ANOVA and Fisher's LSD test). Values for r^2 are shown with relevant *P* values in parentheses unless non-significant (NS).

7.4.4 Rhythmic variation of *Pparγ* is maintained during pregnancy

Cosinor analysis showed significant rhythmic variation in the expression of *Pparγ* on all days measured (other than day 6 when a strong trend was observed; see Table 7.3 for r^2 and *P* values). The mesor of *Pparγ* fell by day 6 of gestation, but then increased to a maximum on day 14 (1.35-fold higher than non-pregnant), before returning to pre-pregnancy levels just before term ($P < 0.05$, one-way ANOVA; Figure 7.3D, Table 7.3). These pregnancy-induced changes in the *Pparγ* mesor closely paralleled those of *Lpl*, a known target gene of *Pparγ* within adipose tissue (Schoonjans et al. 1996). While the amplitude of *Pparγ* was not altered by pregnancy, the acrophase on day 10 was 4-h later than on day 18 of pregnancy ($P < 0.05$, one-way ANOVA; Table 7.3).

7.4.5 Correlations between adipose clock genes and downstream metabolic genes

Significant correlations between adipose tissue clock genes and downstream metabolic genes were relatively infrequent, particularly during pregnancy (Supplementary Tables 7.1 – 7.4). Interestingly, several correlations were significant only prior to pregnancy; for example, *Lpl* was negatively correlated with *Bmal1* and *Clock* and positively correlated with *Per2*, whereas *Lipe* was negatively correlated with *Bmal1* and *Cry1* and positively correlated with *Per1* ($P < 0.05$). Consistent with the maintenance of *Pparγ* rhythmicity in pregnancy, its correlation with the expression of various clock genes was largely maintained across pregnancy. Of particular note, *Pparγ* was positively associated with *Per2* at all stages except day 18 ($P < 0.05$; Supplementary Table 7.4).

7.4.6 The mesor and amplitude of core body temperature rhythms are altered by pregnancy

The T_c mesor increased by day 6 of gestation and remained elevated until day 10 (Figure 7.4A and 7.4B). Thereafter T_c mesor decreased 0.23°C by day 14, followed by a further 0.28°C decrease by day 18 ($P < 0.05$, one-way ANOVA). The T_c mesor at day 18 closely approximated the pre-pregnancy value.

Pregnancy also substantially altered the amplitude of the T_c rhythm, which was maximal before pregnancy (Figure 7.4C). By day 10, the amplitude had fallen 44% and decreased a further 43% by day 14 and remained at this low level at day 18 ($P < 0.05$, one-way ANOVA; Figure 7.4C). The acrophase of the T_c rhythm was unaffected by the onset and progression of pregnancy.

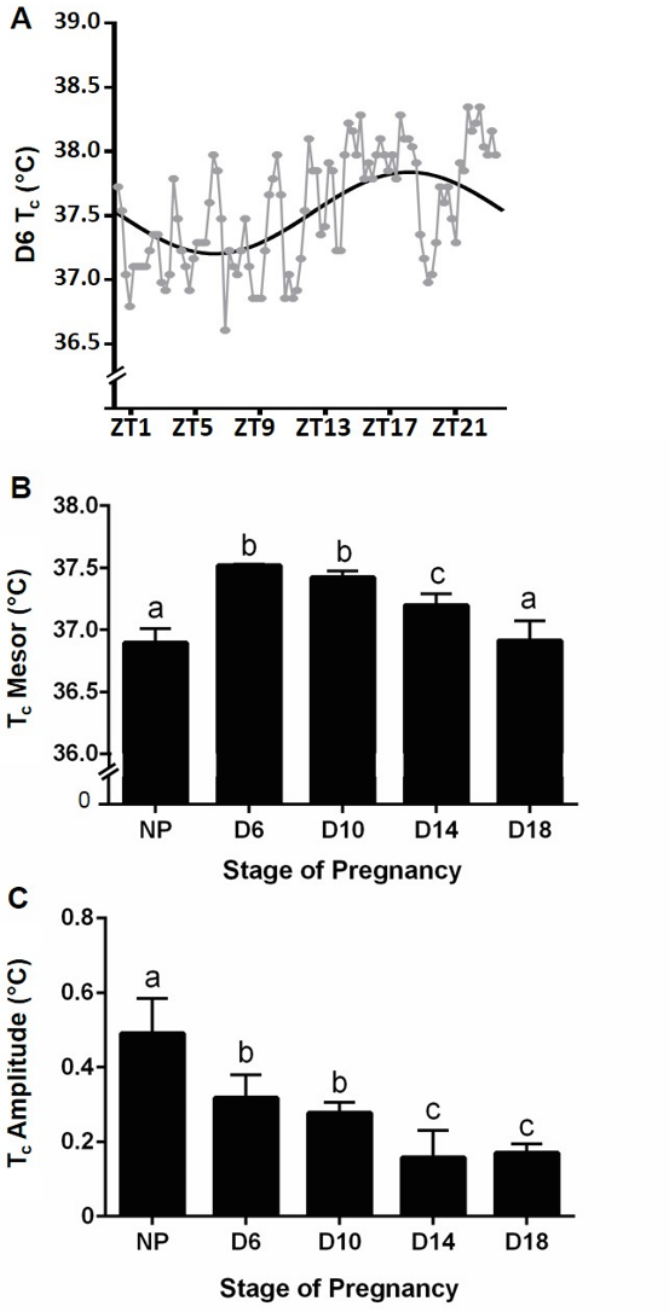

Figure 7.4 Core body temperature (T_c) in pregnant and non-pregnant mice. (A) Representative daily T_c profile in a day 6 pregnant animal. (B) Mesor and (C) amplitude of T_c rhythms in non-pregnant mice and in pregnant mice on days 6, 10, 14 and 18. Values are the mean ± SEM (n = 3/group). Values without common notation differ significantly ($P < 0.05$; one-way ANOVA and *post hoc* Fisher's LSD test).

7.4.7 Plasma progesterone rhythms across gestation

Overall, plasma progesterone varied significantly with stage-of-pregnancy ($P < 0.001$, two-way ANOVA) with levels increasing substantially by day 6 (8-fold) and further by day 14. Progesterone remained high on day 18, reaching levels that were up to 14-fold higher than before pregnancy (Figure 7.5). Although progesterone did not show time-of-day variation overall, there was a significant *time-of-day* x *stage-of-pregnancy* interaction ($P < 0.001$, two-way ANOVA). Accordingly, progesterone varied with time-of-day on day 6 only ($P < 0.001$, one-way ANOVA), whereas significant cosinor rhythms were present on days 10 and 18 ($r^2 = 0.098$ and 0.155; $P < 0.05$; Figure 7.5). This rhythmic variation was most pronounced at day 18, when peak progesterone levels occurred during the light phase. Consistent with this rhythmic variation, overall progesterone levels in the light phase (248 ± 11 nM) were approximately 20% higher than those in the dark phase (201 ± 11 nM; $P < 0.01$, unpaired *t*-test).

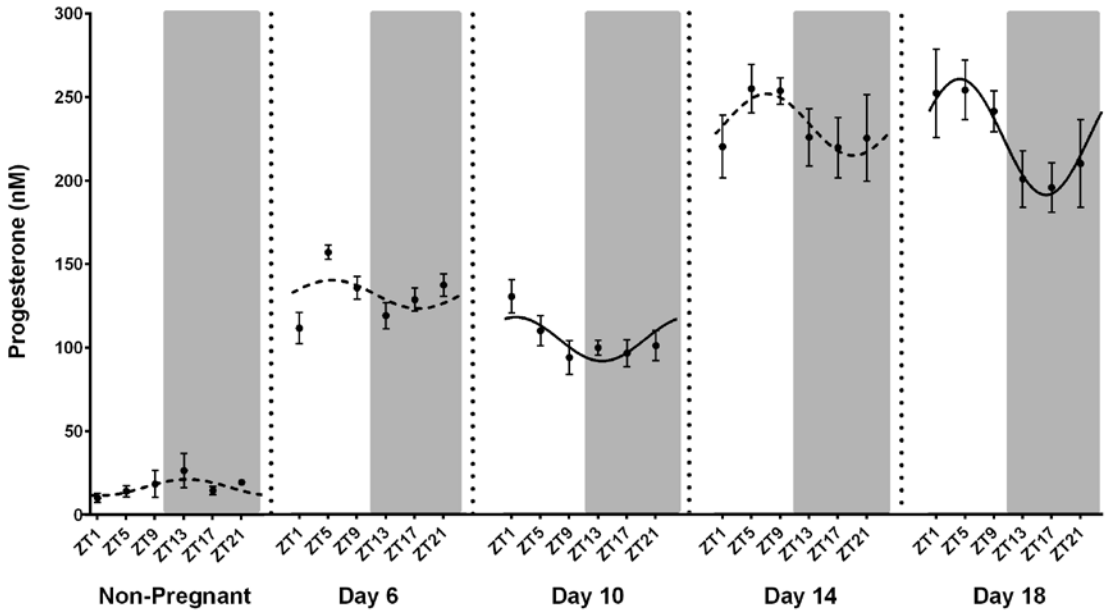

Figure 7.5 Plasma progesterone (nM) at ZT1, 5, 9, 13, 17 and 21 in non-pregnant mice and in pregnant mice on days 6, 10, 14 and 18. Values are the mean ± SEM (n = 6-8/group). Grey shading represents the dark phase of the light cycle. The best-fit curve derived by cosinor analysis is shown as a solid line when significant ($P < 0.05$) and as a dashed line when non-significant.

7.5 Discussion

This study demonstrates for the first time that maternal adaptation to pregnancy in the mouse involves significant changes in the expression of adipose clock genes (*Bmal1*, *Clock, Per1, Per2, Cry1, Cry2, Rev-erbα, Rorα*) across gestation. Importantly, although clock gene rhythmicity remained robust throughout, daily variation in the expression of key rate-limiting genes involved in lipid metabolism (*Lpl, Lipe, Pnpla2*) was lost with the onset of pregnancy. We also demonstrated reduced rhythmicity of T_c across pregnancy, but the pattern of change for T_c appeared unrelated to the pregnancy-induced shifts of adipose clock gene expression.

We hypothesised that the rhythmicity in adipose expression of clock genes and downstream metabolic genes would be suppressed in late pregnancy, similar to previous observations in the mouse liver (Wharfe et al. 2016b). This hypothesis was based on the premise that a dampening of clock gene rhythmicity may be adaptive by providing a more sustained supply of substrate to the rapidly growing fetus. While adipose expression of all clock genes did vary with the progression of pregnancy, expression of each remained robustly rhythmic throughout and so this aspect of the hypothesis was not supported. Interestingly, there were distinct differences in the patterns of change between early and late pregnancy. The first half of gestation was characterised by an attenuation of the mesor for all clock genes (with the exception of *Clock*) by day 6, whereas in the second half the majority of clock genes showed higher mesors together with a slightly reduced amplitude.

Despite the maintenance of robust clock gene rhythms, the rhythmicity of the rate–limiting genes involved in lipid metabolism was lost with the onset of pregnancy. Specifically, the lipolytic genes *Lipe* and *Pnpla2* lost their rhythmicity from day 6, whereas rhythmic variation of *Lpl* was absent on days 10 and 18 of pregnancy. Thus, the second aspect of our hypothesis related to suppression of metabolic gene rhythms was supported. Interestingly, there were two unexpected findings in this context: firstly, the changes in rhythmic variation of downstream metabolic genes across pregnancy appeared unrelated to clock genes and secondly, the loss of rhythmicity occurred even earlier in gestation than hypothesised. Thus, the decoupling of clock and metabolic gene rhythms and the associated loss of metabolic gene rhythmicity is likely to be adaptive for sustained fetal development and growth. For instance, the continuous expression of

Lipe and *Pnpla2* across a 24-h period may enable constant, rather than time-dependent, mobilisation of fatty acids from adipose tissue to meet the continuous demands of the fetus/embryo. During early pregnancy fatty acids are essential for neurogenesis (Innis 2007), whereas late in pregnancy they are required for fetal growth (Schaefer-Graf et al. 2008). Importantly, despite this constant expression across each 24-h period, absolute levels of these lipolytic genes did vary across pregnancy, presumably to meet the changing demand for fatty acids and glycerol throughout gestation. Given the sustained high demand for the products of lipid mobilisation in late pregnancy (Herrera et al. 1988) it is perhaps surprising that the expression of both genes was decreased on day 18. A similar decrease in *Lipe* mRNA expression has been observed in the rat near term (Martin-Hidalgo et al. 1994).

The apparent dissociation of downstream gene expression from that of clock genes is perhaps surprising given the purported role of clock genes in the regulation of lipid metabolism in non-pregnant animals (Koike et al. 2012; Shostak, Meyer-Kovac & Oster 2013). Accordingly, the strong negative correlation between *Bmal1* and *Lipe* that was evident prior to pregnancy was not apparent on any day of gestation. A similar decoupling was observed for several other clock gene and metabolic gene associations in pregnancy. Interestingly, a comparable loss of rhythmicity of adipose metabolic genes (e.g. *Lipe* and *Lpl*) despite robust clock gene expression has been observed in adrenalectomised rats (Su et al. 2015). These findings are suggestive of a role for corticosterone rhythms in the maintenance of rhythmic expression of metabolic genes. In our study, however, the loss of metabolic rhythmicity does not appear to be associated with corticosterone rhythmicity as robust rhythms are maintained up to day 14 of gestation in these animals (Wharfe et al. 2016a). That said, changes might occur in the sensitivity of maternal tissues to glucocorticoids or in the molecular interactions between glucocorticoids and these metabolic genes across gestation. Thus, further studies are required to determine the causes of this pregnancy-induced dissociation.

In contrast to the changes in the lipogenic and lipolytic genes, the rhythmic expression of *Pparγ* was robustly maintained throughout gestation and involved further adaptation. *Pparγ* is involved in the regulation of several physiological processes in white adipose tissue including adipogenesis, glyceroneogenesis (via regulation of adipose phosphoenolpyruvate carboxykinase 1) and the production of adiponectin and leptin (reviewed by Ferré (2004)). As such, it is possible that the rhythmic expression of *Pparγ*

ensures that other adipose tissue functions maintain circadian variation. Interestingly, previous studies suggest there is a reciprocal relationship between adipose *Pparγ* and clock gene expression, possibly indicative of direct, bi-directional regulation (e.g. *Pparγ* regulates transcription of *Bmal1*, *Per2* regulates activity of *Pparγ*) (Grimaldi et al. 2010; Yang et al. 2012). Our observation that *Pparγ* expression correlated with that of several clock genes is consistent with such regulation.

Recent studies have identified a role for the circadian rhythm of temperature as an entraining cue for *Bmal1* and *Per2* expression in peripheral tissues both *in vitro* and *in vivo* (Saini et al. 2012; Oishi et al. 2013). As T_c rhythms are suppressed in late gestation in both rats and mice (Fewell 1995; Eliason & Fewell 1997; Gamo et al. 2013), we had hypothesised that attenuated T_c rhythms are linked to suppressed adipose clock gene expression during pregnancy. This was not supported by our data, however, since changes in T_c rhythms were unrelated to the pregnancy-induced changes in clock gene expression; specifically, the amplitude of *Per2* expression was not decreased in late gestation and the magnitude of amplitude suppression for *Bmal1* was substantially smaller than that for T_c by late gestation. While our data showing that the amplitude of maternal T_c was reduced in late pregnancy are consistent with previous observations in the mouse (Gamo et al. 2013), the early onset of this reduced rhythm (from day 6) is novel. Interestingly, the changes in body temperature rhythmicity appear more similar to the marked suppression of clock genes observed in the liver during late gestation and specifically those of *Bmal1* and *Per2*, the amplitudes of which were up to 64% smaller than in non-pregnant animals (Wharfe et al. 2016b). That said, an effect of the early reduction in amplitude of T_c was not reflected in hepatic clock gene expression.

The mesor of T_c was also substantially decreased across pregnancy. This reduction, however, only reversed the increase that occurred between diestrus I and day 6, consistent with findings in MF1 mice (Gamo et al. 2013). Interestingly, this differs substantially from rats in which T_c is significantly lower on day 20 of gestation (term = day 23) than in the non-pregnant animal (Eliason & Fewell 1997). It has been proposed that this reduction in T_c is due to the progesterone withdrawal that occurs in late gestation, since progesterone has thermogenic effects in some species (Freeman et al. 1970). In our study, however, the decrease in T_c on days 14 or 18 was not associated with lower progesterone levels, which remained at maximal levels across the two days. While we did expect to see a decrease in progesterone on day 18 in our mice, we

presume we were not close enough to term to observe this. Nevertheless, the decreased concentration of progesterone during the dark phase on day 18 may indicate the beginning of the prepartum progesterone withdrawal.

The progressive increase in plasma progesterone from early pregnancy may influence clock gene expression since several clock genes contain progesterone response elements within their promoter regions (Nakamura et al. 2005; He et al. 2007; Nakamura et al. 2010). Although no studies have been carried out in adipose tissue, in the rat uterus progesterone upregulates *Per1* and *Clock* and downregulates *Rev-erbα* (He et al. 2007; Rubel et al. 2012). Interestingly, the increasing concentration of progesterone does correlate with the patterns of adipose *Per1* (upregulated) and *Rev-erbα* (downregulated) expression. On the other hand, the late gestation decrease in *Clock* suggests that factors other than progesterone regulate its adipose expression during pregnancy.

In conclusion, this study shows that the adipose circadian clock is substantially adapted during pregnancy, although unlike the liver clock, its robust rhythmicity is maintained. Furthermore, the regulation of adipose lipogenic and lipolytic genes appears to be decoupled from rhythmic variation in clock genes, possibly to meet the continuous demands of fetal development and growth. Although maternal T_c rhythms undergo substantial adaptations across mouse gestation, these do not appear to be associated with either pregnancy-induced changes in adipose clock genes or progesterone levels.

7.6 Supplementary data

Supplementary Table 7.S1 Linear regression analysis of the adipose clock genes with *Lpl* throughout pregnancy.

	Non-Pregnant	Day 6	Day 10	Day 14	Day 18
Bmal1 : Lpl	-0.31	-0.2	0.04	0.18	-0.26
	($P < 0.05$)	(NS)	(NS)	(NS)	(NS)
Clock : Lpl	-0.35	-0.12	0.3	0.06	-0.12
	($P < 0.05$)	(NS)	(NS)	(NS)	(NS)
Per1 : Lpl	0.21	0.24	0.08	-0.06	-0.07
	(NS)	(NS)	(NS)	(NS)	(NS)
Per2 : Lpl	0.46	0.24	-0.09	0.14	-0.13
	($P < 0.05$)	(NS)	(NS)	(NS)	(NS)
Cry1 : Lpl	0.08	0.18	-0.23	0.45	-0.16
	(NS)	(NS)	(NS)	($P < 0.05$)	(NS)
Cry2 : Lpl	0.19	0.22	0.03	0.46	0.04
	(NS)	(NS)	(NS)	($P < 0.05$)	(NS)
Rev-erbα : Lpl	-0.13	-0.03	0.2	-0.4	0.26
	(NS)	(NS)	(NS)	($P < 0.05$)	(NS)
Rorα : Lpl	0.2	0.54	0.17	0.04	0.1
	(NS)	($P < 0.001$)	(NS)	(NS)	(NS)

Correlation coefficients (r) and significance levels are shown for each day of pregnancy.

Supplementary Table 7.S2 Linear regression analysis of the adipose clock genes with *Lipe* throughout pregnancy.

	Non-Pregnant	Day 6	Day 10	Day 14	Day 18
Bmal1 : Lipe	-0.71	-0.15	-0.02	0.13	-0.27
	($P < 0.0001$)	(NS)	(NS)	(NS)	(NS)
Clock : Lipe	-0.54	0.04	0.33	0.06	-0.01
	($P < 0.001$)	(NS)	($P < 0.05$)	(NS)	(NS)
Per1 : Lipe	0.56	0.1	0.12	-0.05	-0.06
	($P < 0.0001$)	(NS)	(NS)	(NS)	(NS)
Per2 : Lipe	0.27	0.22	-0.05	0.11	-0.07
	(NS)	(NS)	(NS)	(NS)	(NS)
Cry1 : Lipe	-0.51	0.18	-0.2	0.38	-0.25
	($P < 0.001$)	(NS)	(NS)	(NS)	(NS)
Cry2 : Lipe	-0.13	0.27	0.16	0.51	0.06
	(NS)	(NS)	(NS)	($P < 0.001$)	(NS)
Rev-erbα : Lipe	0.67	-0.03	0.25	-0.27	0.32
	($P < 0.0001$)	(NS)	(NS)	(NS)	($P < 0.05$)
Rorα : Lipe	0.61	0.35	0.43	0.1	0.07
	($P < 0.0001$)	($P < 0.05$)	($P < 0.01$)	(NS)	(NS)

Correlation coefficients (r) and significance levels are shown for each day of pregnancy.

Supplementary Table 7.S3 Linear regression analysis of the adipose clock genes with *Pnpla2* throughout pregnancy.

	Non-Pregnant	Day 6	Day 10	Day 14	Day 18
Bmal1 : Pnpla2	0.02	-0.23	-0.09	-0.13	-0.03
	(NS)	(NS)	(NS)	(NS)	(NS)
Clock : Pnpla2	-0.07	-0.23	0.21	-0.03	0.1
	(NS)	(NS)	(NS)	(NS)	(NS)
Per1 : Pnpla2	-0.1	0.36	0.11	0.32	0.23
	(NS)	($P < 0.05$)	(NS)	($P < 0.05$)	(NS)
Per2 : Pnpla2	0.27	0.3	0.08	0.23	0
	(NS)	($P < 0.05$)	(NS)	(NS)	(NS)
Cry1 : Pnpla2	0.41	0.03	-0.07	0.14	-0.04
	($P < 0.01$)	(NS)	(NS)	(NS)	(NS)
Cry2 : Pnpla2	0.28	0.1	0.34	0.34	0.26
	(NS)	(NS)	($P < 0.05$)	($P < 0.05$)	(NS)
Rev-erbα : Pnpla2	-0.33	-0.04	0.21	-0.07	-0.06
	($P < 0.05$)	(NS)	(NS)	(NS)	(NS)
Rorα : Pnpla2	0.03	0.38	0.2	0.42	0.14
	(NS)	($P < 0.05$)	(NS)	($P < 0.05$)	(NS)

Correlation coefficients (r) and significance levels are shown for each day of pregnancy.

Supplementary Table 7.S4 Linear regression analysis of the adipose clock genes with *Pparγ* throughout pregnancy.

	Non-Pregnant	Day 6	Day 10	Day 14	Day 18
Bmal1 : Pparγ	-0.32	-0.22	-0.12	-0.39	-0.32
	($P < 0.05$)	(NS)	(NS)	($P < 0.05$)	($P < 0.05$)
Clock : Pparγ	-0.2	-0.3	-0.18	-0.15	-0.07
	(NS)	(NS)	(NS)	(NS)	(NS)
Per1 : Pparγ	0.17	0.45	0.07	0.47	0.46
	(NS)	($P < 0.05$)	(NS)	($P < 0.001$)	($P < 0.001$)
Per2 : Pparγ	0.33	0.38	0.5	0.35	0.1
	($P < 0.05$)	($P < 0.05$)	($P < 0.001$)	($P < 0.05$)	(NS)
Cry1 : Pparγ	-0.01	-0.02	0.23	-0.13	-0.41
	(NS)	(NS)	(NS)	(NS)	($P < 0.05$)
Cry2 : Pparγ	0.2	0.24	-0.56	0.29	0.27
	(NS)	(NS)	($P < 0.0001$)	($P < 0.05$)	(NS)
Rev-erbα : Pparγ	0.09	0.05	-0.29	0.17	0.35
	(NS)	(NS)	($P < 0.05$)	(NS)	($P < 0.05$)
Rorα : Pparγ	0.17	0.63	-0.1	0.4	0.13
	(NS)	($P < 0.0001$)	(NS)	($P < 0.05$)	(NS)

Correlation coefficients (r) and significance levels are shown for each day of pregnancy.

Chapter 8 General Discussion

The overall objective of the studies in this thesis was to characterise the impact of pregnancy on clock gene expression in maternal tissues, and to determine subsequent downstream effects on the circadian expression of tissue-specific genes in normal mouse pregnancy. The findings of each study have been presented and discussed in detail within their respective chapters. In this final chapter, the major findings are re-iterated, integrated, the limitations discussed and the potential for further research considered.

The studies presented in this thesis show for the first time that maternal clock gene expression is substantially altered in the anterior hypothalamus, liver and adipose tissue throughout normal mouse pregnancy. The effect of pregnancy on clock gene expression, however, appears to be highly tissue-dependent. Specifically, in the anterior hypothalamus (Chapter 5) the mesor of each clock gene was elevated above pre-pregnancy levels on day 10 of gestation and in the majority of cases expression was highest at this stage. In the liver (Chapter 6), the majority of clock genes had greatest amplitude and mesor either prior to pregnancy or on day 6, with both decreasing from mid-gestation to reach minimal levels on either day 14 or day 18. In contrast, absolute levels of clock genes were lowest on day 6 of pregnancy in the adipose tissue (Chapter 7), after which the mesor reached maximal levels on either day 14 or day 18. While late pregnancy was also characterised by reduced amplitude of expression of adipose clock genes, this reduction in rhythmicity was not as great as that seen in the liver.

Interestingly, although significant changes in the hypothalamus were evident they were not as extensive as those seen in either the liver or adipose tissue. This is perhaps not surprising given that under normal conditions peripheral clocks need to be relatively flexible to adapt to the changing metabolic demands of the animal (Damiola et al. 2000). In contrast, the central clock is required to remain relatively rigid to ensure time-of-day information is conveyed to the rest of the body (Abraham et al. 2010). Indeed, while peripheral clocks are responsive to a range of entraining cues, the SCN appears resistant to changes in T_c (Goh, Mark & Maloney 2016) and to the direct effects of glucocorticoids due to the absence of GR within the SCN (Rosenfeld et al. 1988; Balsalobre et al. 2000; Kalsbeek et al. 2012). That said, the central clock is likely

influenced by glucocorticoids indirectly via afferent inputs from other brain regions sensitive to glucocorticoid signalling (Amir et al. 2004; Lamont et al. 2005; Malek et al. 2007). While the mechanisms underlying the pregnancy-induced changes in the central clock remain an avenue to be explored, importantly the findings presented in this thesis provide a comprehensive account of the changes during pregnancy. As such, they supplement and extend previous findings of Schrader and colleagues (2010), by showing that clock gene-specific changes occur throughout gestation in the central clock.

The changes observed in the hypothalamus are suggestive of a shift in the function of the central clock, presumably to contribute to gestational adaptations in maternal physiology and behaviour. Because of the diverse number of SCN efferent pathways, the effects of changes in the central clock are potentially widespread. Alterations in central clock function may impact maternal physiology via changes in the local hypothalamic secretion of a range of humoral factors or via efferent projections to hypothalamic nuclei involved in the regulation of circadian physiological processes. For example, the central clock regulates T_c rhythms via inputs into the preoptic area, the brain region responsible for thermoregulation (Saper, Scammell & Lu 2005). T_c rhythms were substantially altered throughout pregnancy, with a 65% reduction in the amplitude of T_c and a 0.61°C decrease in T_c mesor by term (Chapter 7). Because the preoptic area is located in the anterior hypothalamus adjacent to the SCN, the section of the anterior hypothalamus isolated in this study included this region (Chapter 5). While this may appear as a limitation, nuclei surrounding the SCN depend upon input from the central clock for regulation of their circadian timing, thus they are expected to be tightly in phase (Kalsbeek et al. 2006). The relatively low variability in hypothalamic clock gene expression at each time point (Chapter 5) is suggestive of synchronicity across the whole tissue. Thus, the observed changes in hypothalamic clock gene expression should be indicative of the altered circadian timing in this thermoregulatory brain region during pregnancy. That said, how these changes relate to the marked reduction in the amplitude of T_c seen across pregnancy remains to be determined. Importantly, while lesions of the SCN eliminate the circadian rhythm of T_c they do not affect mean T_c (Refinetti & Menaker 1992). This suggests that changes in SCN clock gene expression are unlikely to be responsible for the changes in the mesor of T_c observed during gestation.

The impact of pregnancy-induced changes in the central clock likely extends to brain regions outside of the anterior hypothalamus. Indeed in the rat, levels of PER2 and FOS, a marker for neuronal activity, are altered on day 6 of pregnancy in two nuclei of the limbic forebrain involved in stress response and autonomic regulation (oval nucleus of the bed nucleus of the stria terminalis and central nucleus of amygdala) (Schrader, Nunez & Smale 2011). Because numerous brain regions receive circadian signals from the SCN it is likely that pregnancy-induced changes in central nervous system are widespread. Thus, a valuable extension of this work would be to determine clock gene expression in these and other specific brain regions throughout pregnancy.

Changes to the central clock likely influence peripheral tissue clocks via neural and/or hormonal pathways. Findings of the first study presented in this thesis (Chapter 5) showed that the clock gene expression in the central clock does not appear to drive the marked pregnancy-induced changes in glucocorticoid secretion via the HPA axis. Nevertheless, the central clock might still influence glucocorticoid secretion by the transmission of neuronal signals to the adrenal cortex via the ANS (Buijs et al. 1999; Buijs et al. 2003). Although no association between hypothalamic clock genes and corticosterone was observed, this remains a valid hypothesis as the multiple regulatory pathways between the central clock and corticosterone secretion may obscure correlations between the two. In this regard, a role for the adrenal peripheral clock itself also requires consideration since transcription of adrenal steroidogenic acute regulatory protein (StAR), the key regulator of the rate-limiting step in steroidogenesis, is directly regulated by local adrenal clock genes (Son et al. 2008). It is possible that the central clock may influence the adrenal clock via a range of synchronising cues (ANS, T_c etc.) and/or that the adrenal clock itself is independently adapted during pregnancy. Indeed, previous studies show that adrenal function is regulated by sex steroids (Atkinson & Waddell 1997; Figueiredo et al. 2007), and so pregnancy-related changes in the adrenal clock seem plausible. Therefore, measurement of adrenal clock gene and StAR rhythms throughout pregnancy would be a useful extension of this study.

Corticosterone levels in the pregnant mouse were increased by around 14-fold across late gestation (Chapter 5). While increased levels of glucocorticoids have previously been observed in both humans (Patrick et al. 1980) and rats (Atkinson & Waddell 1995), the magnitude of the increase observed in the mouse is several fold greater. Overall, plasma corticosterone levels on day 14 and 18 appear substantially higher than

levels reported in the literature for mice (Vaughan et al. 2015). Importantly, however, this is the first time that the full circadian profile of maternal corticosterone has been reported in this species, thus the marked increase in amplitude that occurs in late gestation has likely been missed due to the common practice of tissue sampling early in the light phase. Indeed, plasma levels at 0800 (ZT1) on day 14 (Chapter 5) are comparable to those measured in C57Bl/6J mice at a similar stage of pregnancy (Vaughan et al. 2015). Interestingly, the higher levels of corticosterone occurred despite a marked fall in absolute levels of plasma ACTH over the same period. While a similar dissociation of ACTH and corticosterone has been observed in rat pregnancy (Atkinson & Waddell 1995), again the magnitude of this change appears far greater in the mouse. Moreover, this dissociation further supports a role for factors outside of the conventional HPA axis in the regulation of plasma corticosterone during rodent pregnancy.

Clock gene expression in the liver was substantially altered with the onset and progression of pregnancy (Chapter 6). Most notably, while the expression of each remained rhythmic throughout, the majority of genes (*Bmal1, Per1, Per2, Rev-erbα*) showed a greatly reduced amplitude towards term. Similarly, the circadian rhythmicity of several key glucoregulatory genes (*Pck1*, *Gk*, *G6pase*) was also greatly attenuated in late gestation. Whether the observed clock gene changes drive those reported for metabolic genes remains unclear, since relationships between the two vary depending on the gene and the timeframe considered. While it appears that the circadian relationship between most hepatic clock genes and glucoregulatory genes is upheld across a 24-h period (with the exception of late gestation when rhythms of both are suppressed), the link between hepatic clock genes and glucoregulatory genes across pregnancy is less clear. This is likely due to a role for the normal regulatory mechanisms of glucose metabolism (e.g. glucocorticoids, glucagon etc.) in response to the changing demands of pregnancy. For instance, since glucocorticoids stimulate the transcription of *Pck1* and *G6Pase* (Jitrapakdee 2012), increased levels of corticosterone in late gestation likely drive the increase in expression of these enzymes observed on day 18.

The expression of clock genes in white adipose tissue also varied markedly throughout pregnancy, but in contrast to the liver the expression of each remained robustly rhythmic throughout (Chapter 7). Interestingly, there were distinct differences in the

patterns of change between the early anabolic phase of pregnancy and the late catabolic phase. For example, the first half of gestation was characterised by an attenuation of the mesor for all clock genes (with the exception of *Clock*) by day 6, whereas in the second half of pregnancy the majority of clock genes showed higher mesors together with a reduced amplitude. These changes, however, did not appear to be associated with the pregnancy-induced changes in lipogenic and lipolytic genes, which lost their circadian rhythmicity with the onset of pregnancy. The cause of this apparent uncoupling of these metabolic genes from circadian variation in clock genes remains to be established. Interestingly, a recent study shows that adrenalectomy in the rat leads to a similar loss of metabolic gene rhythmicity in epididymal white adipose tissue (Su et al. 2015). That said, corticosterone levels were not altered by day 6 of gestation in the present study, with both levels and rhythmicity increasing as gestation progressed. It is possible that reduced levels of aldosterone and/or catecholamines may contribute to the arrhythmic metabolic gene expression seen after adrenalectomy.

A consistent aspect of pregnancy-induced metabolic gene changes in liver and adipose tissue was the reduction in their circadian oscillations. These changes may be metabolically adaptive for sustained supply of nutrients to the fetus, at least during late gestation. In this regard, a useful extension of this study would be to measure transplacental passage of nutrients to the fetus to determine whether supply is in fact relatively constant across a 24-h period. Indeed, preliminary data in the rat suggests that this may be the case, since only minor circadian variation is detectable in the placental glucose transporters 1, 3 and 4 and in the fatty acid transporter (CD36) in the labyrinth zone of the placenta on day 21 of pregnancy (term = day 23; Waddell et al. 2012).

Maternal physiological adaptations to pregnancy are thought to be driven primarily by increased concentrations of estradiol, progesterone and glucocorticoids in maternal circulation. Because numerous clock genes contain hormone response elements including GREs within their promoter regions, it seems likely that these hormones contribute to the pregnancy-induced changes in clock gene expression. This may be particularly important in the regulation of adipose clock gene expression, since significant correlations between plasma corticosterone and clock genes were present across the majority of pregnancy (*Bmal1*, *Clock*, *Per1*, *Per2*, *Rorα*). Most notably, corticosterone and *Per1*, which contains a positive GRE (Yamamoto et al. 2005), were strongly positively correlated prior to and on all stages of pregnancy. Furthermore, the

increasing concentration of plasma progesterone may contribute to higher expression of adipose *Per1* and lower expression of *Rev-erbα* both of which are regulated by progesterone in the rat uterus (He et al. 2007; Rubel et al. 2012). In contrast the stimulatory effects of progesterone on uterine *Clock* expression was not evident in adipose tissue in late gestation (Rubel et al. 2012). These differences within a tissue suggest that clock genes are regulated by a combination of factors, which may include corticosterone and sex steroids.

The tissue-specific effect of these steroids on clock gene expression has been previously observed (Balsalobre et al. 2000; Nakamura et al. 2005; Pezuk et al. 2012) and may reflect differences in the cellular context between tissues, and with the progression of pregnancy. For example, the effect of corticosterone on gene expression is mediated by numerous factors, including the presence of co-activators and co-repressors within a specific cell type, as well as the density of glucocorticoid- and mineralocorticoid-receptor expression in the tissue (Beato & Klug 2000; Bamberger, Schulte & Chrousos 1996). Moreover, tissue-specific concentrations of 11β-hydroxysteroid dehydrogenases, which catalyse the interconversion of active corticosterone and inactive 11-DHC, modulate the effect of glucocorticoids within a cell (Seckl & Walker 2001). In this regard, a measure of intracellular corticosterone and 11-DHC levels would have provided valuable insight to our understanding of the effect of corticosterone in specific maternal tissues. Furthermore, an interesting extension of these studies would be to determine the activities of the 11-βHSD enzymes across pregnancy in maternal metabolic tissues.

Because the overall aim of this thesis was to characterise changes in normal, uninterrupted mouse pregnancy, it is difficult to separate out the effects of corticosterone and sex steroids on *in vivo* clock gene expression. Ultimately, it is likely that during pregnancy clock gene expression in peripheral tissues is regulated by a combination of these factors. It is also possible that other pregnancy-related factors including prolactin and the placental lactogens, for example, may contribute to changes in gene expression, and so this remains an avenue for future research.

Despite the important findings presented in this thesis, there are a number of study limitations that warrant discussion. Firstly, because the anterior hypothalamus contains a number of different nuclei that express clock genes, use of hypothalamic blocks rather

than isolated SCN tissue (Chapter 5) could be considered a limitation. However, the relatively low variability in hypothalamic clock gene expression within each time point suggests that all cells in each hypothalamic block of tissue exhibited similar temporal profiles for each of the clock genes. Secondly, blood glucose levels (Chapter 6) appeared substantially higher than expected for non-diabetic, healthy mice (Sorhede Winzell & Ahren 2004). It is possible that the Accu-Chek glucose meter, which is normally used to measure blood glucose in humans, is not accurate for use with mice. The major focus of this work was the relative changes in blood glucose levels across the 24-h period and throughout pregnancy, which showed very low variability within time points. Consequently, although the absolute glucose levels may have been inaccurate, the low variability suggests the Accu-Chek meter was sufficiently precise, for the purposes of this study. Lastly, the scope of these studies was limited by the quantitation of mRNA only, for each clock gene and metabolic target. It would have been interesting and informative to measure corresponding protein levels, to supplement and expand on the gene expression results presented in this thesis.

While the focus of this thesis was to characterise normal adaptation to pregnancy, there is growing recognition that abnormal adaptations during gestation can lead to low birth weight and adverse developmental programming effects in adult offspring (Langley-Evans & McMullen 2010; Gallo et al. 2012). As the incidence of shift work continues to increase, an emerging area of interest is the effect of circadian disruption during pregnancy (e.g. shift work) and subsequent effects on offspring health outcomes. Several epidemiological studies show associations between shift work and negative pregnancy outcomes including spontaneous abortion, preterm birth and low birth weight (Cone et al. 1998; Knutsson 2003; Zhu et al. 2004), of which the latter two factors are strong predictors of chronic disease in later life. Shift work has also been associated with a wide range of endocrine and metabolic disorders including diabetes and obesity (Delezie & Challet 2011; Eckel-Mahan et al. 2012). Given the considerable metabolic challenges faced by the mother during pregnancy this is of particular concern. Indeed, studies mimicking shift work during pregnancy in animal models show long-term adverse programming effects including insulin resistance and altered glucose tolerance in adult offspring (Varcoe et al. 2011; Varcoe et al. 2013). These studies highlight the importance of appropriate maternal circadian rhythms during gestation for sufficient maternal adaptation and subsequent offspring health. Thus, improving our knowledge of the changes that occur in normal gestation may advance our understanding of the

mechanisms underlying pregnancy complications that result from maternal chronodisruption, an issue likely to become more prevalent as the incidence of shift work increases in our society.

In conclusion, pregnancy-induced changes in the circadian oscillations of both clock genes and metabolic genes are substantial and thus, should be considered part of the normal maternal physiological adaptation to pregnancy. These findings provide a strong basis for investigation into the effect of maternal insults such as high maternal stress and maternal over- and under-nutrition on clock gene and metabolic gene adaptations during pregnancy, which may shed some light on the mechanisms underlying abnormal fetal growth and adverse developmental programming outcomes of these conditions.

Chapter 9 References

Abraham, U, Granada, AE, Westermark, PO, Heine, M, Kramer, A & Herzel, H 2010, 'Coupling governs entrainment range of circadian clocks', *Molecular Systems Biology*, vol. 6, no. 438, pp. 1-13.

Abrahamsohn, PA & Zorn, TMT 1993, 'Implantation and decidualization in rodents', *The Journal of Experimental Zoology*, vol. 266, pp. 603-628.

Adeva, M, Gonzalez-Lucan, M, Seco, M & Donapetry, C 2013, 'Enzymes involved in l-lactate metabolism in humans', *Mitochondrion*, vol. 13, pp. 615-629.

Ahren, B 2000, 'Diurnal variation in circulating leptin is dependent on gender, food intake and circulating insulin in mice', *Acta Physiologica Scandinavica*, vol. 169, pp. 325-331.

Akashi, M, Tsuchiya, Y, Yoshino, T & Nishida, E 2002, 'Control of intracellular dynamics of mammalian period proteins by casein kinase I epsilon (CKIepsilon) and CKIdelta in cultured cells', *Molecular and Cellular Biology*, vol. 22, no. 6, pp. 1693-1703.

Akhtar, RA, Reddy, AB, Maywood, ES, Clayton, JD, King, VM, Smith, AG, Gant, TW, Hastings, M & Kyriacou, CP 2002, 'Circadian cycling of the mouse liver transcriptome, as revealed by cDNA microarray, is driven by the suprachiasmatic nucleus', *Current Biology*, vol. 12, pp. 540-550.

Akiyama, S, Ohta, H, Watanabe, S, Moriya, T, Hariu, A, Nakahata, N, Chisaka, H, Matsuda, T, Kimura, Y, Tsuchiya, S, Tei, H, Okamura, K & Yaegashi, N 2010, 'The uterus sustains stable biological clock during pregnancy', *Journal of Experimental Medicine*, vol. 221, pp. 287-298.

Albers, HE 1981, 'Gonadal hormones organize and modulate the circadian system of the rat', *Am J Physiol*, vol. 241, pp. R62-R66.

Amir, S, Lamont, EW, Robinson, B & Stewart, J 2004, 'A circadian rhythm in the expression of PERIOD2 protein reveals a novel SCN-controlled oscillator in the oval nucleus of the bed nucleus of the stria terminalis', *The Journal of Neuroscience*, vol. 24, no. 4, pp. 781-790.

Ando, H, Yanagihara, H, Hayashi, Y, Obi, Y, Tsuruoka, S, Takamura, T, Kaneko, S & Fujimura, A 2005, 'Rhythmic messenger ribonucleic acid expression of clock genes and adipocytokines in mouse visceral adipose tissue', *Endocrinology*, vol. 146, no. 12, pp. 5631-5636.

Ansari, N, Agathagelidis, M, Lee, C, Korf, H-W & von Gall, C 2009, 'Differential maturation of circadian rhythms in clock gene proteins in the suprachiasmatic nucleus and the pars tuberalis during mouse ontogeny', *European Journal of Neuroscience*, vol. 29, pp. 477-489.

Aschoff, J 1984, 'Circadian Timing', *Annals New York Academy of Science*, pp. 442-468.

Atkinson, HC & Waddell, BJ 1995, 'The hypothalamic-pituitary-adrenal axis in rat pregnancy and lactation: circadian variation and interrelationship of plasma adrenocorticotrophin and corticosterone', *Endocrinology*, vol. 136, no. 2, pp. 512-520.

Atkinson, HC & Waddell, BJ 1997, 'Circadian variation in basal plasma corticosterone and adrenocorticotropin in the rat: Sexual dimorphism and changes across the estrous cycle', *Endocrinology*, vol. 138, no. 9, pp. 3842-3848.

Bailey, SM, Udoh, US & Young, ME 2014, 'Circadian regulation of metabolism', *Journal of Endocrinology*, vol. 222, pp. R75-R96.

Balsalobre, A, Brown, SA, Marcacci, L, Tronche, F, Kellendonk, C, Reichardt, HM, Schutz, G & Schibler, U 2000, 'Resetting of circadian time in peripheral tissues by glucocorticoid signalling', *Science*, vol. 289, pp. 2344-2347.

Balsalobre, A, Damiola, F & Schibler, U 1998, 'A serum shock induces circadian gene expression in mammalian tissue culture cells', *Cell*, vol. 93, pp. 929-937.

Bamberger, CM, Schulte, HM & Chrousos, GP 1996, 'Molecular determinants of glucocorticoid receptor function and tissue sensitivity to glucocorticoids', *Endocrine Reviews*, vol. 17, no. 3, pp. 245-258.

Bamshad, M, Aoki, VT, Adkison, G, Warren, WS & Bartness, TJ 1998, 'Central nervous system origins of the sympathetic nervous system outflow to white adipose tissue', *American Journal of Physiology - Regulatory, Integrative and Comparative Physiology*, vol. 44, pp. R291-R299.

Barkley, MS, Bradford, GE & Geschwind, II 1978, 'The pattern of plasma prolactin concentration during the first half of mouse gestation', *Biology of Reproduction*, vol. 19, pp. 291-296.

Barkley, MS, Geschwind, II & Bradford, GE 1979, 'The gestational pattern of estradiol, testosterone and progesterone secretion in selected strains of mice', *Biology of Reproduction*, vol. 20, no. 4, pp. 733-738.

Barkley, MS, Michael, SD, Geschwind, II & Bradford, GE 1977, 'Plasma testosterone during pregnancy in the mouse', *Endocrinology*, vol. 100, pp. 1472-1475.

Barlow, SM, Morrison, PJ & Sullivan, FM 1974, 'Plasma corticosterone levels during pregnancy in the mouse: the relative contributions of the adrenal glands and foeto-placental units', *Journal of Endocrinology*, vol. 60, no. 3, pp. 473-483.

Barlow, SM, Morrison, PJ & Sullivan, FM 1975, 'Effects of acute and chronic stress on plasma corticosterone levels in the pregnant and non-pregnant mouse', *Journal of Endocrinology*, vol. 66, no. 1, pp. 93-99.

Baxter, JD & Rousseau, GG 1979, 'Glucocorticoid hormone action: an overview', *Monographs on Endocrinology*, vol. 12, pp. 1-24.

Beale, EG, Hammer, RE, Antoine, B & Forest, C 2004, 'Disregulated glyceroneogenesis: PCK1 as a candidate diabetes and obesity gene', *Trends in Endocrinology & Metabolism*, vol. 15, pp. 129-135.

Beato, M & Klug, J 2000, 'Steroid hormone receptors: an update', *Human Reproduction Update*, vol. 6, no. 3, pp. 225-236.

Benavides, A, Siches, M & Llobera, M 1998, 'Circadian rhythms of lipoprotein lipase and hepatic lipase activities in intermediate metabolism of adult rat', *American Journal of Physiology, Regulatory, Integrative and Comparitive Physiology*, vol. 275, pp. 811-817.

Bittman, EL, Doherty, L, Huang, L & Paroskie, A 2003, 'Period gene expression in mouse endocrine tissues', *American Journal of Physiology - Regulatory, Integrative and Comparative Physiology*, vol. 285, pp. R561-R569.

Blaustein, JD, King, JC, Toft, DO & Turcotte, J 1988, 'Immunocytochemical localization of estrogen-induced progestin receptors in guinea pig brain', *Brain Research*, vol. 474, no. 1, pp. 1-15.

Blaustein, JD & Wade, GN 1978, 'Progestin binding by brain and pituitary cell nuclei and female rat sexual behavior', *Brain Research*, vol. 140, no. 2, pp. 360-367.

Boden, MJ, Varcoe, TJ, Voultsios, A & Kennaway, DJ 2010, 'Reproductive biology of female Bmal1 null mice', *Reproduction*, vol. 139, pp. 1077-1090.

Bollen, M, Keppens, S & Stalmans, W 1998, 'Specific features of glycogen metabolism in the liver', *Journal of Biochemistry*, vol. 336, pp. 19-31.

Bonica, JJ 1973, 'Maternal respiratory changes during pregnancy and parturtion', *Clinical Anesthesia*, vol. 10, no. 2, pp. 1-19.

Bowen-Shauver, JM & Gibori, G 2003, 'The corpus luteum of pregnancy', in *The ovary*, Second edn, eds PCK Leung & EY Adashi, Elsevier Academic Press.

Brown, R, Diaz, R, Robson, A, Kotelevtsev, Y, Mullins, J, Kaufman, M & Seckl, J 1996, 'The ontogeny of 11 beta-hydroxysteroid dehydrogenase type 2 and mineralocorticoid receptor gene expression reveal intricite control of glucocorticoid action in development', *Endocrinology*, vol. 137, pp. 794-797.

Brown, SA, Zumbrunn, G, Fleury-Olela, F, Preitner, N & Schibler, U 2002, 'Rhythms of mammalian body temperature can sustain peripheral circadian clocks', *Current Biology*, vol. 12, pp. 1574-1583.

Brunton, PJ 2010, 'Resetting the dynamic range of hypothalamic-pituitary-adrenal axis stress responses through pregnancy', *Journal of Neuroendocrinology*, vol. 22, pp. 1198-1213.

Brunton, PJ, McKay, AJ, Ochedalski, T, Piastowska, A, Rebas, E, Lachowicz, A & Russell, JA 2009, 'Central opiod inhibition of neuroendocrine stress responses in pregnancy in the rat is induced by the neurosteroid allopregnanolone', *Journal of Neuroscience*, vol. 29, pp. 6449-6460.

Buhr, ED, Yoo, S-H & Takahashi, JS 2010, 'Temperature as a universal resetting cue for mammalian circadian oscillators', *Science*, vol. 330, pp. 379-385.

Buijs, FN, Cazarez, F, Basualdo, MC, Scheer, FAJL, Perusquia, M, Centurion, D & Buijs, RM 2014, 'The suprachiasmatic nucleus is part of a neural feedback circuit adapting blood pressure response', *Neuroscience*, vol. 266, pp. 197-207.

Buijs, RM, Van Eden, CG, Goncharuk, VD & Kalsbeek, A 2003, 'The biological clock tunes the organs of the body: timing by hormones and the autonomic nervous system', *Journal of Endrocrinology*, vol. 177, pp. 17-26.

Buijs, RM, Wortel, J, Van Heerikhuize, JJ, Feenstra, MGP, Ter Horst, GJ, Romijn, HJ & Kalsbeek, A 1999, 'Anatomical and functional demonstration of a multisynaptic suprachiasmatic nucleus adrenal (cortex) pathway', *European Journal of Neuroscience*, vol. 11, no. 5, pp. 1535-1544.

Cailotto, C, La Fleur, SE, Van Heijningen, C, Wortel, J, Kalsbeek, A, Feenstra, M, Pevet, P & Bujis, RM 2005, 'The suprachiasmatic nucleus controls the daily variation of plasma glucose via the autonomic output to the liver: are the clock genes involved?', *European Journal of Neuroscience*, vol. 22, pp. 2531-2540.

Cailotto, C, van Heijningen, C, van der Vliet, J, van der Plasse, G, Habold, C, Kalsbeek, A & Buijs, RM 2008, 'Daily rhythms in metabolic liver enzymes and plasma glucose require a balance in the autonomic output to the liver', *Endocrinology*, vol. 149, no. 4, pp. 1914-1925.

Caligioni, C 2009, 'Assessing reproductive status/stages in mice', *Current Protocols Neuroscience*, vol. 48, no. 4I, pp. A.4I.1-A.4I.8.

Canaple, L, Rambaud, J, Dkhissi-Benyahya, O, Rayet, B, Tan, NS, Michalik, L, Delaunay, F, Wahli, W & Laudet, V 2006, 'Reciprocal regulation of brain and muscle arnt-like protein 1 and peroxisome-proliferator activated receptor alpha defines a novel positive feedback loop in the rodent liver circadian clock', *Molecular Endocrinology*, vol. 20, no. 8, pp. 1715-1727.

Casey, T, Patel, O, Dykema, K, Dover, H, Furge, K & Plaut, K 2009, 'Molecular signatures reveal circadian clocks may orchestrate the homeorhetic response to lactation', *PloS One*, vol. 4, no. 10, p. e7395.

Cheng, MY, Bullock, CM, Chuanyu, L, Lee, AG, Bermak, JG, Belluzzi, J, Weaver, DR, Leslie, FM & Qun-Yong, Z 2002, 'Prokineticin 2 transmits the behavioural circadian rhythm of the suprachiasmatic nucleus', *Nature*, vol. 417, no. 6887, pp. 405-410.

Choudary, JB & Greenwald, GS 1969, 'Luteotropic complex of the mouse', *The Anatomical Record*, vol. 163, no. 3, pp. 373-387.

Cone, JE, Vaughan, LM, Huete, A & Samuels, SJ 1998, 'Reproductive health outcomes among female flight attendants: an exploratory study', *Journal of Occupational & Environmental Medicine*, vol. 40, no. 3, pp. 210-216.

Constancia, M, Hemberger, M, Hughes, J, Dean, W, Ferguson-Smith, AC, Fundele, R, Stewart, F, Kelsey, G, Fowden, A, Sibley, C & Reik, W 2002, 'Placental-specific IGF-II is a major modulator of placental and fetal growth', *Nature*, vol. 417, pp. 945-948.

Costrini, NV & Kalhkhoff, RK 1971, 'Relative effects of pregnancy, estradiol and progesterone on plasma insulin and pancreatic islet insulin secretion', *The Journal of Clinical Investigation*, vol. 50, pp. 992-999.

Cottrell, EC, Holmes, MC, Livingstone, DE, Kenyon, CJ & Seckl, JR 2012, 'Reconciling the nutritional amd glucocorticoid hypotheses of fetal programming', *The FASEB Journal*, vol. 26, no. 5, pp. 1866-1874.

Dallman, MF, Akana, SF, Jacobson, L, Levin, N, Cascio, CS & Shinsako, J 1987, 'Characterization of corticosterone feedback regulation of ACTH secretion', *Annals of the New York Academy of Sciences*, vol. 512, pp. 402-414.

Damiola, F, Le Minh, N, Preitner, N, Kornmann, B, Fleury-Olela, F & Schibler, U 2000, 'Restricted feeding uncouples circadian oscillators in peripheral tissues from the central pacemaker in the suprachiasmatic nucleus', *Genes and Development*, vol. 14, pp. 2950-2961.

Dardente, H, Fortier, EE, Martineau, V & Cermakian, N 2007, 'Cryptochromes impair phosphorylation of transcriptional activators in the clock: a general mechansm for circadian repression', *Biochemical Journal*, vol. 402, pp. 525-536.

Delezie, J & Challet, E 2011, 'Interactions between metabolism and circadian clocks: reciprocal disturbances', *Annals of the New York Academy of Sciences*, vol. 1243, pp. 30-46.

Delezie, J, Dumont, S, Dardente, H, Oudart, H, Grechez-Cassiau, A, Klosen, P, Teboul, M, Delaunay, F, Pevet, P & Challet, E 2012, 'The nuclear receptor REV-ERBα is required for the daily balance of carbohydrate and lipid metabolism', *The FASEB Journal*, vol. 26, pp. 3321-3335.

Do, M & Yau, KW 2010, 'Intrinsically photoreceptive retinal ganglion cells', *Physiology Reviews*, vol. 90, pp. 1547-1581.

Doi, R, Oishi, K & Ishida, N 2010, 'CLOCK regulates circadian rhythms of hepatic glycogen synthesis through transcriptional activation of Gys2', *The Journal of Biological Chemistry*, vol. 285, no. 29, pp. 22114-22121.

Douglas, AJ, Brunton, PJ, Bosch, OJ, Russell, JA & Neumann, ID 2003, 'Neuroendocrine responses to stress in mice: hyporesponsiveness in pregnancy and parturition', *Endocrinology*, vol. 144, no. 12, pp. 5268-5276.

Ebihara, S, Marks, T, Hudson, DJ & Menaker, M 1986, 'Genetic control of melatonin synthesis in the pineal gland of the mouse', *Science*, vol. 231, pp. 491-493.

Eckel-Mahan, KL, Patel, VR, Mohney, RP, Vignola, KS, Baldi, P & Sassone-Corsi, P 2012, 'Coordination of the transcriptome and metabolome by the circadian clock', *PNAS*, vol. 109, no. 14, pp. 5541-5546.

Eide, EJ, Woolf, MF, Kang, H, Woolf, P, Hurst, W, Camacho, F, Vielhaber, EL, Giovanni, A & Virshup, DM 2005, 'Control of mammalian circadian rhythm by CKIε-regulated proteosome-mediated PER2 degradation', *Molecular and Cellular Biology*, vol. 25, no. 7, pp. 2795-2807.

Eliason, HL & Fewell, JE 1997, 'Thermoregulatory control during pregnancy and lactation in rats', *Journal of Applied Physiology*, vol. 83, pp. 837-844.

Escobar, C, Diaz-Munoz, M, Encinas, F & Aguilar-Roblero, R 1998, 'Persistance of metabolic rhythmicity during fasting and its entrainment by restricted feeding schedules in rats', *American Journal of Physiology - Regulatory, Integrative and Comparative Physiology*, vol. 43, pp. R1309-R1316.

Ferre, P 2004, 'The biology of peroxisome proliferator-activated receptors. Relationship with lipid metabolism and insulin sensitivity', *Diabetes*, vol. 53, no. Supplementary 1, pp. S43-S50.

Ferre, P & Foufelle, F 2007, 'SREBP-1c transcription factor and lipid homeostasis: Clinical perspective', *Hormone Research*, vol. 68, pp. 72-82.

Fewell, JE 1995, 'Body temperature regulation in rats near term of pregnancy', *Canadian Journal of Physiological Pharmocology*, vol. 73, pp. 364-368.

Figueiredo, HF, Ulrich-Lai, YM, Choi, DC & Herman, JP 2007, 'Estrogen potentiates adrenocortical responses to stress in female rats', *American Journal of Physiology, Endocrinology and Metabolism*, vol. 292, pp. E1173-E1182.

Frayn, KN, Arner, P & Yki-Jarvinen, H 2006, 'Fatty acid metabolism in adipose tissue, muscle and liver in health and disease', *Essays in Biochemistry*, vol. 42, pp. 89-103.

Frayn, KN, Coppack, SW, Fielding, BA & Humphreys, SM 1995, 'Coordinated regulation of hormone-sensitive lipase and lipoprotein lipase in human adipose tissue in vivo: Implications for the control of fat storage and fat mobilization', *Advances in Enzyme Regulation*, vol. 35, pp. 163-178.

Freeman, ME, Crissman, JKJ, Louw, GN, Butcher, RL & Inskeep, EK 1970, 'Thermogenic action of progesterone in the rat', *Endrocrinolgy*, vol. 86, no. 717, pp. 717-720.

Froy, O 2010, 'Metabolism and circadian rhythms - implications for obesity', *Endocrine Reviews*, vol. 31, no. 1, pp. 1-24.

Fruhbeck, G, Mendez-Gimenez, L, Fernandez-Formoso, J-A, Fernandez, S & Rodriguez, A 2014, 'Regulation of adipocyte lipolysis', *Nutrition Research Reviews*, vol. 27, pp. 63-93.

Gala, RR & Westphal, U 1967, 'Corticosteroid-binding activity in serum of mouse, rabbit and guinea pig during pregnancy and lactation: possible involvement in the initiation of lactation', *Acta Endocrinologica*, vol. 55, pp. 47-61.

Gallo, LA, Tran, M, Master, JS, Moritz, KM & Wlodek, ME 2012, 'Maternal adaptations and inheritance in the transgenerational programming of adult disease', *Cell and Tissue Research*, vol. 349, pp. 863-880.

Galosy, SS & Talamantes, F 1995, 'Luteotropic actions of placental lactogens at midpregnancy in the mouse', *Endocrinology*, vol. 136, no. 9, pp. 3993-4003.

Gamo, Y, Bernard, A, Mitchell, SE, Hambly, C, Al Jothery, A, Vaanholt, LM, Krol, E & Speakman, JR 2013, 'Limits to sustained energy intake. XVI. Body temperature and physical activity of female mice during pregnancy', *The Journal of Experimental Biology*, vol. 216, no. 12, pp. 2328-2338.

Georgiades, P, Ferguson-Smith, AC & Burton, GJ 2002, 'Comparative developmental anatomy of the murine and human definitive placentae', *Placenta*, vol. 23, no. 1, pp. 3-19.

Gery, S & Koeffler, P 2010, 'Circadian rhythms and cancer', *Cell Cycle*, vol. 9, no. 6, pp. 1097-1103.

Gery, S, Virk, RK, Chumakov, K, Yu, A & Koeffler, HP 2007, 'The clock gene Per2 links the circadian system to the estrogen receptor', *Oncogene*, vol. 26, pp. 7916-7920.

Goh, GH, Mark, PJ & Maloney, SK 2016, 'Altered energy intake and the amplitude of the body temperature rhythm are associated with changes in phase, but not amplitude, of clock gene expression in the rat suprachiasmatic nucleus in vivo', *Chronobiology International*, vol. 33, no. 1, pp. 1-13.

Gonzalez, CG, Alonso, A, Balbin, M, Diaz, F, Fernandez, S & Patterson, AM 2002, 'Effects of pregnancy on insulin receptor in liver, skeletal muscle and adipose tissue', *Gynecological Endocrinology*, vol. 16, no. 3, pp. 193-205.

Gooley, JJ, Lu, J, Chou, TC, Scammell, TE & Saper, CB 2001, 'Melanopsin in cells of origin of the retinohypothalamic tract', *Nature Neuroscience*, vol. 4, no. 12, p. 1165.

Goto, M, Oshima, I, Tomita, T & Ebihara, S 1989, 'Melatonin content of the pineal gland in different mouse strains', *Journal of Pineal Research*, vol. 7, pp. 195-204.

Gozeri, E, Celik, H, Ozercan, I, Gurates, B, Poltat, SA & Hanay, F 2008, 'The effect of circadian rhythm changes on fetal and placental development (experimental study)', *Neuroendocrinology Letters*, vol. 29, no. 1, pp. 87-90.

Grattan, DR & Averill, RLW 1990, 'Effect of ovarian steroids on a nocturnal surge of prolactin secretion that precedes parturition in the rat', *Endocrinology*, vol. 126, no. 2, pp. 1199-1205.

Grattan, DR, Ladyman, SR & Augustine, RA 2007, 'Hormonal induction of leptin resistance during pregnancy', *Physiology & Behavior*, vol. 91, pp. 366-374.

Grimaldi, B, Bellet, MM, Katada, S, Astarita, G, Hirayama, J, Amin, RH, Granneman, JG, Piomelli, D, Leff, T & Sassone-Corsi, P 2010, 'PER2 controls lipid metabolism by direct regulation of PPAR-gamma', *Cell Metabolism*, vol. 12, pp. 509-520.

Hamosh, M, Clary, TR, Chernick, SS & Scow, RO 1970, 'Lipoprotein lipase activity in adipose and mammary tissue and plasma triglyceride in pregnant and lactating rats', *Biochimica et Biophysica Acta*, vol. 210, no. 3, pp. 473-482.

Hara, R, Wan, K, Wakamatsu, H, Aida, R, Moriya, T, Akiyama, M & Shibata, S 2001, 'Restricted feeding entrains liver clock without participation of the suprachiasmatic nucleus', *Genes to Cells*, vol. 6, pp. 269-278.

Harris, A & Seckl, J 2011, 'Glucocorticoids, prenatal stress and the programming of disease', *Hormones and Behavior*, vol. 59, pp. 279-289.

Hastings, M, O'Neill, J & Maywood, ES 2007, 'Circadian clocks: regulators of endocrine and metabolic rhythms', *Journal of Endrocrinology*, vol. 195, pp. 187-198.

He, P-J, Hirata, M, Yamauchi, N & Hattori, M 2007, 'Up-regulation of *Per1* expression by estradiol and progesterone in the rat uterus', *Journal of Endrocrinology*, vol. 194, pp. 511-519.

Henriksson, E & Lamia, KA 2015, 'Adipose clocks: burning the midnight oil ', *Journal of Biological Rhythms*, p. 0748730415581234.

Henson, MC & Castracane, VD 2000, 'Leptin in pregnancy', *Biology of Reproduction*, vol. 63, pp. 1219-1228.

Herrera, E 2000, 'Metabolic adaptations in pregnancy and their implications for the availability of substrates to the fetus', *European Journal of Clinical Nutrition*, vol. 54, pp. 47-51.

Herrera, E, Knopp, RH & Freinkel, N 1969, 'Carbohydrate metabolism in pregnancy VI. Plasma fuels, insulin, liver composition, gluconeogenesis and nitrogen metabolism during late gestation in the fed and fasted rat', *The Journal of Clinical Investigation*, vol. 48, pp. 2260-2272.

Herrera, E, Lasuncion, MA, Gomez-Coronado, D, Aranda, P, Lopez-Luna, P & Maier, I 1988, 'Role of lipoprotein lipase activity on lipoprotein metabolism and the fate of circulating triglyercides in pregnancy', *American Journal of Obstetrics and Gynecology*, vol. 158, pp. 1575-1583.

Herrera, E, Lasuncion, MA, Huerta, L & Martin-Hidalgo, A 2000, 'Plasma leptin levels in rat mother and offspring during pregnancy and lactation', *Biology of the Neonate*, vol. 78, no. 4, pp. 315-320.

Herrera, E, Palacin, M, Martin, A & Lasuncion, MA 1985, 'Relationship between maternal and fetal fuels and placental glucose transfer in rats with maternal diabetes of varying severity', *Diabetes*, vol. 34 (Supplement 2), pp. 42-46.

Hitier, Y, Champigny, O, Homayoon, P & Bourdel, G 1982, 'Circadian feeding pattern in pregnant rats fed three levels of protein', *Annals of Nutrition and Metabolism*, vol. 26, pp. 129-137.

Holinka, CF, Tseng, Y-C & Finch, CE 1979, 'Reproductive aging in C57BL/6J mice: Plasma progesterone, viable embryos and resorption frequency throughout pregnancy', *Biology of Reproduction*, vol. 20, pp. 1201-1211.

Horard, B, Rayet, B, Triqueneaux, G, Laudet, V, Delaunay, F & Vanacker, JM 2004, 'Expression of the orphan nuclear receptor ERRalpha is under circadian regulation in estrogen-responsive tissues', *Journal of Molecular Endocrinology*, vol. 33, pp. 87-97.

Innis, SM 2007, 'Dietary (n-3) fatty acid and brain development', *The Journal of Nutrition*, vol. 137, pp. 855-859.

Ishida, A, Mutoh, T, Ueyama, T, Bando, H, Masubuchi, S, Nakahara, D, Tsujimoto, G & Okamura, H 2005, 'Light activates the adrenal gland: Timing of gene expression and glucocorticoid release', *Cell Metabolism*, vol. 2, pp. 297-307.

Ishikawa, K & Shimazu, T 1976, 'Daily rhythms of glycogen synthetase and phosphorylase activities in rat liver: influences of food and light', *Life Sciences*, vol. 19, pp. 1873-1878.

Jacobson, L 2005, 'Hypothalamic-pituitary-adrenal axis regulation', *Endocrinology and Metabolism Clinics of North America*, vol. 34, no. 2, pp. 271-292.

Jiang, G & Zhang, BB 2003, 'Glucagon and regulation of glucose metabolism', *American Journal of Physiology - Endocrinology and Metabolism*, vol. 284, pp. E671-E678.

Jitrapakdee, S 2012, 'Transcription factors and coactivators controlling nutrient and hormonal regulation of hepatic gluconeogenesis', *The International Journal of Biochemistry and Cell Biology*, vol. 44, pp. 33-45.

Jones, CT & Rolph, TP 1985, 'Metabolism during fetal life: A fucntional assessment of metabolic development', *Physiological Reviews*, vol. 65, no. 2, pp. 357-430.

Jones, MT, Hillhouse, EW & Burden, JL 1977, 'Dynamics and mechanics of corticosteroid feedback at the hypothalamus and anterior pituitary gland', *Journal of Endocrinology*, vol. 73, pp. 405-417.

Kalhan, S & Parimi, P 2000, 'Gluconeogenesis in the fetus and neonate', *Seminars in perinatology*, vol. 24, no. 2, pp. 94-106.

Kalkhoff, RK, Kissebah, AH & Kim, H-J 1978, 'Carbohydrate and lipid metabolism during normal pregnancy: relationship to gestational hormone action', *Seminars in Perinatology*, vol. 2, pp. 291-307.

Kalkhoff, RK, Richardson, BL & Beck, P 1969, 'Relative effects of pregnancy, human placental lactogen and prednisolone on carbohydrate tolerance in normal and subclinical subjects', *Diabetes*, vol. 18, pp. 153-163.

Kalsbeek, A, La Fleur, SE, Van Heijningen, C & Buijs, RM 2004, 'Suprachiasmatic GABAergic inputs to the paraventricular nucleus control plasma glucose concentrations in the rat via sympathetic innervation of the liver', *The Journal of Neuroscience*, vol. 24, no. 35, pp. 7604-7613.

Kalsbeek, A, Palm, IF, La Fleur, SE, Scheer, FAJL, Perreau-Lenz, S, Ruiter, M, Kreier, F, Cailotto, C & Buijs, RM 2006, 'SCN outputs and the hypothalamic balance of life', *Journal of Biological Rhythms*, vol. 21, pp. 458-469.

Kalsbeek, A, Van der Spek, R, Lei, J, Endert, E, Buijs, RM & Fliers, E 2012, 'Circadian rhythms in the hypothalamo–pituitary–adrenal (HPA) axis', *Molecular and Cellular Endocrinology*, vol. 349, no. 1, pp. 20-29.

Kaneko, M, Kaneko, K, Shinsako, J & Dallman, MF 1981, 'Adrenal sensitivity to adrenocorticotropin varies diurnally', *Endocrinology*, vol. 109, no. 1, pp. 70-75.

Kennaway, DJ 2005, 'The role of circadian rhythmicity in reproduction', *Human Reproduction Update*, vol. 11, no. 1, pp. 91-101.

Kennaway, DJ, Owens, JA, Voultsios, A, Boden, MJ & Varcoe, TJ 2007, 'Metabolic homeostasis in mice with disrupted Clock gene expression in peripheral tissues', *American Journal of Physiology - Regulatory, Integrative and Comparative Physiology*, vol. 293, no. 4, pp. R1528-R1537.

Kennaway, DJ, Owens, JA, Voultsios, A & Wight, N 2012, 'Adipokines and adipocyte function in Clock mutant mice that retain melatonin rhythmicity', *Obesity*, vol. 20, no. 2, pp. 295-305.

Kennaway, DJ, Varcoe, TJ, Voultsios, A & Boden, MJ 2013, 'Global loss of Bmal1 expression alters adipose tissue hormones, gene expression and glucose metabolism', *PLOS One*, vol. 8, no. 6, p. e65255.

Kennaway, DJ, Voultsios, A, Varcoe, TJ & Moyer, RW 2003, 'Melatonin and activity rhythm responses to light pulses in mice with the Clock mutation', *Am J Physiol Regul Integr Comp Physiol*, vol. 284, pp. R1231-R1240.

Kennaway, DJ & Wright, H 2002, 'Melatonin and Circadian Rhythms', *Current Topics in Medicinal Chemistry*, vol. 2, pp. 199-209.

King, DP, Zhao, Y, Sangoram, AM, Wilsbacher, LD, Tanaka, M, Antoch, MP, Steeves, TDL, Vitaterna, MH, Kornhauser, JM, Lowrey, PL, Turek, FW & Takahashi, JS 1997, 'Positional cloning of the mouse circadian clock gene', *Cell*, vol. 89, pp. 641-653.

Klein, DC, Coon, SL, Roseboom, PH, Weller, JL, Bernard, M, Gastel, JA, Zatz, M, Iuvone, PM, Rodriguez, IR, Begay, V, Falcon, J, Cahill, GM, Cassone, VM & Baler, R 1997, 'The melatonin rhythm-generating enzyme; molecular regulation of serotonin N-actyltransferase in the pineal gland', *Recent Progress in Hormone Research*, vol. 53, pp. 307-357.

Klover, PJ & Mooney, RA 2004, 'Hepatocytes: critical for glucose homeostasis', *The International Journal of Biochemistry and Cell Biology*, vol. 36, pp. 753-758.

Knopp, RH, Herrera, E & Freinkel, N 1970, 'Carbohydrate metabolism in pregnancy. VIII. Metabolism of adipose tissue isolated from fed and fasted pregnant rats during late gestation', *The Journal of Clinical Investigation*, vol. 49, no. 7, pp. 1438-1446.

Knopp, RH, Ruder, HJ, Herrera, E & Freinkel, N 1970, 'Carbohydrate metabolism in pregnancy. VII. Insulin tolerance during late pregnancy in the fed and fasted rat', *Acta Endocrinologica*, vol. 65, pp. 352-360.

Knopp, RH, Saudek, CD, Arky, RA & O'Sullivan, JB 1973, 'Two phases of adipose tissue metabolism in pregnancy: maternal adaptations for fetal growth', *Endocrinology*, vol. 92, pp. 984-988.

Knutsson, A 2003, 'Health disorders of shift workers', *Occupational Medicine*, vol. 53, no. 2, pp. 103-108.

Koike, N, Yoo, S-H, Huang, H-C, Kumar, V, Lee, C, Kim, T-K & Takahashi, JS 2012, 'Transcriptional architecture and chromatin landscape of the core circadian clock in mammals', *Science*, vol. 338, pp. 349-354.

Kornmann, B, Schaad, O, Bujard, H, Takahashi, JS & Schibler, U 2007, 'System-driven and oscillator-dependent circadian transcription in mice with a conditionally active liver clock', *Plos Biology*, vol. 5, no. 2, pp. 179-189.

Kramer, A, Yang, F-C, Snodgrass, P, Li, X, Scammell, TE, Davis, FC & Weitz, CJ 2001, 'Regulation of daily locomotor acitivity and sleep by hypothalamic EGF receptor signalling', *Science*, vol. 294, no. 2511-2515.

Kraves, S & Weitz, CJ 2006, 'A role for cardiotrophin-like cytokine in the circadian control of mammalian locomotor activity', *Nature Neuroscience*, vol. 9, pp. 212-219.

La Fleur, SE, Kalsbeek, A, Wortel, J & Buijs, RM 1999, 'A suprachiasmatic nucleus generated rhythm in basal glucose concentrations', *Journal of Neuroendocrinology*, vol. 11, pp. 643-652.

La Fleur, SE, Kalsbeek, A, Wortel, J & Buijs, RM 2000, 'Polysnaptic neural pathways between the hypothalamus, including the suprachiasmatic nucleus, and the liver', *Brain Research*, vol. 871, pp. 50-56.

Lamia, KA, Papp, SJ, Yu, RT, Barish, GD, Uhlenhaut, NH, Jonker, JW, Downes, M & Evans, RM 2011, 'Cryptochromes mediate rhythmic repression of the glucocorticoid receptor', *Nature*, vol. 480, pp. 552-556.

Lamia, KA, Storch, KF & Weitz, CJ 2008, 'Physiological significance of a peripheral tissue circadian clock', *PNAS*, vol. 105, no. 39, pp. 15172-15177.

Lamont, EW, Robinson, B, Stewart, J & Amir, S 2005, 'The central and basolateral nuclei of the amygdala exhibit opposite diurnal rhythms of expression of the clock protein Period2', *PNAS*, vol. 102, no. 11, pp. 4180-4184.

Landgraf, D, Shochtak, A & Oster, H 2012, 'Clock genes and sleep', *European Journal of Physiology*, vol. 463, pp. 3-14.

Landgraf, RM, Landgraf-Leurs, MC, Weissman, A, Horl, R, von Werder, K & Scriba, PC 1977, 'Prolactin: a diabetogenic hormone', *Diabetologia*, vol. 13, pp. 99-104.

Langley-Evans, SC & McMullen, S 2010, 'Developmental origins of adult disease', *Medical Principles and Practice*, vol. 19, no. 2, pp. 87-98.

Le Minh, N, Damiola, F, Tronche, F, Schutz, G & Schibler, U 2001, 'Glucocorticoid hormones inhibit food-induced phase-shifting of peripheral circadian oscillators', *The EMBO Journal*, vol. 20, no. 24, pp. 7128-7136.

Leturque, A, Ferre, P, Satabin, P, Kervran, A & Girard, J 1980, 'In vivo insulin resistance during pregnancy in the rat', *Diabetologia*, vol. 19, pp. 521-528.

Lincoln, DW & Porter, DG 1976, 'Timing of the photoperiod and the hour of birth in rats', *Nature*, vol. 260, pp. 780-781.

Liu, C, Li, S, Lui, T, Borjigin, J & Lin, JD 2007, 'Transcriptional coactivator PGC-1a integrates the mammalian clock and energy metabolism', *Nature*, vol. 447, pp. 447-481.

Lovegrove, BG 2009, 'Modification and miniaturization of Thermochron iButtons for surgical implantation into small animals', *Journal of Comparitive Physiology B*, vol. 179, no. 179, pp. 451-458.

Lowrey, PL & Takahashi, JS 2000, 'Genetics of the mammalian circadian system: Photic entrainment, circadian pacemaker mechanisms and posttranslational regulation', *Annual Review of Genetics*, vol. 34, pp. 533-562.

Lucas, RJ, Freedman, MS, Lupi, D, Munoz, M, David-Gray, ZK & Foster, RG 2001, 'Identifying the photoreceptive inputs to the mammalian circadian system using trasngenic and retinally degenerate mice', *Behavioural Brain Research*, vol. 125, pp. 97-102.

Luppi, P 2003, 'How immune mechanisms are affected by pregnancy', *Vaccine*, vol. 21, pp. 3352-3357.

Malassine, A, Frendo, J-L & Evain-Brion, D 2003, 'A comparison of placental development and endocrine functions between the human and mouse model', *Human Reproduction Update*, vol. 9, no. 6, pp. 531-539.

Malek, S, Sage, D, Pevet, P & Raison, S 2007, 'Daily rhythm of tryptophan hydroxylase-2 messenger ribonucleic acid within Raphe neurons is induced by corticoid daily surge and modulated by enhanced locomotor activity', *Endocrinology*, vol. 148, pp. 5165-5172.

Mark, PJ, Augustus, S, Lewis, JL, Hewitt, DP & Waddell, BJ 2009, 'Changes in placental glucocorticoid barrier during rat pregnancy: impact on placental corticosterone levels and regulation by progesterone', *Biology of Reproduction*, vol. 80, pp. 1209-1215.

Martin-Hidalgo, A, Holm, C, Belfrage, P, Schotz, MC & Herrera, E 1994, 'Lipoprotein lipase and hormone-sensitive lipase activity and mRNA in rat adipose tissue during pregnancy', *American Journal of Physiology - Endocrinology And Metabolism*, vol. 266, no. 6, pp. E930-E935.

Maywood, ES, Reddy, AB, Wong, GKY, O'Neill, JS, O'Brien, JA, McMahon, DG, Harmar, AJ, Okamura, H & Hastings, M 2006, 'Synchronization and maintenance of timekeeping in suprachiasmatic circadian clock cells in neuropeptidergic signaling', *Current Biology*, vol. 16, pp. 599-605.

McCormack, JT & Greenwald, GS 1974, 'Evidence for a preimplantation rise in oestradiol-17B levels on day 4 of pregnancy in the mouse', *Journal of Reproduction and Fertility*, vol. 41, no. 2, pp. 297-301.

McLennan, IS & Taylor-Jeffs, J 2004, 'The use of sodium lamps to brightly illuminate mouse houses during their dark phases', *Laboratory Animals*, vol. 38, pp. 384-392.

McNamara, JP & Bauman, DE 1978, 'Partitioning of nutrients between mammary and adipose tissue of the rat during lactogenesis', *Journal of Dairy Science*, vol. 61, no. Supplementary 1, p. 156.

Metcalfe, J, Stock, MK & Barron, DH 1988, 'Maternal physiology during gestation', in *The Physiology of Reproduction*, 1 edn, vol. 2, eds E Knobil & JD Neill, Raven Press, Ltd., New York, pp. 2145-2176.

Mohawk, JA, Green, CB & Takahashi, JS 2012, 'Central and peripheral circadian clcoks in mammals', *Annual Review of Neuroscience*, vol. 35, pp. 445-462.

Montes, A, Humphrey, J, Knopp, RH & Tolbert Childs, M 1978, 'Lipid Metabolism in Pregnancy. VI. Lipoprotein Composition and Hepatic Lipids in the Fed Pregnant Rat', *Endocrinology*, vol. 103, no. 4, pp. 1031-1038.

Moore, RY & Eichler, VB 1972, 'Loss of a circadian adrenal corticosterone rhythm following suprachiasmatic lesions in the rat', *Brain Research*, vol. 42, no. 1, pp. 201-206.

Munck, A & Koritz, SB 1962, 'Studies on the mode of action of glucocorticoids in rats I. Early effects of cortisol on blood glucose and on glucose entry into muscle, liver and adipse tissue', *Biochemica et Biophysica Acta*, vol. 57, no. 1, pp. 310-317.

Munoz, C, Lopez-Luna, P & Herrera, E 1995, 'Glucose and insulin tolerance tests in the rat on different days of gestation', *Neonatology*, vol. 68, pp. 282-291.

Nader, N, Chrousos, GP & Kino, T 2010, 'Interactions of the circadian CLOCK system and the HPA axis', *Trends in Endocrinology & Metabolism*, vol. 21, no. 5, pp. 277-286.

Nakamura, TJ, Moriya, T, Inoue, S, Shimazoe, T, Watanabe, S, Ebihara, S & Shinohara, K 2005, 'Estrogen differentially regulates expression of *Per1* and *Per2* gene between central and peripheral clocks and between reproductive and nonreproductive tissues in female rats', *Journal of Neuroscience Research*, vol. 82, pp. 622-630.

Nakamura, TJ, Sellix, MT, Kudo, T, Nakao, N, Yoshimura, T, Ebihara, S, Colwell, CS & Block, GD 2010, 'Influence of the estrous cycle on clock gene expression in reproductive tissues: Effects of fluctuating ovarian steroid hormone levels', *Steroids*, vol. 75, no. 3, pp. 203-212.

Nakamura, TJ, Shinohara, K, Funabashi, T & Kimura, F 2001, 'Effect of estrogen on the expression of *Cry1* and *Cry2* mRNAs in the suprachiasmatic nucleus of female rats', *Neuroscience Research*, vol. 41, no. 3, pp. 251-255.

Nielsen, JH, Svensson, C, Galsgaard, ED, Moldrup, A & Billestrup, N 1999, 'Beta cell proliferation and growth factors', *Journal of Molecular Medicine*, vol. 77, pp. 62-66.

Ogren, L, Southard, JN, Colosi, P, Linzer, DIH & Talamantes, F 1989, 'Mouse placental lactogen-I: RIA and gestational profile in maternal serum', *Endocrinology*, vol. 125, no. 5, pp. 2253-2257.

Oishi, K, Miyazaki, K, Kadota, K, Kikuno, R, Nagase, T, Atsumi, G, Ohkura, N, Azama, T, Mesaki, M, Yukisama, S, Kobayashi, H, Iitaka, C, Umehara, T, Horikoshi, M, Kudo, T, Shimizu, Y, Yano, M, Monden, M, Machida, K, Matsuda, J, Horie, S, Todo, T & Ishida, N 2003, 'Genome-wide expression analysis of mouse liver reveals CLOCK-regulated output genes', *The Journal of Biological Chemistry*, vol. 278, no. 42, pp. 41519-41527.

Oishi, K, Uchida, D & Itoh, N 2012, 'Low-carbohydrate, high-protein diet affects rhythmic expression of gluconeogenic regulatory and circadian clock genes in mouse peripheral tissues', *Chronobiology International*, vol. 29, no. 7, pp. 799-809.

Oishi, K, Yamamoto, S, Uchida, D & Doi, R 2013, 'Ketogenic diet and fasting induce expression of cold-inducible RNA-binding protein with time-dependent hypothermia in the mouse liver', *FEBS Open Bio*, vol. 3, pp. 192-195.

Olcese, J 2012, 'Circadian aspects of mammalian parturition: A review', *Molecular and Cellular Endocrinology*, vol. 349, no. 1, pp. 62-67.

Oster, H, Damerow, S, Kiessling, S, Jakubcakova, V, Abraham, D, Tian, J, Hoffmann, MW & Eichele, G 2006, 'The circadian rhythm of glucocorticoids is regulated by a gating mechanism residing in the adrenal cortical clock', *Cell Metabolism*, vol. 4, pp. 163-173.

Palacin, M, Lasuncion, MA, Asuncion, M & Herrera, E 1991, 'Circulating metabolite utilization by periuterine adipose tissue in situ in the pregnant rat', *Metabolism*, vol. 40, no. 5, pp. 534-539.

Panda, S, Antoch, MP, Miller, BH, Su, AI, Schook, AB, Straume, M, G., SP, Kay, SA, Takahashi, JS & Hogenesch, JB 2002, 'Coordinated transcription of key pathways in the mouse by the circadian clock', *Cell*, vol. 109, pp. 307-320.

Parkening, TA, Collins, TJ & Smith, ER 1982, 'Plasma and pituitary concentrations of LH, FSH and prolactin in aging C57Bl/6 mice at various times of the estrous cycle', *Neurobiology of Aging*, vol. 3, pp. 31-35.

Partch, CL, Green, CB & Takahashi, JS 2014, 'Molecular architecture of the mammalian circadian clock', *Trends in Cell Biology*, vol. 24, no. 2, pp. 90-99.

Patrick, J, Challis, J, Campbell, K, Carmichael, L, Natale, R & Richardson, B 1980, 'Circadian rhythms in maternal plasma cortisol and estriol concentrations at 30 to 31, 34 to 35, and 38 to 39 weeks gestational age', *American Journal of Obstetrics and Gynecology*, vol. 136, pp. 325-334.

Perez, S, Murias, L, Fernandez-Plaza, C, Diaz, I, Gonzalez, C, Otero, J & Diaz, E 2015, 'Evidence for clock genes circadian rhythms in human full-term placenta', *Systems Biology in Reproductive Medicine*, vol. 61, no. 6, pp. 360-366.

Pezuk, P, Mohawk, JA, Wang, LA & Menaker, M 2012, 'Glucocorticoids as entraining signals for peripheral oscillators', *Endocrinology*, vol. 153, pp. 4775-4783.

Pocai, A, Lam, TK, Gutierrez-Juarez, R, Obici, S, Muse, ED, Arduini, A & Rossetti, L 2006, 'Restoration of hypothalamic lipid sensing normalizes energy and glucose homeostasis in overfed rats', *Journal of Clinical Investigation*, vol. 116, pp. 1081-1091.

Pocai, A, Lam, TK, Gutierrez-Juarez, R, Obici, S, Schwartz, GJ, Bryan, J, Aguilar-Bryan, L & Rossetti, L 2005a, 'Hypothalamic K(ATP) channels control hepatic glucose production', *Nature*, vol. 434, pp. 1026-1031.

Pocai, A, Obici, S, Schwartz, GJ & Rossetti, L 2005b, 'A brain-liver circuit regulates glucose homeostasis', *Cell Metabolism*, vol. 1, pp. 53-61.

Preitner, N, Damiola, F, Molina, LL, Duboule, D, Albrecht, U & Schibler, U 2002, 'The orphan nuclear receptor REV-ERBalpha controls circadian transcription within the positive limb of the mammalian circadian oscillator', *Cell*, vol. 110, pp. 251-260.

Ptitsyn, AA, Zvonic, S, Conrad, SA, Scott, LK, Mynatt, RL & Gimble, JM 2006, 'Circadian clocks are resounding in peripheral tissues', *PloS Computational Biology*, vol. 2, no. 3, p. e16.

Quennell, JH, Howell, CS, Roa, J, Augustine, RA, Grattan, DR & Anderson, GM 2011, 'Leptin deficiency and diet-induced obesity reduce hypothalamic kisspeptin expression in mice', *Neuroendocrinology*, vol. 152, no. 4, pp. 1541-1550.

Ralph, MR, Foster, RG, Davis, FC & Menaker, M 1990, 'Transplanted suprachiasmatic nucleus determines circadian period', *Science*, vol. 247, pp. 975-978.

Ramos, MP, Crespo-Solans, S, del Campo, S, Cacho, J & Herrera, E 2003, 'Fat accumulation in the rat during early pregnancy is modulated by enhanced insulin responsiveness', *American Journal of Physiology - Endocrinology and Metabolism*, vol. 285, no. 2, pp. E318-E328.

Ratajczak, CK, Herzog, ED & Muglia, LJ 2010, 'Clock gene expression in gravid uterus and extra-embryonic tissues during late gestation in the mouse', *Reproduction, Fertility and Development*, vol. 22, pp. 743-750.

Reddy, AB, Karp, NA, Maywood, ES, Sage, EA, Deery, M, O'Neill, JS, Wong, GKY, Chesham, J, Odell, M, Lilley, KS, Kyriacou, CP & Hastings, M 2006, 'Circadian

orchestration of the hepatic proteome', *Current Biology*, vol. 16, pp. 1107-1115.

Reddy, AB, Maywood, ES, Karp, NA, King, VM, Inoue, Y, Gonzalez, FJ, Lilley, KS, Kyriacou, CP & Hastings, M 2007, 'Glucocorticoid signaling synchronizes the liver circadian transcriptome', *Hepatology*, vol. 45, no. 6, pp. 1478-1488.

Refinetti, R 1996, 'Comparison of the body temperature rhythms of diurnal and nocturnal rodents', *The Journal of Experimental Zoology*, vol. 275, no. 1, pp. 67-70.

Refinetti, R & Menaker, M 1992, 'The circadian rhythm of body temperature', *Physiology & Behavior*, vol. 51, pp. 613-637.

Reppert, SM, Henshaw, D, Schwartz, WJ & Weaver, DR 1987, 'The circadian-gated timing of birth in rats: disruption by maternal SCN lesions or by removal of fetal brain', *Brain Research*, vol. 403, pp. 398-402.

Reppert, SM & Schwartz, WJ 1984, 'The suprachiasmatic nuclei of the fetal rat: characterization of a functional circadian clock using C-labeled deoxyglucose', *The Journal of Neuroscience*, vol. 4, no. 7, pp. 1677-1682.

Reppert, SM & Weaver, DR 2002, 'Coordination of circadian timing in mammals', *Nature*, vol. 418, no. 29, pp. 935-941.

Rey, G, Cesbron, F, Rougemont, J, Reinke, H, Brunner, M & Naef, F 2011, 'Genome-wide and phase specific DNA-binding rhythms of BMAL1 control circadian output functions in mouse liver', *Plos Biology*, vol. 9, no. 2, p. e1000595.

Richards, MP 1966, 'Activity measured by running wheels and observation during the oestrous cycle, pregnancy and pseudopregnancy in the golden hamster', *Animal Behaviour*, vol. 14, pp. 450-458.

Robson, SC, Hunter, S, Boys, RJ & Dunlop, W 1989, 'Serial study of factors influencing changes in cardiac output during human pregnancy', *American Journal of Physiology*, vol. 256, pp. H1060-H1065.

Roseboom, PH, Namboodiri, MAA, Zimonjic, DB, Popescu, NC, Rodriguez, IR, Gastel, JA & Klein, DC 1998, 'Natural melatonin 'knockdown' in C57BL/6J mice: rare mechanism truncates serotonin N-acetyltransferase', *Molecular Brain Research*, vol. 63, no. 1, pp. 189-197.

Rosen, ED & Spiegelman, BM 2006, 'Adipoctyes as regulators of energy balance and glucose homeostasis', *Nature*, vol. 444, pp. 847-853.

Rosenfeld, P, Van Eekelen, JAM, Levine, S & De Kloet, ER 1988, 'Ontogeny of the type 2 glucocorticoid receptor in discrete brain regions: an immunocytochemical study', *Developmental Brain Research*, vol. 42, pp. 119-127.

Rosenwasser, AM, Hollander, SJ & Adler, NT 1987, 'Effects of pregnancy and parturition on free-running circadian activity rhythms in the rat', *Chronobiology International*, vol. 4, no. 2, pp. 183-187.

Rousham, EK, Clarke, PE & Gross, H 2006, 'Significant changes in physical activity among pregnant women in the UK as assessed by accelerometry and self reported activity', *European Journal of Clinical Nutrition*, vol. 60, pp. 393-400.

Rubel, CA, Lanz, RB, Kommagani, R, Franco, HL, Lydon, JP & DeMayo, FJ 2012, 'Research resource: Genome-wide profiling of progesterone receptor binding in the mouse uterus', *Molecular Endocrinology*, vol. 26, no. 8, pp. 1428-1442.

Rudic, RD, McNamara, P, Curtis, AM, Boston, RC, Panda, S, Hogenesch, JB & FitzGerald, GA 2004, 'BMAL1 and CLOCK, two essential components of the

circadian clock, are involved in glucose homeostasis', *Plos Biology*, vol. 2, no. 11, pp. 1893-1899.

Rugh, R 1968, *The mouse: its reproduction and development*, Burgess Publishing Company.

Rusak, B & Zucker, I 1979, 'Neural regulation of circadian rhythms', *Physiological Reviews*, vol. 59, no. 3, pp. 449-526.

Saderi, N, Cazarez-Marquez, F, Buijs, FN, Salgado-Delgado, RC, Guzman-Ruiz, MA, del Carmen Basualdo, M, Escobar, C & Buijs, RM 2013, 'The NPY intergenticulate leaflet projections to the suprachiasmatic nucleus transmit metabolic conditions', *Neuroscience*, vol. 246, pp. 291-300.

Saini, C, Morf, J, Stratmann, M, Gos, P & Schibler, U 2012, 'Simulated body temperature rhythms reveal the phase-shifting behavior and plasticity of mammalian circadian oscillators', *Genes & Development*, vol. 26, pp. 567-580.

Salgado-Delgado, RC, Saderi, N, del Carmen Basualdo, M, Guerrero-Vargas, NN, Escobar, C & Buijs, RM 2013, 'Shift work or food intake during the rest phase promotes metabolic disruption and desynchrony in male rats', *PLOS One*, vol. 8, no. 4, p. e60052.

Saltiel, AR & Kahn, R 2001, 'Insulin signalling and the regulation of glucose and lipid metabolism', *Nature*, vol. 414, pp. 799-806.

Saper, CB, Scammell, TE & Lu, J 2005, 'Hypothalamic regulation of sleep and circadian rhythms', *Nature*, vol. 437, pp. 1257-1263.

Sato, TK, Panda, S, Miraglia, LJ, Reyes, TM, Rudic, RD, McNamara, P, Naik, KA, Fitzgerald, GA, Kay, SA & Hogenesch, JB 2004, 'A functional genomics strategy reveals Rora as a component of the mammalian circadian clock', *Neuron*, vol. 43, no. 4, pp. 527-537.

Schaefer-Graf, UM, Graf, K, Kulbacka, I, Kjos, SL, Dudenhausen, J, Vetter, K & Herrera, E 2008, 'Maternal lipids as strong determinants of fetal environment and growth in pregnancies with gestational diabetes mellitus', *Diabetes Care*, vol. 31, no. 9, pp. 1858-1863.

Schoonjans, K, Peinado-Onsurbe, J, Lefebvre, A, Heyman, RA, Briggs, M, Deeb, S, Staels, B & Auwerx, J 1996, 'PPARα and PPARγ activators direct a distinct tissue-specific transcriptional response via a PPRE in the lipoprotein lipase gene', *The EMBO Journal*, vol. 15, no. 19, pp. 5336-5348.

Schrader, JA, Nunez, AA & Smale, L 2010, 'Changes in and dorsal to the rat suprachiasmatic nucleus during early pregnancy', *Neuroscience*, vol. 171, pp. 513-523.

Schrader, JA, Nunez, AA & Smale, L 2011, 'Site-specific changes in brain extra-SCN oscillators during early pregnancy in the rat', *Journal of Biological Rhythms*, vol. 26, no. 363-367.

Scott, DE 1972, 'Anemia in pregnancy', *Obstetrics and Gynecology Annual*, vol. 1, pp. 219-244.

Scribner, SJ & Wynne-Edwards, KE 1994, 'Disruption of body temperature and behavior rhythms during reproduction in dwarf hamsters *(Phodopus)*', *Physiology & Behavior*, vol. 55, no. 2, pp. 361-369.

Seckl, J & Walker, BR 2001, 'Minireview: 11beta-hydroxysteroid dehydrogenase type 1 - a tissue-specific amplifier of glucocorticoid action', *Endrocrinolgy*, vol. 142, no. 4, pp. 1371-1376.

Sellix, MT, Egli, M, Poletini, MO, McKee, DT, Bosworth, MD, Fitch, CA & Freeman, ME 2006, 'Anatomical and functional characterization of clock gene expression in neuroendocrine dopaminergic neurons', *American Journal of*

Physiology, Regulatory, Integrative and Comparative Physiology, vol. 290, pp. R1309-R1323.

Serón-Ferré, M, Ducsay, CA & Valenzuela, GJ 1993, 'Circadian rhythms during pregnancy', *Endocrine Reviews*, vol. 14, no. 5, pp. 594-609.

Serón-Ferré, M, Mendez, N, Abarzua-Catalan, L, Vilches, N, Valenzuela, FJ, Reynolds, HE, Llanos, AJ, Rojas, A, Valenzuela, GJ & Torres-Farfan, C 2012, 'Circadian rhythms in the fetus', *Molecular and Cellular Endocrinology*, vol. 349, no. 1, pp. 68-75.

Shimba, S, Ogawa, T, Hitosugi, S, Ichihashi, Y, Nakadaira, Y, Kobayashi, M, Tezuka, M, Kosuge, Y, Ishige, K, Ito, Y, Komiyama, K, Okamatsu-Ogura, Y, Kimura, K & Saito, M 2011, 'Deficient of a clock gene, brain and muscle arnt-like protein-1 (BMAL1), induces dyslipedima and ectopic fat formation', *Plos One*, vol. 6, no. 9, p. e25231.

Shimomura, H, Moriya, T, Sudo, M, Wakamatsu, H, Akiyama, M, Miyake, Y & Shibata, S 2001, 'Differential daily expression of Per1 and Per2 mRNA in the suprachiasmatic nucleus of fetal and early postnatal mice', *European Journal of Neuroscience*, vol. 13, pp. 687-693.

Shostak, A, Meyer-Kovac, J & Oster, H 2013, 'Circadian regulation of lipid mobilization in white adipose tissues', *Diabetes*, vol. 62, pp. 2195-2203.

Sladek, M, Jindrakova, Z, Bendova, Z & Sumova, A 2007, 'Ontogeny of circadian organization in the rat', *American Journal of Physiology - Regulatory, Integrative and Comparative Physiology*, vol. 292, pp. R1224-R1229.

Sladek, M, Sumova, A, Kovacikova, Z, Laurinova, K & Illnerova, H 2004, 'Insight into molecular core clock mechanism of embryonic and early postnatal rat suprachiasmatic nucleus', *PNAS*, vol. 101, no. 16, pp. 6231-6236.

So, AYL, Bernal, TU, Pillsbury, ML, Yamamoto, KR & Feldman, BJ 2009, 'Glucocorticoid regulation of the circadian clock modulates glucose homeostasis', *PNAS*, vol. 106, no. 41, pp. 17582-17587.

Soares, MJ, Colosi, P & Talamantes, F 1982, 'The development and characterization of a homologous radioimmunoassay for mouse placental lactogen', *Endocrinology*, vol. 110, no. 2, pp. 668-670.

Soares, MJ, Faria, TN, Roby, KF & Deb, S 1991, 'Pregnancy and the prolactin family of hormones: coordination of anterior pituitary, uterine, and placental expression ', *Endocrine Reviews*, vol. 12, no. 4, pp. 402-423.

Solt, LA, Wang, Y, Banerjee, S, Hughes, T, Kojetin, DJ, Lundasen, T, Shin, Y, Liu, J, Cameron, MD, Noel, R, Yoo, S-H, Takahashi, JS, Butler, AA, Kamenecka, TM & Burris, TP 2012, 'Regulation of circadian behaviour and metabolism by synthetic REV-ERB agonists', *Nature*, vol. 485, pp. 62-68.

Son, GH, Chung, S, Choe, HK, Kim, H-D, Baik, S-M, Lee, H, Lee, H-W, Choi, S, Sun, W, Kim, H, Cho, S, Lee, KH & Kim, K 2008, 'Adrenal peripheral clock controls the autonomous circadian rhythm of glucocorticoid by causing rhythmic steroid production', *Proceedings of the National Academy of Sciences*, vol. 105, no. 52, pp. 20970-20975.

Sorhede Winzell, M & Ahren, B 2004, 'The high-fat diet-fed mouse: A model for studying mechanisms and treatment of impaired glucose tolerance and type 2 diabetes', *Diabetes*, vol. 53, no. Supplement 3, pp. S215-S219.

Spiga, F, Walker, JJ, Terry, JR & Lightman, SL 2014, 'HPA axis-rhythms', *Comprehensive Physiology*, vol. 4, pp. 1273-1298.

Stehle, JH, von Gall, C & Korf, H-W 2003, 'Melatonin: a clock-output, a clock-input', *Journal of Neuroendocrinology*, vol. 15, pp. 383-389.

Stokkan, K-A, Yamazaki, S, Tei, H, Sakaki, Y & Menaker, M 2001, 'Entrainment of the circadian clock in the liver by feeding', *Science*, vol. 291, no. 5503, pp. 490-493.

Storch, KF, Lipan, O, Leykin, I, Viswanathan, N, Davis, FC, Wong, WH & Weitz, CJ 2002, 'Extensive and divergent circadian gene expression in liver and heart', *Nature*, vol. 417, pp. 78-82.

Strauss, JFI, Martinez, F & Kiriakidou, M 1996, 'Placental steroid hormone synthesis: unique features and unanswered questions', *Biology of Reproduction*, vol. 54, no. 2, pp. 303-311.

Su, Y, Cailotto, C, Foppen, E, Jansen, R, Zhang, Z, Buijs, RM, Fliers, E & Kalsbeek, A 2016, 'The role of feeding rhythm, adrenal hormones and neuronal inputs in synchronizing daily clock gene rhythms in the liver', *Molecular and Cellular Endocrinology*, vol. 422, pp. 125-131.

Su, Y, van der Spek, R, Foppen, E, Kwakkel, J, Fliers, E & Kalsbeek, A 2015, 'Effects of adrenalectomy on daily gene expression rhythms in the rat suprachiasmatic and paraventricular nuclei and in white adipose tissue', *Chronobiology International*, vol. 32, no. 2, pp. 211-224.

Sukumaran, S, Xue, B, Jusko, WJ, DuBois, DC & Almon, RR 2010, 'Circadian variations in gene expression in rat abdominal adipose tissue and relationship to physiology', *Physiological Genomics*, vol. 42A, pp. 141-152.

Suman Rao, PN, Shashidhar, A & Ashok, C 2013, 'In utero fuel homeostasis: lessons for a clinician', *Indian Journal of Endrocrinology and Metabolism*, vol. 17, no. 1, pp. 60-68.

Summa, KC, Vitaterna, MH & Turek, FW 2012, 'Environmental perturbation of the circadian clock disrupts pregnancy in the mouse', *Plos One*, vol. 7, no. 5, p. e37668.

Sumova, A, Bendova, Z, Sladek, M, El-Hennamy, R, Mateju, K, Polidarova, L, Sosniyenko, S & Illnerova, H 2008, 'Circadian molecular clocks tick along ontogenesis', *Physiological Research*, vol. 57, no. Suppl 3, pp. S139-S148.

Sutter-Dub, M-T, Dazey, B, Hamdan, E & Vergnaud, M-T 1981, 'Progesterone and insulin-resistance: studies of progesterone action on glucose transport, lipogenesis and lipolysis in isolated fat cells of the female rat', *Journal of Endocrinology*, vol. 88, pp. 455-462.

Suzuki, M, Shimomura, Y & Satoh, Y 1983, 'Diurnal changes in lipolytic activity of isolated fat cells and their increased responsiveness to epinephrine and theophylline with meal feeding in rats', *Journal of Nutritional Science and Vitaminology*, vol. 29, no. 4, pp. 399-411.

Tei, H, Okamura, H, Shigeyoshi, Y, Fukuhara, C, Ozawa, R, Hirose, M & Sakaki, Y 1997, 'Circadian oscillation of a mammalian homologue of the Drosophila period gene', *Nature*, vol. 389, pp. 512-516.

Terazono, H, Mutoh, T, Yamaguchi, S, Kobayashi, M, Akiyama, M, Udo, R, Ohdo, S, Okamura, H & Shibata, S 2003, 'Adrenergic regulation of clock gene expression in mouse liver', *PNAS*, vol. 100, no. 11, pp. 6795-6800.

Thorens, B 1996, 'Glucose transporters in the regulation of intestinal, renal and liver glucose fluxes', *American Physiological Society*, pp. G541-G553.

Torres-Farfan, C, Mendez, N, Abarzua-Catalan, L, Vilches, N, Valenzuela, GJ & Seron-Ferre, M 2011, 'A circadian clock entrained by melatonin is ticking in the rat fetal adrenal', *Endocrinology*, vol. 152, pp. 1891-1900.

Torres-Farfan, C, Seron-Ferre, M, Dinet, V & Korf, H-W 2006, 'Immunocytochemical demonstration of day/night changes of clock gene protein levels in the murine adrenal gland: differences between melatonin-proficient (C3H) and

melatonin-deficient (C57BL) mice', *Journal of Pineal Research*, vol. 40, pp. 64-70.

Travnickova-Bendova, Z, Cermakian, N, Reppert, SM & Sassone-Corsi, P 2002, 'Bimodal regulation of mPeriod promoters by CREB-dependent signalling and CLOCK/BMAL1 activity', *PNAS*, vol. 99, no. 11, pp. 7728-7733.

Turek, FW, Joshu, C, Kohsaka, A, Lin, E, Ivanova, G, McDearmon, E, Laposky, A, Losee-Olson, S, Easton, A, Jensen, DR, Eckel, RH, Takahashi, JS & Bass, J 2005, 'Obesity and metabolic syndrome in circadian clock mutant mice', *Science*, vol. 308, pp. 1043-1045.

Uchikawa, M, Kawamura, M, Yamauchi, N & Hattori, M 2011, 'Down-regulation of circadian clock gene Period 2 in uterine endometrial stromal cells of pregnant rats during decidualization', *Chronobiology International*, vol. 28, no. 1, pp. 1-9.

Ueda, HR, Hayashi, S, Chen, W, Sano, M, Machida, M, Shigeyoshi, Y, Iino, M & Hashimoto, S 2005, 'System-level identification of transcriptional circuits underlying mammalian circadian clocks', *Nature Genetics*, vol. 37, no. 2, pp. 187-192.

Uesa, BU, Seal, US & Doe, RP 1965, 'Elevation of certain plasma proteins in man following estrogen administraton: a dose-response relationship', *Journal of Clinical Endocrinology*, vol. 25, pp. 1163-1166.

Ulrich-Lai, YM, Arnhold, MM & Engeland, WC 2006, 'Adrenal splanchnic innervation contributes to the diurnal rhythm of plasma corticosterone in rats by modulating adrenal sensitivity to ACTH', *American Journal of Physiology - Regulatory, Integrative and Comparative Physiology*, vol. 290, pp. R1128-R1135.

Vandesompele, J, De Preter, K, Pattyn, F, Poppe, B, Van Roy, N, De Paepe, A & Speleman, F 2002, 'Accurate normalization of real-time quantitative RT-PCR data by geometric averaging of multiple internal control genes', *Genome Biology*, vol. 3, no. 7, pp. 1-12.

Varcoe, TJ, Boden, MJ, Voultsios, A, Salkeld, MD, Rattanatray, L & Kennaway, DJ 2013, 'Characterisation of the maternal response to chronic phase shifts during gestation in the rat: implications for fetal metabolic programming', *Plos One*, vol. 8, no. 1, p. e53800.

Varcoe, TJ, Wight, N, Voultsios, A, Salkeld, MD & Kennaway, DJ 2011, 'Chronic phase shifts of the photoperiod throughout pregnancy programs glucose intolerance and insulin resistance in the rat', *Plos One*, vol. 6, no. 4, p. e18504.

Vaughan, OR, Fisher, HM, Dionelis, KN, Jefferies, EC, Higgins, JS, Musial, B, Sferruzzi-Perri, AN & Fowden, AL 2015, 'Corticosterone alters materno-fetal glucose partitioning and insulin signalling in pregnant mice', *The Journal of Physiology*, vol. 593, no. 5, pp. 1307-1321.

Vegiopoulos, A & Herzig, S 2007, 'Glucocorticoids, metabolism and metabolic diseases', *Molecular and Cellular Endocrinology*, vol. 275, pp. 43-61.

Vida, B, Hrabovszky, E, Kalamatianos, T, Coen, CW, Liposits, Z & Kalló, I 2008, 'Oestrogen receptor α and β immunoreactive cells in the suprachiasmatic nucleus of mice: distribution, sex differences and regulation by gonadal hormones', *Journal of Neuroendocrinology*, vol. 20, no. 11, pp. 1270-1277.

Vidal-Puig, AJ, Considine, RV, Jimenez-Linan, M, Werman, A, Pories, WJ, Caro, JF & Flier, JS 1997, 'Peroxisome proliferator-activated receptor gene expression in human tissues. Effects of obesity, weight loss and regulation by insulin

and glucocorticoids.', *Journal Of Clinical Investigation*, vol. 99, no. 10, pp. 2416-2422.

Vollmers, C, Schmitz, RJ, Nathanson, J, Yeo, G, Ecker, JR & Panda, S 2012, 'Circadian oscillations of protein-coding and regulatory RNAs in a highly dynamic mammalian liver epigenome', *Cell Metabolism*, vol. 16, pp. 833-845.

Waddell, BJ 1993, 'The placenta as hypothalamus and pituitary: possible impact on maternal and fetal adrenal function', *Reproduction, Fertility and Development*, vol. 5, pp. 479-497.

Waddell, BJ & Atkinson, HC 1994, 'Production rate, metabolic clearance rate and uterine extraction of corticosterone during rat pregnancy', *Journal of Endocrinology*, vol. 143, pp. 183-190.

Waddell, BJ, Benediktsson, R, Brown, RW & Seckl, JR 1998, 'Tissue-specific messenger ribonucleic acid expression of 11beta-hydroxysteroid dehydrogenase types 1 and 2 and the glucocorticoid receptor within rat placenta suggests exquisite local control of glucocorticoid action', *Endocrinology*, vol. 139, no. 4, pp. 1517-1523.

Waddell, BJ & Burton, PJ 1993, 'Release of bioactive ACTH by perifused human placenta at early and late gestation', *Journal of Endrocrinology*, vol. 136, no. 2, pp. 345-353.

Waddell, BJ, Wharfe, MD, Crew, RC & Mark, PJ 2012, 'A rhythmic placenta? Circadian variation, clock genes and placental function', *Placenta*, vol. 33, pp. 533-539.

Wallace, JC & Barritt, GJ 2002, in Encyclopedia of Life Sciences, Macmillian Publishers Ltd Nature Publishing Group.

Walmer, DK, Wrona, MA, Hughes, CL & Nelson, KG 1992, 'Lactoferrin expression in the mouse reproductive tract during the natural estrous cycle: correlation with circulating estradiol and progesterone', *Endrocrinolgy*, vol. 131, no. 3, pp. 1458-1466.

Watts, AG, Tanimura, S & Sanchez-Watts, G 2004, 'Corticotropin-releasing hormone and arginine vasopressin gene transcription in the hypothalamic paraventricular nucleus of unstressed rats: daily rhythms and their interactions with corticosterone', *Endocrinology*, vol. 145, no. 2, pp. 529-540.

Weissgerber, TL & Wolfe, LA 2006, 'Physiological adaptation in early human pregnancy: adaptation to balance maternal-fetal demands', *Applied Physiology, Nutrition, and Metabolism*, vol. 31, no. 1, pp. 1-11.

Weizenbaum, F, Kenney, NJ & Adler, NT 1979, 'Similarities in the regulatory patterns of pregnant and cycling rats', *Physiology and Behaviour*, vol. 23, pp. 891-896.

Wharfe, MD, Mark, PJ & Waddell, BJ 2011, 'Circadian variation in placental and hepatic clock genes in rat pregnancy', *Endocrinology*, vol. 152, no. 9, pp. 3552-3560.

Wharfe, MD, Mark, PJ, Wyrwoll, CS, Smith, JT, Yap, C, Clarke, MW & Waddell, BJ 2016a, 'Pregnancy-induced adaptations of the central circadian clock and maternal glucocorticoids', *Journal of Endocrinology*, vol. 228, no. 3, pp. 135-147.

Wharfe, MD, Wyrwoll, CS, Waddell, BJ & Mark, PJ 2016b, 'Pregnancy-induced changes in the circadian expression of hepatic clock genes: implications for maternal glucose homeostasis', *American Journal of Physiology - Endocrinology And Metabolism*, vol. 311, no. 3, pp. E575-E586.

Yamamoto, T, Nakahata, Y, Soma, H, Akashi, M, Mamine, T & Takumi, T 2004, 'Transcirptional oscillation of canonical clock genes in mouse peripheral tissues', *BMC Molecular Biology*, vol. 5, no. 18, pp. 1-9.

Yamamoto, T, Nakahata, Y, Tanaka, M, Yoshida, M, Soma, H, Shinohara, K, Yasuda, A, Mamine, T & Takumi, T 2005, 'Acute physical stress elevates mouse *Period1* mRNA expression in mouse peripheral tissues via a glucocorticoid-responsive element', *Journal of Biological Chemistry*, vol. 280, no. 51, pp. 42036-42043.

Yamazaki, S, Numano, R, Abe, M, Hida, A, Takahashi, R-I, Ueda, M, Block, GD, Sakaki, Y, Menaker, M & Tei, H 2000, 'Resetting central and peripheral circadian oscillators in transgenic rats', *Science*, vol. 288, pp. 682-685.

Yang, G, Jia, Z, Aoyagi, T, McClain, D, Mortensen, RM & Yang, T 2012, 'Systemic PPARgamma deletion impairs circadian rhythms of behavior and metabolism', *PLoS One*, vol. 7, no. 8, p. e38117.

Yang, X, Downes, M, Yu, RT, Bookout, AL, He, W, Straume, M, Mangelsdorf, DJ & Evans, RM 2006, 'Nuclear receptor expression links the circadian clock to metabolism', *Cell*, vol. 126, pp. 801-810.

Ye, J, Coulouris, G, Zaretskaya, I, Cutcutache, I, Rozen, S & Madden, TL 2012, 'Primer-BLAST: A tool to design target-specific primers for polymerase chain reaction', *BMC Bioinformatics*, vol. 13, no. 134, pp. 1-11.

Yi, C-X, van der Vliet, J, Dai, J, Yin, G, Ru, L & Buijs, RM 2006, 'Ventromedial arcuate nucleus communicates peripheral metabolic information to the suprachiasmatic nucleus', *Endocrinology*, vol. 147, no. 1, pp. 283-294.

Yin, L, Wu, N, Curtin, JC, Qatanani, M, Szwergold, NR, Reid, RA, Waitt, GM, Parks, DJ, Pearce, KH, Wisely, GB & Lazar, MA 2007, 'Rev-erbα, a heme sensor that coordinates metabolic and circadian pathways', *Science*, vol. 318, pp. 1786-1789.

Yoo, S-H, Mohawk, JA, Siepka, SM, Shan, Y, Huh, SK, Hong, HK, Kornblum, I, Kumar, V, Koike, N, Xu, M, Nussbaum, J, Liu, X, Chen, Z, Chen, ZJ, Green, CB & Takahashi, JS 2013, 'Competing E3 ubiquitin ligases govern circadian periodicity of degradation of CRY in nucleus and cytoplasm', *Cell*, vol. 152, no. 5, pp. 1091-1105.

Yoo, S-H, Yamazaki, S, Lowrey, PL, Shimomura, K, Ko, CH, Buhr, ED, Siepka, SM, Hong, HK, Oh, WJ, Yoo, OJ, Menaker, M & Takahashi, JS 2004, 'Period2::Luciferase real-time reporting of circadian dynamics reveals persistent circadian oscillations in mouse peripheral tissues', *PNAS*, vol. 101, no. 15.

Young, ME, Razeghi, P & Taegtmeyer, H 2001, 'Clock genes in the heart - Characterization and attenuation with hypertrophy', *Circulation Research*, vol. 88, no. 11, pp. 1142-1150.

Zani, F, Breasson, L, Becattini, B, Vukolic, A, Montani, J, Albrecht, U, Provenzani, A, Ripperger, J & Solinas, G 2013, 'PER2 promotes glucose storage to liver glycogen during feeding and acute fasting by inducing *Gys2*, *PTG* and *GL* expression', *Molecular Metabolism*, vol. 2, pp. 292-305.

Zhang, EE, Liu, Y, Dentin, R, Pongsawakul, PY, Liu, AC, Hirota, T, Nusinow, DA, Sun, X, Landais, S, Kodama, Y, Brenner, DA, Montminy, M & Kay, SA 2010, 'Cryptochrome mediates circadian regulation of cAMP signaling and hepatic gluconeogenesis', *Nature Medicine*, vol. 16, no. 10, pp. 1152-1156.

Zhang, Y, Chen, W, Li, R, Ge, Y & Chen, G 2011, 'Insulin-regulated Srebp-1c and Pck1mRNA expression in primary hepatocytes from zucker fatty but not lean rats is affected by feeding conditions', *PLoS One*, vol. 6, no. e21342.

Zhu, JL, Hjollund, NH, Andersen, AM & Olsen, J 2004, 'Shift work, job stress and late fetal loss: The national birth cohort in Denmark', *Journal of Occupational & Environmental Medicine*, vol. 46, no. 11, pp. 1144-1149.

Zuber, AM, Centeno, G, Pradervand, S, Nikolaeva, S, Maquelin, L, Cardinaux, L, Bonny, O & Firsov, D 2010, 'Molecular clock is involved in predictive circadian clock adjustment of renal function', *PNAS*, vol. 106, no. 38, pp. 16523-16528.

Zvonic, S, Ptitsyn, AA, Conrad, SA, Scott, LK, Floyd, EZ, Kilroy, G, Wu, X, Goh, BC, Mynatt, RL & Gimble, JM 2006, 'Characterization of peripheral circadian clocks in adipose tissues', *Diabetes*, vol. 55, pp. 962-970.